DOCTORAL DISSERTATION

Improvement of Indoor Environment based on Cooking Heating Wall and Sunlight Room in Traditional Chinese Housing

September 2022
YANG SIMIN

Graduate School of Environmental Engineering
Dewancker Bart Lab
The University of Kitakyushu, Japan

Acknowledgements

After three years' study in the University of Kitakyushu, this thesis was finally accomplished. Without of the help of many people, it could never be completed. Thus, here I would like to express my sincere gratitude towards them.

First of all, I owe my heartfelt thanks to my distinguished and cordial supervisor, Professor Bart Julien Dewancker. He is knowledgeable and rigorous, and motivates students with his excellent professionalism and serious work attitude. He has been inspiring and guiding me with his original insights and practical academic advice. The completion of this thesis is inseparable from his careful guidance and confusion.

In addition, I would also like to thank Professor Xu Juan, who was my first tutor. I would not have started my academic research without her guidance. At the same time, I am also very grateful to Prof. Weijun Gao, Prof. Kido and Prof. Imai. for their great help to my study and research in Japan.

Then, I would also like to thank to all university colleagues and students, Dr. Gaochuan Zhang, Dr. Yuang Guo, Dr. Xinbo Yao, Dr. Shuo Chen, Dr. Di Wang, Dr. Jinming Wang, Dr. Jialu Dai, Dr. Wensheng Mo, Ms. Xiaodi Sun and Ms. Yang Cao. Their support has enriched my research and life.

Finally, I would like to thank my parents. It is very difficult for me to complete the whole learning process without their support.

In a word, thank you so much for all of you!

Abstract

In China, research on winter heating and energy saving for residential buildings mainly focuses on urban residences rather than rural ones. According to the 2018 China Building Energy Consumption Research Report, rural residential buildings emit about 423 million tons of carbon, accounting for 21% of the country's total carbon emissions. Rural houses are generally independent houses, with flexible layout, spacious courtyards, easier to use people's way of life and production to develop passive energy saving characteristics. Therefore, rural housing has great energy saving potential. Through the field investigation of more than 60 villages in southern Shaanxi, the characteristics of the houses in southern Shaanxi are collected and sorted out. Twelve villages were selected as the key research objects, and the status quo of the spatial function, construction technology, features and characteristics, indoor thermal comfort and other four aspects of residential houses were summarized and analyzed in depth by literature induction, induction and summary, field research and software simulation. It is found that the indoor temperature of residential houses in southern Shaanxi is low in winter and the traditional heating equipment can only raise the local temperature of human body but not the whole indoor temperature. In addition, the paper also summarizes the function, technology and image of residential space and reveals its influencing factors.

In view of the current situation, relevant theories and heat transfer principles are applied. First, according to the research on China's greenhouse gas inventory, the main sources of carbon emissions in rural areas are from cooking and the burning of fuelwood and biomass for heating in winter. In this study, the southern Shaanxi area, which is hot in summer and cold in winter, was selected as the research site, and a cooking heating wall system was planned that combines cooking and heating facilities in residential buildings. The system uses the heat generated by cooking and the heat storage capacity of the wall, as well as the principle of thermal radiation and heat convection, to increase the indoor temperature. The advantage is that the hot air generated is mainly concentrated in the inside of the wall, which reduces the direct contact with the cold outdoor air and avoids excess heat loss.

Secondly, in the process of studying the cooking heating wall system, it is found that the system is affected by the cooking time and the heating time is less. Therefore, a sunlight heating system with an additional cooking heating wall is put forward. The system is composed of a cooking heating wall system and a sunlight system. The combination of the two systems prolongs the heating time and makes up for the lack of intermittent heating. The cooking heating wall principle involves using the heat generated by cooking through the heat storage and heat release capacity of the wall, and using the principle of heat radiation and convection to increase the indoor temperature. Meanwhile, the principle of the additional sunlight room involves using the external facade of the building to establish an additional sunlight room, by absorbing the heat radiation of the sun and using the principle of heat transfer from the wall. The rapid loss of indoor hot air is avoided, the heating time is prolonged, and part of the heat is retained, thereby improving the heating efficiency. A model was established based on the typical residential model in southern Shaanxi, and the presence or absence of solar radiation on the wall was used as the research variable. Using ANSYS software to simulate the analysis, it is concluded that the cooking heating wall–sunlight system can extend the heating time and meet the continuous heating demand, and the heating effect is better than that of the cooking heating wall system alone.

Finally, the optimization measures for the heating system between the cooking heating wall and additional sunlight are put forward. It mainly includes the material of glass between additional sunlight, depth of building, wall material and window-wall ratio. The simulation analysis and comparison are carried out, and the passive heating technology suitable for traditional houses in southern Shaanxi is summarized.

Keywords: cooking heating wall–additional sunlight system; passive heating; rural residential buildings; southern Shaanxi; software analysis.

Contents

List of Figures

List of tables

List of Nomenclature

1. Gross Domestic Product (GDP)
2. Tons of Standard Coal Equivalent (TCE)
3. Household Energy Consumption (HEC)
4. Window-to-Wall Ratio (WWR)
5. Severe Cold Regions (SCR)
6. Cold Regions (CR)
7. Hot Summer and Cold Winter Regions (HSCW)
8. Mild Regions (MR)
9. Hot Summer and Warm Winter Regions (HSWW)
10. Solar Heat Gain Coefficient (SHGC)
11. Average Radiation Temperature (MRT)
12. Predicted Mean Vote (PMV)
13. Predicted Percentage of Dissatisfied People (PPD)
14. Wall Solar Radiation (WSR)
15. National Fenestration Rating Council Incorporated (NFRC)
16. Low Emissivity (Low - e)
17. Geometric Shadow Coefficient (GSC)
18. Designer's Simulation Toolkit (DeST)
19. Design of Experiments (DOE)
20. Expanded Polystyrene Board (EPS)
21. Extruded Polystyrene Board (XPS)

Chapter 1. Introduction

1.1 Research Background

Nowadays, with the rapid growth in the global economic GDP, the demand for energy in construction, agriculture, industry, and other industries has increased [1]. As is shown in figure 1-1, from 2016 to 2018, the construction industry accounted for 12.5% of the global energy requirement, increasing to 21.22% [2]. Therefore, as is shown in figure 1-2, the demand for energy in the construction industry is on the rise. The total annual energy demand of the building industry was 2.147 billion TCE (tons of standard coal equivalent—1 ton standard coal equivalent is the conversion index for calculating various energy quantities according to the calorific value of standard coal), accounting for 46.5% of the whole energy requirement in 2018 (Figure 1-3). The total carbon emissions generated by the construction industry is 4.93 billion TCE, accounting for 51.3% of the national carbon emissions [3]. It is expected that in 2050, this value will double [4]. According to China's construction Industry Energy Report 2016, residential buildings account for 77% of building energy consumption [5]. Thus, residential buildings are an important part of building energy consumption. In response to this phenomenon, some experts have proposed the use of renewable sources, such as geothermal and hydroelectric power generation, to save energy [6]. Neupane et al. [7] evaluated the development space of wind energy in provincial areas of Nepal and established an energy model based on the local geographical environment, economic conditions, and other factors. Through the calculation of the open source system platform, 1686 MW of local wind energy can be generated. In addition, the local area has the potential to generate 267.0 MW of wind power, and the construction cost is 46 USD/MWh. The development of wind energy has a good impact on resource utilization in Nepal. Yuan et al. [8] found, through high density instruments, that there is a high-temperature underground heat storage layer deep underground in the Yang bajing area. When using five-point configuration with multiple wellheads, the flow rate of a single geothermal heat generation is 17 kg/s. The total capacity of geothermal power can reach 66.0 MW, which can effectively reduce greenhouse gas emissions. Rauf et al. [9] designed a combination of solar photovoltaic and hydropower, analyzing the impact of solar photovoltaic on hydropower. Using a combination of the two methods, the total power of the hydropower generation increased by 3.5%.

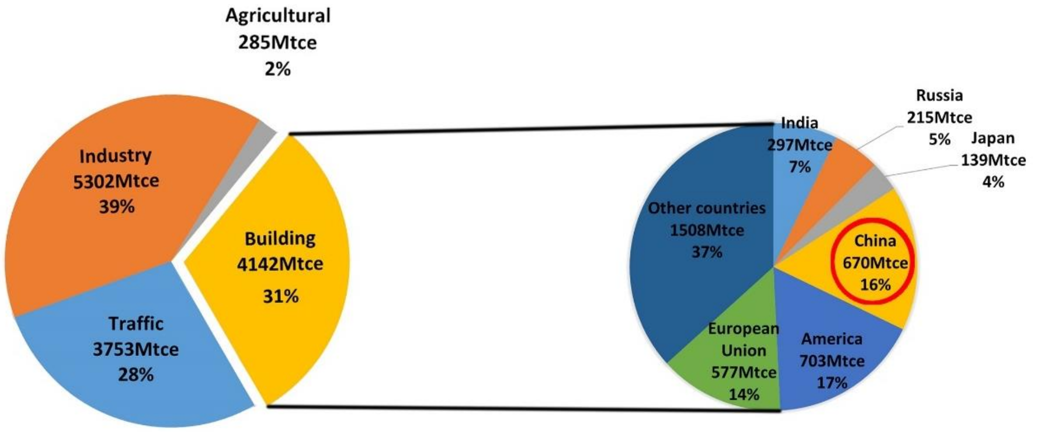

Figure 1-1. Proportion and regional distribution of global building terminal energy.

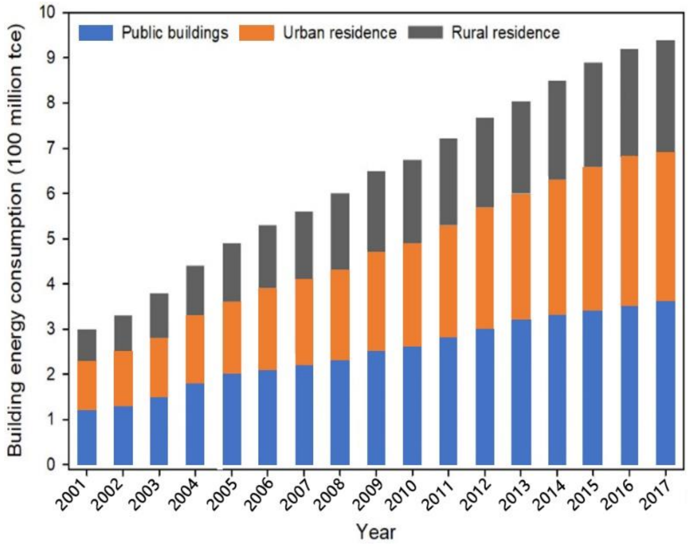

Figure 1-2. Building energy variation in China.

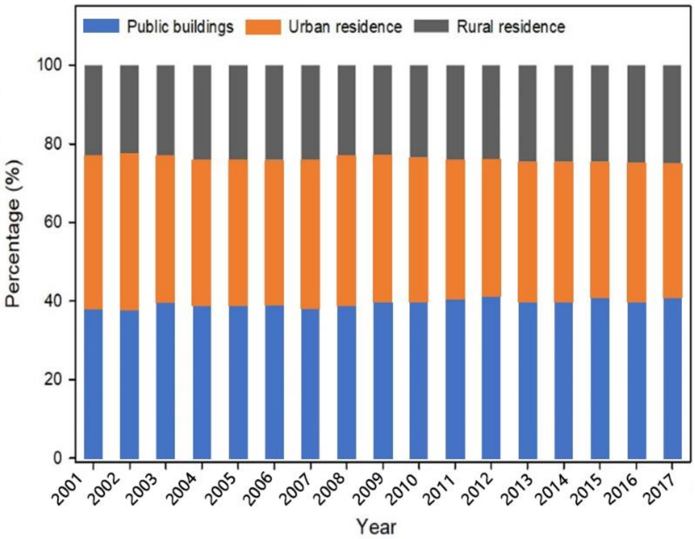

Figure 1-3. The proportion of energy consumption for different building types

In China, to effectively reduce the energy demand of residences, the housing and urban–rural construction departments have proposed a series of urban residential energy saving design specifications and have achieved some results [10]. Many scholars have put forward corresponding urban residential building energy-saving design strategies through a variety of research methods [11]. However, there are few considerations for the energy-saving design of rural residences. Urban houses are different from rural houses in terms of architectural design, climatic conditions, and behavior of occupants [12]. In terms of architectural design, in order to reduce energy demand, urban residential buildings generally adopt centralized high-rise buildings. High-rise residential buildings are divided according to the internal space, and there are two types: the corridor type and the unit type. Its characteristics are a long service life and a large demand [13]. Rural housing is generally self-built, with the residents getting involved in the construction mainly based on their years of construction experience. Therefore, residential houses not only have the function of use, but also have the function of cultural inheritance [14]. In terms of climatic conditions, urban residences are greatly affected by solar radiation, and electrical appliances are mainly used for indoor adjustment [15]. The indoor temperature of rural houses in the summer is mainly regulated by natural ventilation, as well as partly by electrical equipment. Heating in winter mainly relies on burning charcoal fires [16]. In terms of occupant behavior, compared to rural residents, urban residents pay more attention to privacy. Therefore, in addition to satisfying the basic space, urban housing has less public communication space [17]. Residents in rural areas live on cultivated land and need space to store agricultural tools and crops. In addition, there is a lot of communication between residents, and these behavioral factors make rural residential building spaces larger, relatively open, and possessing other characteristics [18]. In the light of the statistics from the National Bureau of Statistics, the per capita housing area of rural residents in 2019 was 48.9 m², an improvement of 97.2% compared to 2000 [19]. Therefore, energy-saving designs for rural houses is very necessary. Rural residential buildings have the advantages of being relatively open, flexible in layout, and large in space [20]. Thus, when studying the energy efficiency of rural residences, the reconstruction of buildings and the utilization of renewable energy have great advantages [21]. In this study, passive cooking and the addition of a sunlight room heating system are proposed for winter, which can effectively improve the indoor temperature and reduce energy requirements.

1.2 Literature Review

In rural areas, energy consumption mainly comes from residential buildings, and nearly one-fifth of the energy demand is used for the heating and cooling of residences [22]. With the increase in energy consumption, environmental pollution and other problems also follow [23]. In China, the demand for the energy consumption of residential buildings in rural areas is even more severe [24]. To solve this problem, relevant departments have made policies to reduce the demand for energy [25]. Wang et al. [26] studied the factors affecting Chinese household energy consumption (HEC) from 2005 to 2017, and explored the difference between HEC in urban and rural areas. The HEC is higher in rural areas, and it is recommended to decrease the demand for energy. Satish et al. [27] established a per capita energy balance for urban and rural households by analyzing the energy transition and requirement patterns in India. They divided the income into three types—high, medium, and low—and analyzed the relationship between energy and income, finding that cooking is one of the main energy demands. These results explain the difference between the urban and rural requirements of each energy option in India. Zi et al. [28] investigated the possibility of HEC and the purchase of energy-consuming products by analyzing the policy of clean energy transition in rural areas of Henan Province. It is believed that with the development of the economy, rural areas should implement an energy transition policy, and it is very necessary to increase the supply of clean energy.

1.2.1 Application of Passive Heating in Buildings

Research on passive heating design is mainly divided into three categories: The first is climate adaptation strategy research [29], mainly including reasonable orientation [30], the optimization of the envelope structure [31], appropriate window-to-wall ratio (WWR). and so on [32]. The second is the use of renewable energy in buildings, such as solar energy and geothermal energy [33]. The third is the study of Kang [34].

The research on building orientation mainly focuses on studying the relationship between different orientations, indoor temperature, and energy savings to find the most reasonable orientation for a building [35]. The research results of Wang et al. [36] show that in cold areas, the orientation of buildings is a factor in obtaining more solar radiation. Torreggiani et al. [37] showed that direction had an effect on indoor temperature through simulation calculation. Chi et al. [24] rotated traditional residential buildings clockwise by 20°. Through simulation calculation and comparisons of temperature, humidity, and lighting in 18 sets of data, the research results showed that the best angle was S and the worst angle was N-W80 for the whole year, and the difference in building electricity consumption between the two was 150 kWh. The research results show that a good orientation has the potential to save energy. The optimization research on envelope structures mainly focusses on improving the thermal performance of the wall structure, thereby improving the thermal comfort of human body and reducing carbon emissions. Liu et al. [38] conducted research on traditional houses and cave houses in northwest China, and their results showed that thick walls can effectively restrain changes in indoor temperature and keep the internal surface temperature of a wall stable. This research provides a scientific basis for reducing energy demand. Xu et al. [16] measured indoor temperature, humidity, and lighting data of brick and earth walls in winter and summer through field measurements of traditional houses with two types of walls in Qinba mountain. The results showed that houses with earth walls were more suitable for the local climate. For brick walls, they recommended using a variety of materials such as concrete, porous brick, and foam concrete to achieve a good thermal insulation performance and low cost. This study provides useful data for future research on folk houses. Research on appropriate WWRs mainly focuses on the influence of WWR on indoor temperature. Chi et al. [39] divided the WWR of traditional houses in Zhejiang into categories of 0.1–0.9 and calculated the indoor lighting, temperature, humidity, and wind speed through software simulation. The range of the three intersecting values is the best WWR. Obrecht et al. [40] studied the glazing ratio of glass facing different directions and concluded that using different glazing ratios in different areas can meet different cooling and heating requirements.

Through the energy-saving design of residential buildings, buildings can use renewable energy to improve their indoor temperatures, such as solar or geothermal energy [41]. Research on passive solar technology mainly comprises two parts: the influence of solar technology on indoor temperature and measures for the improvement of solar technology. Passive solar technology generally uses a combination of different types of glass and buildings to effectively increase indoor temperature, such as the roof of a greenhouse [42], the Trombe wall [43], and the solar chimney [44]. Cossu et al. [45] stated that the roof of a greenhouse mainly refers to the use of a glass device covering a roof to increase the solar radiation and contribute to indoor heat, thus affecting indoor temperature. Trombe walls are another passive solar technology [46]. From the perspective of reducing the dependence on energy and carbon emissions, Irshad et al. [47] proved that double-layer glass with argon gas can effectively improve indoor temperature when placed on a Trombe wall. By comparing the thermal performance of traditional and composite Trombe walls, Chen et al. [48] used the ANSYS software to simulate the calculation, and the research results showed that composite Trombe walls had a better thermal performance. Solar chimneys usually protrude from the roof and absorb solar energy to increase indoor temperature [49]. To obtain more solar radiation, in addition to the use of a glass chimney, one also needs to have a certain angle of tilt. Solar-powered chimneys alone can reduce electricity consumption by 10 to 20 percent per day [50]. Jing et al. [51] conducted a software simulation study on gaps between 0.2 and 0.6 when a solar chimney was used, and their research results showed that when the gap was 0.5, the airflow rate of flue gas had the best effect. In addition, this also showed that the improved scheme is more consistent with test results.

In addition to the passive heating technology mentioned above, Kang is one of the traditional heating methods used in northern China, Its working principle is using the heat generated by burning biomass to heat a bed, which can effectively improve the local thermal comfort of human body and reduce the demand for energy [52,53]. Similar heating methods have been used in the design of residential buildings in other developed countries, such as Ondol in South Korea and Hypocaus in ancient Rome [54,55]. Traditional Kang is one of the floor heating systems in northern China and first appeared in the Zhou Dynasty [56]. It is a rectangular platform composed of bricks, concrete, stone, and other materials. The cavity inside the platform is used as a flue, and the hot smoke generated by cooking utensils is used to add to heated Kang body. Traditional Kang consists of three parts: a stove, Kang body (similar to a bed), and a chimney [57]. A stove is a place where wood is burned [58]. The heat generated during the burning of biomass is used on the one hand for cooking and heating food, and on the other hand heat is added to Kang body by conveying heat [59]. Traditional Kang heating assembly is composed of two parts: Kang body and an internal flue. High-temperature flue gas enters Kang body, flows through the flue, and finally the flue gas leaves through the chimney. The setting of the flue resistance has a great impact on the flow of flue gas. The greater the flow resistance, the greater the heat conduction time of Kang will be [60]. The surface of Kang body absorbs the heat and raises the local temperature of human body through heat transfer processes such as convection and heat conduction [61]. In rural area of north China, 85% of families use Kang for heating in winter [62]. The research on Kang mainly covers three parts: the development of Kang, the evaluation of the thermal performance of Kang, and the joint application of Kang and other technologies. Yu et al. [63] discussed the development and classification of Kang in terms of cultural background and ethnic divisions; analyzed the composition, structure, flue, and thermal performance of Kang; and proposed a new optimized design. The research shows that Kang improves the local thermal comfort of human body; this creates the possibility of influencing indoor temperature and reducing indoor pollutants by optimizing heated Kang equipment. Wang et al. [64] studied and set up a heating wall, tested its thermal performance, and found that the heating wall could store 70% of the heat in a furnace. Through practical measurements and mathematical modeling, it was found that the two results were consistent. This study enhances our understanding of heating walls and provides a reference for rural residential heating design. Chen et al. [65] used a method involving combining solar heating technology and traditional Kang to improve indoor temperature through the investigation of three family houses in the northeast of China. Research results show that when using this technology, the temperature is evenly distributed in the vertical direction, but the initial investment needs to increase by about 10%.

At present, there are few researches on cooking heating walls, and they are just some simple introductions. It mainly includes what equipment is needed to adopt cooking heating wall technology. There are few references on the simulation analysis of the influence of cooking heating wall on indoor temperature.

1.2.2 Research on Passive Heating and Energy Saving Design

At present, the research on passive energy saving in buildings mainly includes three aspects: the first approach is to change the maintenance structure of the phase-change materials [66,67], the second is to effectively use renewable energy [68], and the third is to burn biomass [33]. Maryam et al. [66] studied the thermal properties of external walls in Morocco and compared and analyzed the thermal properties of different materials through the calculation of the four-bar method. The research results showed that the selection of hemp and cotton material can effectively reduce greenhouse gas emissions, with an average annual reduction of 30%. Ahmed et al. [69] built a mathematical model to calculate the heat gain value, economic cost, and sunshine conditions of different materials. By optimizing the objective function, the heat gain value of a building can be reduced by 34% and the daylighting situation can be increased by 11%, thereby effectively improving energy utilization. Ji et al. [70] believed that biochar can improve the damp and heat performance of buildings through the comparison of multiple groups of experiments. The thermal conductivity of biochar–mortar can be reduced by 57.6% and the water vapor resistance coefficient increased by 50.9% compared to the single mortar. The research results showed that the mortar exterior wall with biochar can improve the strength, heat, and humidity performance of mortar.

Facing the problem of increasing energy consumption in residential buildings, some experts believe that the effective use of solar energy has potential [71]. For nearly a decade, solar energy has been used to design energy-efficient residential buildings [72]. The research on the effective use of solar energy mainly includes the following two points: The first is to study the types of solar energy storage, such as glass boxes [73], Tromble walls [74], and solar spaces [75]. The second uses solar energy to reduce the energy consumption of buildings [76]. Hilliaho et al. [73] studied 156 different types of glass balconies in Finnish apartments in the 1970s. Five important factors affecting the design of glass balconies were summarized, including the airtightness of glass, the heat absorption coefficient, heat loss, and the building ventilation system. Simões et al. [77] combined solar energy with Trombe walls based on the Mediterranean climate type and used software to compute the energy performance of the system. The new system can reduce heating demand by 20%. Duan et al. [78] put phase-change materials into Tromble walls and compared the best combination of phase-change materials and Tromble walls in Beijing, Jiuquan, and Shenyang. The melting temperature and layer thickness of the material were 23 ℃ and 5 mm (Beijing, Jiuquan) and 21 ℃ and 5 mm (Shenyang), respectively. Li et al. [79] took cold rural areas as an example and compared solar space with solar space containing PCM shutters. The results showed that the solar space heating effect with PCM blinds is obvious, saving 5.27% energy. Barrencua et al. [80] combined solar space with a mechanical ventilation system, combined with software calculation and an experiment, and showed that the energy saving of this system is 38.48 $kWh \cdot m^{-2}$, with 58% in heating. Using solar energy has been proven to decrease the energy consumption of buildings. Mihalakakou et al. [81] conducted simulation calculations by setting different parameter values of the solar heating system to simulate the thermal performance and thermal environment of the winter and summer seasons. The results showed that a solar heating system is an effective heating system in cold seasons. Mottard et al. [82] studied an additional solar energy system and demonstrated the reliability of the model by comparing the calculation with the measured experimental data through the mathematical model. The additional solar energy system is effective at saving energy.

Satisfying the temperature of the human body by burning the heat generated by biomass is also a passive heating method [52]. This heating mode first appeared in the spring and autumn periods of China and has been handed down to this day, which is called a kang [53]. As of 2014, the main method in China for 174 million people in winter is heating on a kang [62,83]. A kang is mainly made of three parts: a body, stove, and chimney [84]. Stoves are generally used for burning firewood and cooking food [85]. In addition to heating food, the heat generated by burning biomass also heats the body through its inner cavity [59]. The hot smoke generated therein is then discharged to the outdoors by the chimney [60]. Heated kang is the use of the body to heat the local temperature of the human body, to meet the temperature of the human body rather than raise the temperature of the whole room [86]. The research on the heating performance of a kang can be divided into two aspects: the first is to put forward the reconstruction scheme of the body [87,64]; the second is the application of combining a kang with other technologies [65]. Zhuang et al. [88] used the heat flow method to simulate the heat transfer process of flue gas entering the body, focusing on analyzing the flue gas flow process to avoid energy waste caused by flue gas backflow. The use of a new type of flue can effectively avoid the backflow of flue gas. Zhao et al. [89] put forward a new system for solar heating kang, which has the advantage of collecting heat throughout the day. The indoor temperature can be increased by approximately 13 ℃, and the surface temperature of a kang can reach 26 ℃, which has a good heating effect. Wei et al. [90] combined a kang with a solar water collector, established a mathematical model, and determined that the water inlet temperature of a kang can reach 35–55 ℃.

1.2.3 Study on Passive Additional Sunlight

Passive solar buildings are typically designed to use solar radiation in winter to raise temperatures inside the building [91]. This process minimizes heat loss through maintenance of the structure and infiltration [92]. In summer, try to reduce the heat caused by solar radiation and indoor equipment cooling [93]. Without the use of mechanical equipment as the premise, completely rely on strengthening the shielding function of the building, through the architectural method, to achieve the purpose of comfortable indoor environment [94]. According to the collection of solar heat radiation, there are four main types: direct benefit type, heat storage wall type, sunlight type and roof pool type [95].

In the early stage of the related research of passive solar house with additional sunlight, it mainly focuses on theoretical research and field testing, and draws conclusions by combining various data simulation software [96]. Hu et al. [97] used the thermal performance dynamic simulation program to conduct sensitivity experiments on related parameters in the additional sunlight of traditional residential houses in Beijing and proposed that transparent glass should be used at the top and in the south for the design of solar houses through simulation results. The results show that 240mm wall has better thermal insulation effect than 370 wall, and the optimization strategy of external thermal insulation is better than internal thermal insulation is put forward. Zheng et al. [98] compiled the computer aided design software package, and calculated the optimization parameters of each region, mainly including the best Angle of heat collection wall is 90° with the ground, the smaller the depth of sunlight is conducive to building energy saving and warmth, the building public wall window should not be too small, 25% ~ 50% is the best. Jin teacher and others through the climate characteristics of cold region of northeast China, residential status, the villagers living habits such as factor analysis, the indoor thermal comfort of the influence in the region, and puts forward the northeast cold region of the farmhouse, winter indoor and suitable temperature for 15 ~ 18 ℃, problems such as the calculation of energy-saving for the region provides a theoretical basis [99]. Liu et al. [100] designed three types of solar houses in Daqing, namely direct benefit type, heat collection and storage wall type and additional sunlight interroom type. Thermal calculation by SLR method showed that the energy saving rates of the three solar houses were 0.66, 0.59 and 0.71 respectively. The results show that the direct benefit passive solar house can save 35077.06 yuan, and the recovery life is 3 years. Ji et al. [101] introduced the winter heat preservation measures of direct benefit type and accessory sunshine type in rural residential buildings in Shanxi province, and put forward improvement measures for the components that affect the heat loss in their use, which has positive significance for the promotion and use of rural residential buildings in Shanxi province. Wang et al. [102] selected the common additional sunlight compartment housing in Kangding area as the research object, and proved through the test method that the additional sunlight compartment has a positive effect on the indoor thermal comfort of adjacent rooms, and can maintain the stability of indoor temperature by setting heat storage walls. Zheng et al. [103] optimized the design of additional sunshine room in northern Shaanxi in terms of high heat consumption in winter and overheating in summer, providing a comfortable, efficient and healthy indoor environment for residents in northern Shaanxi, and promoting the promotion and application of additional sunshine room in this area.

At present, the research on additional sunlight is mainly based on the optimization of additional sunlight. By applying the additional sunlight room to the active system, Bai et al. [104] found that the heat collected by the additional sunlight room was not enough to be used as the active system, but it could preheat the HVAC system. Furthermore, the thermal effect of the system is compared with that of the traditional passive structure, and the economic evaluation of the active solar chamber is made. Through on-site investigation, Li et al. [105] put forward the conclusion that most of the existing residential buildings in Lhasa adopt passive solar house design spontaneously based on experience, so that the thermal environment in the area can hardly meet the thermal demand. Therefore, a thermal simulation calculation model is established to provide a design method for new residential buildings by analyzing the design elements of passive components. The research of Sun et al. [106] on passive solar ecological house is based on form design, residential layout and site planning, which has certain reference value for the study of the effect performance of solar energy. Based on software simulation, laboratory experiments and real investigation. Sun et al. [107] created a corresponding energy-saving technology system for rural residential buildings in cold regions, including shape control, residential planning and layout, etc. The applicability of the technology system in rural residential buildings in cold regions was verified on the basis of field tests of demonstration projects. Based on field research, scholar Han made an in-depth study of passive solar houses in rural areas in cold regions, and made comprehensive consideration of the enclosure structure system and planar form characteristics of rural houses, which further improved the living environment quality of rural houses and reduced heating energy consumption [108].

1.2.4 Comprehensive Review

To sum up, the previous research conclusions regarding passive building heating are as follows: Avoid outdoor cold air entering the room (cold enclosure) [109], encourage hot air to enter the room (cold conditioning) [110], and remove indoor local cold air (heat collection) [111]. Cold enclosures are mainly used to change the phase change material of the building envelope structure, affecting the thermal performance of the walls, roof, glass, and other building materials, so as to improve indoor temperature, but the cost is high. Cold conditioning is based on the greenhouse principle and adopts a solar passive design. The indoor temperature is completely determined by the amount of solar radiation entering the building. This method is more suitable for areas with sufficient solar radiation. A combination of solar energy and earth source heat pumps can be used, and equipment units are needed to realize this. Heat collection refers to the use of a fire Kang, but only for heating local parts of human body, rather than for increasing the overall indoor temperature. However, passive heating technology for traditional houses should not only consider the construction cost and effect, but also consider the production and lifestyle of local people.

Passive heating in the above three aspects has been proven to raise the indoor temperature and decrease the demand for energy, but there are still some problems. In the study of improving the phase-change material of enclosure structures, most buildings in rural areas are restricted by factors such as the building structure and cost, and it is difficult to improve the phase-change material of a maintenance structure. At the same time, phase-change materials only improve the process of heat transfer, not from the heat source; for all the research, there is still a lack of energy saving. In addition to considering the construction cost when using solar energy, it is also necessary to determine whether the weather influences the solar radiation on the indoor temperature. In terms of biomass combustion, a large amount of carbon will be produced during the combustion process, which will lead to environmental pollution. Therefore, proposing a cooking heating wall system with an additional sunlight room system, which can effectively raise the indoor thermal comfort in winter, can achieve energy saving.

1.3 Research Purpose

Through field research, it was found that traditional heating equipment such as hot coals, fire pits, and braziers can increase the local temperature in the room but cannot increase the overall indoor temperature to satisfy the needs of human body. In this study, a cooking heating wall system is proposed to improve indoor temperature and the effectiveness of the cooking heating wall equipment is confirmed using ANSYS software simulation. Its specific objectives are as follows:

- To investigate, with or without solar radiation on an external wall, the time required for the natural heating system to work, as well as the balanced temperature and the heating efficiency.
- To investigate, with or without solar radiation on an external wall, the time required for the cooking heating wall heating system to work, as well as the balanced temperature and the heating efficiency.
- To evaluate the appropriate time when the open cooking heating wall heating system can work throughout the year.
- To use the cooking heating wall heating system to increase indoor temperature in an effective timeframe. To investigate the annual heat load reduction outside a wall with or without solar radiation in two cases.
- To optimize the passive design of traditional houses to provide a reference for the design of rural houses in the future.

For increasing the indoor temperature of residences and reducing the heat load of the building, this research proposes a passive heating system between a cooking heating wall and an additional sunlight room. Based on the model, the new system was added for comparison with traditional residential buildings in various aspects. The specific research objectives were as follows:

- By comparing the heating conditions of traditional residential buildings with or without the new passive system, the heat load reduction when adopting the new system in winter was estimated.
- In the absence of solar radiation, the heating effects of the ordinary heating system and the new passive system were analyzed. The purpose was to calculate the heating rate, the time required, and the decrease in the annual heat load of the building.
- Considering the presence or absence of solar radiation, the new system was compared to the ordinary heating of residential buildings to simulate and calculate the change in indoor temperature, heating efficiency, heating time, and the value of the annual building heat load.
- Through software simulation computation, the appropriate use time of the whole year after adopting the new system was estimated.
- According to the standard minimum value of indoor thermal comfort temperature, under basic heating, the total time to meet the minimum value of the comfort standard throughout the year was calculated. Compared to the use of the new system with or without solar radiation, the total time to meet the lowest value of the comfort standard throughout the year was estimated.

1.4 Scientific Originality

Under the influence of the subtropical continental monsoon climate in southern Shaanxi, traditional houses feel wet and cold indoors in winter. Most traditional houses are ancient and limited by their construction technology and materials, as there was little consideration for heating measures at the beginning of the design process. To improve indoor temperatures, people use heating equipment such as charcoal, fire ponds, and braziers. However, these types of heating equipment can only improve the indoor local temperature and cannot improve indoor temperature. A passive cooking heating wall heating system is proposed that uses the heat storage capacity of a wall to store the heat generated by smoke when cooking and then release stored heat into the room so as to enhance indoor temperature.

This kind of heating equipment has three characteristics: cold conditioning, cold enclosure, and heat collection. Cold conditioning is when the heat from cooking heats aluminum tubes inside the walls. Cold enclosure refers to the heat generated by the aluminum tube, which heats the wall, and the wall stores the heat. Heat collection refers to the heat generated by heating the wall, which increases the temperature of the room through thermal radiation and convection. The heating effect completely depends on the heat generated by cooking and does not rely on any mechanical equipment. The increase in the indoor temperature relies on heat radiation and heat convection. Therefore, the heating system does not need any power and is a completely passive heating system. This system is suitable for vast rural areas where the winters are relatively humid and cold. In previous passive heating design research, fewer factors were considered, with the influence of heating technology on indoor temperature being the main aspect analyzed. In this paper, in addition to the heating technology, the influence of solar radiation on indoor temperature is also considered.

In previous studies, a new passive heating design strategy for rural residential buildings has been proposed, combining the characteristics of cooking and heating methods, and studying the basic working principles of cooking heating wall and energy saving [112]. Based on this principle, this research added new heating equipment, combined the cooking cooking heating wall system with solar energy technology, and comprehensively analyzed the heating time, effect, and energy saving.

First of all, in previous research, the time for cooking and heating and the heat transfer of the wall have been analyzed and discussed. The main purpose was to extend the thermal time and improve the heating effect. The specific method was based on the cooking heating wall cooking and heating system, and a glass sun room was built in conjunction with the kitchen on the sunny side of the building. Its function is to collect the heat generated from cooking and prevent the accelerated loss of hot air in the room. The principle is that the hot air is stored in the glass sunlight room through the heat transfer of the wall, while preventing direct contact between the hot air and the outdoor cold air, causing the indoor temperature to drop rapidly, similarly to the design principle of a thermos cup.

Second, the use of the greenhouse effect makes the internal temperature of the glass sunlight room increase when receiving solar radiation and keeps the temperature constant. The principle is that the airtight space between sunlight forms a heat preservation effect due to the lack of heat exchange with the outside, so as to achieve the effect of heating and heat preservation. At the same time, it can also make up for the discontinuity of cooking and heating in time. On the basis of whether the wall has solar radiation as a separate reference, systematic analysis and research on whether the new system takes this factor into consideration was carried out, which verifies the importance of whether the wall has solar radiation for winter heating.

Finally, compared to a separate cooking and heating system, the new system also has functions such as building wall insulation and the greenhouse effect of the glass sun room. In essence, this study used completely passive heating technology. The results showed a greater reduction in the heat load of the building compared to previous research, as well as an improvement in the heating effect to a new level. This makes up for the blank passive comprehensive energy-saving design in rural residence.

1.5 Research Framework

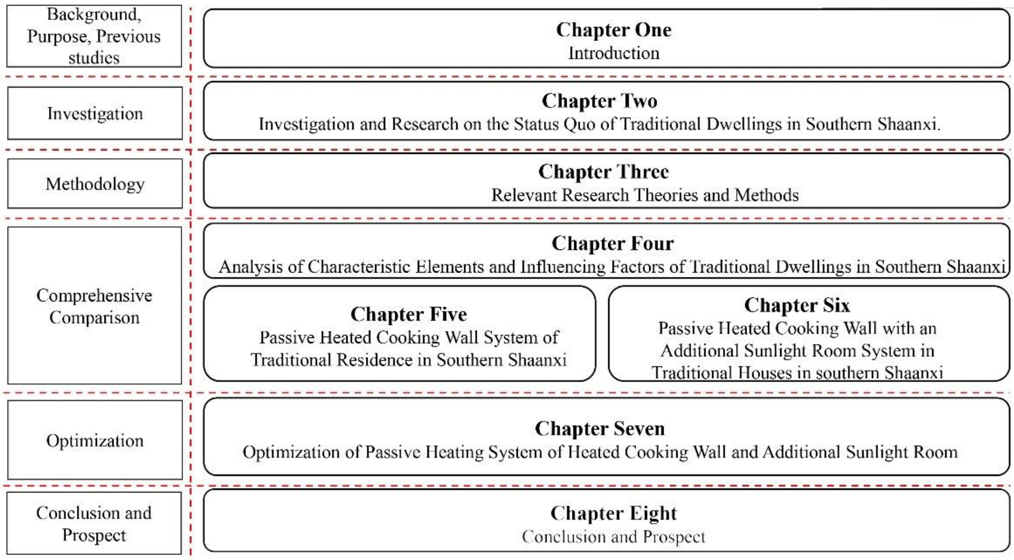

Figure 1-4. Research framework.

1.6 Chapter Summary

This chapter mainly introduces the research background, research purpose and research innovation. This paper reviews the application of passive heating in architecture, passive heating and energy saving design, and passive additional sunlight. Through the analysis of the references, the passive heating technology is summarized. Combined with research methods and research objectives, this paper tries to solve the passive winter heating of traditional residential houses in southern Shaanxi. It is found that there are some problems in heating and energy saving in traditional residential houses, and the rational application of passive heating technology in traditional residential houses in southern Shaanxi is explored.

References

[1] Luo, Y.; Zeng, W.; Wang, Y.; Li, D.; Hu, X.; Hua, Z. A hybrid approach for examining the drivers of energy consumption in Shanghai. Renew. Sustain. Energy Rev. 2021, 151, 111571.

[2] IEA. IEA Online Data Services. Available online: https://www.iea.org/subscribe-to-data-services/world-energy-balances-and-statistics (accessed on 4 August 2021).

[3] China Association of Building Energy Efficiency. 2018 China building energy research report. Available online: https://www.cabee.org/site/term/107.html (accessed on 4 August 2021).

[4] Mi, Z.; Zheng, J.; Meng, J.; Shan, Y.; Zheng, H.; Ou, J.; Guan, D.; Wei, Y.-M. China's Energy Consumption in the New Normal. Earths Future 2018, 6, 1007–1016.

[5] China Association of Building Energy Efficiency. 2016 China Building Energy Research Report. Available online: https://www.efchina.org/Attachments/Report/report-20170710-1/report-20170710-1(accessed on 4 August 2021).

[6] Liu, C.; Xu, W.; Li, A.; Sun, D.; Huo, H. Energy balance evaluation and optimization of photovoltaic systems for zero energy residential buildings in different climate zones of China. J. Clean. Prod. 2019, 235, 1202–1215.

[7] Neupane, D.; Kafle, S.; Kaji, R.K.; Dae, H.K.; Pradhan, P. Solar and wind energy potential assessment at provincial level in Nepal: Geospatial and economic analysis. Renew. Energy 2022, 181, 278–291.

[8] Yuan, Y.; Xu, T.; Jiang, Z.; Feng, B. Prospects of power generation from the deep fractured geothermal reservoir using a novel vertical well system in the Yangbajing geothermal field, China. Energy Rep. 2021, 7, 4733–4746.

[9] Rauf, H.; Muhammad, S.G.; Arshad, N. Complementing hydroelectric power with floating solar PV for daytime peak electricity demand. Renew. Energy 2020, 162, 1227–1242.

[10] Liu, Z.; Liu, Y.; He, B.-J.; Xu, W.; Jin, G.; Zhang, X. Application and suitability analysis of the key technologies in nearly zero energy buildings in China. Renew. Sustain. Energy Rev. 2019, 101, 329–345.

[11] Siwei, L.; Yu Joe, H. Energy conservation standard for space heating in Chinese urban residential buildings. Energy 1993, 18, 871–892.

[12] Fallmann, J.; Emeis, S. How to bring urban and global climate studies together with urban planning and architecture? Dev. Built Environ. 2020, 4, 2666–1659.

[13] Barros, P.; Linda, N.F.; Garcia, L.M.T.; Anne, D.S.; Thomopoulos, N.; Thiago, H.S.; Morais, P.; Mindell, J.S. Social consequences and mental health outcomes of living in high-rise residential buildings and the influence of planning, urban design and architectural decisions: A systematic review. Cities 2019, 93, 263–272.

[14] Fu, J.; Zhou, J.; Deng, Y. Heritage values of ancient vernacular residences in traditional villages in Western Hunan, China: Spatial patterns and influencing factors. Build. Environ. 2021, 188, 107473.

[15] Surasit, T.; Tuan, A.D.; Pana, S.; Mona, Y. Energy reduction of split-type air conditioners using a pre-cooling system for the condenser. Energy Rep. 2021, 7, 1–6.

[16] Juan, X.; Ziliang, L.; Weijun, G.; Mengsheng, Y.; Menglong, S. The comparative study on the climate adaptability based on indoor physical environment of traditional dwelling in Qinba mountainous areas, China. Energy Build. 2019, 197, 140–155.

[17] Zhou, D.; Li, Z.; Wang, S.; Tian, Y.; Zhang, Y.; Jiang, G. How does the newly urban residential built-up density differ across Chinese cities under rapid urban expansion? Evidence from residential FAR and statistical data from 2007 to 2016. Land Use Policy 2021, 104, 105365.

[18] Chi, F.; Borys, I.; Jin, L.; Zhu, Z.; Bart, D. The strategies and effectiveness of climate adaptation for the thousand pillars dwelling based on passive elements and passive spaces. Energy Build. 2019, 183, 17–44.

[19] National Bureau of Statistics. Report on Residential Floor Area Per Capita. Available online: http://www.stats.gov.cn/tjsj/sjjd/202007/t20200727_1778643.html (accessed on 4 August 2021).

[20] Ding, J.; Ma, S. Comparative analysis of habitation behavioral patterns in spatial configuration of traditional houses in Anhui, Jiangsu, and Zhejiang provinces of China. Front. Archit. Res. 2020, 9, 54–66.

[21] He, B.-j.; Yang, L.; Ye, M.; Mou, B.; Zhou, Y. Overview of rural building energy efficiency in China. Energy Policy 2014, 69, 385–396.

[22] Ignjatovi´c, D.; Jovanovi´c Popovi´c, M.; Kavran, J. Application of sunspaces in fostering energy efficiency and economical viability of residential buildings in Serbia. Energy Build. 2015, 98, 3–9.

[23] Ismail, K.A.R.; Salinas, C.T.; Henriquez, J.R. Comparison between PCM filled glass windows and absorbing gas filled windows. Energy Build. 2008, 40, 710–719.

[24] Chi, F.a.; Zhang, J.; Li, G.; Zhu, Z.; Bart, D. An investigation of the impact of Building Azimuth on energy consumption in sizhai traditional houses. Energy 2019, 180, 594–614.

[25] Acheampong, A.O., Boateng, E., Amponsah, M., Dzator, J. Revisiting the economic growth–energy consumption nexus: Does globalization matter? Energy Econ. 2021, 102, 105472.

[26] Wang, S.; Sun, S.; Zhao, E.; Wang, S.; Urban and rural differences with regional assessment of household energy consumption in China. Energy 2021, 232, 121091.

[27] Yawale, S.K.; Hanaoka, T.; Kapshe, M. Development of energy balance table for rural and urban households and evaluation of energy consumption in Indian states. Renew. Sustain. Energy Rev. 2021, 136, 110392.

[28] Zi, C.; Qian, M.; Baozhong, G. The consumption patterns and determining factors of rural household energy: A case study of Henan Province in China. Renew. Sustain. Energy Rev. 2021, 146, 111142.

[29] Zhao, X.; Nie, P.; Zhu, J.; Tong, L.; Liu, Y. Evaluation of thermal environments for cliff-side cave houses in cold region of China. Renewable Energy 2020, 158, 154-166.

[30] Morrissey, J.; Moore, T.; Horne, R.E. Affordable passive solar design in a temperate climate: an experiment in residential building orientation. Renew Energy 2011, 36, 568-577.

[31] Zhu, X.; Liu, J.; Yang, L.; Hu, R. Energy performance of a new Yao dong dwelling, in the Loess Plateau of China. Energy and Buildings 2014, 70, 159-166.

[32] Wen, L.; Hiyama, K.; Koganei, M. A method for creating maps of recommended window-to-wall ratios to assign appropriate default values in design performance modeling: A case study of a typical office building in Japan. Energy and Buildings 2017, 145, 304-317.

[33] Liu, Y.W.; Feng, W. Integrating passive cooling and solar techniques into the existing building in South China. In: 4th international conference on technology of architecture and structure (ICTAS 2011). pp. 3717–3720.

[34] Zhai, Z.; Yates, A.P.; Duanmu, L.; Wang, Z. An evaluation and model of the Chinese Kang system to improve indoor thermal comfort in northeast rural China – Part-1: Model development. Renewable Energy 2015, 84, 3-11.

[35] Abanda, F.H.; Byers, L. An investigation of the impact of building orientation on energy consumption in a domestic building using emerging BIM (Building Information Modelling). Energy 2016, 97, 517-527.

[36] Fan, Q.; Wong, K.d. Building information modelling (BIM) for sustainable building design. Facilities 2013, 31, 138-157.

[37] Torreggiani, D.; Barbaresi, A.; Dallacasa, F.; Tassinari, P. Effects of different architectural solutions on the thermal behaviour in an unconditioned rural building. The case of an Italian winery. Journal of Agricultural Engineering 2018, 49, 52-63.

[38] Liu, J.; Wang, L.; Yoshino, Y.; Liu, Y. The thermal mechanism of warm in winter and cool in summer in China traditional vernacular houses. Building and Environment 2011, 46, 1709-1715.

[39] Chi, F.a.; Wang, Y.; Wang, R.; Li, G.; Peng, C. An investigation of optimal window-to-wall ratio based on changes in building orientations for traditional houses. Solar Energy 2020, 195, 64-81.

[40] Potrč Obrecht, T.; Premrov, M.; Žegarac Leskovar, V. Influence of the orientation on the optimal glazing size for passive houses in different European climates (for non-cardinal directions). Solar Energy 2019, 189, 15-25.

[41] Al-Shahri, O.A.; Ismail, F.B.; Hannan, M.A.; Lipu, M.S.H.; Al-Shetwi, A.Q.; Begum, R.A.; Al-Muhsen, N.F.O.; Soujeri, E. Solar photovoltaic energy optimization methods, challenges and issues: A comprehensive Review. Journal of Cleaner Pro-duction 2021, 284, 0959-6526.

[42] Fiaschi, D.; Bertolli, A. Design and energy analysis of solar roofs: a viable solution with esthetic appeal to collect solar heat. Renewable Energy 2012, 46, 60–71.

[43] Hami, K.; Draoui, B.; Hami, O. The thermal performances of a solar wall. Energy 2012, 39, 11–6.

[44] Zhai, X.Q.; Song, Z.P.; Wang, R.Z. A review for the applications of solar chimneys in buildings. Renewable and Sustainable Energy Reviews 2011, 15, 3757–3767.

[45] Cossu, M.; Yano, A.; Li, Z.; Onoe, M.; Nakamura, H.; Matsumoto, T.; Nakata, J. Advances on the semi-transparent modules based on micro solar cells: first integration in a greenhouse system. Applied Energy 2016, 162, 1042–1051.

[46] Briga-Sá, A.; Martins, A.; Boaventura-Cunha, J.; Lanzinha, J.C.; Paiva, A. Energy performance of Trombe walls: adaptation of ISO 13790:2008(E) to the Portuguese reality. Energy and Buildings 2014, 74, 111–119.

[47] Irshad, K.; Habib, K.; Thirumalaiswamy, N. Energy and cost analysis of photo voltaic Trombe wall system in tropical cli-mate. Energy Procedia 2014, 50, 71–78.

[48] Shen, J.; Lassue, S.; Zalewski, L.; Huang, D. Numerical study of classical and composite solar walls by TRNSYS. Journal of Thermal Science 2007, 16, 46–55.

[49] Lal, S.; Kaushik, S.; Bhargav, P. Solar chimney: a sustainable approach for ventilation and building space conditioning. International Journal of Development and Sustainability 2013, 2, 277-279.

[50] Khedari, J.; Rachapradit, N.; Hirunlabh, J. Field study of performance of solar chimney with air-conditioned building. Energy 2003, 28, 1099–1140.

[51] Jing, H.; Chen, Z.; Li, A. Experimental study of the prediction of the ventilation flow rate through solar chimney with large gap-to-height ratios. Building and Environment 2015, 89, 150-159.

[52] Li, G.; Bi, X.; Feng, G.; Chi, L.; Zheng, X.; Liu, X. Phase change material Chinese Kang: Design and experimental performance study. Renewable Energy 2020, 150, 821-830.

[53] Men, R. Origin of everything; China Economy Press: Beijing, China, 2004.

[54] Yeo, M.-S.; Yang, I.-H.; Kim, K.-W. Historical changes and recent energy saving potential of residential heating in Korea. Energy and Buildings 2003, 35, 715-727.

[55] Forbes, R.J. Studies in ancient technology; Brill Archive: Netherlands, 1957; Volume 1.

[56] Zhuang, Z.; Li, Y.; Chen, B.; Guo, J. Chinese kang as a domestic heating system in rural northern China—A review. Energy and Buildings 2009, 41, 111-119.

[57] Ayres de Mello, L.; Moura, L.M.; Mendes, N. A model for assessment of heat and moisture transfer through hollow porous buildings elements. Case Studies in Thermal Engineering 2019, 14, 100446.

[58] Wang, J.; Lou, H.H.; Yang, F.; Cheng, F. Development and performance evaluation of a clean-burning stove, Journal of Cleaner Production 2016, 134, 447-455.

[59] Zhang, H.; Chen, Y.; Rui, J.; Yoshino, H.; Zhang, J.; Chen, X.; Liu, J. Effects of thermal environment on elderly in urban and rural houses during heating season in a severe cold region of China, Energy and Buildings 2019,198, 61-74.

[60] Niu, H.-F.; Wei, L.-J.; Yu, J.-P.; Lian, Z.; Zhao, J.; Wu, Z.-Z.; Liu, J.-T. Is adjuvant chemotherapy necessary for patients with microinvasive breast cancer after surgery? Cancer biology & medicine 2016, 13, 142.

[61] Gao, X.; Liu, J.; Hu, R.; Akashi, Y.; Sumiyoshi, D. A simplified model for dynamic analysis of the indoor thermal environ-ment of rooms with a Chinese kang. Building and Environment 2017, 111, 265-278.

[62] Cao, G.; Jokisalo, J.; Feng, G.; Duanmu, L.; Vuolle, M.; Kurnitski, J. Simulation of the heating performance of the Kang system in one Chinese detached house using biomass. Energy and Buildings 2011, 43, 189-199.

[63] Yu, K.; Tan, Y.; Zhang, T.; Zhang, J.; Wang, X. The traditional Chinese kang and its improvement: A review. Energy and Buildings 2020, 218, 110051.

[64] Wang, P.; Yang, M.; Yang, X.; Shan, M. Thermal performance of a traditional Chinese heated wall with the in-series flow pass: Experiment and modeling. Energy and Buildings 2014, 84, 46-54.

[65] Chen, B.; Zhuang, Z.; Chen, X.; Jia, X. Field survey on indoor thermal environment of rural residences with coupled Chinese kang and passive solar collecting wall heating in Northeast China. Solar Energy 2007, 81, 781-790.

[66] Dlimi, M.; Iken, O.; Agounoun, R.; Kadiri, I.; Sbai, K. Dynamic assessment of the thermal performance of hemp wool insu-lated external building walls according to the Moroccan climatic zoning. J. Energy Storage 2019, 26, 101007.

[67] Fumo, N.; Mago, P.; Luck, R. Methodology to estimate building energy consumption using EnergyPlus Benchmark Models. Energy Build. 2010, 42, 2331–2337.

[68] Al-Shahri, O.A.; Ismail, F.B.; Hannan, M.A.; Lipu, M.S.H.; Al-Shetwi, A.Q.; Begum, R.A.; Al-Muhsen, N.F.O.; Soujeri, E. Solar photovoltaic energy optimization methods, challenges and issues: A comprehensive Review. J. Clean. Prod. 2021, 284, 125465.

[69] Ahmed, W.A.; Hammad, F.K.; Rosa, A.C.; Vazquez, E.; Haddad, A. Enhancing the passive design of buildings: A mixed integer non-linear programming approach for the selection of building materials and construction building systems. Energy Rep. 2021, 458, 2352–4847.

[70] Ji, H.; Kim, Y.; Jeon, J.; Yun, B.; Kang, Y.; Kim, S. Analysis of biochar-mortar composite as a humidity control material to improve the building energy and hygrothermal performance. Sci. Total Environ. 2021, 775, 145552.

[71] Ma, L.; Zhang, X.; Li, D.; Arıcı, M.; Yıldız, Ç.; Li, Q.; Zhang, S.; Jiang, W. Influence of sunspace on energy consumption of rural residential buildings. Sol. Energy 2020, 211, 336–344.

[72] Harkouss, F.; Fardoun, F.; Biwole, P.H. Passive design optimization of low energy buildings in different climates. Energy 2018, 165, 591–613.

[73] Hilliaho, K.; Makitalo, E.; Lahdensivu, J. Energy saving potential of glazed space: Sensitivity analysis. Energy Build. 2015, 99, 87–97.

[74] Kim, T.; Ahn, S.; Leigh, S.-B. Energy consumption analysis of a residential building with phase change materials under various cooling and heating conditions. Indoor Built Environ. 2014, 23, 730–741.

[75] Wang, W.; Li, C.; Li, Y.-Z.; Yuan, M. A novel on-top inverse sunspace conception and the passive heating effects on a typical northern China rural house. Indoor Built Environ. 2019, 28, 1406–1421.

[76] Girard, A.; Muneer, T.; Caceres, G. A validated design simulation tool for passive solar space heating: Results from a monitored house in West Lothian, Scotland. Indoor Built Environ. 2014, 23, 353–372.

[77] Simões, N.; Manaia, M.; Simões, I. Energy performance of solar and Trombe walls in Mediterranean climates. Energy 2021, 234, 121197.

[78] Duan, S.; Li, H.; Zhao, Z.; Wang, L. Investigation on heating performance of an integrated phase change material Trombe wall based on state space method. J. Energy Storage 2021, 38, 102460.

[79] Li, Q.; Wang, Y.; Ma, L.; Arıcı, M.; Li, D.; Yıldız, Ç.; Zhu, Y. Effect of sunspace and PCM louver combination on the energy saving of rural residences: Case study in a severe cold region of China. Sustain. Energy Technol. Assess. 2021, 45, 101126.

[80] Barrencua, J.G.; Maritorena, M.O.; Minguillon, R.H.; Arriaran, I.G. Energy savings using sunspaces to preheat ventilation intake air: Experimental and simulation study. J. Build. Eng. 2021, 40, 102343.

[81] Mihalakakou, G.; Ferrante, A. Energy conservation and potential of a sunspace: Sensitivity analysis. Energy Convers. Manag. 2000, 41, 1247–1264.

[82] Mottard, J.M.; Fissore, A. Thermal simulation of an attached sunspace and its experimental validation. Sol. Energy 2007, 81, 305–315.

[83] Zhuang, Z.; Li, Y.; Chen, B. Simulation and analysis of the thermal process in a house with an elevated Chinese kang heating system. HV&AC 2009, 12, 96–98.

[84] Ayres de Mello, L.; Moura, L.M.; Mendes, N. A model for assessment of heat and moisture transfer through hollow porous buildings elements. Case Stud. Therm. Eng. 2019, 14, 100446.

[85] Wang, J.; Lou, H.; Yang, F.; Cheng, F. Development and performance evaluation of a clean-burning stove. J. Clean. Prod. 2016, 134, 447–455.

[86] Yu, K.; Tan, Y.; Zhang, T.; Zhang, J.; Wang, X. The traditional Chinese kang and its improvement: A review. Energy Build. 2020, 218, 110051.

[87] Bian, M. Numerical simulation research on heat transfer characteristics of a Chinese kang. Case Stud. Therm. Eng. 2021, 25, 100922.

[88] Zhuang, Z.; Li, Y.; Chen, B. Thermal storage performance analysis on Chinese kangs. Energy Build. 2009, 41, 452–459.

[89] Zhao, D.; Ji, J.; Yu, H.; Wei, W.; Zheng, H. Numerical and experimental study of a combined solar Chinese kang and solar air heating system based on Qinghai demonstration building. Energy Build. 2017, 143, 61–70.

[90] Wei, H.; Jiang, Q.Y., Ji, J.; Wei, W. A study on thermal performance, thermal comfort in sleeping environment and solar energy contribution of solar Chinese Kang. Energy Build. 2013, 58, 66–75.

[91] Michaelj Cr. The passive solar design and construction handbook. Steven Winter Associates. 1997, 16-18.

[92] Swisher, J.N. Measured performance of 50 passive solar residences in the United States. Proceedings of NPSC. 1983, 5.

[93] Bakos, G.C. Electrical energy saving in a passive-solar-heated residence using a direct gain attached sunspace. Energy and Buildings. 2003, 35, 147-151.

[94] Ana, S.O.; Aurora, M.B.; Silvia, D.I. Design and experimental study of an industrialized sunspace with solar heat storage. Energy and Buildings. 2014, 806, 231-246.

[95] DePt, U.S. Passive Solar Design Handbook, Volley. 1980, 19-27.

[96] Wang, D.; Wu, S.; Xi, W. Mathematical model and simulation program of passive solar heating room I. Direct benefit type and heat collection wall type PSHDC (part 1). Journal of Gansu Science. 1990, 2 1.

[97] Hu, J.; LU, W.; Zheng, M. Sensitivity analysis of solar chamber with additional sunlight. Acta Heliotica Sinica. 1989, 1, 64-69.

[98] Zheng, R.; Lu, B.; Wang D. Optimization design technology of passive solar heating building. Architecture Science. 1997, 1, 10-15.

[99] Jin, H.; Zhao, H.; Wang, X. Study on indoor thermal comfort environment of rural houses in winter in cold region. Ha Journal of Erbin University of Technology. 2006, 38, 2108-2111.

[100] Liu, X.; li, Y.; Ma, C. Comparative analysis of three types of passive solar houses in daqing area. Energy Conservation Technology. 2007, 25, 334-336, 377.

[101] Ji, X.R.; Du, J.F.; Shen, T. Application of passive solar energy in rural residential buildings in Shanxi Province. Building Energy Conservation. 2013, 5, 39-40, 44.

[102] Wang, Q.Q.; He, Q.; Yang, L. Thermal environment test of inter-house with additional sunlight in winter in Kangding area. Construction Building Energy Conservation. 2015, 9, 89-92.

[103] Zheng, H.; Yang, H.; Wu, W. Optimization design of Additional sunlight interval in Northern Shaanxi. Journal of Yan 'an University (Natural Science Edition). 2016, 35, 100-102.

[104] Bai, S. Research on Thermal Performance Analysis Method of Passive Heating Building. Dalian University of Technology. 2011.

[105] Li, En.; Yang, L.; Liu, J. Research on passive optimal design of Residential buildings with additional sunlight in Lhasa. Journal of Xi 'an university of Architecture and Technology (natural science edition). 2016, 48, 258-264.

[106] Sun, C.; Han, Y. Theoretical research on building digital energy saving Design based on Green Performance. Architectural Journal. 2016, 11, 89-93.

[107] Sun, C.; Han, Y. Study on energy-saving design of office building form in cold region considering photothermal performance. Architectural Journal. 2016, 38-42.

[108] Han, Y. Research on the Method of building Form Generation Based on the Influence of Sunshine and Wind Environment. Harbin Institute of Technology Science. 2013.

[109] Sangma, S.; Tripura, D.D. Experimental study on shrinkage behavior of earth walling materials with fibers and stabilizer for cob building. Construction and Building Materials 2020, 256, 119449.

[110] Rabani, M.; Kalantar, V.; Dehghan, A.A.; Faghih, A.K. Experimental study of the heating performance of a Trombe wall with a new design. Solar Energy 2015, 118, 359-374.

[111] Li, A.; Gao, X.; Yang, L. Field measurements, assessments and improvement of Kang: Case study in rural northwest China. Energy and Buildings 2016, 111, 497-506.

[112] Yang, S.; Bart, D.; Chen, S. Study on the Passive Heating System of a Cooking Heating Wall in Dwellings: A Case Study of Traditional Dwellings in Southern Shaanxi, China. Int. J. Environ. Res. Public Health 2021, 18, 3745.

Chapter 2. Investigation and Research on traditional Houses in southern Shaanxi.

2.1 General Situation of Southern Shaanxi

2.1.1 Geographical Location

As is shown in figure 2-1 a, the southern Shaanxi region is located in the south of Shaanxi province, including Hanzhong, Ankang and Shangluo [1]. As is shown in figure 2-1 b, Shaanxi is bordered by the Qinling Mountains to the north and the Bashan Mountains to the south, and the Han River flows from west to east [2]. The region is bordered by Henan province to the east, Gansu province to the west, and Sichuan province, Chongqing Municipality and Hubei province to the south. Due to the qinling Mountains in the north and daba Mountain in the south, its topography is mainly mountainous and hilly [3].

The landform of southern Shaanxi is characterized by "two mountains sandwiching a river", namely the Qinling Mountains in the north and the Dabashan mountains in the south. "Yi Chuan" is the central Han River Valley and danjiang plain composed of plain area [4]. The river systems in southern Shaanxi are mainly composed of the Han River, jialing River and Danjiang river [5]. The Qinling Mountains run east-west, with the main body of the mountains above 3000 meters above sea level [6]. The terrain in the region is complex and the vertical landscape is distributed significantly [7]. Bashan mountain is northwest - southeast trend, karst landform development, average elevation of 2000 meters. The Hanjiang River flows through Hanzhong and Ankang from Ningqiang to Hubei, constituting the largest tributary of the middle reaches of the Yangtze River. Danjiang, a tributary of the Han River in the east, enters Hubei province from Shangluo [8].

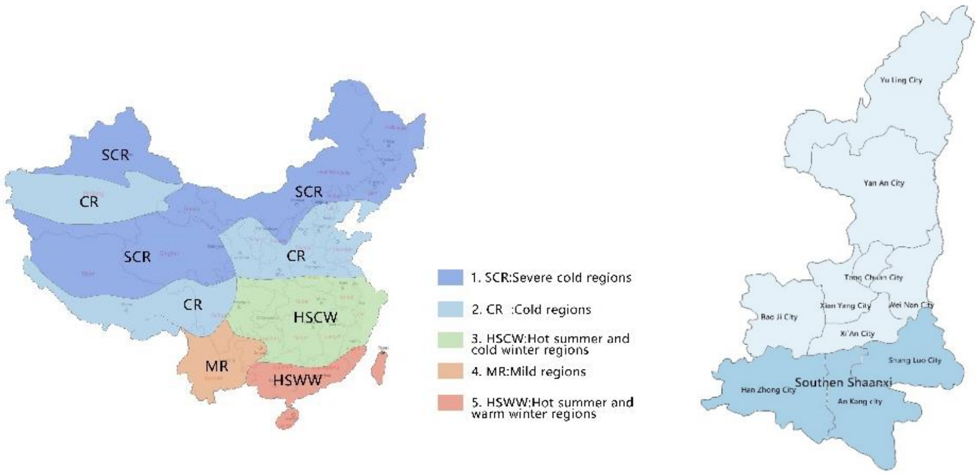

(a) (b)

Figure 2-1. (a) China climate zone map; (b) Location map of Southern Shaanxi.

2.1.2 Climatic Conditions

The geographical coordinates of southern Shaanxi region are 31°42 "~34°25 '40" north latitude and 105°30' 30 "~111°1 '25" East longitude [9]. The region has a subtropical continental monsoon climate with four distinct seasons, abundant rainfall in summer and mild and little rainfall in winter [10]. In terms of building thermal design division, it belongs to the region with hot summer and cold winter, mild climate, and the average temperature in January is above 0℃ [11]. The annual frost-free period is long, with an average of 253 days/year. The annual average temperature is 15℃, including the average temperature of 3℃-4℃ in January and 22℃-26℃ in July [12]. The average sunshine duration is 1610 hours/year, and the annual total radiation is 106 kcal/cm^2. It is rainy from July to September every year in southern Shaanxi, with an annual rainfall of 840-900mm [13]. The climate is humid and the rainfall is abundant [14]. The average number of rainfall days in Ankang is 94 days per year, with a maximum of 145 days and a minimum of 68 days. Extreme annual maximum rainfall 1240mm, extreme annual minimum rainfall 450mm (Table 2-1).

Table 2-1. Climatic conditions in southern Shaanxi.

Region	Annual mean temperature (℃)	Average annual sunshine hours (H)	Mean annual precipitation (mm)	Altitude (m)
Shang luo	11-14	1874-2124	706-845	215.4-2802.1
An kang	12-15.7	1495-1840	700-1280	170-2964.6
Han zhong	10.6-19.2	1273-2031	598-1463	371.2-2610

2.1.3 Topography and Landform

Shaanxi province is located in the inland hinterland of northwest China [15]. In terms of natural regionalization, shaanxi province straddles north and south due to the Qinling-Huaihe River line, and straddles the middle of the Yellow River and Yangtze River basins. Southern Shaanxi is located between the Qinling mountains and bashan Mountains in the south of Shaanxi Province [16]. There are various landforms in southern Shaanxi, including mountains, flat dams and hills, but they are mainly mountainous. However, compared with Ankang Basin, Hanzhong Basin is flat and open in terms of terrain [17]. Ankang Basin is small and has large topographic fluctuations and narrow space. This difference in terrain also affects the form of villages.

2.2 Cultural Inheritance and Historical Development of Traditional Houses in Southern Shaanxi

2.2.1 Cultural Inheritance of Folk Houses in Southern Shaanxi

(1) Qin and Jingchu Cultures

As is shown in figure 2-2, qin culture is an important part of Chinese culture with a long history. The qin culture mainly inherited the culture of the Western Zhou Dynasty, and at the same time, the Qin culture also constantly improved the continuation of the culture of its ancestors in the process of historical development [18]. The wooden frame that uses carry beam type is more. The style of the building has been generated, and the composition is neat and symmetrical throughout [18]. The sculpture and decoration of the courtyard building are various and the colors are also bright. Jingchu culture mainly refers to the ancient Jingchu culture in Hubei province [18].

Jingchu architecture is mainly dry architecture, it is also the main form of chu architecture, and the integration of nature, fully embodies the concept of "unity of nature and man" [19]. The ground floor of a dry building is usually treated on stilts to enhance air circulation and protect against moisture [20]. The second floor is for living. Because of the rich wood resources in Jingchu area, the whole building is mostly made of bamboo and wood [21].

(2) Bashu Cultures

Bashu culture is also an important part of Chinese culture and a regional culture in Sichuan Basin [22]. It mainly covers sichuan, Chongqing and Hanzhong in southern Shaanxi. Because there are many mountainous areas in Sichuan and Chongqing, the terrain is skillfully used in the construction of residential buildings, which is well combined with the natural environment [23]. Most of the residential buildings in Sichuan are built near mountains and rivers, and the buildings behind are higher than those in front, which is suitable for the terrain [24]. Due to the limitations of the terrain, the layout of the building is relatively flexible and free, and the houses have an obvious central axis [25]. Stilted buildings are also often used in mountain buildings to expand the use of space, as well as ventilation and moisture resistance [26]. Buildings in western Sichuan are mostly shaped like "one" and "L", forming open courtyards inside and outside, and allowing air circulation [27].

(3) Jingchu Cultures

The Jingchu culture, named after the state of Chu and its people, was a regional culture that emerged in the Jianghan Valley from the Zhou Dynasty to the Spring and Autumn Period and the Warring States Period [28]. It mainly refers to the ancient Jingchu history and culture with the present Hubei area as the main radiation area [29].

The so-called Jingchu culture, as a cultural form with distinct regional characteristics, from the static point of view of dating, it mainly refers to the ancient Jingchu historical culture with the present Hubei region as the main body, from the dynamic point of view, it not only includes ancient history and culture also includes the culture with local characteristics formed in Hubei from ancient times to the present and even in the future [30]. Therefore, "Jingchu culture" can also be understood as a culture with local characteristics of Hubei [31].

Generally speaking, Hanzhong city is greatly influenced by Bashu culture, but it has formed a unique Hanshui culture in the central hanzhong region and part of Ankang region [32]. Ankang is adjacent to Sichuan and Hubei, and is greatly influenced by Bashu culture and Jingchu culture [33]. The northern part of Shangluo city is mainly influenced by Qin culture, while the southern part of Shangluo city is greatly influenced by Jingchu culture [34].

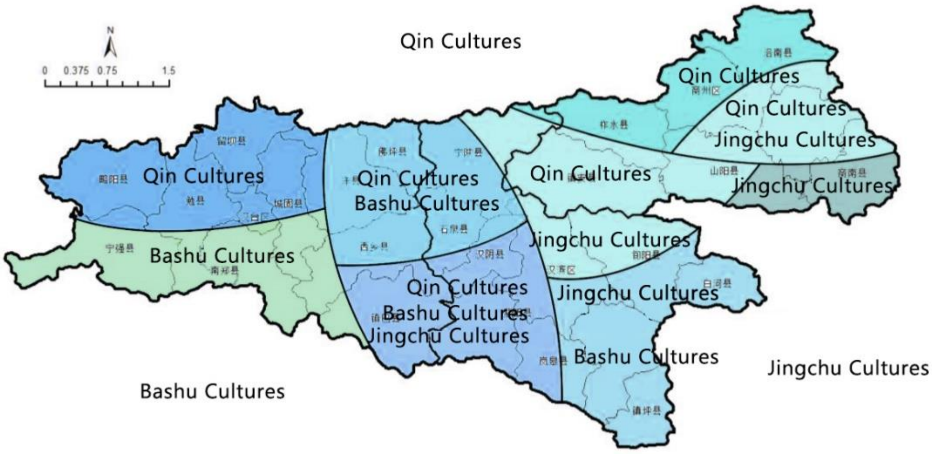

Figure 2-2. Multicultural intersection map of Southern Shaanxi.

2.2.2 Historical Development of Folk Houses in Southern Shaanxi

The traditional houses in southern Shaanxi have been formed for a long time, and the earliest traditional settlements can be traced back to the Yuan Dynasty and before [35]. During the Ming and Qing Dynasties, the number of traditional settlements in southern Shaanxi increased sharply due to a large number of immigration activities, while the economy and culture in southern Shaanxi also began to develop rapidly [36]. The Qing Dynasty was a vigorous period for the development of residential houses in southern Shaanxi, which could not be separated from large-scale immigration and trade activities [37]. Residential houses in this period are mainly wooden houses and slate houses, and the building materials are local materials [38].

In the Neolithic age, the houses in southern Shaanxi were mainly nested [39]. During the Xia, Shang and Zhou dynasties, the houses in southern Shaanxi were mainly built on the ground [40]. From The Qin and Han dynasties to the Sui and Tang Dynasties, the residential houses in southern Shaanxi should be dominated by courtyards [41]. From Song Dynasty to

Ming Dynasty, the forms of residential houses in southern Shaanxi were mainly tile-roofed houses, plate houses, thatched houses, slate houses and so on [42]. The traditional houses in southern Shaanxi were shaped in the Qing Dynasty and the Republic of China [43]. The main types are courtyard, earthwork tile house, SLATE house, bamboo and wood house, thatched house, stilted house and so on [44].

2.3 Research on Traditional Houses in Southern Shaanxi

2.3.1 Survey Overview

(1) Research Scope

Combined with the topic selection of the paper, field research was carried out on the villages in southern Shaanxi region, including Shangluo, Ankang and Hanzhong. Because there are a large number of traditional villages in southern Shaanxi in the Chinese traditional directory, in order to achieve the uniform distribution of villages in the selection process, the selection should also be carried out according to different regions, and each kind of landform should be involved. The selection of traditional village samples is mainly based on the selection of traditional villages recorded in the directory of Traditional villages in Shaanxi Province and famous historical and cultural towns. Among the recorded traditional houses in southern Shaanxi, Ankang city has the most, with 85 recorded in the directory of traditional villages in Shaanxi Province, mainly distributed in the central area of Ankang. Among them, traditional villages are screened, basic information of each village is searched, and the plan of key traditional residential houses is drawn. In the research part, the basic data of traditional villages and folk houses are sorted out. In the quantitative part, the plane, elevation and section of typical traditional buildings are listed for analysis. The statistical table 2-2 of rural survey is as follows:

Table 2-2. Rural survey statistics.

Research of time	Province	City	District/County	Rural
2018.10	Shaanxi	An kang	Xun Yang	Jiedao village, Kaihua village, Lijiatai village, Changsha village, Jiangbei village, Xianhekou village.
2018.11	Shaanxi	An kang	Xun Yang	Yunlongshan village, Wanyangchang village, Yellow mud village, Xigou mouth village, Lao Yangtian village, Sajiagou village, jianshangou village.
2019.7	Shaanxi	Han zhong	Cheng gu	Fangjiayan Village, Hejiaqiao village, Junwang Village, Wujia Village, Huangjiaying village, Wenguang Village.
			Cheng gu	Wenxing Village, Wensu village,

2020.1	Shaanxi	Shang luo	Cheng gu	Guangou Village Wangjia Village, Zhanggao Village, Xixiwang Village, Tian Cross village.
			Zhen An	Green locust village, Yumin village, Wujia village, Yanwan village, Huayuan village.
			Zhen An	Dongdong Village, Jinzhong Village, Jianjun village, Yonghong Village.
			Zhen An	Ping 'an Village, Taoyuan village, Victory village, Guilin village.

(3) Research Content

A. Basic rural conditions

Through questionnaire visits, inquiries, consulting and collection of local residents, basic data of rural areas are collected, including basic data of rural areas, village pattern, architectural style, industrial type and population.

B. Information related to residential buildings

Through field research and tool mapping, relevant information of folk houses was collected, including functions, technologies and images of folk houses, and the current situation was analyzed and the existing problems of folk houses were summarized. The specific research content is shown in the table 2-3.

Table 2-3. Table of research contents of residential houses.

Number	Category	Content
1	Basic Situation of countryside	Natural environment, historical evolution, rural scale, village layout, economic development, intangible cultural heritage, local cultural customs, way of life and production, basic family composition, economic income.
2	Related information of residential buildings	Functions: homestead area, house type area, architectural form, architectural space, courtyard form Technology: physical environment, construction technology Image: Architectural era, architectural style

(3) Research Methods

Using questionnaire interview, photo recording and on-site surveying and mapping methods, this paper conducted a detailed survey of rural houses in southern Shaanxi, selected key villages as the research object, collected and sorted out relevant information, and laid a foundation for the next research of the subject.

2.3.2 Key Research

(1) Shang Luo Region

Shang Luo city is located in the southeast of Shaanxi Province, east and Henan Province Nanyang City, Ling bao city, Lu shi County, Xi xia County, Xi chuan county and other counties border [45]. Southeast and Shiyan City, Hubei Province Yun yang District, Yun xi county adjacent, west and southwest and An kang Ningshan County, Xun yang city borders. North and northwest of Wei nan city tong guan County, Hua zhou District, Hua yin County and Xi 'an City of Lan tian County, Chang 'an district adjacent. Located between 108°34 '20 "-- 111°1' 25" east longitude and 33°2 '30 "-- 34°24' 40" north latitude, it is about 229 kilometers long from east to west and 138 kilometers wide from north to south. It covers a total area of 19,292 square kilometers, accounting for 9.36% of the total area of Shaanxi Province [46].

A. Huayuan Village, Zhen 'an County

a. Basic information

As is shown in figure 2-3, Hua yuan Village in Zhen an County is located in the northwest of Zhen an County. The village is located between two mountains and develops in a belt. There are 10 groups of villagers in the village, 405 households and 1512 people. The village is far from the urban area and develops slowly, and most of them are modern houses. Traditional houses account for about 20% of the total, and were mainly built in the Ming and Qing dynasties.

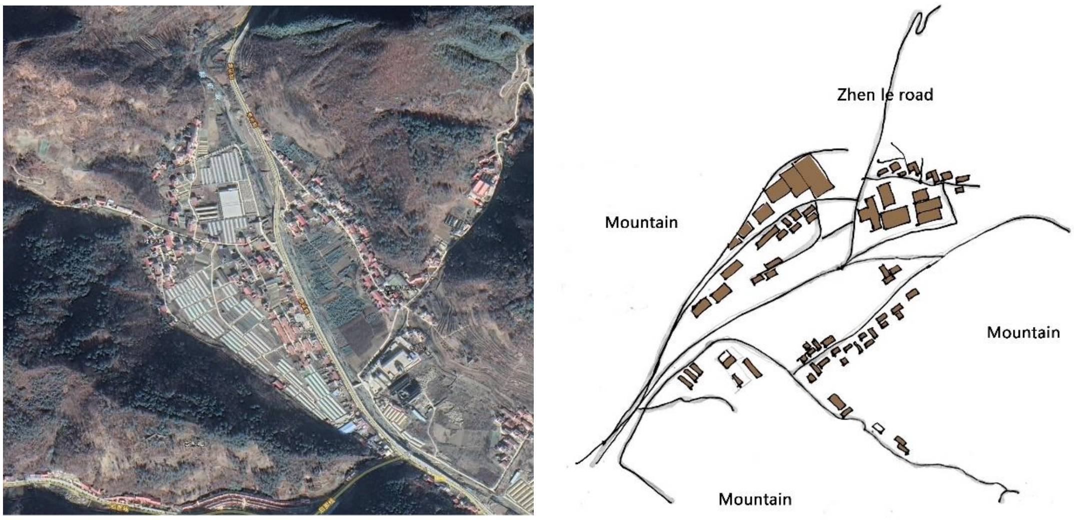

Figure 2-3. Topographic map of Huayuan village.

b. The status quo of traditional houses

The traditional houses of Huayuan Village in Zhen 'an County are mainly divided into one- shape, L-shape and courtyard type, among which one-character houses occupy a large proportion. The existing traditional residential buildings are mainly wooden structure, mainly with the combination of the through-beam type and the lift beam type structure. The interior is generally the lift beam type structure, and the through-beam type structure is exposed on the gable. A small number of courtyard buildings are two-story structures with two entrances and two exits, as well as some traditional residential houses with front shops and back houses. As is shown in figure 2-4, there are also a large number of farmhouses in Hua yuan Village, Zhen 'an County, where the preservation of all traditional buildings has reached 40%.

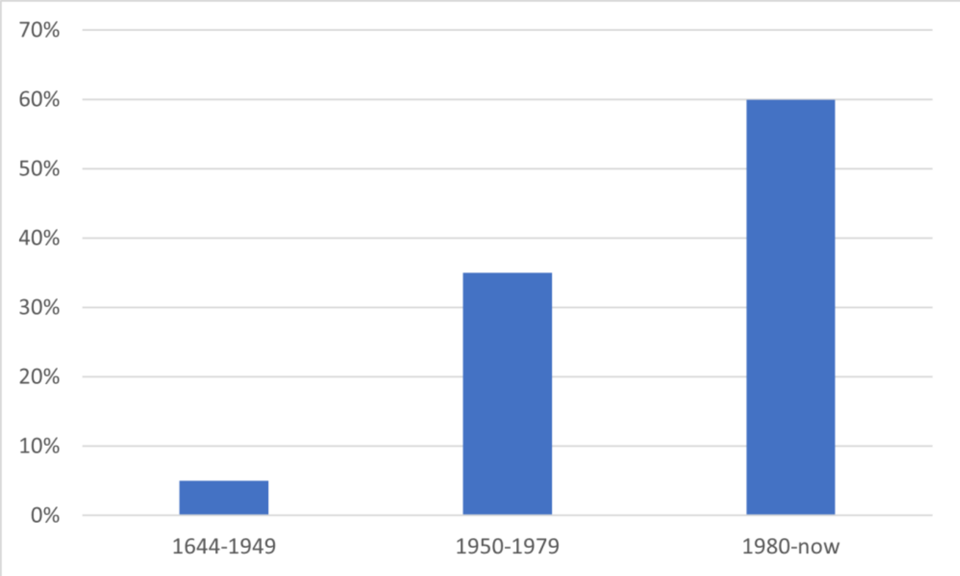

Figure 2-4. Statistical map of Huayuan Village residential buildings.

c. Cooking heating method

In the traditional houses of Hua yuan Village, Zhen 'an County, firewood stoves are the main cooking methods, as well as coal-fired stoves, gas stoves and electric cookers. According to the number of burning eyes, firewood stoves are divided into single-eye stoves, double-eye stoves and three-eye stoves. Electric cookers include electric rice cookers, electric frying pans, induction cookers and so on. The gas source of gas stove includes canned liquefied petroleum gas, biomass gasification gas and so on. The main energy used in cooking is biomass fuel (Figure 2-5).

Figure 2-5. Firewood stoves.

d. Residential building space

Space form: mostly courtyard type or "one" type, "L" type, civil structure, roof for green tile, double slope hard mountain form.

Space function: Courtyard type is composed of main room, side rooms on both sides, courtyard wall, etc. The main room is composed of main room and wing room. The main room is used for receiving guests and living, the wing room is bedroom, and the wing room is storage and kitchen. The "one" type houses are composed of the main house, with the main house in the middle and the ear rooms on both sides. "L" type residential houses are similar to courtyard type, the difference is that there is only one side wing without courtyard wall.

Spatial scale: Courtyard type house area is 120~150 square meters, of which the building area is 90~120 square meters, the courtyard area is 40~70 square meters, the main room is 3~6 rooms wide, the main room is 5~6 m deep, the traditional houses are mostly one layer, the height is 4~5m, the foundation is 2~3 steps, the step height is 15~20 cm, the step width is 20~25 cm. The main room area is 40~80m2, the wing area is 54~75 m², the patio area is 20~40 m². The base area of "one" type houses is 80~100 square meters, of which the building area is 60~70 square meters, the courtyard area is 20~30 square meters, the width of the face is 3 carves, the depth of the main house is 5~6m, and the area of the main house is 40~75 square meters. The base area of "L" type houses is 90~130 square meters, of which the building area is 80~100 square meters, the courtyard area is 20~30 square meters, the main room area is 40~80 square meters, the wing area is 40~65 square meters. According to the investigation and statistics, courtyard type accounts for 10% of traditional houses, "one" type accounts for 60%, and "L" type accounts for 30% (Table 2-4).

Table 2-4. Spatial index statistics of traditional residential buildings in Huayuan Village.

Category	Courtyard type	Stripe type	"L" type
Photo			
Floor plan	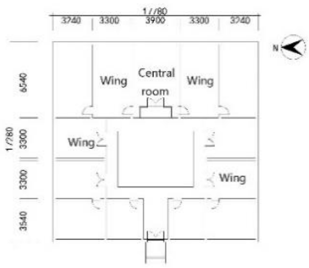	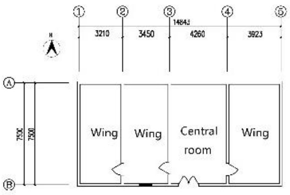	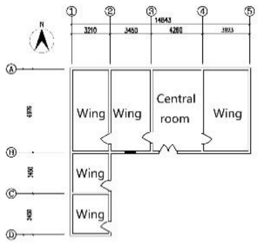
Homestead Area (m²)	120~150	80~100	90~130
Total construction area (m²)	90~120	60~70	80~100
Yard area (m²)	40~70	20~30	20~30
Entrance of main Room (m)	5~6		
Storey height (m)	4~5		
Base size (cm)	Base 2~3 steps, step height 15~20, step width 20~25		
Main room (m²)	40~80	40~75	40~80
Wing (m²)	54~75	-	40~65
Patio (m²)	20~40	-	-

B. Jinzhong Village, Zhen an County

a. Basic information

Jin Zhong Village of Zhen an County is located in the northwest of Zhenan County, Shang zhou District, Shang luo City, and adjacent to Xing jia Ditch, Wan jia Slope and Wan jia Ditch. There are 8 groups of villagers, 400 households and 1320 people in the village. The village is far from the urban area and is generally developed. The number of traditional houses is more than that of Hua yuan Village in Chen Zhen 'an County. The layout of Jin zhong Village in Zhen 'an County has the characteristics of a typical valley type village. Affected by topography and landform, the village develops along the transit road in a strip (Figure 2-6).

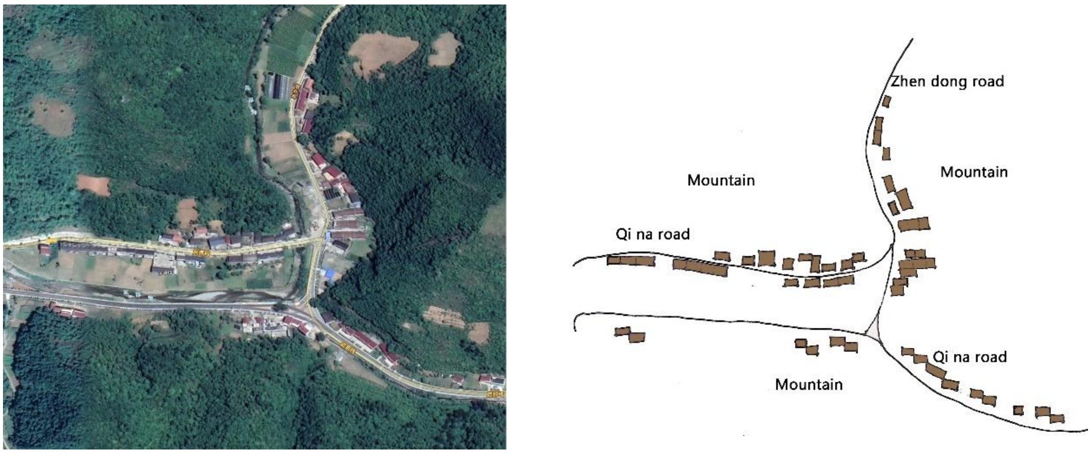

Figure 2-6. Topographic map of Jinzhong village.

b. The status quo of traditional houses

The streets of Jin zhong Village in Zhen an County are narrow and crowded with the ups and downs of the terrain. The traditional houses are also layered and scattered because of the topography. The traditional houses of Jin zhong Village in Zhen an County are mainly divided into one-font, L-shape and U-shape. Many of the houses on the west side of the street have been renovated. The preservation rate of traditional buildings in Jin zhong Village, Zhen 'an County is 30%. Typical for the Li family courtyard (Figure 2-7).

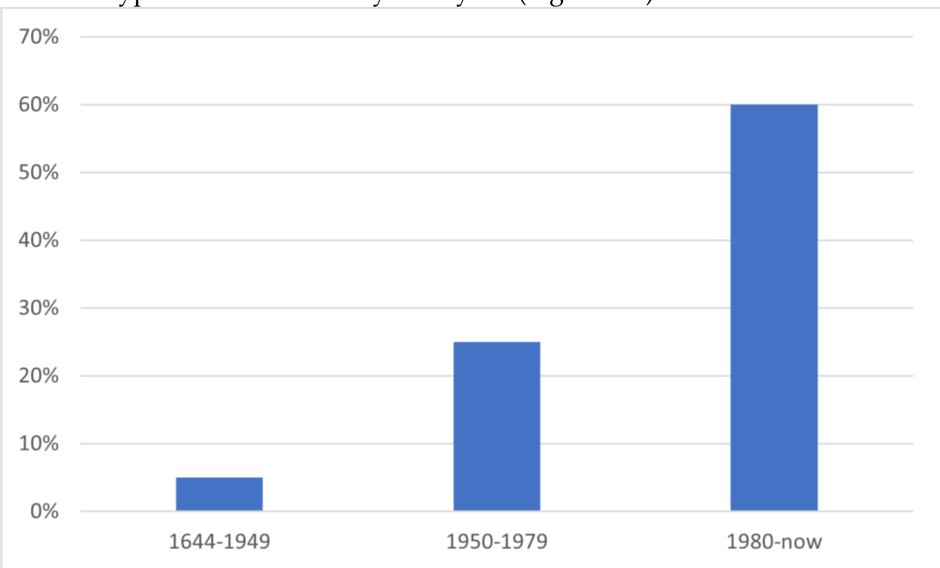

Figure 2-7. Statistical map of Jin zhong Village residential buildings.

c. Cooking heating method

In the traditional residential houses of Jinzhong Village, Zhenan County, firewood stoves are the main cooking methods, as well as coal stoves, gas stoves and electric cookers. A small number of residents use gas stoves from canned LPG and biomass gasification gas. The main energy used in cooking is biomass fuel (Figure 2-8).

Figure 2-8. Firewood stoves.

d. Residential building space

Space form: mostly "one" type, "L" type, "U" type, civil structure, roof for green tile, double slope hard mountain form.

Spatial function: the "one" type houses are composed of the main room, with the main room in the middle and ear rooms on both sides. The main room is composed of the main room and the ear room. The main room is used for receiving guests and living, while the ear room is the bedroom. "L" type houses have one more ear room than "one" type houses. The ear room is used for storage and kitchen. "U" shaped houses are composed of wing rooms and main rooms.

Spatial scale: The base area of "one" type houses is 70~90 square meters, of which the building area is 50~60 square meters and the yard area is 10~20 square meters. The main room is 3~6 rooms wide and the main room is 5~6 m deep. The traditional houses are mostly one layer, the height is 3~5 m, the base is 2~3 levels, the steps are 15~25 cm high and the stepping width is 15~25 cm. The main room area is 44~70 square meters. The base area of "L" type houses is 80~120 m^2, including 70~90 m^2 building area, 20~30 m^2 courtyard area, 40~75 m^2 main house area and 40~60 m^2 wing area. "U" type base area of 80~120 m^2, including building area of 70~100 m^2, courtyard area of 30~40 m^2, main room area of 40~75 m^2, wing area of 40~80 m^2. According to the survey statistics, "one" shaped houses accounted for 65%, "L" shaped houses accounted for 20%, "U" shaped houses accounted for 15% (Table 2-5).

Table 2-5. Spatial index statistics of traditional residential buildings in Jinzhong Village.

Category	Stripe type	"U" type	"L" type
Photo			
Floor plan	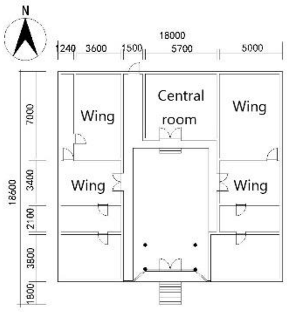	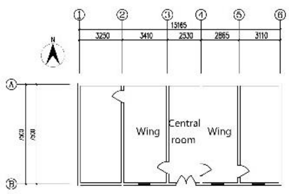	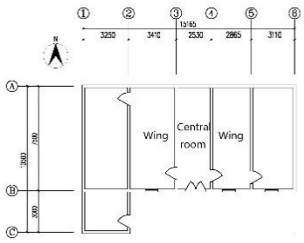
Homestead Area (m^2)	70~90	80~120	80~120
Total constructio	50~60	70~100	70~90

n area (m^2)			
Yard area (m^2)	10~20	30~40	20~30
Entrance of main Room (m)		5~6	
Storey height (m)		3~5	
Base size (cm)		Base 2~3 steps, step height 15~25, step width 15~25	
Main room (m^2)	44~70	40~75	40~75
Wing (m^2)	30-60	40~80	40~60

C. Ping an Village, Zhen 'an County

a. Basic information

Zhen 'an County pingan village is located in Shang zhou District, close to Liang jiazhuang, Miao Concave. The local scenery is beautiful, the sky is blue and the water is clear. The village of 10 groups of villagers, 405 households, 1512 people, the village is close to the urban development is better. Ping an village in Zhen 'an County is located between two mountains and develops along the transit road in a belt shape, with the characteristics of a typical valley type village (Figure 2-9).

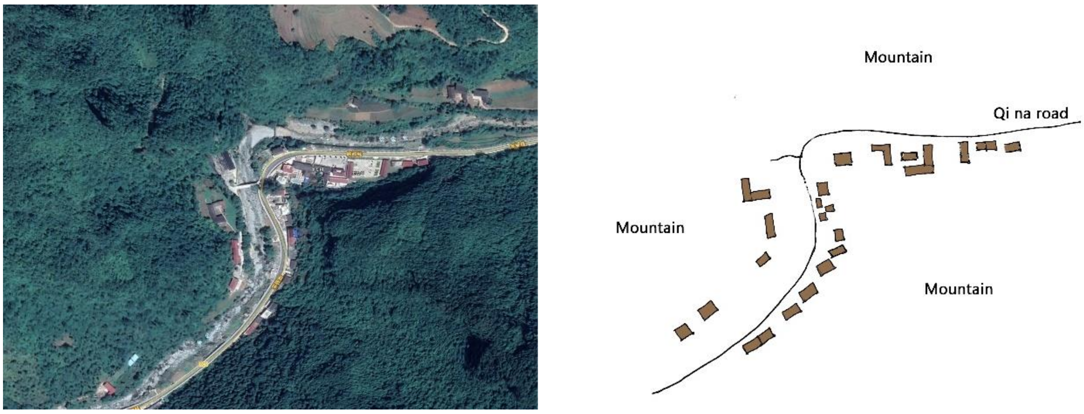

Figure 2-9. Topographic map of Ping an village.

b. The status quo of traditional houses

Ping 'an Village in Zhen 'an County is surrounded by mountains, and the village as a whole presents a "ribbon" form. The construction of residential houses is relatively clustered and relatively well integrated with nature. The traditional houses of Ping 'an Village in Zhen 'an County are mainly one-character houses, while the rest are L-shape, U-shape and courtyard type. The local traditional residential houses are mainly brick and wood structure, the height of the building is generally one or two stories. In Ping an Village, Zhen 'an County, 45 percent of traditional buildings are preserved (Figure 2-10).

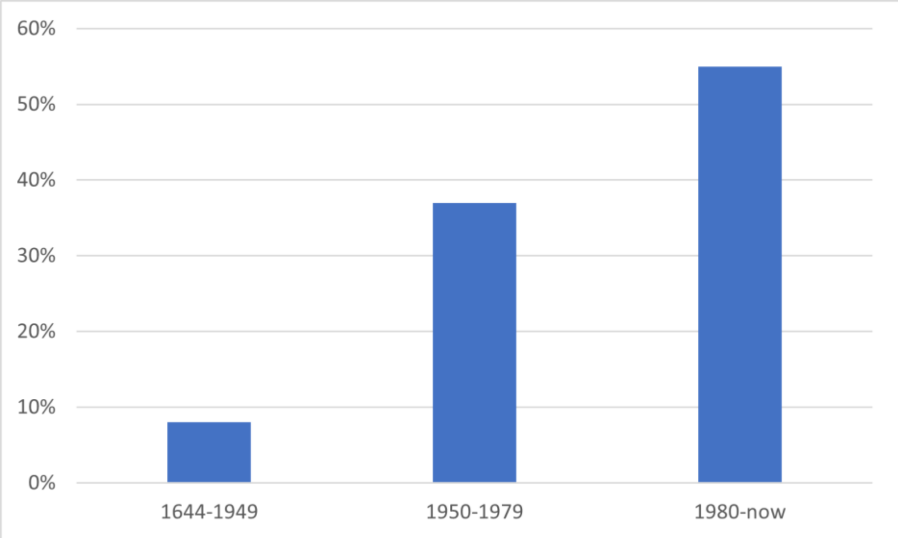

Figure 2-10. Statistical map of Ping 'an Village residential buildings.

c. Cooking heating method

In the traditional houses of Ping 'an Village, Zhen 'an County, firewood stoves are the main cooking methods, as well as coal-fired stoves, Electric baking pan, gas stoves and electric cookers. Today, gas stoves are also widely used by residents (Figure 2-11).

(a)

(b)

Figure 2-11. (a) Induction cooker; (b) Electric baking pan.

d. Residential building space

Space form: mostly courtyard type or Stripe type, "L" type, civil structure, roof for green tile, double slope hard mountain form.

Space function: Courtyard type is composed of main room, side rooms on both sides and courtyard wall. The main room is composed of main room and wing room. The main room is used for receiving guests and living, the wing room is bedroom, and the wing room is storage and kitchen. The Stripe type houses are composed of the main house, with the main house in the middle and the ear rooms on both sides. "L" type residential houses are similar to courtyard type, the difference is that there is only one side wing without courtyard wall.

Spatial scale: Courtyard type house area is 130~160 square meters, of which the building area is 100~130 square meters, the courtyard area is 30~50 square meters, the main room is 3~6 rooms wide, the main room is 5~6 m deep, the traditional houses are mostly one layer, the height is 4~5 m, the foundation is 2~3 levels, the steps are 15~20 cm high, the stepping width is

20~25 cm. Main room area of 40~80 square meters, wing area of 40~70 square meters, patio area of 20~40 square meters. The base area of Stripe type houses is 90~110 m², of which the building area is 70~80 m², the yard area is 30~40 m², the face width is 3 bareness, the hall depth is 5~6 m, the main room area is 45~60 m². The base area of "L" type houses is 100~140 m², of which the building area is 90~110 m², the courtyard area is 30~50 m², the main room area is 45~70 m², and the wing area is 40~60 m². According to the investigation and statistics, courtyard type accounts for 10% of traditional houses, Stripe type accounts for 55%, and "L" type accounts for 35% (Table 2-6).

Table 2-6. Spatial index statistics of traditional residential buildings in Ping an Village.

Category	Courtyard type	Stripe type	"L" type
Photo			
Floor plan	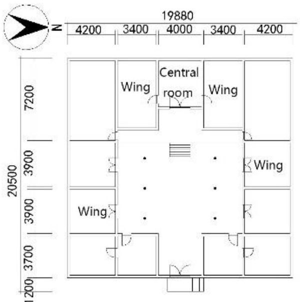	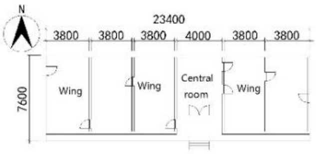	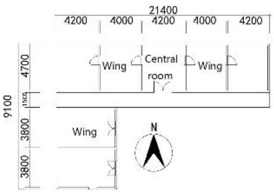
Homestead Area (m²)	130~160	90~110	100~140
Total construction area (m²)	100~130	70~80	90~110
Yard area (m²)	30~50	30~40	30~50
Entrance of main Room (m)		5~6	
Storey height (m)		4~5	
Base size (cm)		Base 2~3 steps, step height 15~20, step width 20~25	
Main room (m²)	40~80	45~60	45~70
Wing (m²)	40~70	-	40~60
Patio (m²)	20~40	-	-

D. Taoyuan Village, Zhen 'an County

a. Basic information

Taoyuan Village in Zhen an County is located in the southwest of Zhen an County, close to tuqiao ditch, Ma Jiafang, south ditch. There are 8 groups of villagers in the village, 652 households and 1212 people. The village is far from the urban area and the development is more general. Taoyuan Village in Zhen an County is surrounded by mountains, and the distribution of villages develops along the mountain belt, which conforms to the characteristics of the Qinling River valley (Figure 2-12).

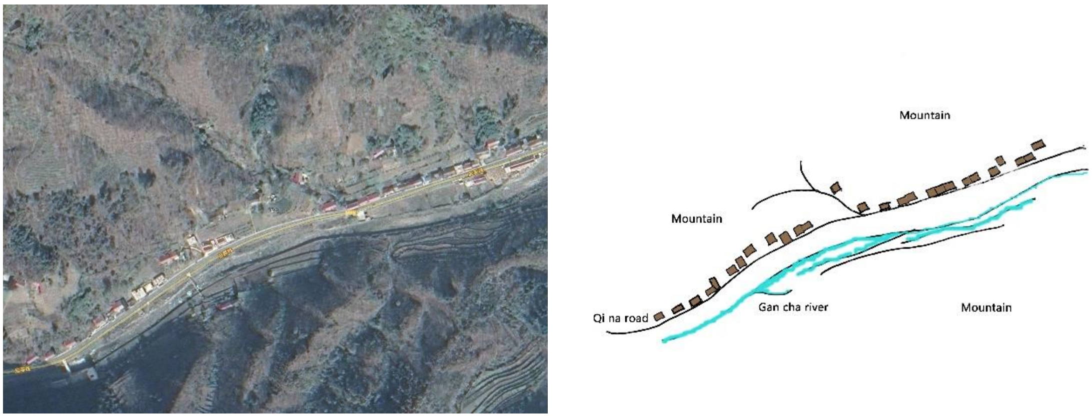

Figure 2-12. Topographic map of Taoyuan village.

b. The status quo of traditional houses

The traditional houses in Taoyuan Village of Zhen 'an County mainly have one font, L and U, among which one font houses are more common. The residential buildings in this village have been badly damaged because of years of disrepair, and some of them can no longer be used. The structure of traditional residential houses is mostly beam type structure, and some buildings need to meet the requirements of sacrifice, so the beam type structure can meet the needs of larger space. Village in a font building, the typical han courtyard and shangjia courtyard. In Taoyuan Village, Zhen 'an County, 38 percent of traditional buildings are preserved (Figure 2-13).

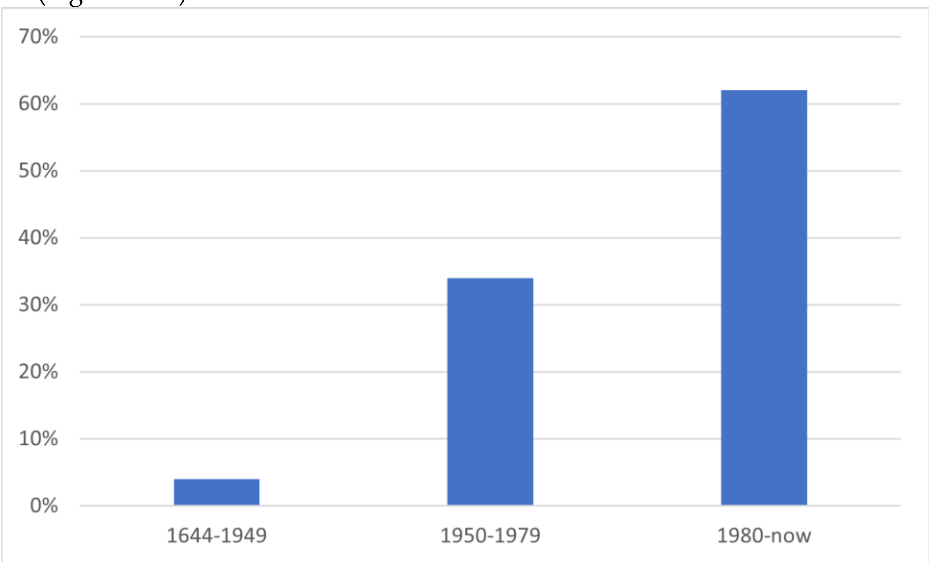

Figure 2-13. Statistical map of Taoyuan Village residential buildings.

c. Cooking heating method

In taoyuan village, Zhen an County, firewood stoves are the main cooking methods, as well as coal-fired stoves, gas stoves and electric cookers. A small number of residents use gas stoves from canned LPG and biomass gasification gas. The main energy used in cooking is biomass fuel (Figure 2-14).


Figure 2-14. Firewood stoves.

d. Residential building space

Space form: mostly Stripe type, "L" type, "U" type, civil structure, roof for green tile, double slope hard mountain form.

Spatial function: the "I" type houses are composed of the main house, with the main house in the middle and the ear rooms on both sides. "L" type houses are similar to "U" type houses, the difference is that there is only one side wing without courtyard walls. "U" shaped houses are composed of the main house and flanking rooms.

Space scale: The base area of Stripe type houses is 90~100 m², including 70~80 m² construction area and 20~30 m² courtyard area. The main room is 3~6 rooms wide, the main room is 5~6 m deep, and the main room is 45~70 m². The base area of "L" type houses is 100~130 m², of which the building area is 90~100 m² and the courtyard area is 30~40 m². The traditional houses are mostly one layer, the height is 4~5 m, the base is 2~3 levels, the step height is 15~20 cm, the step width is 20~25 cm, the main room area is 50~80 m², the wing room area is 40~50 m². The base area of "U" type houses is 100~130 m², of which the building area is 90~105 m² and the yard area is 30~40 m². The traditional houses are mostly one layer, the height is 4~5 m, the base is 2~3 levels, the step height is 15~20 cm, the step width is 20~25 cm, the main room area is 50~60 m², the wing room area is 40~50 m². According to the investigation and statistics, Stripe shaped houses account for 65%, "L" shaped houses 25%, and "U" shaped houses 10% (Table 2-7).

Table 2-7. Spatial index statistics of traditional residential buildings in Taoyuan Village.

Category	**Stripe type**	**"U" type**	**"L" type**
Photo			

Floor plan	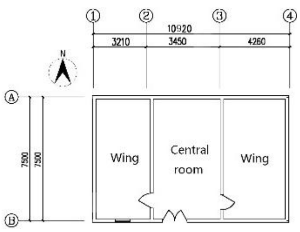	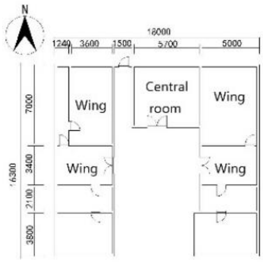	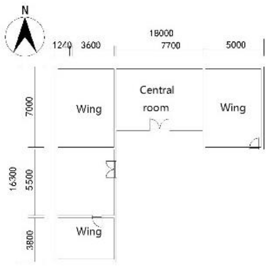
Homestead Area (m²)	90~100	100~130	100~130
Total construction area (m²)	70~80	90~100	90~105
Yard area (m²)	20~30	30~40	40~50
Entrance of main Room (m)		5~6	
Storey height (m)		4~5	
Base size (cm)		Base 2~3 steps, step height 15~20, step width 20~25	
Main room (m²)	45~70	50~80	50~60
Wing (m²)	-	40~50	40~50

(2) An Kang Region

An kang city, located in the southeast of Shaanxi Province, north qin ling Mountains, south Bashan Mountain, Han River across the east and west, valley basin in the middle, the territory between 31°42 '~33°49' north latitude, 108°01 '~110°01' east longitude. Under the jurisdiction of Hanbin District, Xun yang County, Bai he County, Shi quan County, Ping li County, Ziyang County, Langao County, Ning shan County, Zhen ping County, Han yin County 1 area 9 counties. An kang covers an area of 23,391 square kilometers, with 289,000 hectares of cultivated land and a population of 2.65 million [47].

A. Lijiatai Village, Xun yang County

a. Basic information

Lijiatai Village is a national key poverty alleviation village and a demonstration village of Xun yang County targeted poverty alleviation and beautiful village construction, with a total population of 1265 in 388 households. The total land area is 5123 mu, of which, cultivated land 2323 mu, woodland 2800 mu. Lijiatai village, Xun yang County, faces the water behind the mountains. The village develops along the direction of the river in a zonal shape, located on both sides of the Xun River and along the national Road 316 (Figure 2-15).

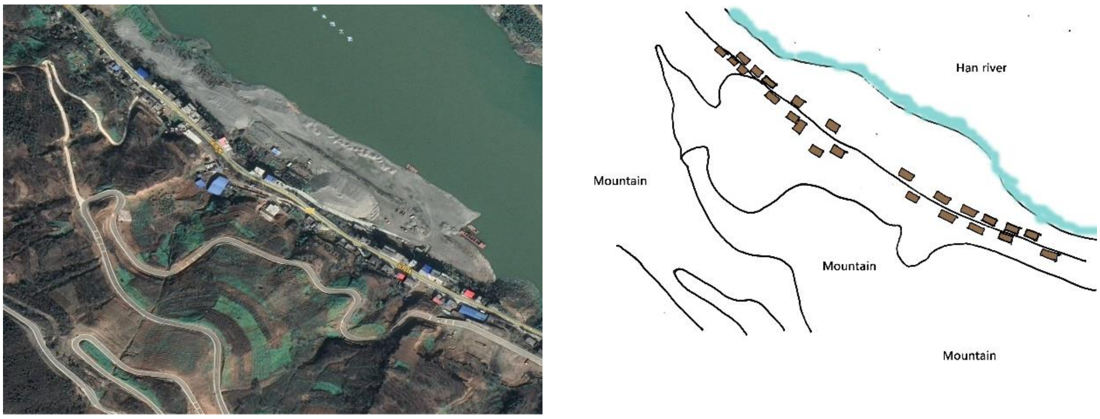

Figure 2-15. Topographic map of Lijiatai village.

b. The status quo of traditional houses

The traditional houses in Lijiatai village are well preserved, including Qianjia courtyard, Huang jia courtyard and Zhang jia Courtyard. The traditional houses are mostly of brick and wood structure, and the lifting beam type is mostly used. The roof form is hard mountain roof, and the entrance of the house has a high platform to highlight the status of the owner. The architectural decoration is very fine, with dragon and phoenix as the main shape. In Lijiatai Village, Zhen 'an County, 47 percent of traditional buildings are preserved (Figure 2-16).

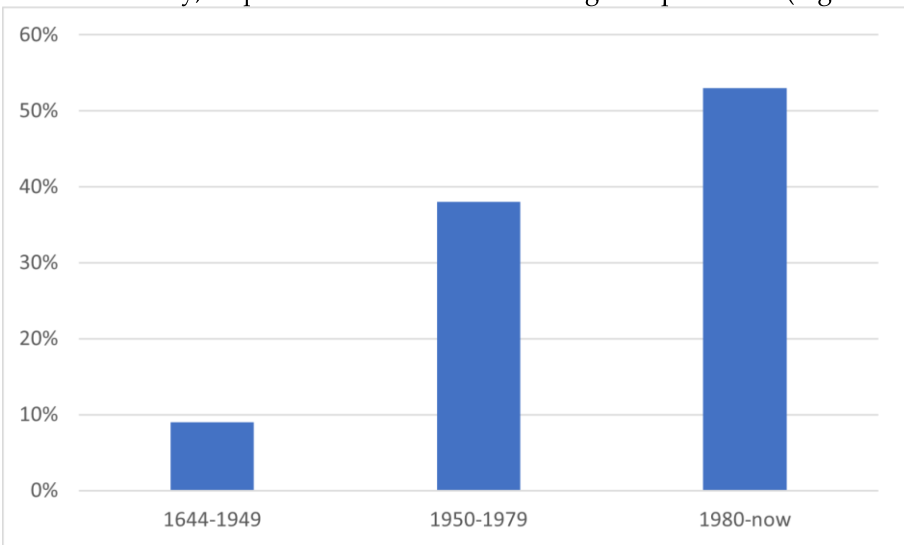

Figure 2-16. Statistical map of Lijiatai Village residential buildings.

c. Cooking heating method

In lijiatai village, Xun yang County, firewood stoves are the main cooking methods, as well as coal stoves, gas stoves and electric cookers. Many residents use gas stoves from liquefied petroleum gas and biomass gasification gas (Figure 2-17).

(a) (b)

Figure 2-17. (a) Liquefied petroleum gas; (b) Firewood stoves.

d. Residential building space

Space form: mostly courtyard type or Stripe type, civil structure, roof is green tile, double slope hard mountain form, A small number of hanging mountain form.

Space function: Courtyard type is composed of main room, side rooms on both sides and courtyard wall. The main room is composed of main room and wing room. The main room is used for receiving guests and living, the wing room is bedroom, and the wing room is storage and kitchen. The Stripe type houses are composed of the main house, with the main house in the middle and the ear rooms on both sides. "L" type houses are composed of main rooms and wing rooms.

Spatial scale: The courtyard house covers an area of 110~150 square meters, of which the building area is 80~130 square meters, and the courtyard area is 50~75 square meters. The main room is 3~6 rooms wide, and the main room is 5~7 m deep. The traditional residential houses are mostly one layer, the height is 5~7 m, the foundation is 2~3 levels, the steps are 15~20 cm high, and the stepping width is 20~25 cm. Main room area of 40~80 square meters, wing area of 45~75 square meters, patio 20~40 square meters. The base area of "L" type houses is 100~120 m^2, of which the building area is 90~100 m^2 and the courtyard area is 30~40 m^2. The traditional houses are mostly one layer, the height is 4~5 m, the base is 2~3 levels, the step height is 15~20 cm, the step width is 20~25 cm, the main room area is 50~80 m^2, the wing room area is 40~50 m^2. The base area of Stripe type houses is 90~105 square meters, of which the building area is 70~90 square meters, and the courtyard area is 10~30 square meters. The main room is 3~6 rooms wide, the main room is 5~7m deep, and the main room area is 40~65 square meters. According to the survey and statistics, courtyard type houses account for 14% of traditional houses, "L" houses account for 21%, and Stripe type houses account for 65% (Table 2-8).

Table 2-8. Spatial index statistics of traditional residential buildings in Lijiatai Village.

Category	**Courtyard type**	**"L" type**	**Stripe type**
Photo			

Floor plan	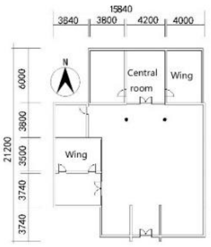	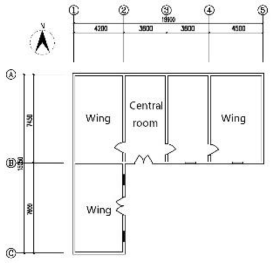	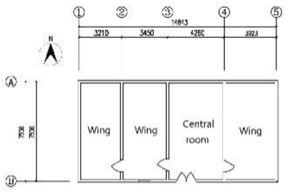
Homestead Area (m²)	110~150	100~120	90~105
Total construction area (m²)	80~130	90~100	70~90
Yard area (m²)	50~75	30~40	10~30
Entrance of main Room (m)		5~7	
Storey height (m)		5~7	
Base size (cm)		Base 2~3 steps, step height 15~20, step width 20~30	
Main room (m²)	40~80	50~80	40~65
Wing (m²)	45~75	40~50	-
Patio (m²)	20~40	-	-

B. Jiangbei Village, Guankou Town

a. Basic information

Jiangbei Village is an administrative village under the jurisdiction of Guankou Town, Xunyang City, An kang City, Shaanxi Province. Jiangbei Village is adjacent to Xuezhuang Village, Damiao Village, Pugou Village, Song ping Village, Hao ta Village, Zhangling Village, Nigou Village, Xipo village and Guan ping community. The whole village 7 villagers group, 500 households, 1520 people, the village is far from the urban development is relatively backward. The layout of Jiangbei Village is surrounded by mountains on all sides, and the whole village develops along the Han River in a belt. In Jiangbei Village, there is a suitable living space for traditional freeform streets and lanes (Figure 2-18).

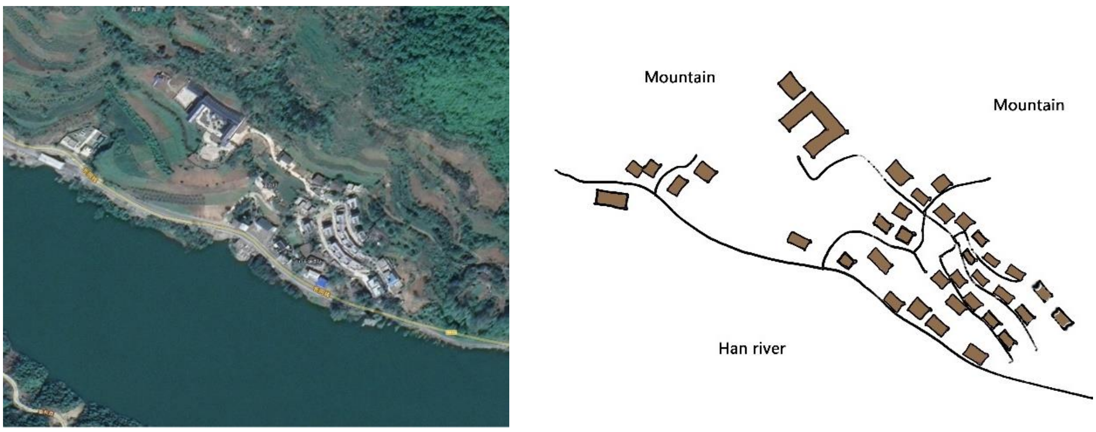

Figure 2-18. Topographic map of Jiangbei village.

b. The status quo of traditional houses

In Jiangbei Village of Guankou Town, traditional houses coexist with modern houses, accounting for about 27% of the total. The spatial form of traditional residential houses is mostly courtyard type or Stripe type or "L" type, which adopts civil structure, roof with green tile and double slope hard mountain form (Figure 2-19).

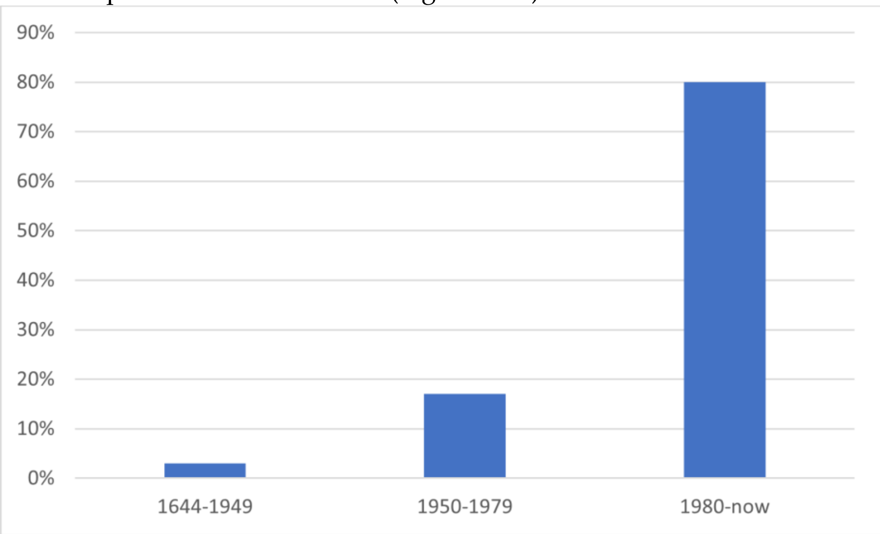

Figure 2-19. Statistical map of Jiangbei Village residential buildings.

c. Cooking heating method

In jiangbei village, Guankou Town, firewood stoves are the main cooking methods, as well as coal-fired stoves, gas stoves and electric cookers. A small number of residents use biomass gasification gas (Figure 2-20).

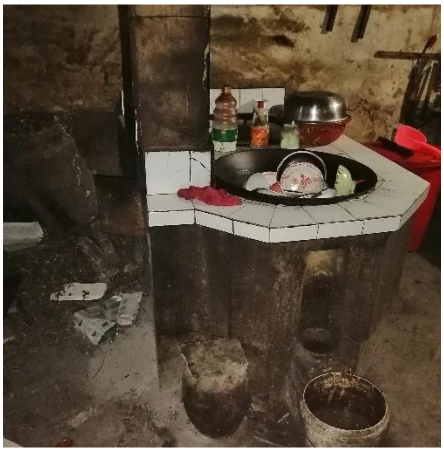

Figure 2-20. Firewood stoves.

d. Residential building space

Space form: mostly courtyard type or Stripe type, "L" type, civil structure, roof for green tile, double slope hard mountain form.

Space function: Courtyard type is composed of main room, side rooms on both sides and courtyard wall. The main room is composed of main room and wing room. The main room is used for receiving guests and living, the wing room is bedroom, and the wing room is storage and kitchen. The Stripe type houses are composed of the main house, with the main house in the middle and the ear rooms on both sides. "L" type residential houses are similar to courtyard type, the difference is that there is only one side wing without courtyard wall.

Spatial scale: Courtyard house area is 130~160 square meters, of which the building area is 100~130 square meters, the courtyard area is 40~60 square meters, the main room width is 3~6 rooms, the main room depth is 5~7 m, the traditional residential houses are mostly one layer, the height is 4~6m, the foundation is 2~3 levels, the steps are 15~25 cm high, the stepping width is 20~30 cm. Main room area of 40~75 square meters, wing area of 40~50 square meters, patio area of 20~40 square meters. The base area of Stripe type houses is 90~110 square meters, of which the building area is 70~90 square meters, the courtyard area is 20~30 square meters, the main room width is 3~6 rooms, the main room depth is 5~7 m, the main room area is 50~70 square meters. "L" type houses base area of 100~140 square meters, including building area of 80~110 square meters, courtyard area of 20~40 square meters, main room area of 40~80 square meters, wing area of 30~55 square meters. According to the survey statistics, courtyard type accounts for 10% of the traditional residential houses, "L" type accounts for 35% of the traditional residential houses, and Stripe type accounts for 55% of the traditional residential houses (Table 2-9).

Table 2-9. Spatial index statistics of traditional residential buildings in Jiangbei Village.

Category	Courtyard type	Stripe type	"L" type
Photo			
Floor plan	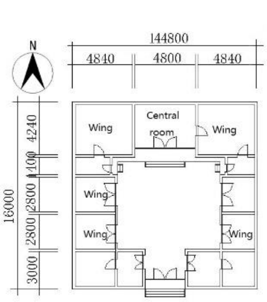	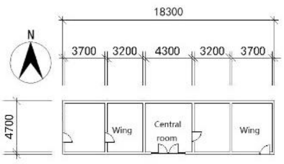	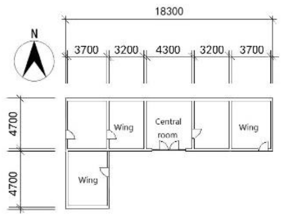
Homestead Area (m^2)	130~160	90~110	100~140
Total construction area (m^2)	100~130	70~90	80~110
Yard area (m^2)	40~60	20~30	20~40
Entrance of main Room (m)		5~7	
Storey height (m)		4~6	
Base size (cm)		Base 2~3 steps, step height 15~25, step width 20~30	
Main room (m^2)	40~75	50~70	40~80
Wing (m^2)	40~50	-	30~55
Patio (m^2)	20~40	-	-

C. Huang nigou village, Xian he Town

a. Basic information

Huang nigou Village is an administrative village under the jurisdiction of Xian he Town, Xun yang City, An kang City, Shaanxi Province. The local climate is temperate continental monsoon climate. Huangnigou village and Xigou Village, Wang ping village, big dragon Wanggou village, Zhuyuan River village, fairy estuary village, jian shan community, Jijiazhuang community, view village community, niujia Yinpo village adjacent. The entire village of 10 groups of villagers, 524 households, 1212 people, the village is far from the urban development is relatively backward. Huangnigou Village is surrounded by mountains. The layout of the whole village develops along the form of the mountain, which is in line with the characteristics of the valley (Figure 2-21).

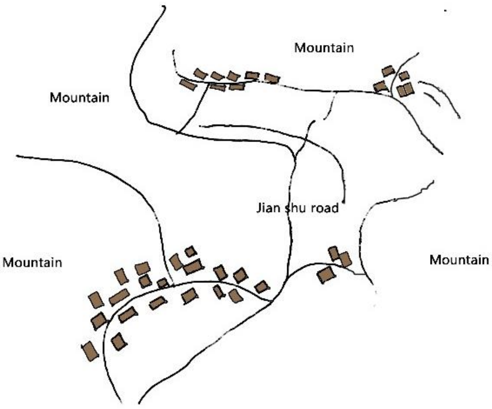

Figure 2-21. Topographic map of Huang nigou village.

b. The status quo of traditional houses

In Huangnigou Village, Xianhe Town, traditional houses coexist with modern houses, accounting for about 38% of the total. The spatial form of traditional residential houses is mostly courtyard type or Stripe type or "L" type, which adopts civil structure, roof with green tile and double slope hard mountain form, and a few are hanging mountain form (Figure 2-22).

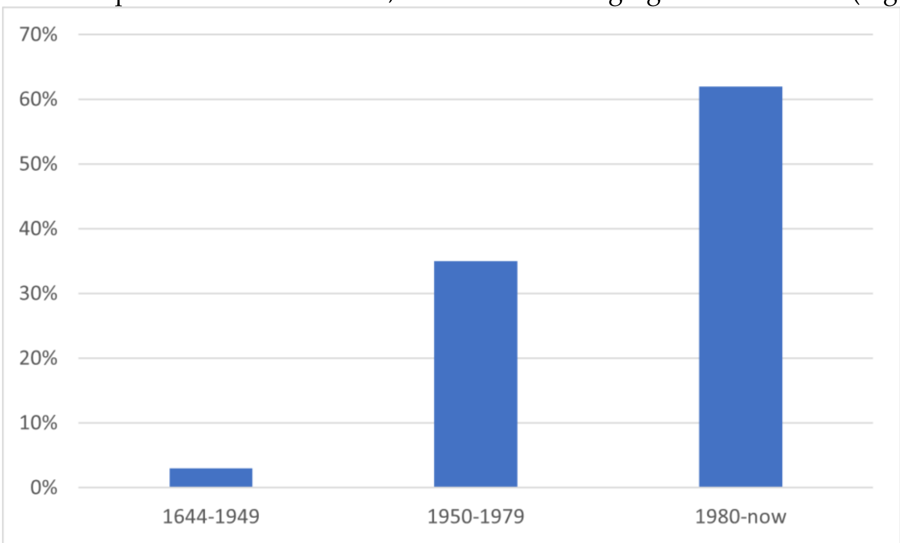

Figure 2-22. Statistical map of Huangnigou Village residential buildings.

c. Cooking heating method

In the traditional houses of Huangnigou Village, Xianhe Town, firewood stoves are the main cooking methods, as well as coal stoves, gas stoves and electric cookers (Figure 2-23).

(a) (b)

Figure 2-23. (a) Electric cookers; (b) Firewood stoves.

d. Residential building space

Space form: mostly courtyard type or Stripe type or "L" type, civil structure, roof with green tiles, double slope hard mountain form, A small number of hanging mountain form.

Space function: Courtyard type is composed of main room, side rooms on both sides and courtyard wall. The main room is composed of main room and wing room. The main room is used for receiving guests and living, the wing room is bedroom, and the wing room is storage and kitchen. The Stripe type houses are composed of the main house, with the main house in the middle and the ear rooms on both sides. "L" type residential houses are similar to a courtyard, the difference is that there is only one side wing without courtyard wall.

Space scale: Courtyard house area is 140~160 m^2, including building area of 90~130 m^2, courtyard area of 50~80 m^2, main room area of 50~85 m^2, wing area of 30~50 m^2, patio area of 20~40 m^2. The base area of Stripe type houses is 100~110 m^2, of which the building area is 70~100 m^2, and the yard area is 20~40 m^2. The main room is 3~6 rooms wide, the main room is 5~7 m deep, and the main room is 40~75 m^2. "L" type houses base area of 100~150 square meters, including building area of 80~100 square meters, courtyard area of 20~50 square meters, main room area of 40~75 square meters, wing area of 20~50 square meters. According to investigation and statistics, courtyard type accounts for 10% of traditional residential houses, and "L" type accounts for 25% of traditional residential houses. The Stripe shape accounts for 65% of traditional houses (Table 2-10).

Table 2-10. Spatial index statistics of traditional residential buildings in Huang nigou Village.

Category	Courtyard type	Stripe type	"L" type
Photo			
Floor plan	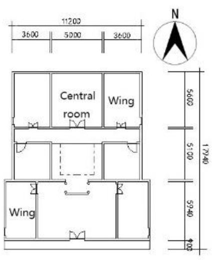	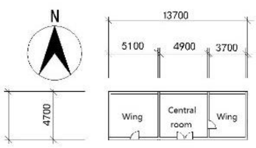	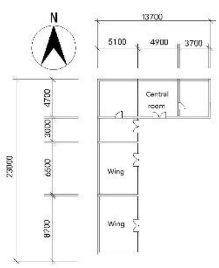
Homestead	140~160	100~110	100~150

Area (m^2)			
Total construction area (m^2)	90~130	70~100	80~100
Yard area (m^2)	50~80	20~40	20~50
Entrance of main Room (m)		5~7	
Storey height (m)		4~6	
Base size (cm)		Base 2~3 steps, step height 15~30, step width 20~40	
Main room (m^2)	50~85	40~75	40~75
Wing (m^2)	30~50	-	20~50
Patio (m^2)	20~40	-	-

D. Shagou Village, Shuhe town

a. Basic information

Shagou Village is shaanxi Province Ankang City Xunyang City Shuhe town under the jurisdiction of the administrative village. Shagou village and ford village, xiaoshan fork village, Longchi village, Luo Jiapo village, Zhujia village, donggou village, Wenjiashan village, Longtan village, Man Bay village, Shi Jiagou village, yellow field village, Zhai Po village, Zhi Jiawan village, guantanggou village adjacent. There are 12 groups of villagers in the village, 724 households and 1563 people. The village is further from the city and closer to development. Shagou Village of Shuhe town is relatively flat, in line with the typical terrain characteristics of "two mountains sandwiched by a river", and the whole village develops along the mountain belt (Figure 2-24).

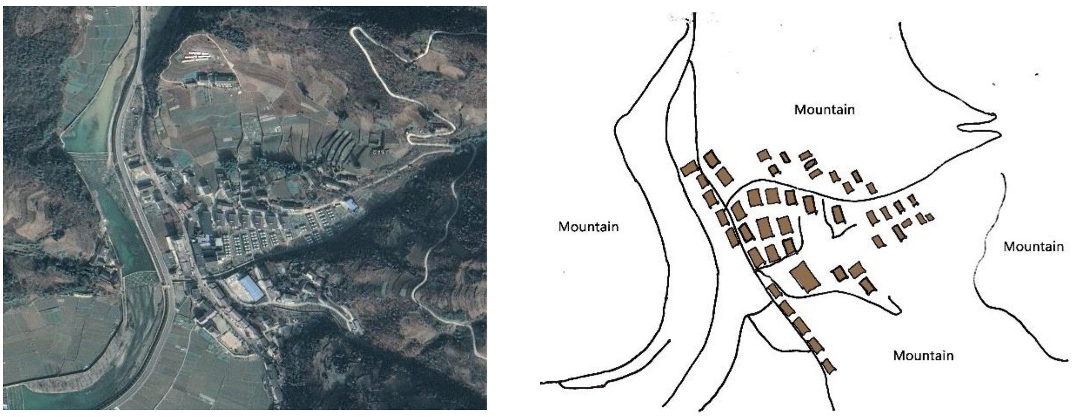

Figure 2-24. Topographic map of Shagou village.

b. The status quo of traditional houses

Traditional houses and modern houses coexist in Shagou Village, Shuhe town, accounting for about 20% of the total. The space form of traditional residential houses is mostly "U" or Stripe type and "L" type, which adopts civil structure, roof with green tile and double slope hard mountain form (Figure 2-25).

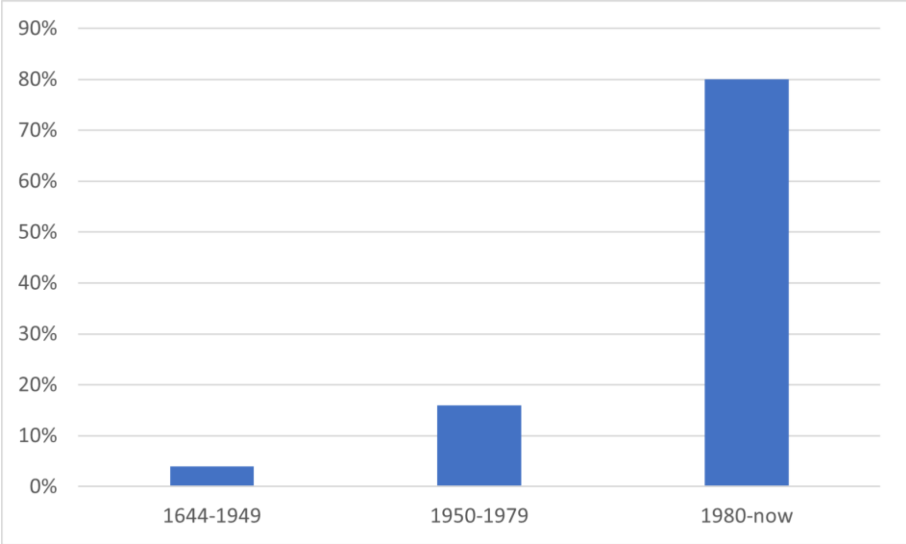

Figure 2-25. Statistical map of shagou Village residential buildings.

c. Cooking heating method

In shagou village, Shuhe town, firewood stoves are the main cooking methods, as well as coal-fired stoves, gas stoves and electric cookers (Figure 2-26).

Figure 2-26. Firewood stoves.

d. Residential building space

Space form: mostly in the form of "U" or Stripe or "L", with civil structure, green tile roof and double slope hard mountain form.

Spatial function: the Stripe type houses are composed of the main room, with the main room in the middle and ear rooms on both sides. "L" type residential houses are similar to a courtyard, the difference is that there is only one side wing without courtyard wall. The "U" shape consists of the main room and the flanks.

Spatial scale: The main room is 3~6 rooms wide and the main room is 5~7 m deep. The traditional houses are mostly one story, the height is 4~6 m, the foundation is 2~3 levels, the steps are 15~25 cm high, and the stepping width is 20~30 cm. The main room is 40~75 square meters, and the wing is 30~50 square meters. The base area of Stripe type houses is 95~110 square meters, of which the building area is 80~90 square meters, the yard area is 20~30 square meters, the face width is 3~6 rooms, the hall depth is 5~7 m, the main room area is 40~55 square meters. The base area of "L" type houses is 110~140 m^2, of which the building area is 85~110 m^2, the courtyard area is 20~40m2, the main room area is 40~65 m^2, and the wing area is 30~50 m^2. According to the survey statistics, "U" shape accounts for 13%, "L" shape for 37% and Stripe shape for 50% of traditional houses (Table 2-11).

Table 2-11. Spatial index statistics of traditional residential buildings in Shagou Village.

Category	"U" type	Stripe type	"L" type
Photo			
Floor plan	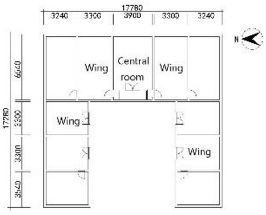	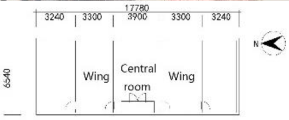	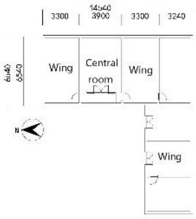
Homestead Area (m²)	120~150	95~110	110~140
Total construction area (m²)	90~120	80~90	85~110
Yard area (m²)	20~40	20~30	20~40
Entrance of main Room (m)		5~7	
Storey height (m)		4~6	
Base size (cm)		Base 2~3 steps, step height 15~25, step width 20~30	
Main room (m²)	40~75	40~55	40~65
Wing (m²)	30~50	-	30~50

(3) Han Zhong Region

Hanzhong City, referred to as Han, known as Nanzheng, Liangzhou, Hanchuan and Xingyuan in ancient times, is a prefecture-level city under the jurisdiction of Shaanxi Province of the People's Republic of China. It is located in the southwest of Shaanxi Province, where shaanxi, Gansu and Sichuan provinces meet. Baoji city, Xi 'an city in the north, Ankang city in the east, Dazhou City, Bazhong City, Guangyuan City in Sichuan province in the south, longnan City in Gansu province in the west. Located in the qinling mountain and daba mountain transition zone, the north of the Qinling mountain, the south of daba mountain, the middle of the low hill basin. Jialing River from north to south across the city in the west, Han Water originated from the west east across the city. The city covers an area of 27,096 square kilometers, with a permanent population of 3,211,500 at the end of 2020 [48].

A. Fangjiayan Village, Chenggu County

a. Basic information

Fangjiayan Village is located in the northwest corner of Chenggu county, Hanzhong City. The local climate is continental monsoon climate. There are 11 groups of villagers, 450 households and 1081 people in the village. Fangjiayan village is relatively close to the urban area and developed well, most of which are modern houses. The terrain of Fangjiayan village is relatively flat and the distribution of residential houses is relatively compact (Figure 2-27).

Figure 2-27. Topographic map of Fangjiayan village.

b. The status quo of traditional houses

Traditional houses and modern houses coexist in Fangjiayan Village, accounting for about 38% of the total. The traditional houses in Fangjiayan Village, Chenggu County, are mostly in the shape of Stripe, "L" and "U", and adopt the form of civil structure, roof with green tiles and double slopes of hard mountain, and a few are in the form of hanging mountain (Figure 2-28).

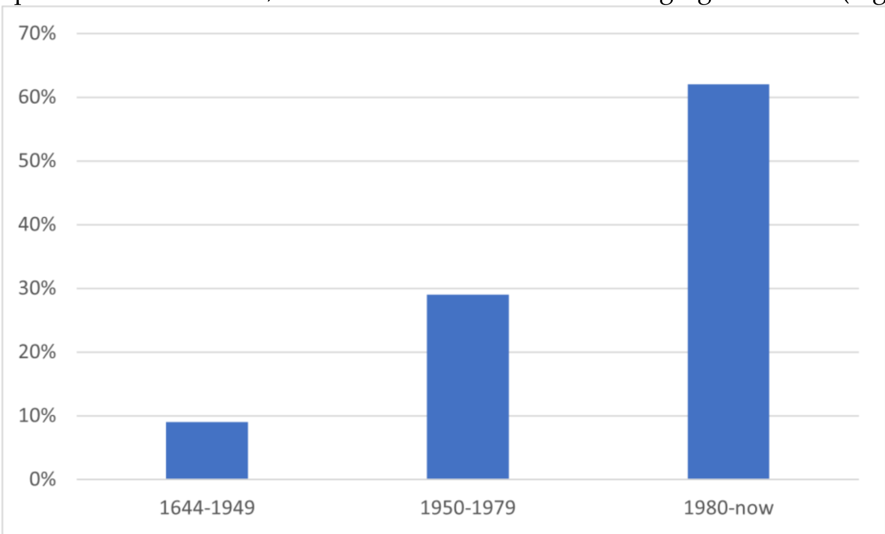

Figure 2-28. Statistical map of Fangjiayan Village residential buildings.

c. Cooking heating method

In the traditional residential houses of Fangjiayan village, firewood stoves are the main cooking methods, as well as coal stoves, gas stoves and electric cookers. More residents use biomass gasification gas (Figure 2-29).

Figure 2-29. Firewood stoves.

d. Residential building space

Space form: mostly Stripe type, "L" type, "U" type, civil structure, roof is green tile, double slope hard mountain form, A small number of hanging mountain form.

Spatial function: the Stripe type houses are composed of the main room, with the main room in the middle and ear rooms on both sides. "L" type houses are similar to Stripe type houses, but the difference lies in that there is only one side wing without courtyard walls. The "U" shape consists of the main room and the flanks.

Spatial scale: Stripe type residential base area of 70~100 square meters, including building area of 60~90 square meters, courtyard area of 20~30 square meters, the main room width of 3~6 rooms, the hall depth of 5~7 m, traditional residential buildings are mostly one layer, the height of 4~6 m, bluestone base 1~2 steps, step height of 10~20 cm, step width of 20~40 cm, The main room area is 40~80 square meters. The base area of "L" type houses is 100~130 m², including 80~100 m² building area, 20~40 m² courtyard area, 45~85 m² main house area and 30~50 m² wing area. "U" type base area of 100~130 square meters, including building area of 80~100 square meters, courtyard area of 20~40 square meters, main room area of 45~85 square meters, wing area of 30~60 square meters. According to the survey statistics, "L" shape accounted for 21% of the traditional residential houses, Stripe shape accounted for 68%, "U" shape accounted for 11% of the traditional residential houses (Table 2-12).

Table 2-12. Spatial index statistics of traditional residential buildings in Fangjiayan Village.

Category	Stripe type	"L" type	"U" type
Photo			
Floor plan	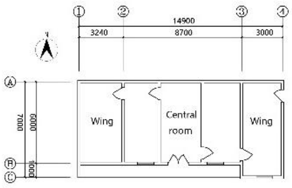	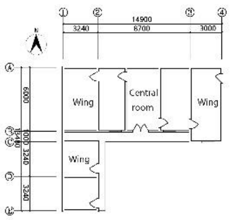	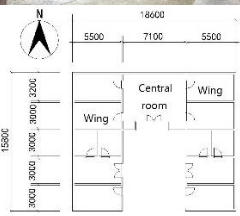
Homestead Area (m²)	70~100	100~130	100~130
Total construction area (m²)	60~90	80~100	80~100
Yard area (m²)	20~30	20~40	20~40
Entrance of main Room (m)	5~7		
Storey height (m)	4~7		
Base size (cm)	Base 2~3 steps, step height 10~20, step width 20~40		
Main room (m²)	40~75	40~55	40~65
Wing (m²)	30~50	-	30~50

B. Wenxing Village, Wenchuan Town

a. Basic information

Wenxing Village is an administrative village under the jurisdiction of Wenchuan Town, Chenggu County, Hanzhong City, Shaanxi Province. There are 13 groups of villagers, 463 households and 1345 people in the village. Wenxing Village and Wenxi village, Wenguang village, Wensu village, Wendong community, Maojialing village, united village adjacent. Xujiaping town medicine yard village distance from the urban area is relatively close to the development of better (Figure 2-30).

Figure 2-30. Topographic map of Wenxing village.

b. The status quo of traditional houses

In Wenxing Village, Wenchuan town, traditional houses coexist with modern houses, accounting for about 35% of the total. The traditional residential houses of Wenxing Village in Wenchuan town are mostly courtyard or Stripe type, "L" type and "U" type. Adopt civil structure, roof is green tile, double slope hard mountain form, a small amount of hanging mountain form (Figure 2-31).

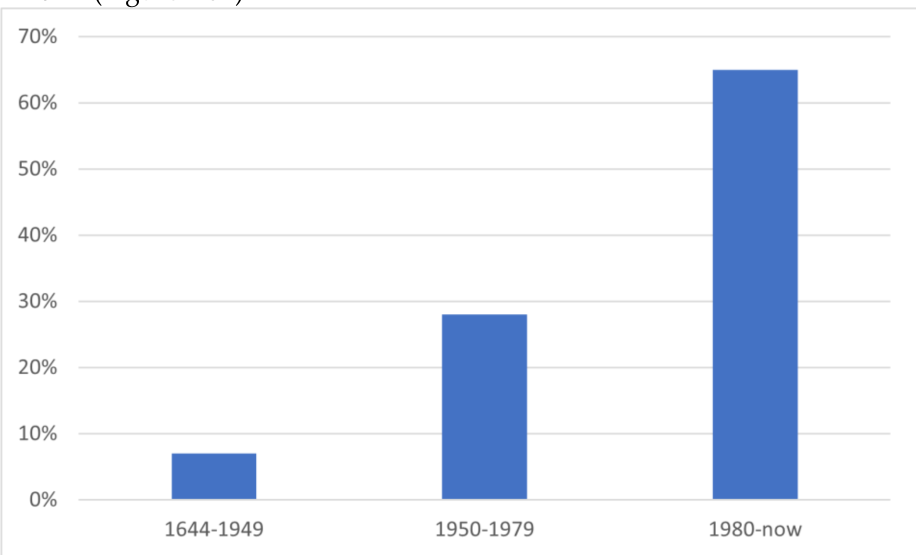

Figure 2-31. Statistical map of Wenxing Village residential buildings.

c. Cooking heating method

In wenxing village, Wenchuan town, firewood stoves are the main cooking methods, as well as coal-fired stoves, gas stoves and electric cookers (Figure 2-32).

Figure 2-32. Firewood stoves.

d. Residential building space

Space form: mostly courtyard type or Stripe type, "L" type, "U" type, civil structure, roof is green tile, double slope hard mountain form, A small number of hanging mountain form.

Space function: Courtyard type is composed of main room, side rooms on both sides and courtyard wall. The main room is composed of main room and wing room. The main room is used for receiving guests and living, the wing room is bedroom, and the wing room is storage and kitchen. The Stripe type houses are composed of the main house, with the main house in the middle and the ear rooms on both sides. "L" type residential houses are similar to courtyard type, the difference is that there is only one side wing without courtyard wall. The "U" shape consists of the main room and the flanks.

Space scale: the area of courtyard house is 120~150 m², of which the building area is 100~130 m², the courtyard area is 30~60 m², the main room area is 40~80 m², the wing area is 30~50 m², the courtyard area is 20~40 m². "U" type residential housing area is 100~150 m², of which the building area is 90~120 m² and the courtyard area is 30~50 m². The main room is 3~6 rooms wide and the main room is 5~7m deep. The traditional residential houses are mostly one story, the height is 4~7 m, the foundation is 2~3 levels, the steps are 15~30cm high and the stepping width is 20~35 cm. The main room is 40~85 square meters, and the wing is 30~60 square meters. The base area of Stripe type houses is 80~100 square meters, of which the building area is 80~120 square meters, and the courtyard area is 20~40 square meters. The main room is 3~6 rooms wide, the main room is 5~7 m deep, and the main room is 40~75 square meters. "L" type houses base area of 80~140 square meters, including building area of 80~100 square meters, courtyard area of 20~30 square meters, main room area of 40~75 square meters, wing area of 30~55 square meters. According to the investigation and statistics, courtyard type accounts for 5%, "U" type 10%, "L" type 25% and Stripe type 60% of the traditional houses (Table 2-13).

Table 2-13. Spatial index statistics of traditional residential buildings in Wenxing Village.

Category	Courtyard type	"U" type	Stripe type	"L" type
Photo				

Floor plan	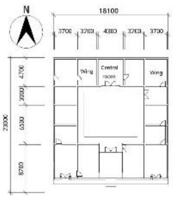	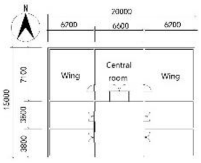	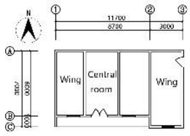	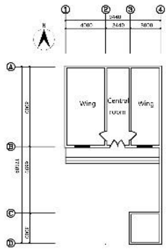
Homestead Area (m^2)	120~150	100~150	80~100	80~140
Total construction area (m^2)	100~130	90~120	80~120	80~100
Yard area (m^2)	30~60	30~50	20~40	20~30
Entrance of main Room (m)	5~7			
Storey height (m)	4~7			
Base size (cm)	Base 2~3 steps, step height 10~30, step width 20~35			
Main room (m^2)	40~80	40~85	40~75	40~75
Wing (m^2)	30~50	30~60	-	30~55
Patio (m^2)	20~40	-	-	-

C. Wensu Village, Wenchuan Town

a. Basic information

Wensu Village is an administrative village under the jurisdiction of Wenchuan Town, Chenggu County, Hanzhong City, Shaanxi Province. There are 12 groups of villagers in the village, 637 households and 1867 people. Wensu Village and Maojialing village, Wenxi village, united village, Wenxing village, Wenguang village, Wendong community adjacent. Wensu village is relatively close to the city and is well developed. The terrain of Wensu village is flat, the development of the whole village is square, and the distribution of residential houses is relatively dense (Figure 2-33).

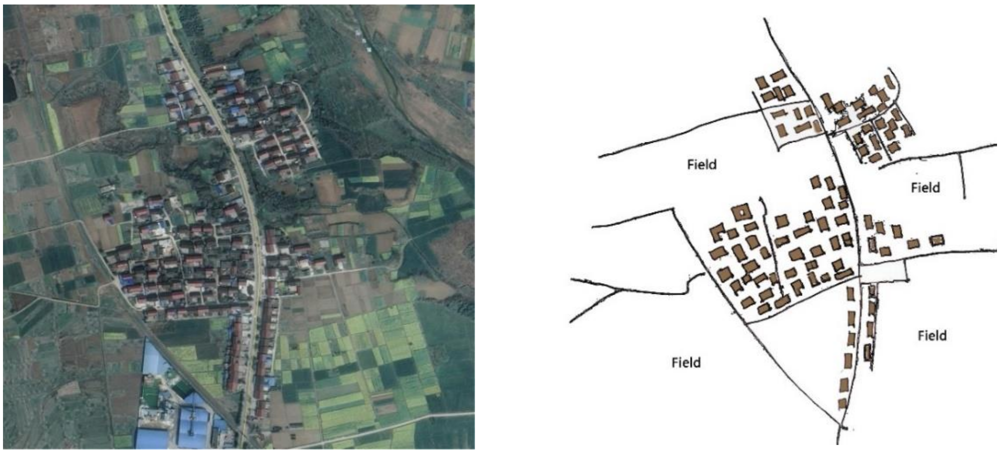

Figure 2-33. Topographic map of Wensu village.

b. The status quo of traditional houses

Traditional and modern houses coexist in Wensu Village, accounting for about 41% of the total. The traditional residential houses in Wensu Village are mostly courtyard or Stripe type or "L" type, with civil structure, roof with green tiles, double slope hard mountain form, and a small number of hanging mountain form (Figure 2-34).

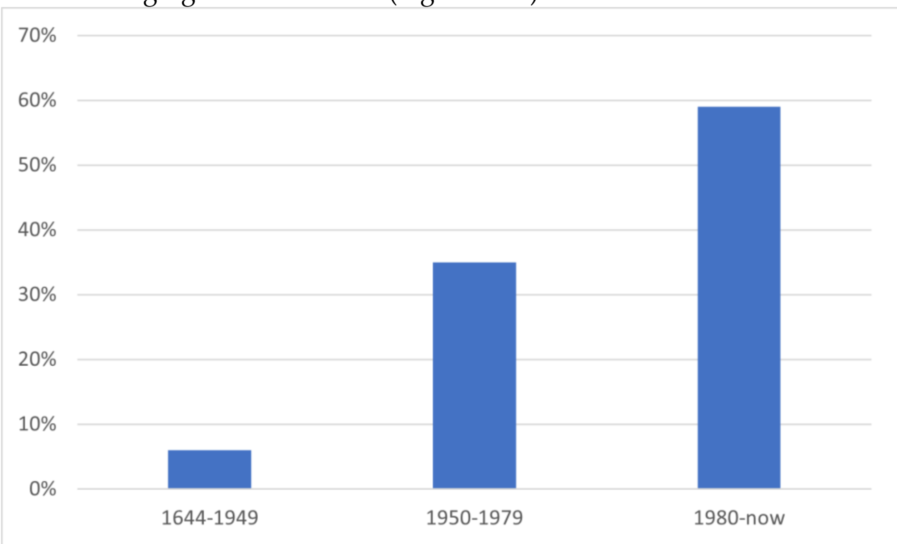

Figure 2-34. Statistical map of Wensu Village residential buildings.

c. Cooking heating method

In the traditional houses of Wensu Village, Wenchuan town, firewood stoves are the main cooking methods, as well as coal-fired stoves, induction cooker, gas stoves and electric cookers (Figure 2-35).

(a) (b)

Figure 2-35. (a) Gas stoves; (b) Induction cooker.

d. Residential building space

Space form: mostly courtyard type or Stripe type, "L" type, "U" type, civil structure, roof is green tile, double slope hard mountain form, A small number of hanging mountain form.

Space function: Courtyard type is composed of main room, side rooms on both sides and courtyard wall. The main room is composed of main room and wing room. The main room is used for receiving guests and living, the wing room is bedroom, and the wing room is storage and kitchen. The Stripe type houses are composed of the main house, with the main house in the middle and the ear rooms on both sides. "L" type residential houses are similar to a courtyard, the difference is that there is only one side wing without courtyard wall.

Space scale: The area of courtyard house is 100~160 m², including 110~130 m² building area, 30~50 m² courtyard area, 40~80 m² main house area, 30~50 m² wing area and 30~50 m² patio area. The base area of Stripe type houses is 90~110 square meters, of which the building area is 80~120 square meters, and the courtyard area is 20~50 square meters. The main room is 3~6 rooms wide, the main room is 5~7 m deep, and the main room area is 40~75 square meters. The base area of "L" type houses is 90~150 m², of which the building area is 80~110 m², the courtyard area is 20~40 m², the main room area is 40~70 m², and the wing area is 30~50 m². "U" type base area of 100~130 square meters, including building area of 80~100 square meters, courtyard area of 20~40 square meters, main room area of 45~85 square meters, wing area of 30~60 square meters. According to the investigation and statistics, courtyard type accounts for 5% of traditional houses, "U" type accounts for 10%, "L" type accounts for 20%, and Stripe type accounts for 65% (Table 2-14).

Table 2-14. Spatial index statistics of traditional residential buildings in Wensu Village.

Category	Courtyard type	"U" type	Stripe type	"L" type
Photo				
Floor plan	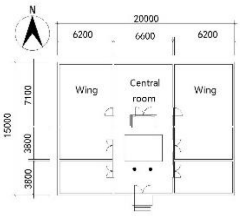	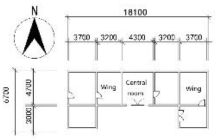	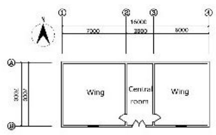	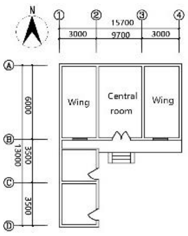
Homestead Area (m²)	100~160	100~130	90~110	90~150
Total construction area (m²)	110~130	80~100	80~120	80~110
Yard area (m2)	30~50	20~40	20~50	20~40

Entrance of main Room (m)	5~7			
Storey height (m)	4~7			
Base size (cm)	Base 2~3 steps, step height 15~30, step width 20~35			
Main room (m^2)	40~80	45~85	40~75	40~70
Wing (m^2)	30~50	30~60	-	30~50
Patio (m^2)	30~50	-	-	-

D. Junwang Village, Bowang Street

a. Basic information

Junwang Village is an administrative village under the jurisdiction of Bowang Street, Chenggu County, Hanzhong City, Shaanxi Province. The climate is characterized by no severe cold in winter and no hot heat in summer, abundant rainfall and rainy seasons. The village has jurisdiction over 10 natural villages, 19 villagers' groups, the village has 812 households, 2711 people. Junwang village and he Jiaqiao village, Wulimiao village, Zhou Jiayan village, Shu Jiaying village, Rao Jiaying village, three villages, Victory village, Dongfanghong village, Dujiaying village, East Village, Bo Wang village, Daxiguan village, Hekan village, liaoyuan company community adjacent. Junwang village is far from the urban area more general development. Junwang Village is rich in forest resources, and its topography is mainly hilly, forming a good landscape pattern (Figure 2-36).

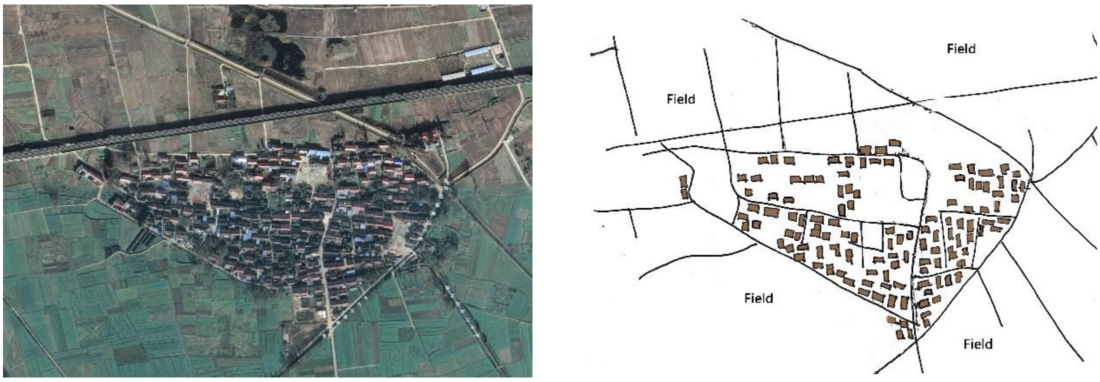

Figure 2-36. Topographic map of Junwang village.

b. The status quo of traditional houses

In Junwang Village, traditional houses coexist with modern houses, accounting for about 25% of the total. The traditional residential houses in Junwang Village are mostly courtyard or Stripe type or "L" type, with civil structure, roof with green tile, double slope hard mountain form, and a small number of hanging mountain form (Figure 2-37).

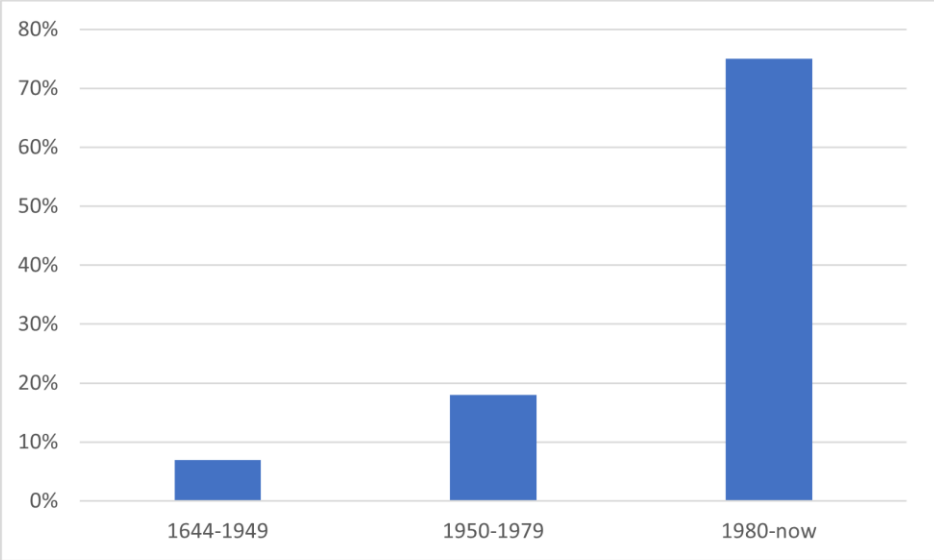

Figure 2-37. Statistical map of Junwang Village residential buildings.

c. Cooking heating method

In the traditional houses of Junwang Village, firewood stoves are the main cooking methods, as well as coal stoves, gas stoves and electric cookers (Figure 2-38).

Figure 2-38. Firewood stoves.

d. Residential building space

Space form: mostly courtyard type or Stripe type or "L" type, civil structure, roof with green tiles, double slope hard mountain form, A small number of hanging mountain form.

Space function: Courtyard type is composed of main room, side rooms on both sides and courtyard wall. The main room is composed of main room and wing room. The main room is used for receiving guests and living, the wing room is bedroom, and the wing room is storage and kitchen. The Stripe type houses are composed of the main house, with the main house in the middle and the ear rooms on both sides. "L" type residential houses are similar to a courtyard, the difference is that there is only one side wing without courtyard wall.

Space scale: the area of courtyard house is 100~150 m^2, including building area of 90~135 m^2, courtyard area of 30~50 m^2, main room area of 30~50 m^2, wing area of 30~65 m^2, patio area of 20~50 m^2. The base area of Stripe type houses is 90~115 square meters, of which the building area is 80~100 square meters, and the courtyard area is 20~50 square meters. The main room is 3~6 rooms wide, the main room is 5~7 m deep, and the main room area is 30~50 square meters. The base area of "L" type houses is 90~140 square meters, including building area of 80~100 square meters, courtyard area of 20~40 square meters, main room area of 30~50 square meters, wing area of 30~50 square meters. According to the survey and statistics, courtyard type accounts for 3%, "L" type 35% and Stripe type 62% of traditional houses (Table 2-15).

Table 2-15. Spatial index statistics of traditional residential buildings in Junwang Village.

Category	Courtyard type	Stripe type	"L" type
Photo			
Floor plan	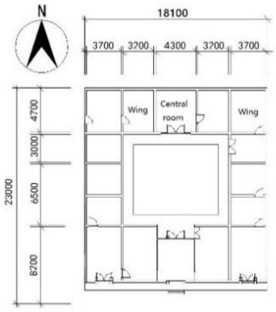	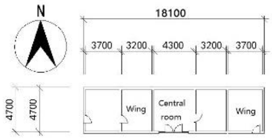	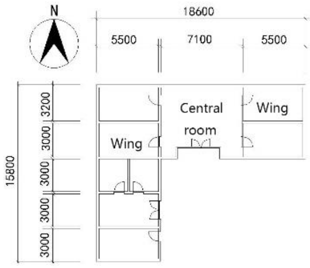
Homestead Area (m²)	100~150	90~115	90~140
Total construction area (m²)	90~135	80~100	80~100
Yard area (m²)	30~50	20~50	20~40
Entrance of main Room (m)		5~7	
Storey height (m)		4~7	
Base size (cm)		Base 2~3 steps, step height 15~30, step width 20~35	
Main room (m²)	30~50	30~50	30~50
Wing (m²)	30~65	-	30~50
Patio (m²)	20~50	-	-

2.3.3 Spatial Functions of Residential Houses

(1) Spatial Form

A. Spatial form investigation and analysis

Among them, Stripe type accounts for the largest proportion, which is due to the reduction of family population, adaptation to the terrain, full use of spatial terrain and meet the basic living needs. There are many l-shaped houses, which are less restricted by geography, and can meet people's living needs. Besides, there is a close connection between indoor and outdoor space. The second is the number of "U" shaped houses, which are in a semi-closed state. Courtyard of siheyuan is the least spatial form of residential houses in southern Shaanxi, the reasons are limited by terrain, family size reduction, economic pressure and other factors (Table 2-16).

Table 2-16. Statistical table of survey on the shape of courtyards in southern Shaanxi.

Number	Village	Courtyard type	"L" type	Stripe type	"U" type
1	Hua yuan	10%	30%	60%	-
2	Jing zhong	-	20%	65%	15%
3	Ping an	10%	35%	55%	-
4	Tao yuan	-	25%	65%	10%

5	Li jiatai	14%	21%	65%	-
6	Jiang Bei	10%	35%	55%	-
7	Huang nigou	10%	25%	65%	
8	Sha gou	-	37%	50%	13%
9	Fang jiayan	-	21%	68%	11%
10	Wen xin	5%	25%	60%	10%
11	Wen gou	5%	20%	65%	10%
12	Jun wang	3%	35%	62%	-
Average value		5.58%	27.42%	61.25%	5.75%

B. Investigation and analysis of apartment type area

The spatial forms of traditional houses in southern Shaanxi are diverse, and there are also differences in house types. Through the investigation and analysis of residential housing type in southern Shaanxi, the following data are obtained.

There is a small difference between the residential area and the total construction area in southern Shaanxi, which is due to the shortage of land in southern Shaanxi, and the building area is greatly affected by topography, so the residential area is small. According to the field survey, the height of residential buildings generally ranges from 4 to 7m, and residents use the building height to design mezzanine lofts to meet their storage needs (Table 2-17).

Table 2-17. Survey and statistics of traditional folk houses in southern Shaanxi.

Region	Homestead Area (m^2)	Total construction area (m^2)	Yard area (m^2)	Entrance of main Room (m)	Storey height (m)	Main room (m^2)	Wing (m^2)	Patio (m^2)
Hua yuan	120~150	90~120	30~70	5~6	4~5	40~80	54~75	20~40
Jing zhong	90~100	60~70	20~40	5~6	3~5	44~70	-	-
Ping an	130~160	100~130	30~50	5~6	4~5	40~80	40~70	20~40
Tao yuan	90~180	70~80	20~50	5~6	4~5	45~70	-	-
Li jiatai	110~150	80~130	20~50	5~7	5~7	40~80	45~75	20~40
Jiang Bei	130~160	100~130	30~60	5~7	4~6	40~75	40~50	20~40
Huang nigou	140~160	90~130	20~50	5~7	4~6	50~85	30~50	20~40
Sha gou	95~110	80~90	20~60	5~7	4~6	40~55	-	-
Fang jiayan	70~180	60~90	20~60	5~7	4~6	40~80	-	-
Wen xin	80~100	80~100	20~60	5~7	4~7	40~75	-	-
Wen gou	90~110	80~100	20~50	5~7	4~7	40~75	-	-
Jun wang	90~115	80~100	20~50	5~7	4~7	30~50	-	-
Average value	120~180	90~150	20~60	5~7	4~7	40~85	30~75	20~40

(2) Constituent Elements

Courtyard is an important element in traditional Chinese architecture, which can give people a strong sense of domain and at the same time connect with the natural environment. Courtyards of residential houses not only satisfy the ventilation and lighting of each room, but also accommodate a variety of activities in daily life, such as receiving guests and treating friends, planting flowers, drying storage and housework.

The main room is the most important activity space in hanzhong folk houses. It is located on the axis of fengshui and used to worship gods, Buddhas or ancestors. It reflects the ethical thought of "centrality is the highest" in traditional Chinese society. The main room is connected to the courtyard and the outside, and is connected to the parents' bedroom on both sides. It is the center of different spatial connections within the house. In modern new residential houses, there are few family worship activities in the bedroom, but the main room space still retains its central character and is used as a special space while connecting various Spaces in the house.

The wing rooms are located on both sides of the axis, arranged symmetrically according to the hierarchical order of Zuo Zhao and Mu, and are generally inhabited by children. The wing is the main rest space, its doors and windows are open to the inner courtyard, the opening and depth is relatively small, conducive to the security and privacy of the space. Most of the traditional residential houses are built on both sides of the gable to serve as kitchen or storage room, while the toilets are set up randomly. Most of them are placed outside the yard, adjacent to pigsty and chicken pen, and some are set up in the yard with independent dry toilets, with relatively simple facilities (Table 2-18).

Table 2-18. Constituent elements.

Constituent Elements	Function	Photo
Courtyard	To meet the ventilation and lighting of each room; Receive a visitor. Kind of Plant; Drying; Adjust microclimate	
central room	Sacrifice; Receive a visitor	
wing	Bedroom, Kitchen	
auxiliary	Toilet	

(3) Layout

By taking real photos and mapping the layout of residential houses, the layout of residential houses can be classified into four forms: one font, L shape, U shape and quadrangle courtyard.

One-character houses are small in size and simple in shape, which is the most common planar layout in Hanzhong area. This kind of residential houses are weakly affected by terrain, and most of them are located in the mountains. They can be flexibly distributed on the mountainside or the foot of the mountain in accordance with the contour line of terrain. Their basic shape is a large open room in the middle and bedrooms or auxiliary rooms on both sides.

L-shaped residential houses are the derivation of one-character residential houses, and their spatial form is to add other use space on the basis of one-character residential houses according to terrain changes. That is, the wing or other auxiliary rooms are arranged on one side of the axis of the hall, so that its plane shape has a semi-enclosed form. But it does not have a closed courtyard surrounded by walls or architectural entities.

U-shaped residential houses are composed of hall and wing, and the overall space shape is U-shaped. Compared with l-shaped houses, the room area is increased. That is, the wing or other auxiliary rooms are arranged on both sides of the axis of the hall, so that its plane shape has a semi-enclosed form.

Courtyard residential houses are a planar system enclosed by the main room, wing room, courtyard wall and auxiliary rooms, with a cohesive and private courtyard space. Through the combination of multi-yard system to form a large scale, high shape of the large house. The architectural space of mouth shaped layout is relatively open and orderly, with multiple houses arranged orderly on both sides of the axis, and the internal courtyard is relatively long and narrow, which is common in the relatively flat Hanzhong Basin (Table 2-19).

Table 2-19. The layout of residential houses.

Layout forms	Schematic diagram	Photo
Courtyard type	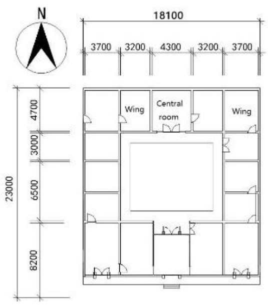	
"U" type	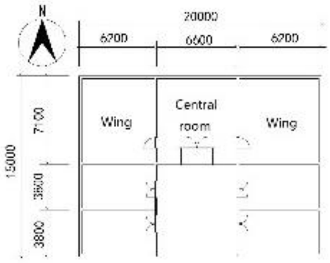	
"L" type	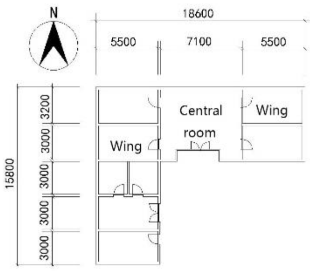	

Stripe type	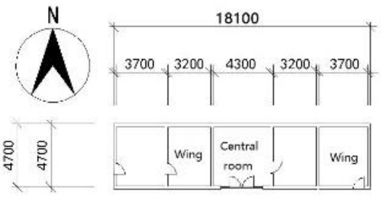	

2.3.4 Construction Technology of Residential Houses

(1) Function Zones Building Structure

With the improvement of economic level, the increase of living space scale and other factors, the traditional residential houses in southern Shaanxi have changed in the process of evolution, and the structure has also changed from the previous through type and civil structure to brick and wood, brick and concrete structure. The height of residential buildings is mostly one story, and a small number of residential buildings are two stories. The construction technology of residential houses has been improved. The brick and concrete structure of residential buildings is relatively high, and the height of the building is mostly one layer. The building material also takes brick as the main material (Table 2-20).

Table 2-20. Residential materials.

Village	Building structure			Building height		Building materials		
	Soil-wood (%)	Brick-wood (%)	Brick (%)	One layer (%)	Two layer (%)	Soil (%)	Wood (%)	Brick (%)
Hua yuan	21.3	21.6	57.1	91.3	8.7	22.3	42.3	35.4
Jing zhong	18.5	20.1	61.4	90.5	9.5	18.2	36.8	45
Ping an	16.3	18.4	65.3	92.1	7.9	19.3	36.4	44.3
Tao yuan	17.3	22.6	60.1	95.3	4.7	24.2	35.6	40.2
Li jiatai	19.4	18.4	62.6	91.5	8.5	18.6	36.9	44.5
Jiang Bei	16.4	16.8	66.8	92.5	7.5	18.6	37.8	43.6
Huang nigou	18.3	17.8	63.9	93.1	6.9	17.2	35.9	46.9
Sha gou	19.4	16.7	63.9	92.1	7.9	18.6	38.9	42.5
Fang jiayan	21.3	22.5	56.2	94.1	5.9	19.1	39.8	41.1
Wen xin	18.4	13.5	68.1	92.3	7.7	18.4	38.6	43
Wen gou	15.6	16.9	67.5	92.6	7.4	17.8	39.8	42.4
Jun wang	17.5	15.6	66.9	91.8	8.2	16.8	40.3	52.9
Average value	18.3	18.4	63.3	92.5	7.5	19	37.6	43.4

(2) Building Materials

The selection of residential building materials depends on the local climate, terrain and economy. Traditional houses in southern Shaanxi have good adaptability to terrain and climate, and the building materials are adapted to local conditions. Rammed earth is usually used as the envelope structure, and gravel is mixed in the adobe to enhance the density of the wall and ensure the shear resistance of the wall.

Stone materials are often used as wall foundations and columns in traditional houses in southern Shaanxi to enhance the stability and firmness of buildings. The mixed masonry wall of pebble and green brick increases the service life of the wall and the ability to prevent rain. Regular or irregular stone paving or masonry is used in steps, patio floor paving, corvees base and so on. The durability of the stone also extends the service life of buildings and other components.

Lumber classics is processed, carve acts the role offing to use as main body bearing component, adornment sex door window and indoor common furniture more. In addition, traditional construction also retains the construction skills of firing clay into green tiles or bricks, which are often used for building roof engineering and ground decoration, adding bricks and tiles to the beautiful appearance of the house (Figure 2-39).

Figure 2-39. Wood carving.

2.3.5 Features and Characteristics of Residential Houses

The regional style of folk houses refers to the mutual integration of folk houses and environment in a certain geographical range, which is marked with the brand of region. Folk houses are unique and representative [49]. Traditional houses in southern Shaanxi are the inheritance of Thousands of years of Chinese culture as well as the accumulation of architectural culture [50]. The analysis of roof shape and color and wall color of traditional houses in southern Shaanxi provides data support for further analysis of traditional houses in southern Shaanxi.

As shown in the figure2-40, the roof shape of traditional houses in southern Shaanxi is mainly sloping roof with deep eaves [51,52]. The roof is mostly made of green tiles, so the roof color is mainly cyan. A small number of residential roofs are made of stone and the color of the roof is black. The walls of the building are yellow and white, and the whole building is primitive [53]. The traditional houses in southern Shaanxi reflect the strong local characteristics [54,55].

Figure 2-40. Residential houses.

The color of building facade can be divided into basic color and decorative color according to the size of the area. The large area of basic color determines the main tone of residential buildings, which is used for the main wall. The area of decorative color is less than the basic color, but it is also very important. It is generally used for the roof, doors, windows and dado of the building, playing the role of ornament and decoration. Through investigation and research of local-style dwelling houses in visit, found the local-style dwelling houses in southern Shaanxi is using a lot of wooden beams and wooden eaves wall with more sophisticated, but most do not use color paint or bottom color process for color, but the more easy tung oil process for wood and its surface protection, as much as possible to keep the color and texture of the nature of the wood Therefore, folk houses in southern Shaanxi like to pursue and show the natural beauty of materials. The main building materials of traditional folk houses in southern Shaanxi are white wall, grey tile and blue brick. These materials set off each other and are interlaced to form the overall style of light and simple and elegant buildings. The color system of white wall, wood door panel and gray tile of traditional residential buildings in southern Shaanxi is extracted, and applied to the design of new buildings, the main color of walls should be white, and the architectural decoration should be gray and wood brown. Through the optimization and refinement of traditional architectural colors, simple and elegant architectural connotations are formed. At the same time, the architecture can be fully integrated into the environment, forming a dialogue with the environment, revealing the primitive and simple local flavor (Table 2-21).

Table 2-21. Residential landscape.

Village	Roof shape		Roof color		Wall color	
	Flat (%)	Slope (%)	Blue (%)	Black (%)	Yellow (%)	White (%)
Hua yuan	88.2	11.8	84.5	15.5	57.5	42.5
Jing zhong	86.2	13.8	89.2	10.8	53.2	56.8
Ping an	88.1	11.9	88.7	11.3	51.6	48.4
Tao yuan	87.5	12.5	89.6	10.4	54.6	45.4
Li jiatai	86.7	13.3	87.9	12.1	56.2	43.8
Jiang Bei	85.6	14.4	89.9	10.1	57.4	42.6
Huang nigou	86.7	13.3	87.9	12.1	55.9	44.1
Sha gou	84.7	15.3	88.7	11.3	58.3	41.7
Fang jiayan	82.6	17.4	86.1	13.9	59.5	40.5
Wen xin	87.6	12.4	86.9	13.1	57.5	42.5
Wen gou	88.7	11.3	88.9	11.1	53.5	46.5
Jun wang	89.4	10.6	89.9	10.1	56.7	43.3
Average value	86.9	13.1	88.2	11.8	56	44

2.4 Indoor Thermal Comfort of Residential Houses

2.4.1 Current Lifestyle

In rural areas of southern Shaanxi, the cooking equipment used in traditional houses is generally a wood stove; the cooking equipment used in modern houses generally includes a gas stove, electric rice cooker, and induction cooker. In our field investigation, it was found that traditional cooking equipment and modern cooking equipment were used together in the same families (Figure 2-42). The frequency of using wood stoves was 79.3%; the frequency of using gas stoves was 4.1%; and the frequencies of using electric rice cookers and induction cookers were 11.3% and 5.3% (Figure 2-43 a), respectively. It can be seen that the use of wood stoves is still common. The stove is generally located in a corner of the kitchen, and a flue is provided on one side of the stove for smoke exhaust.

(a)

(b)

(c)

(d)

(e)

Figure 2-41. (a) Infrared imager; (b) Temperature measuring instrument; (c) Wind speed measuring instrument; (d) Measuring distance instrument; (e) Illuminance instrument.

Mainly used the following instruments (Figure 2-41): infrared imager, wind speed measuring instrument, measuring distance instrument, illuminance instrument, temperature measuring instrument (Table 2-22).

Table 2-22. Instrument data.

Equipment	Type	Range	Accuracy
Infrared imager	HM-TPH11-3AXF	-20～350 ℃	±0.5 ℃
Temperature and humidity measuring instrument	AS847	-10～50 ℃ 5%RH ~ 100% RH	±1.5 ℃ ±3% RH
Anemometer	AR866A	0～30 m/s	±1 m/s
Distance measuring equipment	DL331070	0～70 m	±3 mm
Illuminance meter	AS823	0～200000 Lux	±5%


Figure 2-42. Photo of the present situation of cooking in southern Shaanxi.

In terms of the duration of a single cooking session, the average durations in summer and winter are 60.3 min and 75.2 min, respectively, with small differences between the winter and summer. The field survey results show sessions of 0–30 min for 20.2% and 21.3% of homes in summer and winter, respectively, and sessions of 30–60 min for 34.6% of homes in summer and 36.3% of homes in winter. The time of 60–90 min was taken in the highest proportion of homes, with 45.3% and 36.6% in summer and winter, respectively. Sessions of more than 90 min, mainly in winter, accounted for 5.9% (Figure 2-43 b). It can be seen that the duration of a single cooking session in winter is generally 60–90 min. The main reason for this is that, in addition to meeting basic human needs, families must also prepare livestock food in winter, as well as heating their houses and water using a wood stove to reduce the cost of living. Cooking is also related to eating activities. Through field research, we can see that, in summer, the proportion of families cooking three meals a day is 86.4%, the proportion of families cooking two meals a day is 10.2%, and the proportion of families cooking one meal a day is 3.4%. In winter, the proportion of families cooking three meals a day is 97.3% and the proportion of families cooking two meals a day is 2.7% (Figure 2-43 c). From this, we can deduce that most families in this area cook three meals a day. Field research was conducted on the times every day when the three meals are cooked. In winter, 89.5% cooked in the period 8:30–9:30 in the morning, 91.6% cooked in the period 11:30–12:30 in the afternoon, and 88.6% cooked in the period 5:30–6:30 in the evening (Figure 2-43 d).

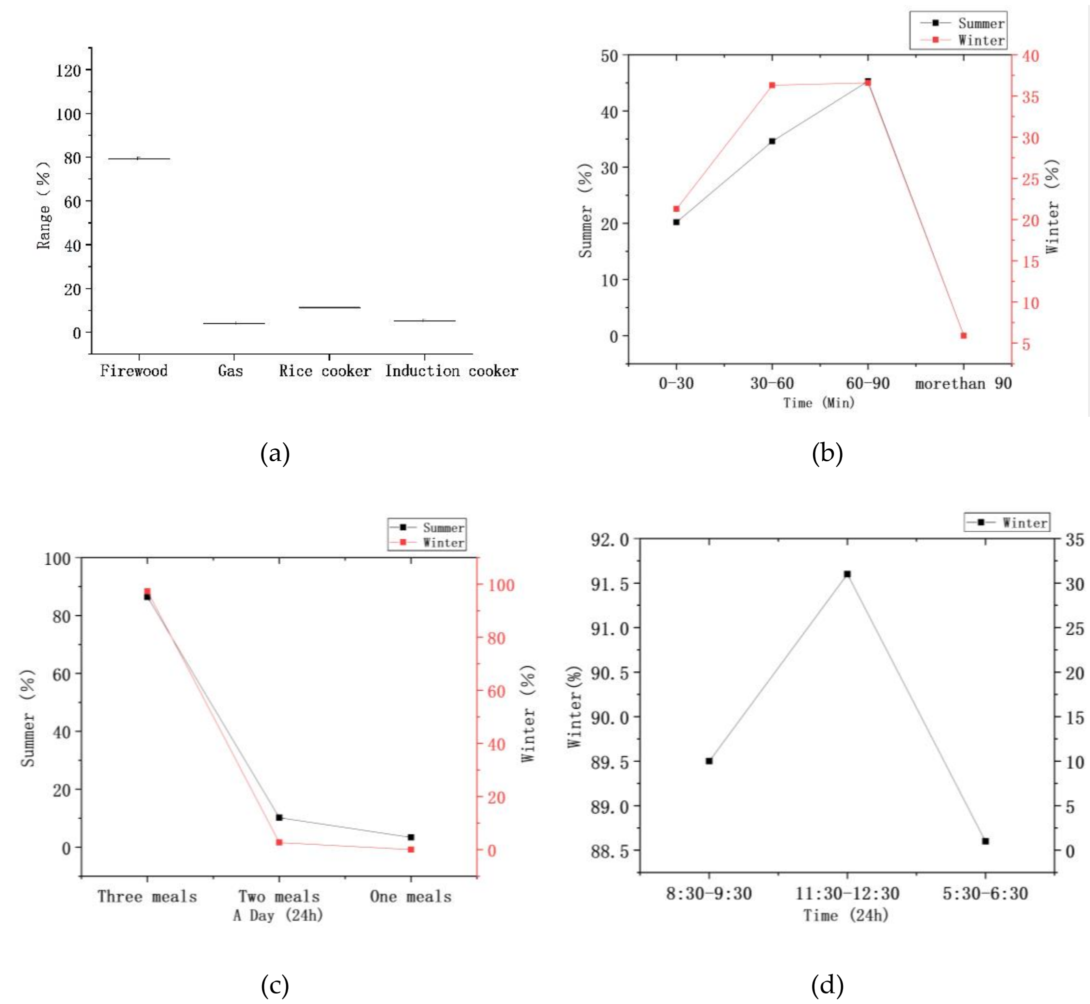

Figure 2-43. (a) Frequency of using cooking equipment; (b) Time taken for a single cooking session; (c) Number of meals a day; (d) Time taken for cooking three meals a day.

2.4.2 Current Heating Methods

As shown in the figure 2-44, traditional heating methods include the use of a fire pit, charcoal fire basin, fire pond, etc., which can also be used for cooking; the main use of firewood and charcoal is as an open heat source, causing indoor pollution during combustion, which is a serious issue. Modern heating equipment uses electric energy—for example, electric heating fans, foot warmers, and electric ovens. Additionally, baking tables burn biomass. In the field survey, 69.3% of residences used firewood for heating energy, 16.7% used carbon, 6.7% used coal, and 7.3% used electricity. The test time was December 26, 2020, and the test location was the traditional residences of Zhongshan Village in southern Shaanxi. The test objects were 5 items: fire ponds, charcoal braziers, fire tables, wood stoves, and electric fans. The instrument used for testing was an infrared imager (Type HM-TPH11-3AXF), which was used to measure the temperature distribution of cooking equipment and the temperature of the surface of human body. The range of the instrument parameters was −20 to 350 ℃, and the sensitivity was 0.5 ℃. The measuring position was 1.5 m away from the cooking equipment and human body. When measuring the data, we tried to keep the object and human body in a stable state and take pictures and measurements at a distance of 1.5 m from the ground. By using an infrared thermal imager to test the temperature distribution of traditional and modern heating equipment, we found that the average heat source temperature of traditional heating equipment is generally higher than that of electric heating equipment. The average fire pond temperature was 103.68 ℃ and the highest temperature was 245.68 ℃ (Figure 2-45 a). The average temperature of the charcoal brazier heat source was 203.43 ℃ and the highest temperature was 241.24 ℃ (Figure 2-45 c). The average temperature of the furnace body of the baking table was 111.32 ℃ and the highest temperature was 142.73 ℃; the average temperature of the table top was about 25.31 ℃ (Figure 2-45 e). The firewood stove was also one of the indoor heat sources analyzed. The average temperature of the stove wall was 110.34 ℃, the highest temperature was 232.32 ℃, and the average temperature of the pot body was 156.35 ℃ (Figure 2-45 g). The highest temperature of the heating element of electric heating equipment was 231.36 ℃, but the average temperature was only 50.26 ℃ (Figure 2-45 i). The surface area of the heat source was generally smaller than that of the traditional heating equipment.

(a) Fire pond

(b) Charcoal brazier

(c) Baking table

(e) Firewood stove

(f) Heating element

Figure 2-44. (a) Fire pond; (b) Charcoal brazier; (c) Baking table (d) Firewood stove; (e) Firewood stove; (f) Heating element.

Using an infrared thermal imager to test the temperature distribution on human body surface when near heating cooking equipment, it was found that the average surface temperature of human body when facing away from the heat source was 37.02 ℃/10.52 ℃ (fire pond) (Figure 2-45 b), 32.93 ℃/14.32 ℃ (charcoal brazier) (Figure 2-45 d), 18.03 ℃/7.07 ℃ (fire table) (Figure 2-45 f), 6.02 ℃/4.21 ℃ (wood stove) (Figure 2-45 h), and 36.68 ℃/13.96 ℃ (electric fan) (Figure 2-45 j). Comparing non-open heat sources (roasting tables, wood stoves) with using open heat sources (fire ponds, charcoal braziers), the body surface temperature rises more. The average temperature differences between the side facing the heat source and the side facing away from the heat source differ by values of 26.5 ℃ (fire pond), 22.72 ℃ (electric fan), 18.76 ℃ (charcoal basin), 10.96 ℃ (fire table), and 1.81 ℃ (firewood stove).

Cooking temperature distribution

Cooking and human body temperature distribution

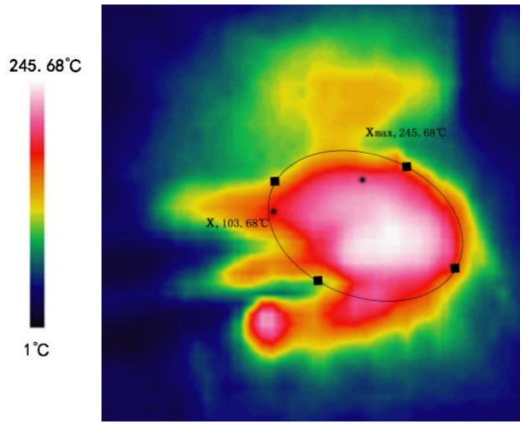

(a) Fire pond

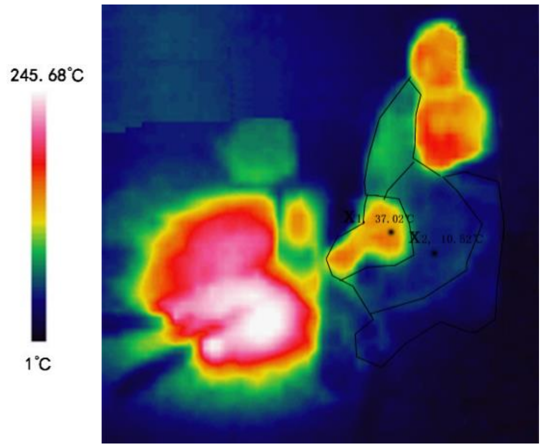

(b) Fire pond

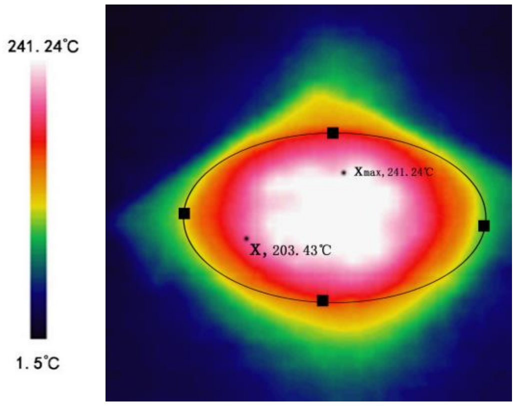

(c) Charcoal brazier

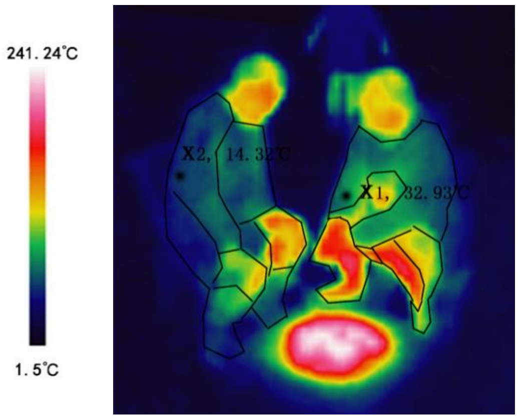

(d) Charcoal brazier

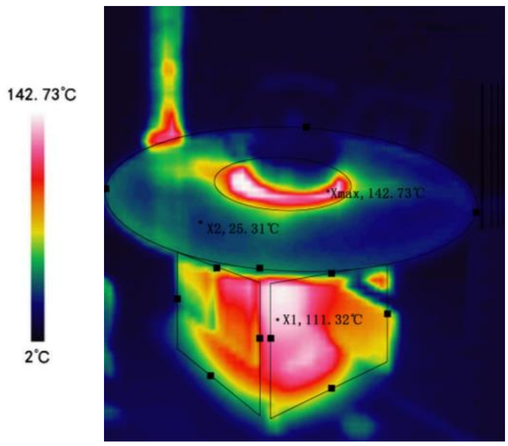

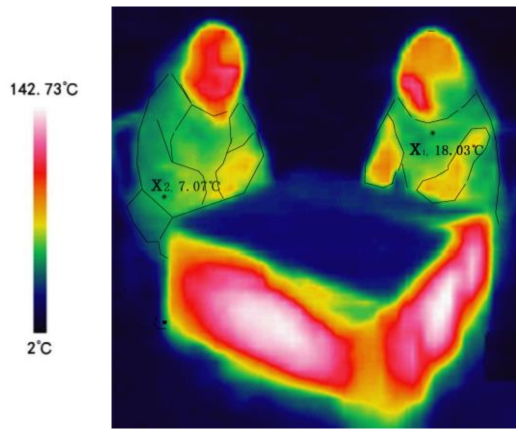

(e) Baking table

(f) Baking table

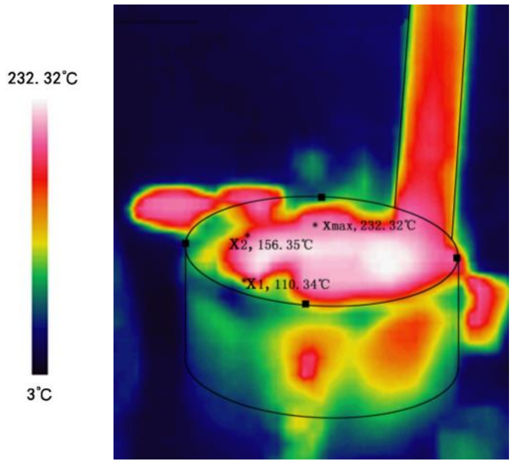

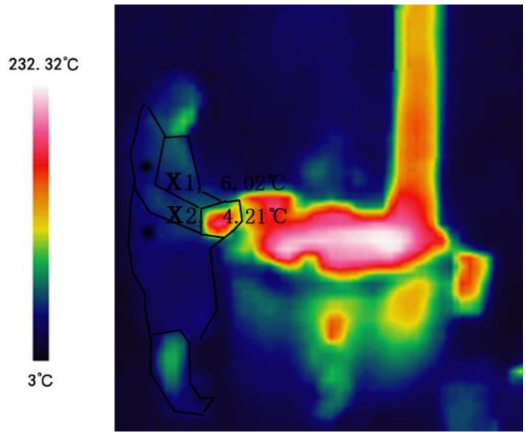

(g) Firewood stove

(h) Firewood stove

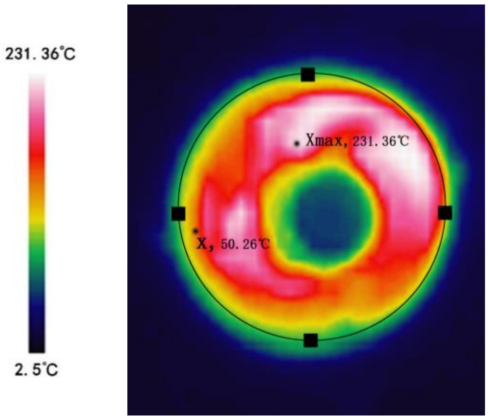

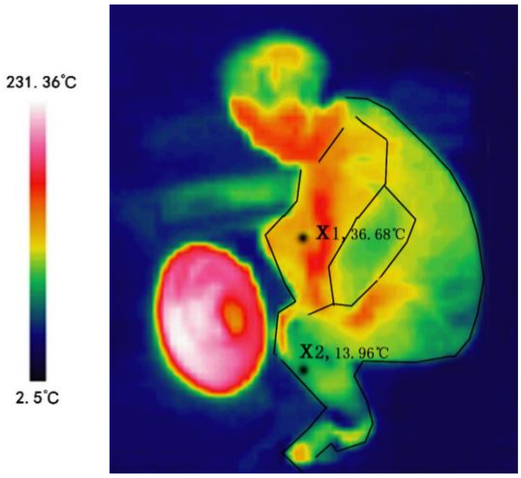

(i) Heating element

(j) Heating element

Figure 2-45. (a) Fire pond temperature distribution; (b) Fire pond and human body temperature distribution; (c) Charcoal brazier temperature distribution; (d) Charcoal brazier and human body temperature distribution; (e) Baking table temperature distribution; (f) Baking table and human body temperature distribution; (g) Firewood stove temperature distribution; (h) Firewood stove and human body temperature distribution; (i) Heating element temperature distribution; (j) Heating element and human body temperature distribution.

According to the modern heating mode of electric heating fan, electric heater, electric oven power and use time statistics. The statistical time is December 26, 2020, and the statistical place is the traditional houses of Zhongshan Village in southern Shaanxi. A total of 43 households were counted effectively. Among them, there are 20 electric fans, 15 foot warmers and 8 electric ovens. In a word, the heating equipment used in rural areas of southern Shaanxi focusses on local heating as its goal. No matter what type of heating equipment is used, it will focus on local heating, improving the local surface temperature of human body (especially in the limbs) and the indoor local temperature (Table 2-23 2-24 2-25).

Table 2-23. The power of the electric fan.

The power of the electric fan(W)	**550-650**	**650-750**	**750-850**
Households	4	5	11

Table 2-24. The power of the electric heater.

The power of the electric heater (W)	1400-1600	1600-1800	1800-2000
Households	4	8	3

Table 2-25. The power of the electric oven.

The power of the electric oven (W)	1200-1500	1500-1800	1800-2100
Households	2	5	1

2.4.3 Current Physical Environment

(1) Test

The physical environment of residential houses involves wind speed, humidity, temperature, ventilation and lighting, noise and other factors. By testing the physical environment of residential houses in southern Shaanxi, the actual values of indoor temperature and humidity, ventilation and other physical environment can be understood.

Hong Village, Houliu Town, Shiquan County, Ankang City, was selected as the physical environment test object through investigation. Because of the special geographical environment, Hong village has a typical valley landform (Figure 2-46). The Stripe shaped residential house was selected as the test object. The residential house was built in 1970. The building walls were made of brick and concrete structure, and the building height was 5m. This study refers to the test method of "Evaluation Standard for Indoor Thermal and Humid Environment of Civil Buildings" (GB/T50785-2012) and "Building Physical Environment and Design", and designs the test experiment of residential houses, selecting 7 temperature and humidity blocks, 2 anemometers, and 2 illuminance meters. Winter testing will be conducted from 9:30 on December 21, 2019 to 9:30 on December 23, 2019 under completely overcast conditions. The selection of this time period is mainly on the winter solstice, which is the extreme point where the sun directly travels southward, and the sun directly hits the Tropic of Capricorn on this day. It is the day with the shortest day and the longest night in the northern hemisphere.

Figure 2-46. Topographic satellite map of Hong village.

Three main rooms (main room, bedroom 1, bedroom 2) and one outdoor space were selected as the tested space. Temperature and humidity blocks were arranged in the center of the plane of the tested space, 1.1m above the ground. The temperature and humidity block was set to record the value every 1h when the outdoor location was 1.1m away from the ground. The anemometer was selected to be placed in the center of the room and instantaneous velocity measurements were made every 2s. The measurement height is 1.7m away from the ground, which belongs to the intuitive position when human body stands, and the horizontal distance between each measurement point and the wall is greater than 0.5m. In the lighting room of residential houses, two measuring lines were vertically arranged in the middle of windows and walls between Windows, with a height of 0.8m from the ground, and measuring points were arranged at intervals of 1.5m. Limited by the instrument, in order to ensure the stability of the optical environment, the instrument takes a reading at every point at an interval of 2s, records 3 times, and finally takes the arithmetic mean value as the illumination value of the measuring point (Figure 2-47).

To avoid adverse effects during the test, the measurement team conducted a standard of personnel behavior: during the wind speed test, ensure that people in the room remain still. During the illuminance test, ensure that the handheld sensor stays up and vertical, and prevent alternating shadows near the window. Avoid doors and windows opening and closing throughout the test. According to the selection of instruments and the needs of the results, the research team will standardize the experimental instruments and reading methods. The temperature numerical accuracy is 0.1℃, and the error is ±0.1. Avoid touching the sensor part of the temperature and humidity block in the whole process. The numerical accuracy of humidity is 0.1% with an error of ±0.1. The numerical accuracy of wind speed is 0.1m/s, and the error is ±0.1. Illuminance value accuracy is 0.01lux, error is ±0.01lux.

A. Temperature

The change of indoor temperature can intuitively reflect the building's indoor thermal environment and provide data support for the user's comfort. The rooms tested are similar in orientation and size. Due to the cold winter, they all need auxiliary heating to meet the requirements of thermal comfort, and the indoor temperature is above 0℃. On the test day, the lowest outdoor temperature was 2.3℃ and the highest temperature was 4.8℃ (Figure 2-48 a). Respectively at 6:30 in the morning and 14:30 in the afternoon, with a temperature difference of up to 6℃. In the case of natural room temperature, the range of indoor temperature change is small. The lowest indoor temperature is 2.5℃, the highest temperature is 6.5℃, and the temperature difference is 4℃. Therefore, the indoor temperature of residential houses is relatively stable and low in winter (Figure 2-48 b).

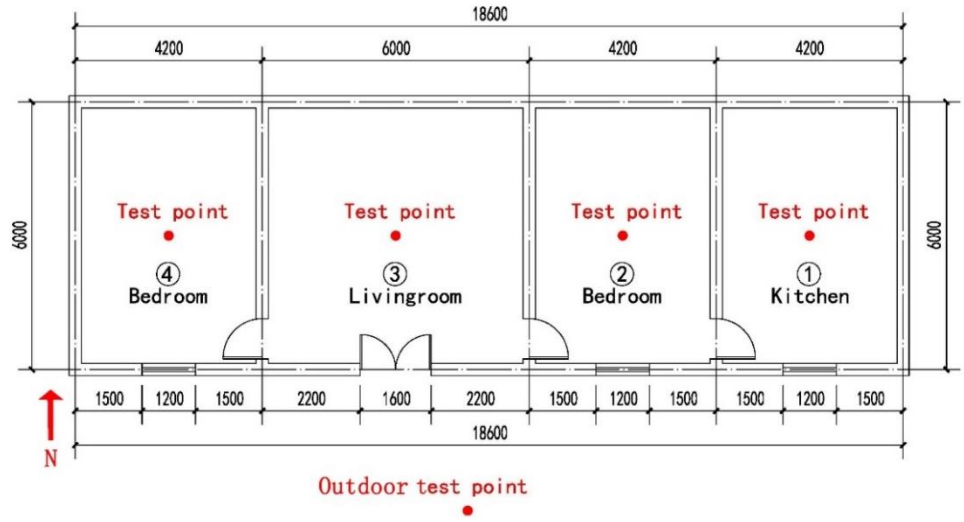

Figure 2-47. Building layout.

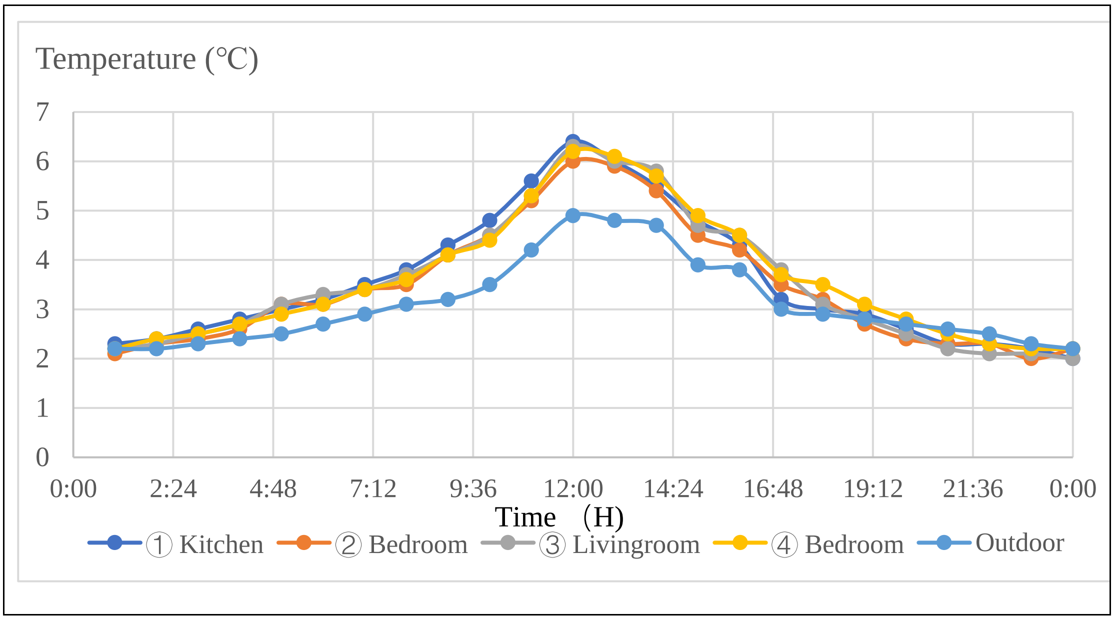

Figure 2-48. Outdoor and indoor temperature distribution map.

B. Humidity

Relative humidity is an important index to measure the indoor comfort of buildings. The actual test results showed that the humidity in Hong Village was high from 9:30 on January 15, 2019 to 9:30 on January 16, 2019. The average outdoor relative humidity was 78.0%, and even reached 99% from 22:30 to 7:30 (Figure 2-49). The outdoor relative humidity varies widely, but the indoor relative humidity of traditional houses varies little. The average indoor relative humidity of residential houses is 63.8%, and the difference between high and low peaks is 22.4% (Figure 2-50). However, according to the indoor air design parameters in The Code for Design of Heating, Ventilation and Air Conditioning for Civil Buildings (GB50736-2012), 40%-60% is the best humidity range to ensure indoor thermal comfort. Therefore, the indoor humidity of traditional houses does not meet the optimal humidity range of indoor thermal comfort.

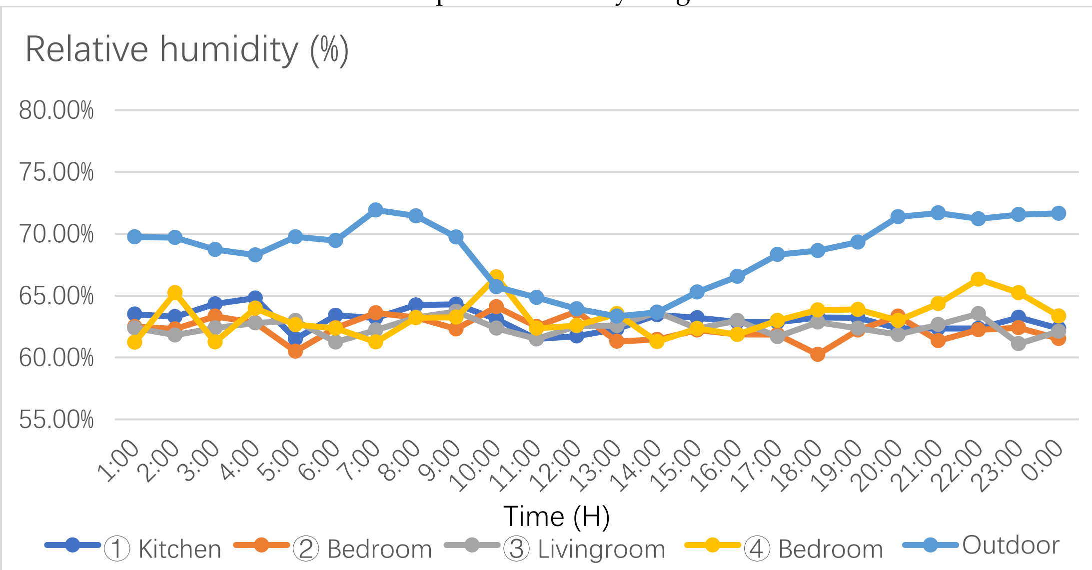

Figure 2-49. Outdoor and indoor relative humidity distribution map.

C. Wind speed

Indoor wind speed is the main factor affecting the comfort of residential buildings, which directly affects the indoor thermal environment and human comfort. According to the measurement, the indoor wind speed tends to be stable, and the average wind speed is 0.18m/s, the highest value is 0.48m/s, the lowest value is 0.14m/s, the difference between the two is 0.44m/s (Figure 2-50). Based on the above tests, the wind speed of the main room, the ear room and other rooms tends to be stable and low from 9:30 on January 15, 2019 to 9:30 on January 16, 2019, and the wind speed of each room is similar.

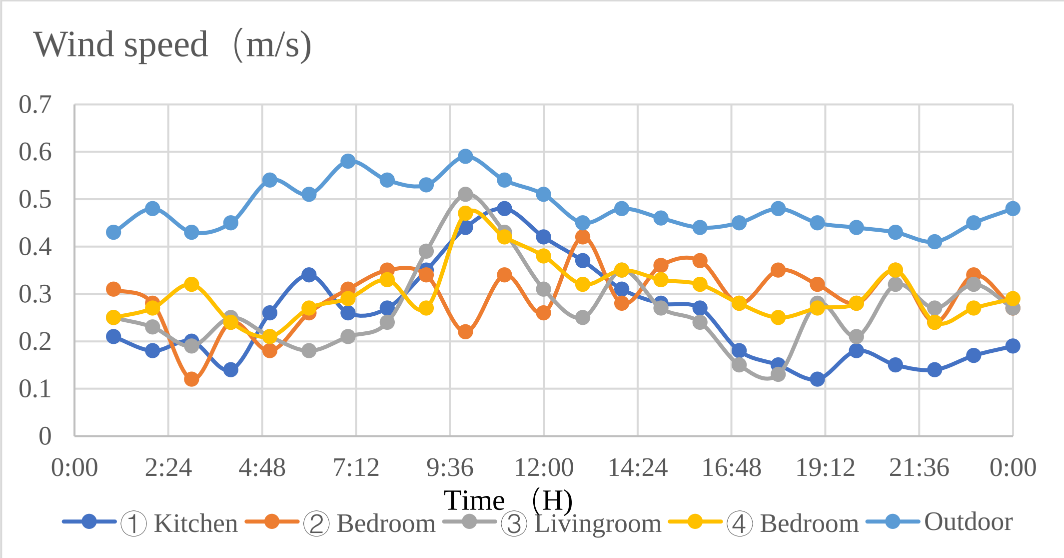

Figure 2-50. Outdoor and indoor wind speed distribution map.

(2) Software Simulation

Located in the south of Shaanxi province, southern Shaanxi includes Hanzhong city, Ankang city and Shangluo city. Qinling mountains in the north, Daba mountains in the south, the Han river from the west to the east through the flow, the main terrain in southern Shaanxi mountains and hills. Under the influence of subtropical continental monsoon climate, it belongs to hot in summer and cold in winter, hot in summer and cold in winter. The research data in this paper mainly come from the following aspects: the arrest of traditional Chinese villages, Energy plus weather, Google Earth, China meteorological data and field research.

There are four research methods in this paper, namely, literature summary, field investigation, summary method and software simulation. Literature summary is to look up more relevant information for reference in a limited time. On-site investigation is an on-site investigation of the folk houses in southern Shaanxi. Inductive summary method: Inductive summary method is to analyze and compare the literature and examples. Software simulation uses Energy plus and Climate Consultant for simulation. Energy plus is a software used to simulate the actual operating conditions of buildings and their ventilation and heating systems and equipment, thereby predicting their hourly energy consumption throughout the year and the total energy consumption of the entire year. Climate Consultant can read the 8760h weather data provided by Energyplus in a certain place throughout the year and can convert these weather data into graphic form. There are four main forms of traditional folk houses in southern Shaanxi, among which "L" type folk houses are more. "L" type folk houses consist of two bedrooms, a meeting room and a kitchen. The bedrooms are located on both sides of the meeting room.

Based on the data on the Fig 2-51 a of the residential houses and the data in the field survey, the height of the residential houses is generally 5.5m, the size of the bedrooms is generally 3.6×6 meters, the size of the living rooms is generally 4×6 meters, and the size of the kitchen is 3.6×7 meters. Model in Open Studio based on the above data, as shown in the Fig 2-51 b. The thermal properties of different rooms are given, and the established modularity is converted into IDF and input into Energy plus.

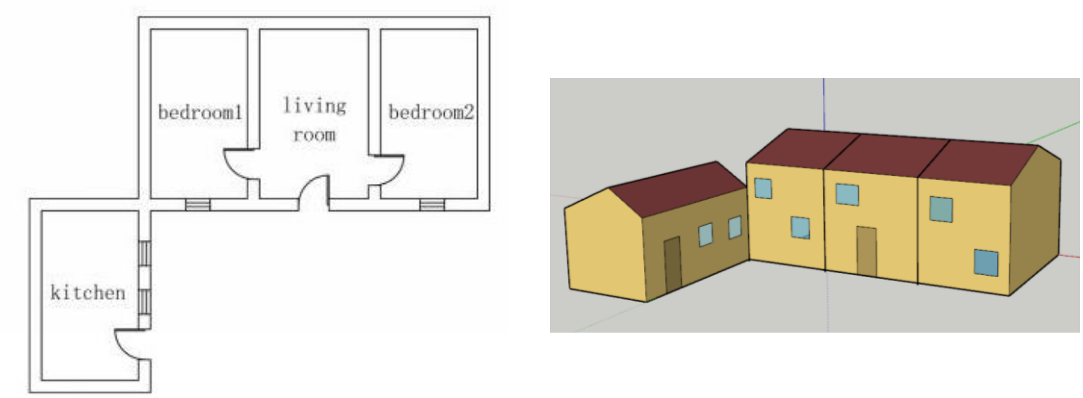

(a) (b)

Figure 2-51. (a)Plan of residence; (b) Residential mode.

The Ankang meteorological data used in this article comes from the "Special Meteorological Data Set for Thermal Environment Analysis of Chinese Buildings", which is based on the meteorological data from 1971 to 2003, and obtained special data for analyzing the thermal environment through reasonable analysis and calculation. set. Using the software climate consultant analysis, the annual temperature range of Ankang area in southern Shaanxi is as follows.

As shown in the Fig 2-52, the temperature is the lowest in February and the temperature is higher in June. The local summer and winter temperature comfort values range from 22° to 27°. The local ground temperature is 26° at the highest and 6° at the lowest, respectively in September and March.

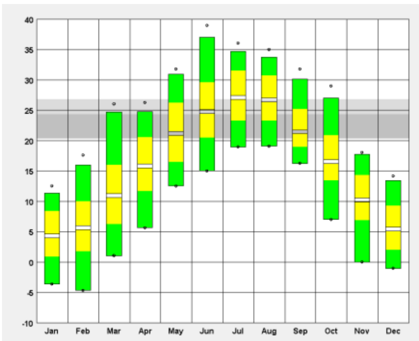

Figure 2-52. Annual temperature profile.

According to the thermal parameter values of the envelope structure of residential buildings in southern Shaanxi, please refer to the table 2-26. Input the parameters into Energy plus, and calculate the solar thermal coefficient value by referring to the solar heat gain coefficient (SHGC), also known as the solar Energy total transmission ratio. The formula is:

$$SHGC = \frac{\sum g \cdot Ag + \sum p \cdot \frac{k}{\partial e} \cdot Af}{Aw}$$

The papers in the formula have the following meanings: g - the total transmission ratio of sunlight in the transmittance part; Ag - light transmission area (m^2); p - the absorption ratio of the non-pervious part of the sun's rays; k - heat transfer coefficient of non-pervious part [$W/(m^2*k)$]; -- coefficient of convective heat transfer on the external surface of the opaque part

[W/(m*k)]; Af -- area of non-transparent part (m^2); Aw -- sum of transmittance and non-transmittance areas (m^2).

Table 2-26. Temperature perception statistics.

Material	Density (Kg/m3)	Heat conductivity coefficient (W/M*K)	Specific heat (J/Kg*K)
Soil	1400	0.58	1010
Marble	2800	2.91	920
Wood	500	0.14	2510

Input personnel, lights, electrical equipment, etc. Before the simulation, the Weather information of Energy plus weather will be input. Through the simulation, the temperature and relevant humidity of the bedroom, kitchen and living room throughout the year will be obtained.

According to the Bedroom annual temperature statistics Fig. 2-53 a, the highest temperature in the bedroom is 35.4℃ and 35.6℃, and the lowest temperature is 7.1℃ and 7.2℃, respectively.

According to the figure 2-53 b, the highest temperature in the living room is 35.5℃, and the lowest temperature is 7.7℃. According to the figure 2-53 c, the highest temperature in the kitchen is 35.9℃. and the lowest temperature is 6.4℃. From this knowable, temperature of bedroom, kitchen, sitting room differs lesser, its performance feels for summer sultry, winter feels wet and cold.

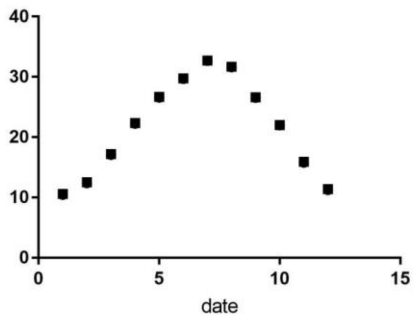

(a)

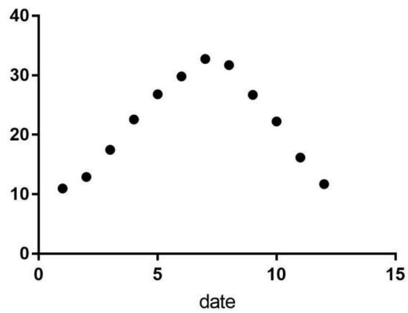

(b)

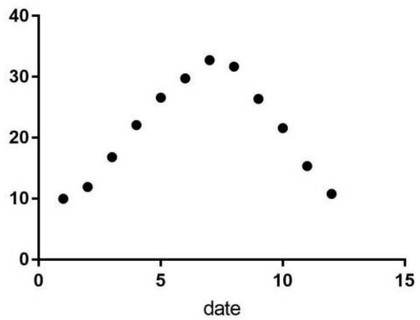

(c)

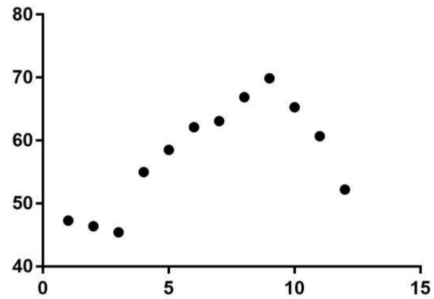

(d)

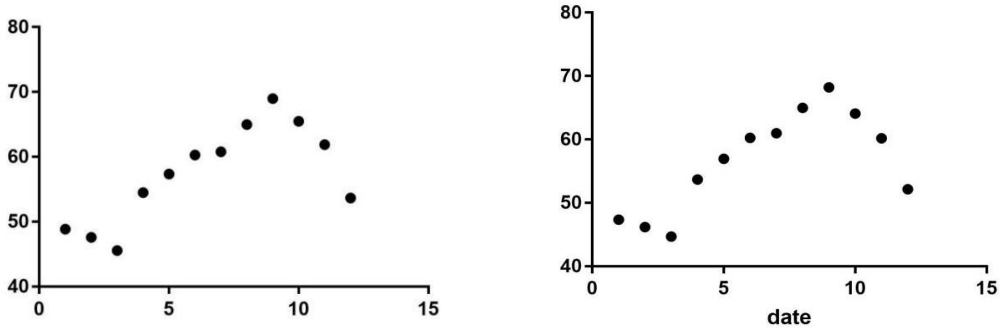

(e) (f)

Figure 2-53. (a) Bedroom annual temperature distribution map; (b) Living room annual temperature distribution map; (c) Kitchen annual temperature distribution map; (d) Living room related humidity distribution map; (e) Kitchen related humidity distribution map; (f)Bedroom related humidity distribution map.

According to the Bedroom related humidity distribution map 2-53 d, the highest relevant humidity in the bedroom is 85.8% and 85.5 %, and the lowest temperature is 23.8 ℃ and 23.6 ℃.

According to Living room related humidity distribution map 2-53 e. The highest temperature in the living room is 87.1%, and the lowest temperature is 23.2 ℃. Respectively. According to Living room related humidity distribution map 2-53 f. The highest temperature in the kitchen is 86.9% and the lowest is 24.0 ℃.

According to the analysis of the above data, the residential houses in southern Shaanxi have high temperature and high humidity in summer and low temperature and high humidity in winter, which are characterized by hot and humid in summer and cold in winter.

Using the above simulation steps and the weather data of Energy plus Weather, the annual outdoor wind speed map 2-56 of residential houses is obtained. The minimum value is 0 m/s, the maximum value is 5.1 m/s, and the average value is 1.2 m/s. According to the above analysis, the outdoor wind speed of the residential buildings in southern Shaanxi is small and stable throughout the year.

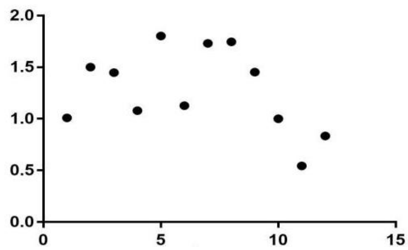

Figure 2-54. Outdoor annual wind speed.

2.4.4 Indoor Thermal Comfort Survey

(1) Definition of Thermal Comfort

Thermal comfort refers to the feeling and preference of human body to the physical environment such as temperature, humidity and wind speed, which can be confirmed by subjective evaluation (ASHRAE 55) [56]. It not only affects the working efficiency of human body, but also may cause health hazards. One of the main objectives of HVAC design is to maintain thermal comfort in buildings (or other Spaces), so thermal comfort is also an important index in building performance simulation. It is often expressed statistically as a percentage of uncomfortable time [57].

If the heat generated by human metabolism can be distributed to the environment, the human body and the environment to achieve a thermal balance [58]. The main factors affecting thermal comfort are some factors related to human heating and cooling, such as metabolic rate, clothing insulation ability, room temperature, average radiation temperature, wind speed and relative humidity [59]. Psychological factors, such as personal expectations, can also affect thermal comfort [60].

The heat balance of human body is a necessary condition for human body to achieve thermal comfort, that is, the heat generated by human metabolism is in a balance state with the heat exchange volume of the environment where human body is located [61]. When the amount of heat released by the human body is less than the amount of heat produced, blood vessels dilate and skin temperature rises [62]. At this time, the human body can regulate its body temperature through sweating, but if this regulation exceeds a certain limit, the body temperature will still rise [63]. When the body emits more heat than it produces, the body will feel cold and even shudder. Blood vessels constrict and sweat pores close. So that the heat release is as low as possible to keep the body temperature within the appropriate range [64]. However, if the heat loss exceeds the limit that the body cannot regulate itself, the body temperature will fall. In a word, hot or cold will bring people uncomfortable feelings. Therefore, in the winter and summer when the climate is not suitable, indoor thermal conditions should be maintained as far as possible [65].

Considering the thermal comfort of human body, it is far from enough to achieve thermal balance only, and the heat exchange between human body and environment should be limited to a certain appropriate range [66]. According to a study, under the condition of heat balance, radiation heat accounted for 45%~50% of the total heat, respiration and sensory evaporation heat accounted for 25%~30% of the total heat, convection heat exchange about 25%~30% of the total heat, the human body can feel thermal comfort, Therefore, this appropriate proportion of indoor thermal environment is a sufficient condition for human thermal comfort [67].

(2) Influencing Factors of Thermal Comfort

Because people's physical and psychological satisfaction varies so much, it can be difficult to find the optimal temperature for everyone in a given space. Laboratory and field data have been collected to define conditions suitable for a specific percentage of test personnel [68]. The six main factors that directly influence thermal comfort can be divided into two categories: personal factors (because they are characteristics of the experimenter) and environmental factors (they are conditions of the thermal environment) [69]. The former is metabolic rate and clothing volume, while the latter is temperature, average radiation temperature, air speed and humidity [71]. Even though all of these factors may vary over time, standards usually study thermal comfort by studying steady-state temperature, allowing only limited temperature variations [72].

A. Environmental parameters

a. Air temperature

Indoor air temperature is bigger to human body thermal feeling, it basically depends on the influence of all sorts of heat sources in solar radiation, atmospheric temperature and living environment [73]. The lower limit of 8 ° C to 10 ° C in winter and the upper limit of 28 ° C to 30 ° C in summer are indoor air temperatures that the human body can tolerate. People in the process of life constantly exchange heat with indoor and outdoor environment, sensitive to temperature changes, especially when the indoor air temperature because the temperature of the surrounding environment change and change, human body by this change will be through their own body temperature regulation system to increase or reduce heat production and heat dissipation, so as to achieve the body temperature is constant and stable [74]. However, if the body's thermoregulatory system has been in the state of frequent regulation, it may affect the stability of the respiratory system, nervous system, digestive system and other systems, reduce the resistance of the human system, then often in a variety of functional disorders and stress state, so as to increase the risk of disease [75].

b. Air humidity

Air humidity refers to the humidity in indoor working or living environment, it is also an important factor that affects human body evaporation and heat dissipation [76]. The drier the indoor air, the more conducive to the evaporation of human sweat and evaporation of heat increase [77]. On the contrary, the more humid the indoor air, evaporation is more difficult, evaporation heat dissipation is smaller. When the relative humidity of the air is less than 30%, the skin of the human body will feel dry, and the respiratory organs will have a sense of inadaptability. When indoor relative humidity is higher than 70%, human skin will feel sticky, and is conducive to the reproduction of most microorganisms, as well as environmental pollution [78]. Therefore, it is generally considered that the most appropriate relative humidity is 30%~70%. Under normal circumstances, humidity in the human body regulation of the role than temperature on the human body. However, if the temperature remains certain or fluctuates little, the air humidity has a very important effect on the regulation of the human body's humidity and heat sensation [79]. Air humidity not only directly affects the thermal balance of human body, but also indirectly affects the breeding of indoor microorganisms, which is not conducive to human health [80].

c. Airflow speed

Indoor airflow speed divides by natural wind power influence besides, the heat source that still is mixed with the shape size of door window, on any account azimuth, area ventilated equipment is concerned, it also is another main factor that affects human body evaporation to come loose heat [81]. The faster the air flow speed is, the greater the evaporation heat loss is. When the gas flow speed is in a static state, a certain saturated air layer will be formed around the surface of the human body, which will largely prevent the evaporation of sweat, and people will feel stuffy when they are in this state [82]. Therefore, there is a certain amount of ventilation and appropriate flow rate in the room, which will play a very good effect on the evaporation and heat dissipation of the human body [83]. When the skin surface temperature is greater than the air temperature, the human body perceives the air temperature to rise by two to three degrees Celsius for every one meter per second decrease in the flow rate of air. A flow rate of 0.15 to 0.25 m/s is sufficient for a comfortable temperature [84]. Gas flow is an important factor in the increase or decrease of heat dissipation of human body. When the air temperature is lower than the surface temperature of human body, the increase of air flow will make the human body lose more heat, which will directly affect the heat balance of human body and thus appear bad condition [85]. In winter when the temperature is low, the airflow will make people feel colder, especially in high humidity and low temperature environment. If the airflow is large, the human body will suffer frostbite due to excessive heat dissipation. When indoor air flow is slow, indoor air can not get effective ventilation, there is insufficient indoor fresh air volume, when all kinds of harmful chemicals can not be discharged to the outdoor in time will lead to indoor air quality deterioration, damage to human health [86].

d. Mean radiation temperature

The mean radiation temperature is the average of the radiation effect of the surrounding surface on the human body [87]. From the point of view of physics, when the surface temperature of any object is higher than absolute temperature zero, it will radiate heat to the outside world. Once there is a certain temperature difference between the relative surface of the object, there will be radiation heat transfer phenomenon. Take the above principle as the basis, when the person is in the indoor environment, there will be radiation heat exchange between the indoor surface, when the average radiation temperature of the indoor surface is lower than the human skin temperature, the human body will use radiation to the surface of the environment [88]. When the average radiation temperature of each indoor surface is higher than the skin temperature of the person, the human body can get radiation heat from each surface of the environment. So controlling the average radiation temperature of the inner surface of the envelope structure has a very important effect on improving the indoor thermal environment [89]. The internal surface temperature of the room envelope structure in our country "civil building thermal design code" is: winter should ensure that the internal surface temperature is greater than or equal to the indoor air dew point temperature, that is, to ensure that the internal surface will not appear condensation phenomenon, the highest temperature limit of the summer internal surface should ensure that the highest temperature is not greater than the highest value of outdoor temperature [90]. In general, the inner surface temperature of the envelope is not evenly distributed and the values are not consistent, so there are many actual points that need to be measured [91]. To simplify the calculation, the average radiation temperature can be expressed as the weighted average of each surface temperature divided by the corresponding surface area. In the formula:

$$MRT=\frac{\sum_i^n T_i\times A_i}{\sum_i^n A_i}$$

MRT -- Average radiation temperature (℃)

Ti -- Temperature of the i-th surface inside the building (℃)

Ai -- Area of the i-th interior surface of the building (m^2)

B. Human parameters

a. Thermal resistance of clothing

There are certain limits to the range of temperature that can be regulated by human's own physiological regulation system, and there are also limits to the physiological regulation methods that a person without any clothes can take in order to keep himself in a comfortable thermal environment. The clothing people wear will directly affect the heat transfer between the human body and the surrounding environment, because the clothing is equivalent to increasing the heat dissipation resistance of the human body surface.

b. Human metabolic rate

For a normal person, his own biological system generates heat to some extent. For example, the human body's respiration is a form of exchange of heat with the outside world [92]. The metabolic rate of the human body is a direct factor affecting the heat exchange between the human body and the surrounding environment [93]. There are many factors affecting it, such as age, gender, physique, psychological state, activity intensity and so on.

c. Other factors

In addition to clothing thermal resistance and metabolic rate, there are also some environmental characteristics that affect human thermal comfort [94]. Be like long-term living habit, local uncomfortable (radiative blow air feeling, uneven radiation, floor temperature, local strong blow air feeling, vertical air temperature difference), transient heat is waited a moment [95].

(3) Investigation of Subjective Reflection of Indoor Thermal Comfort

Due to the inconsistency of age, gender, economic status and regional conditions, residents have different feelings about the indoor thermal environment, and the standard of thermal comfort will also be different. In the residential areas in the mountainous areas of southern Shaanxi, almost no residents use air conditioning equipment. In summer, natural ventilation, fans and electric fans are mainly used for cooling, and in winter, fire kang and furnace are mainly used for heating. Affected by long-term living habits, residents used to chat or work in winter, often in the state of frequent indoor and outdoor walking, in the indoor and outdoor clothing rarely change, if the indoor temperature is too high, with the outdoor temperature difference is large, it is easy to cause a cold. So we can't measure and design rural buildings by urban thermal comfort standards. The subjective response of residents to the indoor thermal conditions of residential houses is investigated below in order to obtain the subjective demand of local residents for the indoor thermal environment and provide basis for the improvement of local indoor thermal comfort (Table 2-27).

A total of 200 households were effectively surveyed by questionnaire. Statistics show that 64 valid questionnaires were collected in Ankang, 65 in Hanzhong and 71 in Shangluo. According to the number of residents, the number of residents of residential houses ranges from 1 to 6, of which 2 people are the majority and there are 100 households. Dwellings with 3 residents were the majority, with a total of 38 households. The number of residential residents is 4, and there are 25 households. The number of residents is 5 and there are 20 households. The number of residents is 5 and there are 7 households. The residential land area varies from $65m^2$ to $100m^2$ in size (the area is estimated by the residents themselves) and is evenly distributed. The basic information of the questionnaire is as follows.

Table 2-27. Basic information of questionnaire.

<table>
<tr><th>Attribute</th><th>Type</th><th>Number</th><th>Proportion</th><th>Attribute</th><th>Type</th><th>Number</th><th>Proportion</th></tr>
<tr><td rowspan="3">Build time</td><td>1960 years ago</td><td>56</td><td>28%</td><td rowspan="3">Building storey</td><td>One floor</td><td>120</td><td>60%</td></tr>
<tr><td>1960-2000 years</td><td>84</td><td>42%</td><td>Second floor</td><td>77</td><td>38.5%</td></tr>
<tr><td>After 2000</td><td>60</td><td>30%</td><td>Three layers</td><td>3</td><td>1.5%</td></tr>
<tr><td rowspan="3">Structure type</td><td>Civil structure</td><td>55</td><td>27.5%</td><td rowspan="3">Independent courtyard</td><td rowspan="2">Yes</td><td rowspan="2">110</td><td rowspan="2">55%</td></tr>
<tr><td>Brick-Wood structure</td><td>60</td><td>30%</td></tr>
<tr><td>Brick structure</td><td>85</td><td>42.5%</td><td>No</td><td>90</td><td>45%</td></tr>
</table>

Statistics are made on the thermal comfort of Stripe type residential houses in winter in terms of temperature, humidity, daylighting, thermal comfort, wind sense and other aspects, and the statistical results are as follows:

A. Temperature

As can be seen from the table, 50% of the residents said that the indoor temperature in winter was cold, and 37.5% said that the indoor temperature in winter was a little cold. 10% of residents said that the indoor temperature in winter is cold, 2.5 % of residents said that the indoor temperature in winter is moderate. The overall indoor temperature for local residents, less satisfied with the indoor temperature is low (Table 2-28).

Table 2-28. Temperature perception statistics.

Hot sensation	Cold	Cool	Slightly cooler	Moderate
Number of households	20	100	75	5
Proportion	10%	50%	37.5%	2.5%

B. humidity

As can be seen from the table, 60% of the residents said that the indoor humidity in winter was slightly humid, and 30% of the residents said that the indoor humidity in winter was humid. Ten percent of residents reported moderate humidity indoors in winter. After analysis, there are two main reasons for the indoor humidity of residential houses in winter. First, the local climate is subtropical continental monsoon climate, and winter is rainy and low temperature. Second, the ground of local houses is not moisture-proof, so the indoor floor will appear dew in winter (Table 2-29).

Table 2-29. Humidity perception statistics.

Hot sensation	Dry	Slightly dry	Moderate	Slightly moist	Moist
Number of households	0	0	20	120	80
Proportion	0%	0%	10%	60%	30%

C. Daylighting

According to the table, 75% of the residents said that the indoor lighting effect in winter is dark, and 15% said that the indoor lighting effect in winter is moderate. The overall brightness of this kind of residential houses is not enough, and the rooms are generally dark, especially in southern Shaanxi, the window holes are generally small, and some use plastic paper with lower transparency instead of glass. This caused indoor daylighting effect poorer, cannot satisfy people normal life demand (Table 2-30).

Table 2-30. Daylighting perception statistics.

Daylighting effect	Dark	Medium	Bright
Number of households	170	30	0
Proportion	75%	15%	0%

(4) Thermal comfort

As can be seen from the table, although the winter temperature of residential houses is lower than the appropriate temperature, 20% of residents generally feel that the thermal comfort is appropriate. 55% of the residents generally felt that the thermal comfort was slightly uncomfortable, and 25% of the residents generally felt that the thermal comfort was inappropriate. This shows that there are some problems worth studying in folk houses (Table 2-31).

Table 2-31. Thermal comfort perception statistics.

Thermal comfort	Comfortable	A little uncomfortable	Uncomfortable
Number of households	40	110	50
Proportion	20%	55%	25%

D. Wind feeling

As can be seen from the table, the ventilation of this kind of houses is not very good, and the proportion of residents with wind sense is small. Due to the problems of living habits, most of the residents of this kind of residential houses almost open their doors when they do not go out during the day, no matter in winter or summer, but they still do not feel in the room, indicating that there are certain ventilation problems in this kind of houses. For there is a clear sense of blowing houses, both before and after the middle of the room with the door, residents from frequent activity room, the two ends of the main door is long in an open position, cause of indoor air temperature of the main basic same as outdoor, which virtually increased the bottom on both sides of the room and outside the contact area, increasing the shape coefficient, the indoor thermal environment have a big impact (Table 2-32).

Table 2-32. Wind feeling perception statistics.

Wind feeling	barely feel	slight wind sensation	distinct blowing sensation
Number of households	150	40	10
Proportion	75%	20%	5%

2.5 Research Question

The villages in southern Shaanxi are widely distributed and the economic development is relatively backward, which makes the traditional houses can not meet the living and spiritual needs of modern people. According to the indoor physical environment test and thermal comfort investigation of Stripe shaped residential houses in southern Shaanxi in winter, the indoor temperature of traditional residential houses is low and residents generally feel cold and wet in winter. Through the analysis of the space, function, construction technology and other aspects of traditional residential houses, it is found that traditional residential buildings in the early stage of heating measures less consideration. In order to improve the indoor temperature, people use fire charcoal, fire pond, fire basin and other heating equipment. According to the present situation of the heating equipment, the infrared thermal imager test results show that the traditional heating equipment can only improve the temperature of human body part, can not improve the indoor temperature. Modern heating methods mainly rely on electrical heating, belong to the active heating will cause energy consumption. According to the above analysis, the indoor temperature and humidity of traditional houses in southern Shaanxi in winter are not suitable for human needs and the thermal comfort is poor.

2.6 Chapter Summary

This chapter selects 12 villages in Shangluo, Ankang, Hanzhong and other places in southern Shaanxi as the key research object. The investigation and data collection of the local houses were carried out. This paper analyzes the general situation of southern Shaanxi, the cultural inheritance and historical development of folk houses, the investigation of traditional folk houses and the indoor thermal comfort of folk houses. Through field research, it can be seen that there are some problems in residential houses. The research problem is that the indoor temperature of traditional houses is low in winter and the residents generally feel wet and cold.

Reference

[1] A Historical Survey of the Yellow River and the River Civilizations.

[2] Liang, Z. On the historical and cultural characteristics of the Han River Basin. Journal of Hanzhong Normal University (Social Science). 2003, 1-7.

[3] Liu, Y.; Wang, Xin. Prehistoric archaeological culture and ethnic distribution in southern Shaanxi. Collection of Chinese Historical Geography. 2017, 32, 43-53.

[4] Chen Liangxue. Tuntian and Immigration in Southern Shaanxi in Ming Dynasty. Journal of Hanzhong Normal University (Social Science). 1998, 16-19.

[5] Wang, J. Compatible characteristics of religious culture in southern Shaanxi. Huaxia Culture. 2012, 03, 17-19.

[6] Yang, X.; Liu, X. An analysis of the site selection behavior of Ba people in the pre-Qin period. Journal of Southwest University for Nationalities (Humanities and Social Sciences Edition). 2009, 30, 20-24.

[7] Liang, Z. On the formation of Hanshui Cultural Belt. Journal of Hanzhong Normal University (Social Science). 2004, 05, 36-40.

[8] Liang, Z. The strategic position of Hanzhong Ankang in the Southern Song Dynasty. Journal of Hanzhong Normal University (Social Science). 1996, 01, 33-41.

[9] Miao, J.; Zhang, Y.; Liu, S. Research on the wisdom of traditional settlements: Taking Fujian Liancun as an example. Huazhong Architecture. 2014, 32, 180-184.

[10] Pu, X.; Huang, L. A review of the public space morphology of traditional rural settlements in China. Architecture and Culture. 2019, 12, 28-30.

[11] Liang, Z. Changes in the natural environment of the Qinba Mountains in the historical period. Collection of Chinese Historical Geography. 2002, 03, 40-48.

[12] Wang, Z. Research on Hanshui Culture and Disciplinary Construction. Journal of Shaanxi Institute of Technology (Social Science Edition). 2012, 30, 02, 37-40+53.

[13] Liang, X. Viewing the Chinese people's view of geomantic omen from the settlement site selection. New Architecture. 1988, 04, 67-71.

[14] Zheng, Z.; Jiao, S.; Jia, L. Analysis of the characteristics and predicaments of ethnic gathering areas in traditional villages. Resource Development and Market. 2019, 35, 504-508.

[15] Liao, R.; Yu, G.; Liu, M. The evolution of settlement location and layout in the process of urban-rural integration. Human Geography. 1997, 04, 35-38+28.

[16] Zhang, X. Analysis of Shaanxi Cultural Division and Its Mechanism. Human Geography. 2000, 03, 17-21+72.

[17] Chen, Q.; Shao, L.; Hou, X.; Zhang, B.; Chen, W.; Xia, X. Detection and attribution of vegetation greening trend across distinct local landscapes under China's Grain to Green Program: A case study in Shaanxi Province, Catena. 2019, 183,104182.

[18] Lin, L.; Bu, F. On the relationship between traditional rural settlements and natural environment. Beijing Agriculture. 2011, 06, 278-280.

[19] Fei, L.; Zhou, M.; Shao, J. Qin, Z. Evolution forms of land systems based on ascendency and overhead: A case study of Shaanxi Province, China. Ecological Modelling. 2020, 419, 108960.

[20] Fan, F.; Wu, D.; Chen, T. Analysis of factors affecting the site selection of rural settlements. Journal of Hainan Normal University (Natural Science Edition). 2009, 22, 462-467.

[21] Hou, K.; Tao, W.; Yue, C.; Yue, Z.; Li, X.; Pei, C. A feasible method for the division of ecological vulnerability and its driving forces in Southern Shaanxi. Journal of Cleaner Production. 2018, 205, 619-628.

[22] Li, P. Research on the site selection of traditional settlements under the background of new rural construction: Taking the planning of market towns and villages in mountainous regions as examples. Housing and Real Estate. 2016, 06, 30.

[23] Yan, J.; Huang, Y.; Ren, X. Research on Environmental Protection Countermeasures of Traditional Settlement Human Settlements. Sichuan Architecture Science Research. 2009, 35, 223-227.

[24] Yang, G. The overall characteristics of traditional settlement space in my country and its sociological significance. Journal of Tongji University (Social Science Edition). 2014, 25, 60-68.

[25] Jing, Z.; Li, Y. Cluster design under the action of field forces——Inspiration of traditional settlement layout ideas on the planning and design of headquarters base. Journal of Tianjin University (Social Science Edition). 2010, 12, 553.

[26] Yang, G. The overall characteristics of traditional settlement space in my country and its sociological significance. Journal of Tongji University (Social Science Edition). 2014, 25, 60-68.

[27] Hu, Z.; Liu, C.; Deng, Y.; Yang, L. Traditional settlement landscape genes and their research progress. Advances in Geographical Sciences. 2012, 31, 1620-1627.

[28] Deng, W.; Hu, H.; Yang, R.; He, Y. The dual-structure characteristics of traditional rural settlement space and its protection enlightenment. Urban Planning Journal. 2019, 06, 101-106.

[29] Xu, X. Research on the Formation of Traditional Settlement Space. Journal of Nanjing University of the Arts (Fine Arts and Design), 2021, 01, 99-104+218.

[30] Wang, L.; Li, X. Landscape renewal of the traditional settlement space of ethnic minorities. Chinese Garden. 2011, 27, 91-93.

[31] Lin, Z. Research on traditional settlement ritual space and its adaptability to contemporary communities. Architecture Journal. 2016, 12, 118-119.

[32] Fan, X.; Du, X. Social structure and spatial structure in traditional settlements. Famous Chinese Cities. 2012, 03, 63-66.

[33] Tao, J.; Zhang, Q.; Xiao, D. The influence of natural environment on the spatial layout of traditional settlements in Meizhou. Southern Architecture. 2013, 06, 60-62.

[34] Fan, X.; Zhang, J. The social structure changes and spatial renewal of traditional settlements. Famous Cities in China. 2013, 03, 65-67.

[35] Ye, Z. Analysis of the spatial structure of traditional settlement environment. Architecture Journal. 2001, 12, 21-24.

[36] Xiao, Y.; Mi, Y. A review of the spatial morphology of traditional rural settlements of ethnic minorities in my country. Architecture and Culture. 2020, 01, 72-73.

[37] Ye, Z. Research on the Spatial Structure of Chinese Traditional Settlement Environment. Journal of Beijing Institute of Civil Engineering and Architecture. 2001, 01, 70-75.

[38] Yan, J. Research on Hanzhong residential architecture—Taking Qingmuchuan, an ancient town, as an example. Huazhong Architecture. 2008, 04, 102-107.

[39] Zhou, X. Research on the spatial form and composition of traditional rural settlements. Nongjia Staff. 2019, 17, 4.

[40] Yuan, F.; Wang, Q. Exploring the origin of Chinese traditional village planning ideas. Construction of Small Cities and Towns. 1998, 06, 36-37.

[41] Wang, L.; Li, C.; Deng, M. Symbolic expression in the layout of ancient villages. Journal of Chongqing Jianzhu University. 2002, 03, 1-4+9.

[42] Wang, L. The future of the village-the experience of traditional villages and contemporary settlement planning. Architecture Journal. 2000, 11, 16-22.

[43] Hu, R.; Shi, F.; He, W.; Li, W. The evolution and development of mountain houses in southern Shaanxi. Journal of Xi'an University of Architecture and Technology (Natural Science Edition). 2009, 41, 841-845.

[44] Zhu, X. On the changes of settlement environment in traditional villages. Journal of Tongji University (Social Science Edition), 1999, 01, 21-24.

[45] Xu, H.; Li, Y.; Li, Z. Research on the local renewal strategy of rural settlements in southern Shaanxi in the new era. Architecture and Culture. 2017, 08, 230-231.

[46] Li, G. Research on the spatial structure of traditional ecological settlements in southern Shaanxi. Ecological Economy. 2014, 30, 150-152+160.

[47] Xing, G.; Xu, Y, Zheng, Y. The types and characteristics of the spatial evolution of rural settlements in the process of urbanization. Economic Geography. 2007, 06, 932-935.

[48] Liu, Q.; Li, Q. Analysis on the street space of traditional villages——Taking Xinzhuang Village of Yangquan as an example. Chinese and Foreign Architecture. 2021, 01, 91-95.

[49] Ma, K.; Li, Y. Analyze the multiple characteristics of traditional courtyard houses in southern Shaanxi. Huazhong Architecture. 2015, 33, 160-163.

[50] Xu, D.; Gu, Z.; Shen, T. A syntactic study on the mechanism of deconstruction and integration of streets and lanes in ancient villages. Shanxi Architecture. 2015, 41, 32-34.

[51] Yang, T. Analysis of the twists and turns of the streets and lanes of rural settlements in southern Shaanxi. Tourism Overview (second half of the month). 2019, 24, 35-37.

[52] Guo, T. "Integration" and "Symbiosis" in the Renewal and Preservation of Historic Buildings: Taking Fenghuang Ancient Town in Shangluo, Shaanxi as an Example. Urban Architecture,.2020, 17, 153-158.

[53] Zhao, Y.; Wang, J. Research on traditional rural settlement planning based on morphological integrity——application of settlement performance improvement planning technology. Urban Planning. 2018, 42, 33-40+53.

[54] Xu, Y. The architectural style of the ancient town of Flatiron in Shaanxi. Architecture, 2020, 07, 67-69.

[55] Liang, Z.; Zhang, H.; Li, Y. Connotation analysis of traditional residential building decoration form in Fenghuang Ancient Town in southern Shaanxi. Art and Design (Theory). 2009, 2, 186-188.

[56] Xie, X.; Xia, F.; Zhao, Y.; Xu, B.; Wang, Y.; Pei, G. Parametric study on the effect of radiant heating system on indoor thermal comfort with/without external thermal disturbance. Energy. 2020, 249, 123708.

[57] Hong, T.; Lin, H. W. Occupant behavior: Impact on energy use of private offices, in: IBPSA (Ed.). ASim2012 Proceedings. 2012.

[58] Hong, T.; Taylor-Lange, S. C.; D'Oca, S.; Yan, D.; Corgnati, S. P. Advances in research and applications of energy-related occupant behavior in buildings. Energy and Buildings. 2016, 116, 694–702.

[59] Schweiker, M.; Huebner, G. M.; Kingma, B. R.; Kramer, M. R.; Pallubinsky, H. Drivers of diversity in human thermal perception - A review for holistic comfort models. Temperature. 2018, 5, 308–342.

[60] Cheng, Y.; Niu, J.; Gao, N. Thermal comfort models: A review and numerical investigation. Building and Environment. 2012, 47, 13–22.

[61] Majcen, D.; Itard, L.; Visscher, H. Theoretical vs. actual energy consumption of labelled houses in the Netherlands: Discrepancies and policy implications. Energy Policy. 2013, 54, 125–136.

[62] Schweiker, M.; Wagner, A. Influences on the predictive performance of thermal sensation indices. Building Research and Information.

[63] Heydarian, A.; McIlvennie, C.; Arpan, L.; Yousefi, S.; Syndicus, M.; Schweiker, M.; Jazizadeh, F.; Rissetto, A.; Pisello, L.; Piselli, C.; Berger, C.; Yan, Z.; Mahdavi, A. What drives our behaviors in buildings? A review on occupant interactions with building systems from the lens of behavioral theories. Building and Environment. 2020, 179, 106928.

[64] Schlu¨ter, M.; Baeza, A.; Dressler, G.; Frank, K.; Groeneveld, J.; Jager, W.; Janssen, M. A. R.; McAllister, R. B.; Müller, K.; Orach, N.; Schwarz, N. A framework for mapping and comparing behavioral theories in models of social-ecological systems. Ecological Economics. 2017, 131, 21–35.

[65] Li, D.; Xu, X.; Chen, C.F.; Menassa, C. Understanding energy-saving behaviors in the American workplace: A unified theory of motivation, opportunity, and ability. Energy Research & Social Science. 2019, 51, 198–209.

[66] Guerreiro, S.; Batel, S.; Lima, M. L.; Moreira, S. Making energy visible: sociopsychological aspects associated with the use of smart meters. Energy Efficiency. 2015, 8, 1149–1167.

[67] Hong, T.; D'Oca, S.; Turner, W. J.; Taylor-Lange, S. C. An ontology to represent energy-related occupant behavior in buildings. Part I: Introduction to the DNAS framework, Building and Environment. 2015, 92, 764–777.

[68] Dear, R. J.; Brager, G. S. Developing an adaptive model of thermal comfort and preference, ASHRAE Transactions.

[69] Schweiker, M.; Wagner, A. A framework for an adaptive thermal heat balance model (ATHB), Building and Environment. 2015, 94, 252–262.

[70] Healey, K.; Webster-Mannison, M. Exploring the influence of qualitative factors on the thermal comfort of office occupants. Architectural Science Review. 2012, 55, 169–175.

[71] Chappells, H.; Shove, E. Debating the future of comfort: environmental sustainability, energy consumption and the indoor environment. Building Research & Information. 2005, 33, 32–40.

[72] Shove, E. Converging conventions of comfort, cleanliness and convenience. Journal of Consumer Policy. 2003, 26, 395–418.

[73] Mishra, A. K.; Derks, M.; Kooi, L.; Loomans, M.; Kort, H. Analysing thermal comfort perception of students through the class hour, during heating season, in a university classroom. Building and Environment. 2017, 125, 464–474.

[74] Montazami, A.; Gaterell, M.; Nicol, F.; Lumley, M.; Thoua, C. Impact of social background and behaviour on children's thermal comfort. Building and Environment. 2017, 122, 422–434.

[75] Kalmár, F. Investigation of thermal perceptions of subjects with diverse thermal histories in warm indoor environment. Building and Environment. 2016, 107, 254–262.

[76] Ning, H.; Wang, Z.; Ji, Y. Thermal history and adaptation: Does a long-term indoor thermal exposure impact human thermal adaptability? Applied Energy. 2016, 183, 22–30.

[77] Schweiker, M.; Shukuya, M. Comparison of theoretical and statistical models of air-conditioning unit usage behavior in a residential setting under Japanese climatic conditions. Building and Environment. 2009, 44, 2137–2149.

[78] Zhang, Y.; Chen, H.; Wang, J.; Meng, Q. Thermal comfort of people in the hot and humid area of China impacts of season, climate, and thermal history. Indoor air. 2016, 26, 820–830.

[79] Luo, M.; Dear, R.; Ji, W.; Bin, C.; Lin, B.; Ouyang, Q.; Zhu, Y. The dynamics of thermal comfort expectations: The problem, challenge and implication. Building and Environment. 2016, 95, 322–329.

[80] Deuble, M.P.; Dear, R. J. Green occupants for green buildings: The missing link? Building and Environment. 2012, 56, 21–27.

[81] Wang, Z.; Dear, R.; Luo, M.; Lin, B.; He, Y.; Ghahramani, A.; Zhu, Y. Individual difference in thermal comfort: A literature review. Building and Environment. 2018, 138, 181–193.

[82] Rupp, R.F.; Kim, J.; Dear, R.; Ghisi, E. Associations of occupant demographics, thermal history and obesity variables with their thermal comfort in air-conditioned and mixed-mode ventilation office buildings. Building and Environment. 2018, 135, 1–9.

[83] Hawighorst, M.; Schweiker, M.; Wagner, A. Thermo-specific self-efficacy (specse) in relation to perceived comfort and control. Building and Environment. 2016, 102, 193–206.

[84] Luo, M.; Cao, B.; Ji, W.; Q. O.; Lin, B.; Zhu, Y. The underlying linkage between personal control and thermal comfort: Psychological or physical effects? Energy and Buildings. 2016, 111, 56–63.

[85] Yun, G.Y. Influences of perceived control on thermal comfort and energy use in buildings. Energy and Buildings. 2018, 158, 822–830.

[86] Auliciems, A. Towards a psycho-physiological model of thermal perception. International Journal of Biometeorology. 1981, 25, 109–122.

[87] Schweiker, M.; Rissetto, R.; Wagner, A. Thermal expectation: Influencing factors and its effect on thermal perception. Energy & Buildings. 2019, 210, 109729.

[88] Luo, M.; Wang, Z.; Brager, G.; Cao, B.; Zhu, Y. Indoor climate experience, migration, and thermal comfort expectation in buildings. Building and Environment, 2018, 141, 262–272.

[89] Grabe, J. How do occupants decide their interactions with the building? From qualitative data to a psychological framework of human-building-interaction. Energy Research & Social Science. 2016, 14, 46–60.

[90] Eccles, J. Expectancies, values, and academic behaviors, in: J. T. Spence (Ed.). Achievement andachievement motives: Psychological and sociological approaches, Free man, San Francisco. 1983, 75–146.

[91] Ajzen, I. The theory of planned behavior, Organizational Behavior and Human Decision Processes 50. 1991, 2 179–211.

[92] Fishbein, M.; Ajzen, I. Predicting and changing behavior: The reasoned action approach. Psychology Press, New York, 2010.

[93] Krosnick, J. A.; Judd, C. M.; Wittenbrink, B. The measurement of attitudes: The handbook of attitudes and attitudes change. 2005, 21-78.

[94] Ding, Z.H.; Li, Y.Q.; Zhao, C.; Liu, Y.; Li, R. Factors affecting heating energy-saving behavior of residents in hot summer and cold winter regions. Natural Hazards. 2019, 95, 193–206.

[95] Lange, I.; Moro, M.; Traynor, L. Green hypocrisy?: Environmental attitudes and residential space heating expenditure. Ecological Economics. 2014, 107, 76–83.

Chapter 3. Relevant Research Theories and Methods

3.1 Theoretical Research

3.1.1 Principle and Application of Heat Transfer

Heat transfer is the transfer of heat from a hot body to a cold body, or from a hot part of the body to a cold part. Heat transfer is a universal phenomenon in nature [1]. As long as there is a temperature difference between bodies or between different parts of the same body, heat transfer occurs and will continue until the temperature is the same [2]. The only condition for heat transfer is that there is a temperature difference, regardless of the state of the objects, regardless of whether they are in contact with each other [3]. The result of heat transfer is the disappearance of temperature difference, that is, the same temperature is reached between objects or between different parts of objects [4]. Heat transfer is mainly divided into three ways: heat conduction, heat radiation and heat convection [5].

(1) Principle of Heat Transfer

A. Heat conduction

Heat conduction refers to the thermal energy transfer generated by the thermal motion of molecules, atoms and free electrons and other microscopic particles without relative displacement between various parts of the object, referred to as heat conduction [6]. The temperature only varies along the X-axis, for any element layer with a thickness of DX along the X-axis [7]. According to Bolier's law, the heat conduction through the layer per unit time is proportional to the local temperature change rate and the area A of the plate.

$$\Phi=-\lambda A(dt/dx) \qquad (1)$$

The proportional coefficient in the formula λ is called thermal conductivity. The minus sign indicates that heat is transferred in the opposite direction of the increase in temperature. The formula is the rate equation for calculating the heat conduction through the plate. According to the provisions of GB 3101-1993, the symbol of a physical quantity represents its magnitude, that is, the numerical x unit. For example, the unit Φ in the formula is W.

B. Thermal convection

Thermal convection refers to the process of heat transfer caused by the relative displacement of each part of the fluid caused by the macroscopic movement of the fluid and the mixing of cold and hot fluids [8]. Thermal convection can only occur in fluid, and because molecules in fluid are moving irregularly at the same time, thermal convection must be accompanied by heat conduction [9]. Of particular interest in engineering is the transfer of heat between a fluid flowing over a surface, called convection.

The basic calculation of convective heat transfer is Newton's cooling formula - when a fluid is heated.

$$q=h(T_W-T_F) \qquad (2)$$

When the fluid is cooled.

$$q=h(T_F-T_W) \qquad (3)$$

In the formula, TW and TF are wall temperature and fluid temperature respectively. If the temperature difference (also known as temperature and pressure) is denoted as Δ T and it is agreed to take a positive value forever, Then Newton's cooling formula can be expressed as:

$$q=h\Delta t \qquad (4)$$

The proportional coefficient h in the formula is called the surface heat transfer coefficient, and the unit is $W/(m^2 \bullet K)$. The surface heat transfer coefficient is related to many factors in the process of convective heat transfer. It not only depends on the physical properties of the fluid (λ, η, etc.) and the shape, size and arrangement of the heat transfer surface, but also has a close relationship with the flow rate. The formula does not reveal the specific relationship of various complicated factors affecting the surface heat transfer coefficient, but only gives the definition of the surface heat transfer coefficient.

C. Thermal radiation

The way in which objects transmit energy through electromagnetic waves is called radiation [10]. Objects emit radiant energy for various reasons, and the phenomenon of radiant energy emitted by heat is called thermal radiation [11]. In nature, all the objects constantly emit heat radiation to space, and at the same time constantly absorb the heat radiation emitted by other objects [12]. The combination of radiation and absorption processes results in the radiative transfer of heat between objects - radiative heat transfer, also known as radiation heat transfer [13]. When the object is in thermal equilibrium with the surrounding environment, the radiative heat transfer is equal to zero, but this is a dynamic equilibrium, radiation and absorption process is still going on [14].

Heat conduction and convection can only be realized in the presence of matter, while thermal radiation can be transmitted in a vacuum, and in fact, the transfer of radiant energy is most effective in a vacuum [15]. This is the basic characteristics of heat radiation different from heat conduction and convection heat transfer [16]. Another characteristic of radiant heat transfer, which is different from heat conduction and convection heat transfer, is that it not only produces the transfer of energy, but also is accompanied by the conversion of energy form, that is, from heat energy to radiation energy when it is transmitted, and from radiation energy to heat energy when it is absorbed [17].

A black body is an object that absorbs all the thermal radiation that falls on its surface. The absorption power and radiation power of the black body are the largest in the same temperature of the object. The amount of heat emitted per unit time by a black body is revealed by Stefan-Bolumann's law:

$$\Phi = A\sigma T^4 \tag{5}$$

In the formula, T is the thermodynamic temperature of the black body, σ is commonly known as the radiation constant of the black body, which is a natural constant and its value is 5.67*108W/ (m^2 • K^4); A is radiation surface area.

$$\Phi = \varepsilon A\sigma T^4 \tag{6}$$

All real objects radiate less than a black body at the same temperature. The empirical modified form of Stephan-Boltzmann's law can be used to calculate the radiant heat flux of real objects: The emissivity of the stuff in the formula is always less than 1, which is related to the type and surface state of the stuff. Stefan-boltzmann moment law, also known as the fourth power law, is the basis of radiation heat transfer calculation.

(2) Application of Heat Transfer Principle

By understanding the three heat transfer modes of heat transfer, the working principles of cooking heating wall system, cooking heating wall system and additional sunlight system and natural heating are analyzed [18]. In order to verify the effectiveness of the system between the cooking heating wall and additional sunlight, the condition is set as whether the wall has solar radiation [19]. By analyzing the principle of heat transfer, the influence of solar radiation on the heating system between the cooking heating wall and additional sunlight is analyzed. In addition, it is beneficial to choose suitable software for analysis and simulation [20].

3.1.2 Evaluation Methods and Standards of Indoor Humid and Thermal Environment.

Indoor thermal and humid environment standard is one of the basic bases of building thermal design [21,22]. There are many indexes for evaluating the heat and humidity environment in the evaluation room, each of which has advantages and disadvantages [23,24]. The simplest, most convenient and most widely used indicator is indoor air temperature [25,26].

(1) Effective Temperature

Effective temperature is a thermal index proposed by Yaglon et al. In 1923 ~ 1925 in the United States, which includes factors such as air temperature, air humidity and air velocity, and is used to evaluate the comprehensive influence of the above three factors on people's subjective thermal sensation when they are resting or sitting at work. This index is based on the subjective response of the subjects [27,28]. In an experiment to determine this, subjects walked back and forth between two rooms with different combinations of environmental factors and adjusted the values of parameters in one room so that subjects experienced the same thermal sensation when they entered the other room [29,30].

Replacing the air temperature with the black sphere temperature is called the new effective temperature. The relationship between the new effective temperature and thermal sensation is as follows table 3-1:

Table 3-1. Effective Temperature.

Effective Temperatu re	**43**	**40**	**35**	**34-31**	**30**	**25**	**20**	**19-16**	**15**	**10**
Subjective thermal sensation	Allow online	Extrem ely hot	Very hot	Hot	Slight ly hot	Mode rate	Slig htly cold	Cold	Very cold	Extre mely cold

(2) PMV-PPD Index of Thermal Sensation

This was put forward by Danish scholar Fanger in the 1970s. The index is based on its famous thermal comfort balance equation, and takes into account six parameters: two human factors, namely the amount of activity and clothing, and four thermal environmental factors [31,32].

The so-called thermal comfort equilibrium equation refers to that in the basic thermal equilibrium equation, Qe is replaced by the body regulation function in a peaceful state, namely Qe* under comfortable conditions, according to the body regulation function in a peaceful state of skin surface temperature Ts. Qr and Qe in the basic heat balance equation are calculated, and the radiation heat transfer and convective heat transfer obtained are expressed as Qr* and Qe* respectively, then:

According to some combination of six parameters, the result obtained by the formula is:

$$Q_m - Qe^{*} \pm Qr^{*} \pm Qc^{*} = \Delta Q^{*} \quad (7)$$

If $\Delta Q^*=0$, the thermal environment is considered to be comfortable.

If $\Delta Q^*=L\neq 0$, that is, the thermal comfort balance is destroyed. In order to maintain normal body temperature, the working intensity of regulating function is bound to change. The greater the absolute value of L, the greater the discomfort degree. According to the experiment, Fanger obtained the functional relationship between PMV index representing thermal sensation and thermal load L and other factors:

PMV is the thermal sensation value of a combination of environmental factors during the experiment. The relationship between this index and human thermal sensation is as follows table 3-2:

Table 3-2. PMV-PPD comfort index.

Hot sensation	**cold**	**cool**	**Slightly cooler**	**neutralize**	**Slightly warmer**	**warm**	**hot**
PMV	-3	-2	-1	0	1	2	3

3.2 Research Methods

3.2.1 Field research

Field research: Field research is one of the most basic research methods. In southern Shaanxi, cooking methods, heating methods, thermal performance of residential building materials and the thermal environment of residential buildings have been deeply understood by means of questionnaire, measurement and interview. By using the methods of analysis, comparison and induction, representative traditional folk houses were selected as the key research objects (Figure 3-1).

Figure 3-1. Field research.

3.2.2 Data Collection

Data collection: Data collection is mainly the classification and sorting of the current survey data. The field investigation of indoor, outdoor, on the surface of the wall inside and outside temperature, different cooking of indoor temperature, different heating means of indoor temperature, the temperature of the hearth in the combustion, wall temperature of the flue, doors, windows and the entrance to the position and size, the size of the room size, and other primary data to be screened, classified and collated.

3.2.3 Induction and Summary

Induction and summary: Induction and summary is to summarize the data according to certain standards, and summarize the properties of the research objects through analysis and comparison. Indoor, outdoor, on the surface of the wall inside and outside temperature, different cooking of indoor temperature, different heating means of indoor temperature, and the influence of human body, the temperature of the hearth in the combustion, wall temperature of the flue, doors, windows and entrances are summarized in relation to the size of the room. The characteristics of thermal environment, cooking mode, heating mode and basic scale of traditional residential buildings in southern Shaanxi were summarized. Table 2 is the related properties of the building materials.

3.2.4 Software Simulation

The simulation software included ANSYS (American ANSYS company, Pittsburgh, America), Open Studio (National renewable energy laboratory, Golden, CO, USA), Ladybug (National renewable energy laboratory, Golden, CO, USA), Energyplus (National renewable energy laboratory, Golden, CO, USA), and MATLAB (MathWorks, Natick, MA, USA). The boundary condition was the presence or absence of solar radiation. ANSYS was mainly used to calculate the heating time and the indoor temperature after the heating balance. Open Studio, Ladybug, and Energyplus mainly calculated the reduction in the heat load of residential buildings throughout the year by using different heating methods. The annual weather data came from the Energyplus weather data package. ANSYS was mainly used for turbulence calculation, steady-state and transient thermal calculation, thermal convection, and thermal radiation calculation. The turbulent calculation primarily simulated the hot gas entering the tube wall and calculated the temperature of the tube and the required time. The steady-state and transient thermal calculation mainly computed the temperature and time of the tube wall heating the wall, as well as the heat transfer time and temperature of the wall between additional sunlight. Heat convection and radiation mainly computed the temperature in the cooking heating wall room, the time and temperature of the additional sunlight heated by solar radiation, and the situations that affect the indoor temperature. The heat load of buildings was calculated with different heating methods. Open Studio, Ladybug, Energyplus and MATLAB were used to simulate the calculations. The steps were to establish a simulation in Open Studio, to put the built model into Ladybug software, and to assign material attributes. The model was carried into Energyplus for simulation analysis, and the heat load results were imported into MATLAB for editing.

(1) Establishing Grids

The model was established according to the measured data and imported into ANSYS. According to the method provided by Arturs et al., the grid was set and divided, and finite element simulation analysis technology was used to analyze the indoor temperature [63]. The k-epsilon format was selected for the model, which is conducive to a more stable model analysis. For ensuring the simulation results were close to the actual situation, it was necessary to set the convergence value. Herein, the convergence value of temperature and energy was 6–10, and the convergence value of the other values was 4–10. The grid setting in ANSYS software is very important, which determines the accuracy of the numerical simulations. Arturs et al. [63] used 1.54, 1.92, 0.55, 0.98, 2.09, and 0.34 million hexagonal sections to divide the grid. In this research, mapped meshing and local refinement were selected. In the process of mapping the grid division, it was divided into 5.324 million cells. In order to reduce the simulation time, the grid size can be controlled by setting the grid size value and the grid growth rate. When setting the grid between the wall and the roof, the grid should be evenly arranged on the roof and the wall. This is conducive to the simulation, with results being closer to the actual situation. As the walls are made of four layers of material, the thickness was 251 mm, and they were kept at 4.5% between adjacent grids.

(2) Interface Conditions

The energy equation was used and k-epsilon and RNG (National Renewable Energy Laboratory, Golden, CO, USA), were used in the turbulence model. The standard in nearwall treatment and buoyancy effects in options was selected. In the thermal radiation model, automatic calculation of the appropriate amount of the sun’s irradiation direction was chosen, and the local longitude, latitude, and date were entered. When setting the material, the relevant thermal properties of the walls, glass, air, and other materials were entered.

(3) Boundary Conditions

After setting the abovementioned parameters, the boundary conditions, such as the walls, glass, floors, floors, and fluids, were set up. Then, detailed parameters in the five boundary conditions were set, including the initial temperature, material, and radiation absorption rate. Finally, the solution was conducted.

(4) Indoor temperature simulation

The steps of ansys software to simulate indoor temperature are shown in the figure 3-2.

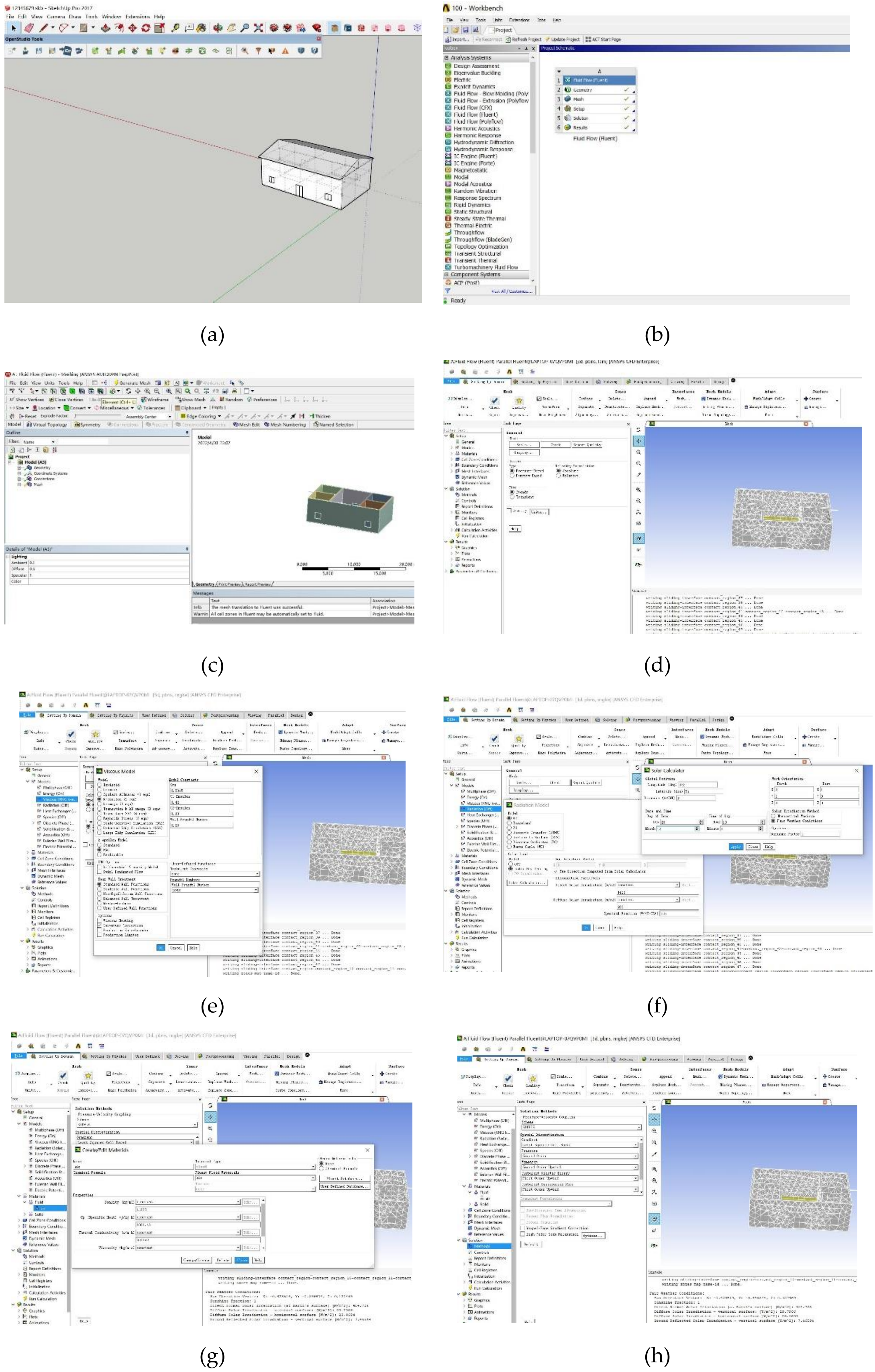

Figure 3-2. (a) Build a model; (b) Import the Ansys; (c) Mesh; (d) Open Fluent; (e) Open the energy equation and select the turbulence model; (f) Set up the radiation model; (g) Set material properties for walls, glass, etc.; (h) Solve.

Table 3-3 includes the basic information of the houses in southern Shaanxi, such as the climate conditions, schedule, number of occupants, size of houses, and construction techniques, such as the walls and roofs. Table 3-4 is the related properties of the building materials.

Table 3-3. Basic information of the houses in southern Shaanxi.

Dwellings	Data Statistics
Research location	Hongcun, Houliu town, Shiquan county, Ankang city, and Shaanxi province
Climatic conditions	Hot summer and cold winter
Time and behavior	09:00–9:00 a.m. at home, 9:00–11:00 a.m. not at home, 11:00 a.m.–3:00 p.m. at home, 3:00–6:00 p.m. at home, 6:00 p.m.–12:00 a.m. at home
Number of occupants	1–2
Room information	Number: 4; sizes: Meeting room 6 m × 6 m, kitchen 4.2 m × 6 m, and bedroom 4.2 m × 6 m; height: 4.8 m
Roof	5 mm tile + 4 mm waterproof coiled material + 20 mm cement mortar + 4 mm lime cement mortar
Wall	4 mm lime cement mortar + 240 mm clay porous brick masonry + 3 mm cement mortar + 4 mm lime cement mortar
Window	Thickness: 6 mm; length: 1200 mm; width: 1300 mm; glass and heat transfer coefficient: 4.7 W/(m2·K); number: 3
Earthen stove	Length: 1800 mm; width: 900 mm; height: 800 mm
Door	45 mm wood; size: 900 mm × 2100 mm; number: 4
Floor	120 mm lime cement mortar
Stoves	Length: 1800 mm; width: 900 mm; height: 800 mm

Table 3-4. Related properties of the building materials.

Material Name	Thermal Storage Coefficient W/(m^2·K)	Specific Heat Capacity (J/kg·K)	Density (Kg/m^3)	Thermal Conductivity (W/m·K)
Tile	6.23	1406	1800	0.43
Waterproof coiled materials	3.302x	1470	600	0.17
Cement mortar	11.37	1050	1800	0.93
Lime cement mortar	10.75	1050	1700	0.87
Clay porous brick masonry	6.602	1356	850	0.52
Wood	3.575	2510	500	0.14
Air	-	-	1.27	-
Aluminum	191.495	920	2700	203

According to the calculation, the lowest indoor temperature on the winter solstice is 2℃, and the highest temperature is 6.5℃ (Figure 3-3). The lowest indoor humidity on the winter solstice is 60.45% and the highest is 66.51% (Figure 3-4). The lowest indoor wind speed was 0.12m /s and the highest was 0.48m /s (Figure 3-5). The difference between the test results and the simulation results is small, indicating that the simulation is close to the actual measurement.

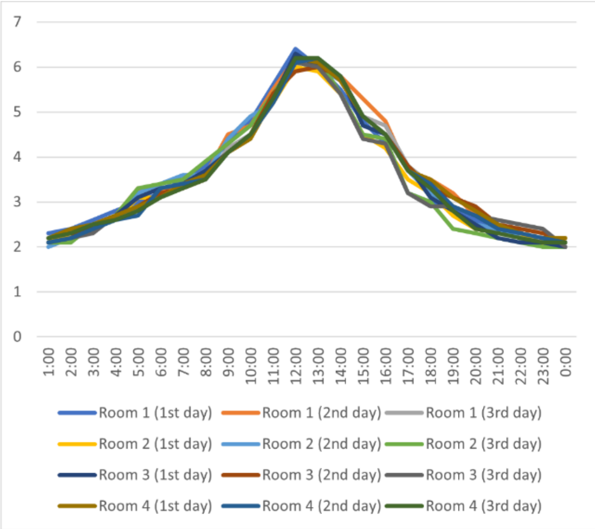

Figure 3-3. Indoor temperature.

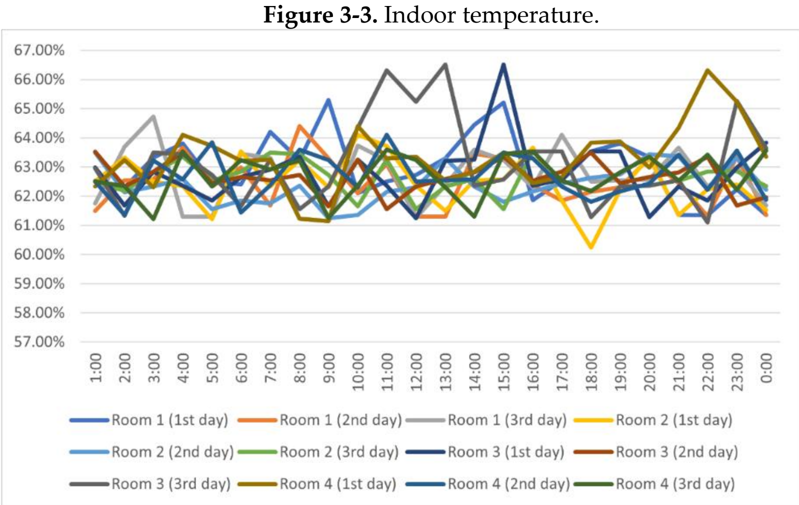

Figure 3-4. Indoor humidity.

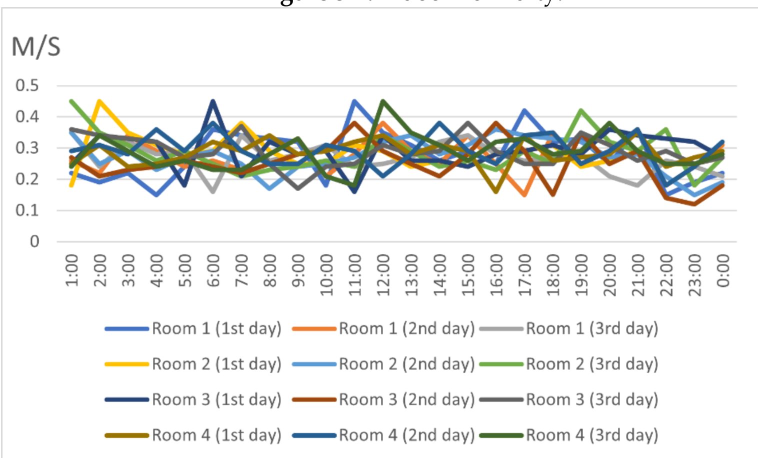

Figure 3-5. Indoor wind speed.

According to the measured data of residential buildings, the model was built in OpenStudio, and thermal attributes were given (Figure 3-2 a). Export the model file to IDF format and import it into Energyplus (Figure 3-2 b). Energyplus sets parameters for walls, Windows, roofs and doors, as well as basic information about people, lighting and equipment. And import the basic information for Energyplus Weather (Figure 3-2 c-d). Click the simulate button and do the calculation (Figure 3-2 e). After the calculation, the indoor temperature statistical table is generated (Figure 3-2 f).

The steps of energyplus software to simulate energy consumption are shown in the figure 3-6.

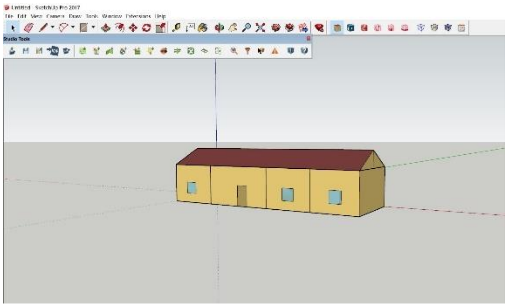

(a)

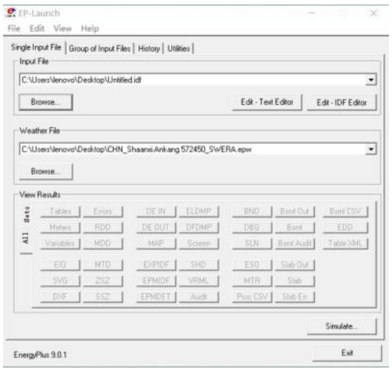

(b)

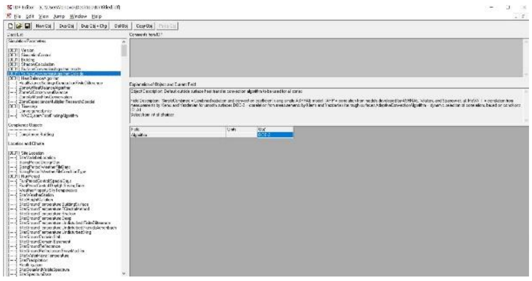

(c)

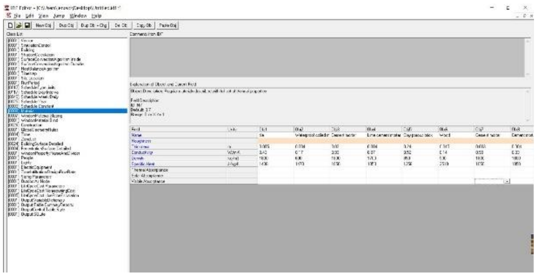

(d)

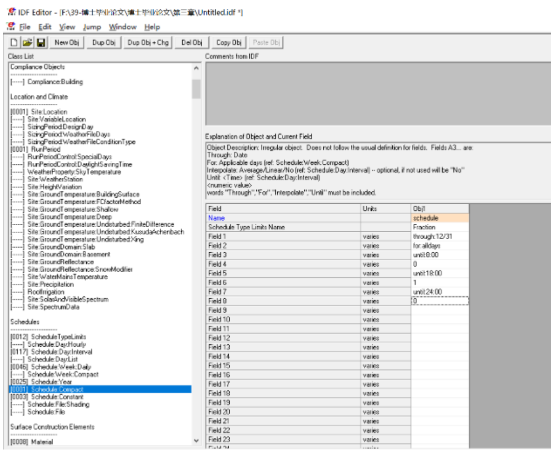

(e)

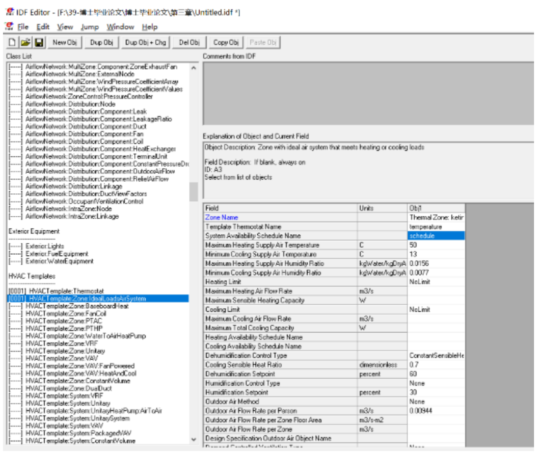

(f)

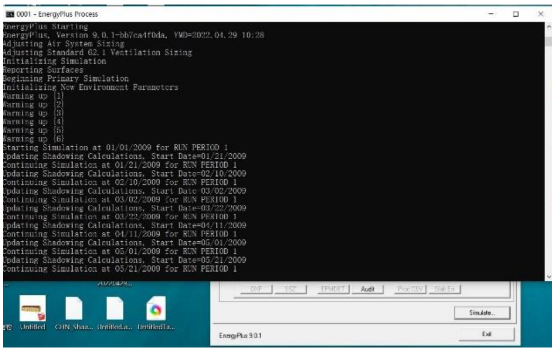

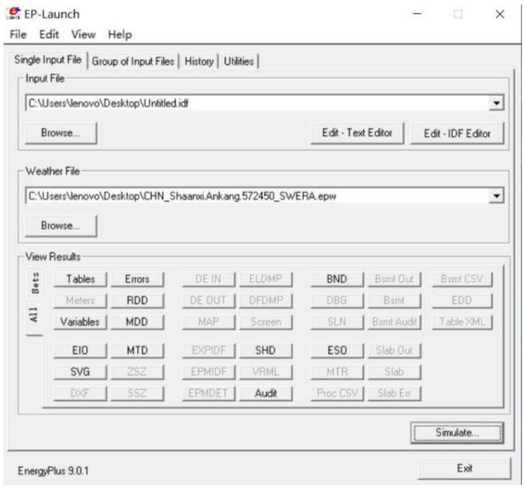

(g) (h)

Figure 3-6. (a) Build a model; (b) Import the Energy-plus; (c) Select DOE-2 kernel computation; (d) Enter parameters such as walls, doors and windows; (e) Set a schedule; (f) Setting Calculated Heat Loads; (g) Run to calculate; (h) Calculate the end.

3.3 Chapter Summary

This section mainly introduces relevant research theories and methods. The research principle mainly includes heat transfer principle and application, effective temperature, and thermal sensation PMV - PPD index. The research methods mainly include field investigation, data collection, induction and summary, and software simulation. Through the application of relevant theories and methods, the paper analyzes the characteristics of traditional houses in southern Shaanxi and verifies the effectiveness of the heating system between passive cooking heating wall and additional sunlight.

Reference

[1] Roh, H. Kinetics of polarization mechanisms, J. Electrochem. Soc. (in press).

[2] Roh, H. Pool boiling mechanisms, Int. J. Heat Mass Transfer (submitted for publication).

[3] Roh, H. Heat transfer mechanisms in solidification, Int. J. Heat Mass Transfer (submitted for publication).

[4] Taine, J.; Petit, J. Heat Transfer. Prentice Hall Ltd. 1993.

[5] Landau, L.D.; Lifshitz, E.M. Fluid Mechanics, second ed. Pergamon Press. 1989.

[6] Lienhard, J.H. A Heat Transfer Textbook, second ed., Prentice-Hall, Inc. 1987.

[7] Collier, J.G. Convective Boiling and Condensation, second ed., McGraw-Hill C. New York. 1972.

[8] Bejan, A. Heat Transfer, John Wiley & Sons Inc. 1993.

[9] Bejan, A. Convection Heat Transfer, John Wiley & Sons Inc. 1984.

[10] Incropera, F.P.; De Witt, D.P. Fundamentals of Heat and Mass Transfer, third ed. John Wiley & Sons Inc. 1990.

[11] Nukiyama, S. The maximum and minimum values of the heat Q transmitted from metal to boiling water under atmospheric process. J. Jap. Soc. Mech. Eng. 1934, 37, 367–374.

[12] McHale, J.P.; Garimella, S.V. Bubble nucleation characteristics in pool boiling ofa wetting liquid on smooth and rough surfaces. Int. J. Multiphase Flow. 2010, 36, 249–260.

[13] Hsu, Y. Graham, R.W. An Analytical and Experimental Study of the Thermal Boundary Layer and Equilibrium Cycle in Nucleate Boiling. Report No. NASATN-D-594, 1961.

[14] Foster, H.K.; Greif, R. Heat transfer to a boiling liquid: mechanism and correlations. J. Heat Transfer 1959, 81, 43–53.

[15] Mikic, B.; Rohsenow, W.M. A new correlation of pool-boiling data including the effect of heating surface characteristics. J. Heat Transfer. 1969, 11, 245–250.

[16] Zuber, N. On the stability of boiling heat transfer, Trans. ASME. 1958, 80, 711–720.

[17] Han, C.; Griffith, P. The mechanism of heat transfer in nucleate boiling, Part I and II. Int. J. Heat Mass Transfer. 1965, 8, 887–914.

[18] Rohsenow, W.M. A method of correlating heat transfer data for surface boiling liquids, Trans. ASME. 1952, 74, 969–976.

[19] Foster, H.K.; Zuber, N. Dynamics of vapor bubbles and boiling heat transfer, Am. Inst. Chem. Eng. J. 1955, 1, 531–535.

[20] Prabhu, K.N.; Kumar, S.T.; Venkataraman, N. Heat transfer at the metal/substrate Interface during solidification of Pb–Sn solder alloys. J. Mater. Eng. Perform. 2002, 11, 265–273.

[21] Malaysia. National Energy Balance 2003 Malaysia. Ministry of Energy, Water and Communication. 2003.

[22] Malaysia, General Report of the Population and Housing Census. Department of Statistics Malaysia. 1970.

[22] Mahlia, T.M.I.; Masjuki, H.H.; Saidur, R.; Amalina, M.A. Viewpoint mitigation of emissions through energy efficiency standards for room air conditioners in Malaysia. Energy Policy. 2004, 32, 1783–1787.

[23] Santamouris, M.; Wouters (Eds.), P. Building Ventilation. The State of the Art, Earth Scan UK. 2006.

[24] Santamouris, M.; Mihalakakou, G.; Argiriou, A.; Asimakopoulos, D. On the efficiency of night ventilation techniques for thermostatically controlled buildings. Solar Energy. 1996, 56, 479–483.

[25] Blondeau, P.; Sperandio, M.; Allard, F. Night ventilation for building cooling in summer. Solar Energy. 1997, 61, 327–335.

[26] Kolokotroni, M.; Aronis, A. Cooling-energy reduction in air-conditioned offices by using night ventilation. Applied Energy. 1999, 63, 241–253.

[27] Kolokotroni, M.; Giannitsaris, I.; Watkins, R. The effect of the London urban heat island on building summer cooling demand and night ventilation strategies. Solar Energy, 2006, 80, 383–392.

[28] Geros, V.; Santamouris, M.; Tsangrasoulis, A.; Guarracino, G. Experimental evaluation of night ventilation phenomena. Energy and Buildings. 1999, 29, 141–154.

[29] V. Geros, M. Santamouris, S. Karatasou, A. Tsangrassoulis, N. Papanikolaou, On the cooling potential of night ventilation techniques in the urban environment. Energy and Buildings. 2005, 37, 243–257.

[30] Artmann, N.; Manz, H.; Heiselberg, P. Climatic potential for passive cooling of buildings by night-time ventilation in Europe. Applied Energy. 2007, 84, 187–201.

[31] Finn, D.P.; Connolly, D.; Kenny, P. Sensitivity analysis of a maritime located night ventilated library building. Solar Energy. 2007, 81, 697–710.

[32] Zhou, J.; Zhang, G.; Lin, Y.; Li, Y. Coupling of thermal mass and natural ventilation in buildings. Energy and Buildings. 2008, 40, 979–986.

Chapter 4. Analysis of Characteristic Elements and Influencing Factors of Traditional Houses in Southern Shaanxi

This chapter makes a detailed analysis of the elements of spatial characteristics of residential houses in southern Shaanxi. Characteristics are a universal law of the existence of things, and also the characteristics of things that are different from other things. This paper analyzes the spatial characteristics of residential houses in southern Shaanxi from three angles: the functional characteristics, the technical characteristics and the image characteristics. The spatial functional characteristics include the shape and volume of space. The technical characteristics of space include the satisfaction of structure form to space and the adaptation of physical environment to space. The image features of space include settlement style, courtyard form and architectural modeling.

4.1 Settlements Features of Traditional Dwellings.

4.1.1 Settlement landscape

Due to the special geographical environment, the landform of southern Shaanxi has the characteristic of typical river valley, namely, two mountains and one river. The complexity of landform creates the diversity of folk houses. Its settlement style is a combination of natural ecological view, social form view and humanistic emotion view, and its characteristics are shown in the formation of groups, according to the shape of the situation, orderly.

Figure 4-1. Distribution map of traditional settlements.

(1) Into the composition of the reunited layout

Due to the limitation of landform in southern Shaanxi, the land for homestead is limited, and the density of houses in villages is large or scattered. There are four forms of folk houses in southern Shaanxi: courtyard type, U type, L type and one type. The selection of folk houses follows the idea of feng shui, with the principle of negative Yin embracing Yang, mountain facing water behind, river in front of base and mountain peak behind (Figure 4-1).

The settlement pattern in southern Shaanxi rises and falls with the slope, and the residents have their own way of site selection. In the area with gentle slope, houses are widely distributed, and the architectural form is mostly courtyard style. They are distributed along both sides of the main road in the village, with a degree of density, which is convenient to connect with neighbors and is not interfered by outsiders. In areas with steeper slope, houses are less distributed, with simple architectural forms, scattered distribution, and relatively independent residence, lacking contact with the outside world. No matter in gentle or steep areas, most buildings are arranged along the axis, which is influenced by the qin and Chu cultures. The spatial form of residents highly respects the system of etiquette, respecting the elderly and caring for the young.

(2) Architectural style due to shape

The slope of the mountain in southern Shaanxi is characterized by steep slope in the north and slow slope in the south. The "small dam" is formed by the erosion of the Han River. This flat terrain results in relatively concentrated distribution of residential houses and farmland. Due to the complex terrain in most areas of southern Shaanxi, the residential buildings are arranged along the contour line of the mountain due to the restriction of the terrain. The residential buildings make use of the height difference, resulting in the fluctuation of the internal space of the building or the change of the courtyard space, and the overall settlement distribution is scattered and irregular. Residents make full use of landform, a natural element, to diversify the space of houses and courtyards, which is the product of the mutual unity and integration of artificial and nature (Figure 4-2 a,b).

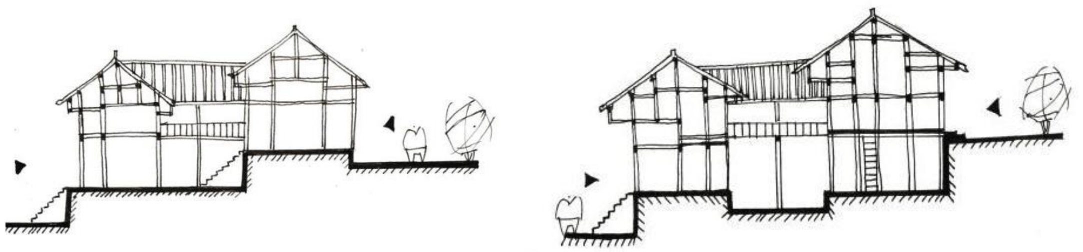

(a) (b)

Figure 4-2. (a) Courtyard space adapts to topographic elevation difference; (b) The interior of the building adapts to topographic elevation differences.

(3) Public space integrated into nature

The public space in the settlements in southern Shaanxi generally adopts free-style layout without clear definition, and the building materials are mostly local materials. In addition to residential buildings, there are other elements in the settlement, among which streets, lanes, places and other Spaces belong to the public space, and the setting of these public Spaces determines the morphological characteristics of the settlement.

1) Street and lane space: Residential buildings are arranged along contour lines on sunny slopes or at the foot of a dam area. Residential buildings are adjacent to each other, and street and lane space is naturally formed between adjacent residential buildings. Due to the limitation of terrain conditions in southern Shaanxi, the layout of streets and lanes is not neatly arranged, and the free layout reflects the characteristics of streets and lanes adapting to terrain. The general street and lane space extends from the main road to both sides, and with the decrease of the width of the street and lane, its grade also decreases, with certain regularity. The width of the street and lane space depends on the area occupied by the residential yard, which is in line with the communication space of people. The streets and lanes are generally paved with green stone or loess. The application of this material makes the streets and lanes complement the residential buildings and echo the nature (Figure 4-3 a).

2) location: location space is commonly used in villagers' communication in villages in southern shaanxi, assembly, and other public venues, its effect is convenient and the communication between residents, the vast majority of places space instead of through detailed

planning and freestyle layout, for places not defined in detail, and the integration of the natural environment, the use of its space dimensions meet basic needs (Figure 4-3 b).

(a) (b)

Figure 4-3. (a) Street spaces; (b) Place the space.

4.1.2 Courtyard Form

Through field research, the treatment of architectural modeling of traditional residential buildings in southern Shaanxi mainly includes four aspects, such as entrance space, facade modeling, body combination and detail decoration, and their characteristics are as follows.

(1) Raise the entrance

The folk houses in southern Shaanxi generally emphasize the entrance space, and the specific method is to set steps in the main entrance. It can be concluded from the survey that there are two forms of the foundation of the folk houses in southern Shaanxi. One is that the building is built according to local conditions and takes advantage of the terrain height difference to form a natural foundation. The height difference between indoor and outdoor is large in this kind of folk houses, and the number of steps is generally 5-10 (Figure 4-4 a). Another kind is artificial construction platform, this kind of indoor and outdoor height difference is lower, the number of steps is 1~3 steps in general (Figure 4-4 b).

(a) (b)

Figure 4-4. (a) Natural stylobate; (b) Artificial stylobate.

(2) Three facades

The traditional folk houses in southern Shaanxi adopt three-stage layout of platform, house and roof. The platform generally adopts two or three steps and the height of the platform is moderate. The house body is divided by pillars, beams and other frames; The roof is pitched to facilitate drainage.

The base is a prominent platform cut with stone slabs under the residential building, which is used to bear the load of the residential building. Through investigation, it can be found that in traditional residential buildings in southern Shaanxi, steps and foundation are combined, among which steps are usually one to three steps.

The roof is the core supporting part of the facade of traditional houses in southern Shaanxi. It is mainly enclosed by pillars, beams, tiebeams and other load-bearing components as well as walls. During construction, the columns are erected on the platform, and the beams are mounted along the longitudinal axis of the columns, and the transverse direction is connected by tiebeams. The architectural space is divided into one room between two columns.

As soil, stone and brick are the main components in southern Shaanxi, the walls of traditional houses are divided into two types. The other is based on earth walls, cement plastering.

The roof is divided into two forms: hard mountain and hanging mountain. Hard mountain roof refers to the building beam and roof bearing structure are built in the gable, the roof slope is gentle, the gable on both sides of the roof for fire prevention; Hanging hill roof refers to the roof hanging over the gable, the roof slope is steep. Both roofs adopt the form of double slope with the eaves projecting far out, and the roof is covered with black green tiles.

The building is generally divided into two colors, mainly composed of gray white plaster earth wall and black blue tile, belonging to the cool color system; With yellow earth wall and black green tiles as the main color composition, belonging to the warm color system (Table 4-1).

Table 4-1. Color combination.

Tone	Color combination	Picture
Warm color	Yellow + black	
Cool color	Lime white + black	

(3) Body combination

The form combination of traditional residential houses in southern Shaanxi is generally the form of the combination of the main building space and the auxiliary building space. The main building space is usually three rooms, and the building height is higher in the form of attic. The roof adopts the double sloping roof with short front and long back, and the green tile roof, to meet the residents' daily life. Auxiliary buildings generally use a lower double slope wing (Figure 4-5).

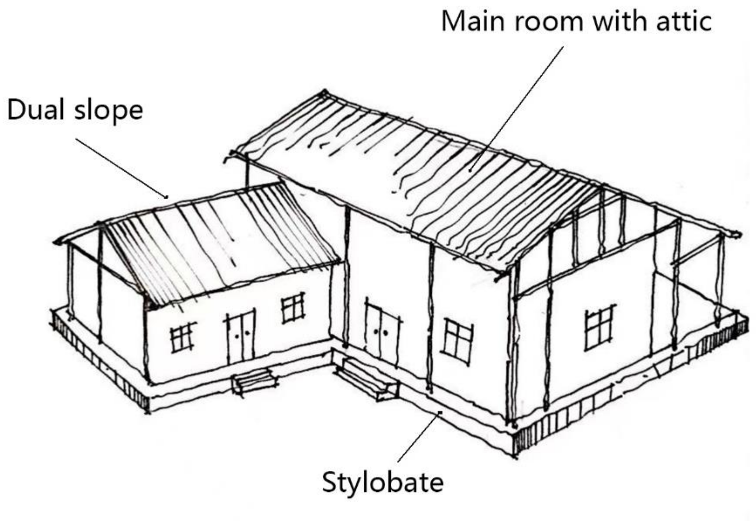

Figure 4-5. Form combination of residential houses.

4.2 Formation Process of Traditional Dwellings

4.2.1 Formation of Traditional Dwellings

Before the founding of New China, China was in a semi-colonial and semi-feudal society. During this period, the earliest residential houses appeared, which were characterized by large houses and small houses, forming a residential community with high concentration. Monomer buildings are courtyard Spaces, which are connected by curved streets and lanes to form a certain scale of settlement space.

Residential buildings are composed of houses with different functions centered on courtyard space. Layout characteristics of residential houses in southern Shaanxi: The architecture is arranged in axis symmetry, including neighborhood (shop), wing, main room, courtyard and courtyard wall, which embodies a strong hierarchical system and certain order. The main function of the courtyard style in this period was to resist foreign enemies, which was caused by the large number of family members and the closed mind of the people at that time.

(1) Spatial form of folk houses

In terms of function, the main room is located in the middle, used for receiving guests and discussing, the ear room is located on both sides for elders to live, and the wing room on both sides for the younger generation to live, which is the traditional layout of one bright and two dark. All activities of residents are carried out around the patio, which is a planar spatial form with strong concentration and introversion. In terms of construction technology, the large wooden frame is mostly made of wood in residential buildings, and the buildings are mostly made of cross beam and lift beam. When creating a large space, the lift beam is used, and when creating a small space, the cross beam is used. In terms of the shape of the houses, the overall shape of the houses is similar to that of the northern quadrangle courtyard. The symmetrical layout with green tiles and yellow walls is made with the courtyard as the center, which shows the thick and grand architecture of the whole houses.

(2) Layout of the yard

Courtyard houses in southern Shaanxi during this period were mainly siheyuan and triheyuan. Siheyuan was the most important form of courtyard, in which the courtyard was dominated by one courtyard, followed by two and three courtyards (Figure 4-6 a). The courtyard is composed of shops, wing rooms, main rooms, corridors, doormen and other Spaces. Some of them have two main floors in one courtyard, the first floor is used for reception and discussion, and the second floor is used for living. The courtyard space is square and small, and each roof is connected with each other, and the eaves are extended to facilitate drainage in rainy days. Two-step and three-step courtyards are developed longitudinally or laterally, and the number of yard space or houses is increased along the axis. Such spatial arrangement increases the ductility and level of space.

Compared with the one-entrance courtyard, the three-courtyard lacks the connection space such as concierge and hall and is dominated by the main room and wing room. The ming hall in the main room is mainly used for receiving guests and discussing. The dark rooms on both sides are bedrooms, and the wing rooms on both sides are auxiliary rooms (Figure 4-6 b).

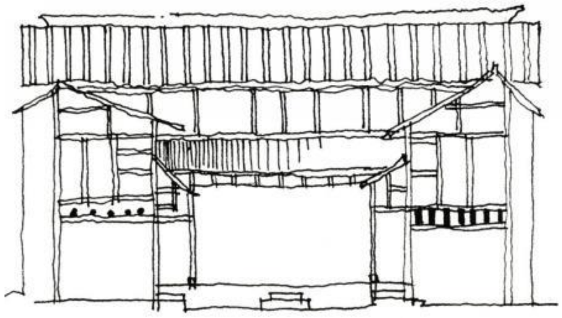

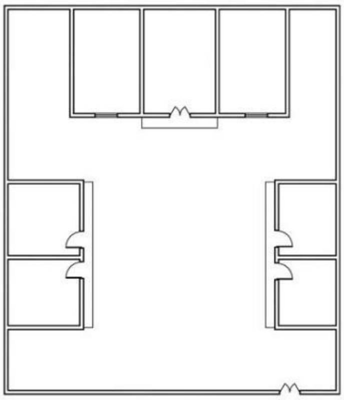

(a) (b)

Figure 4-6. (a) Residential elevation; (b) Plan of the “U” shape.

4.2.2 Development of Traditional Dwellings

From the founding of new China to the reform and opening up period, residential houses were divided into many households for one house. During this period, the architectural space of residential houses changed from the original architecture pattern of adjacent courtyard to the combination of house and courtyard, family joint construction and freestyle joint construction. Residential houses in this period adopted the pattern of big destruction and small new construction.

(1) Spatial form of folk houses

During the period of reform and opening up, the planar space form of folk houses changed from the previous space form, and two planar space forms emerged, namely, one-font and "L". Among them, the plane space of Stripe type is relatively simple, with the Ming Hall in the middle as the function of meeting and receiving guests, and the rooms on both sides as the function of living and bedrooms. This plane space lacks the connection with the courtyard space.

The "L" type plane is generally composed of the main building and the auxiliary building on one side. Generally, the main building is the main living room, and the auxiliary building on the other side is the auxiliary living room. The shape is also divided into two kinds, one is connected with the auxiliary building, but its internal functions are separated from each other, and the other is separated from the main body and the auxiliary building, and its internal functions are separated from each other. Functionally, the main building is used for discussion, reception, living, bedroom and other functions, and the auxiliary rooms are toilet, kitchen and storage. In terms of volume, the main building is obviously higher than the auxiliary building. The main building is no longer the traditional three-room building mode, but lengthened horizontally. The internal functional space of the building adopts the form of series, and the height of the main building is generally 7-9m.

(2) Layout of the yard

In this period, the courtyard space layout of folk houses no longer pursued the symmetrical layout with the courtyard as the center on both sides, and the courtyard space changed from closed to semi-open and open. This kind of courtyard layout also reflected the thoughts of people at that time from closed to open. The reason for the appearance of this kind of courtyard layout is that the enclosed courtyard not only gives people a sense of security, but also can resist foreign enemies. The courtyard space of Stripe and "L" shape deepens the connection between people (Table 4-2).

Table 4-2. "L" shape residential space.

"L"-shaped	Model diagram	Picture
One master one slave		
One main one attached		
One main and two attachments		

4.2.3 Decline of Traditional Dwellings

By the end of the 20th century, with the development of construction technology, the transformation of family population, the improvement of economic capacity, the pursuit of wealth symbols and other factors, people's thoughts have been liberated, and the form of traditional residential houses in southern Shaanxi has changed again.

The traditional houses of this period were demolished and small buildings were built. Residential buildings are mostly self-built. The plane of residential buildings does not pursue horizontal and vertical extension, and the original horizontal development is changed to vertical development. The building covers less area and the building height increases.

Modeling, the building is 2~4 layers, concrete or tile. Functionally, the central room extends to all sides, reflecting the concentration of residents in life. In terms of volume, each room of the building is not built according to the standard, the room is too large or too small; Construction technology, with the development of construction technology, the use of brick-concrete structure, reinforced concrete frame structure.

4.2.4 Revival of Traditional Dwellings

From the beginning of the 21st century, with the destruction of the surface caused by the Wenchuan earthquake in 2008, the traditional folk houses in southern Shaanxi began to revive. The construction method is to splice the elements of traditional folk houses, and residents adopt the slope roof and the beacon wall of the building. In terms of shape, the building is usually two-story, cement plastering, and archaize architectural elements are used to design the houses. Functionally, the central room is developed to all sides, so that the concentration of residents' life can be maintained. Construction technology, the use of brick - concrete structure (Figure 4-7).

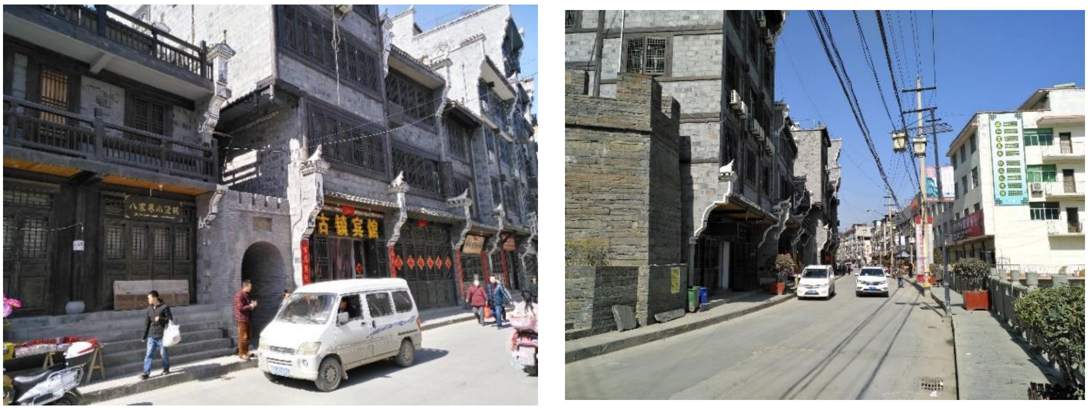

Figure 4-7. Traditional Dwellings.

To sum up, in the early society in southern Shaanxi, influenced by traffic conditions, residents' life and production almost depended on the natural environment, and the construction of residential buildings depended on residents' own experience and response to the natural environment, which made the residential buildings have local characteristics. In terms of spatial form, traditional houses have always been integrated with nature and adapted to nature. In the plane layout, the symmetrical, compact and regular form of the houses is retained because it is conducive to improving the seismic performance of the buildings. With the improvement of economy and the transformation of social form, the spatial layout of residents has changed, but the introversion has been continued. Functionally, the plane layout of "one bright and two dark" meets people's basic living needs, making this plane layout pattern has been continued; In terms of construction techniques, folk houses adapt to local conditions and make use of the height difference, climate and materials of the terrain to make the folk houses local. With the development of economic and social conditions, the architectural modeling of the houses in southern Shaanxi pursues simple imitation, the room area is too large, the integration of the natural environment is less, the dialogue of the natural environment is ignored, and the characteristics of the traditional houses are lost.

4.3 Spatial characteristics of Traditional Dwellings

4.3.1 Spatial Shape

Shape refers to the manifestation of things under certain conditions. From the perspective of language, "shape" can be grasped or perceived. Shape reflects people's thinking form and is subjective or objective, that is, the "appearance" of "form" and the "state" of "form" [1].

Space shape refers to the overall performance of the shape of things in a specific environment, which is used to explain the cause, organization, relationship, development and trend of shape in subjective and objective space, so as to facilitate the grasp of the nature of shape development [2,3].

(1) Courtyard Shape

Influenced by many factors, the folk houses in southern Shaanxi can be divided into courtyard type, U type, L type and one type (Table 4-3).

Table 4-3. Residential space form.

Classification	Features	Form
Courtyard	Few such courtyards; homestead is large; The courtyard is the center, and the building units are arranged symmetrically along the courtyard.	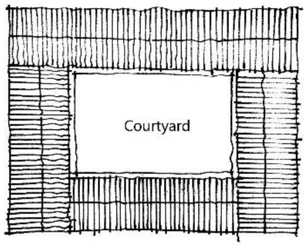
U shape	This architectural form has a large courtyard space for residents' activities and exchanges, and the building units are symmetrically arranged along the central axis.	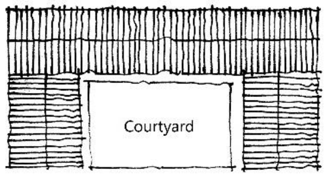
L shape	This architectural have a larger courtyard space, which is convenient for residents to communicate with each other and to dry food.	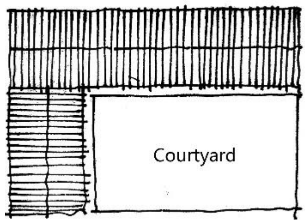
one- shape	The buildings are arranged in a line, and the open space in front of the door is defaulted as a communication space.	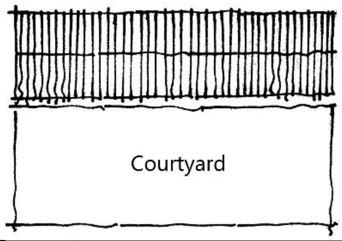

(2) The shape of the functional space

There are two shapes of residential houses in southern Shaanxi, including courtyard shape and house shape. The space shape of the courtyard is generally square, round, trapezoidal and irregular, which can meet the space of drying, planting, communication and storage. The shape of the house is generally rectangular, and its functional features include bedrooms, toilets, halls, kitchens and storage to meet people's basic living needs (Table 4-4).

Table 4-4. Shape features of functional space.

Residential houses	Functional characteristics	space shape	Picture

Courtyard space	drying plant socialize storage	Square, Round, Trapezoid, Irregular	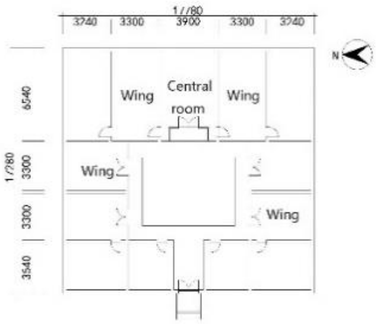
Residential space	Mingtang	Square, Rectangle	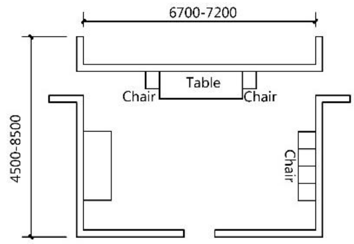
	Bedroom	Square, Rectangle	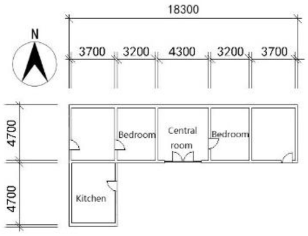
	Kitchen	Square, Rectangle	
	Bathroom	Square, Rectangle	-
	Storage	Square, Rectangle	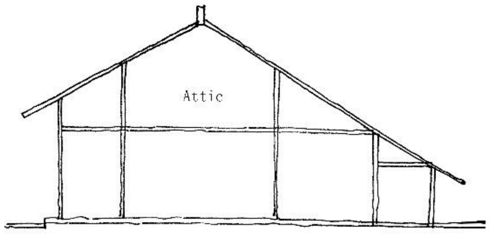

4.3.2 Function Layout

The architectural space of the houses in southern Shaanxi is composed of the hall, bedroom, storage, kitchen and other functional Spaces [4]. The hall is located in the middle and axisymmetric, and is an important place for residents to live and receive guests, as well as the center of people's activities [5]. The main room is composed of a bright hall and two dark rooms. "Room" is a spatial organization unit. The "room" in the main room ranges from 3.6m to 7.5m and the depth ranges from 4.5m to 9.9m. The Ming Hall is used for receiving guests and meeting. Its room layout is relatively simple, mainly with simple furniture such as tables and chairs. Darkroom is used for living in the bedroom for elders, mainly with cabinets, beds, tables and other furniture.

Bedrooms are generally located on both sides of the hall or one side of the wing, symmetrically arranged, and are multi-functional rooms such as living and storage. Bedrooms are generally 1 to 2 rooms, which are combined in series or parallel connection The bedroom is 3.2-3.9m in width and 3.6-4.5m in depth. The elderly live on both sides of the main room, and the young are located on the side of the wing. In addition to meeting the basic living requirements, the bedroom is also used for dining, storage and other functions.

The kitchen is generally located on the side of the wing or the hall to meet the basic needs of people's life. The kitchen is generally a single room with 3.0~3.9m opening, 3.6~4.6m depth and 3.0~3.5m building height. In addition to basic living cooking, the kitchen also meets the needs of storage.

Storage is generally located in the attic above the bedroom, occupying half of the area of the bedroom. This spatial layout is conducive to the insulation of the bedroom or arranged in the lower room on both sides of the entrance, symmetrical layout, used for storage space.

4.4. Technical Characteristics of Traditional Dwellings

4.4.1 Structural Form

(1) The structural form of traditional houses

Due to the unique geographical environment and abundant forestry resources, the folk houses in southern Shaanxi are mostly made of local materials. Therefore, the folk houses in southern Shaanxi can be generally divided into three structural forms: civil folk houses, brick-wood folk houses and wood folk houses [6].

The traditional civil structure adopts the wooden frame system, the wooden frame is composed of columns, wear fang, purlin to bear the weight of the house, the wall does not bear the weight, its role is mainly used for enclosing and dividing the space, the wall uses soil, wood, stone, brick and other building materials [7]. There are two kinds of frame techniques: cross type and beam lifting type. The beam lifting type is to mount the beam on the column and lift the beam on the beam. There are no columns or fewer columns in the indoor houses of this frame, which has large space and many consumables [8]. The cross type is to use the crossbeam to connect the columns in series to form a truss [9]. Purlin is placed in the column head, and the column is connected in series with the crossbeam along the purlin direction. This kind of frame houses use less material, strong integrity and small indoor space (Table 4-5).

Table 4-5. Structural form.

Classification	Features	Form
Lift beam	There are few or no columns indoors, and the space is large	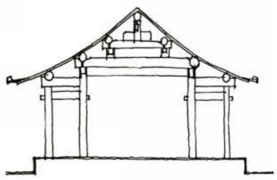
Cross type	Less material, strong integrity, small indoor space	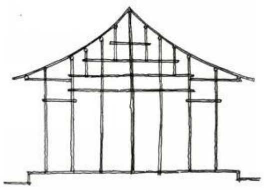

Both of the two frame forms take columns and beams as load-bearing systems, and the wall only plays the role of enclosing the space and distinguishing the indoor and outdoor, which has the security of "wall falling house does not collapse".

The main materials of residential houses are wood, soil, brick, stone and bamboo (Figure 4-8). Brick and wood structure residential houses refer to the walls and columns of the vertical load-bearing structure of the building are built with bricks or blocks, while the floor and roof truss are built with wood structure [10]. The use of brick-concrete maintenance structure, the combination of concrete and wood frame technology, its interior is mainly divided by pillars, the wall between two pillars, the interior space with the size of the partition. Brick-concrete structure refers to the wall and column of the vertical load-bearing structure in the building are made of bricks or blocks, while the beams, floors and roof plates of the horizontal load-bearing structure are made of reinforced concrete [11]. That is to say, the brick structure is a small part of reinforced concrete and most of the brick wall bearing structure. Compared with brick-wood structure, the construction technology of brick-concrete structure makes the building wall more stable and significantly improved, and the building space layout is more flexible and changeable.

Wood Soil

Stone Brick

Figure 4-8. Traditional houses in southern Shaanxi.

(2) Detail decoration

Folk houses in southern Shaanxi are divided into wood carving and stone carving according to building materials and techniques.

A. Wood carving:

Wood carving mainly adopts three carving techniques of relief, through carving and three-dimensional carving. Relief is mainly distributed in the details of residential houses, such as partitions, furniture and skirt boards. Through the carving mainly in the window, the theme is mostly plants, animals; Three-dimensional carving is mainly in independent components, such as columns (Figure 4-9).

Figure 4-9. Wood carving.

B. Stone

Stone carving is mainly located in the column base, using line carving, bas-relief. The theme of the carving is mostly animals, plants and other materials, and the carving is meticulous and exquisite (Figure 4-10).

Figure 4-10. Stone carving.

4.4.2 Physical Environment

(1) Spatial characteristics of thermal environment adaptation

Under the influence of monsoon climate, the overall climate in southern Shaanxi is hot and humid in summer and cold and humid in winter. During the construction of residential houses, different architectural techniques are used to meet the requirements of natural ventilation in summer and windproof in winter. The characteristics of thermal environment to space adaptation are as follows:

A. Adapt to the space characteristics of heat dissipation

Compared with modern houses, traditional houses in southern Shaanxi have more advantages of ventilation and heat dissipation in summer. In southern Shaanxi, the wind is southerly in summer. The houses use the shading effect of eaves and corridors, heat insulation of attic, courtyard and other forms of ventilation to improve ventilation and heat dissipation of houses by changing the indoor and outdoor space.

a. The shading of eaves and roof gallery

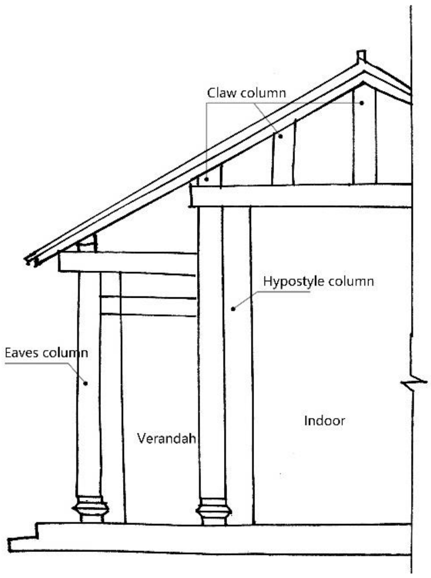

Figure 4-11. Eaves gallery.

In traditional residential houses in southern Shaanxi, eaves corridor can connect different architectural Spaces, which can be used for walking, shelter from wind and rain, lighting and ventilation (Figure 4-11). Residents take advantage of the characteristics of high sun height Angle in summer and low in winter, and use eaves corridor, roof, which can effectively reduce sun exposure, and form a transition space between indoor and outdoor, also known as "gray space" (Figure 4-12).

(a) (a)

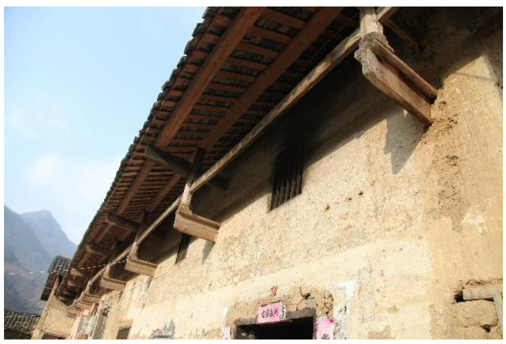

(b) (b)

Figure 4-12. (a) Roofs; (b) Eaves.

b. The insulation of the attic

The dark room on both sides of the hall is used for living in the lower layer and storage in the upper layer. The gable wall is generally a wall of fire, with holes left on the wall to form the effect of draught, so that the indoor space is well ventilated (Figure 4-13).

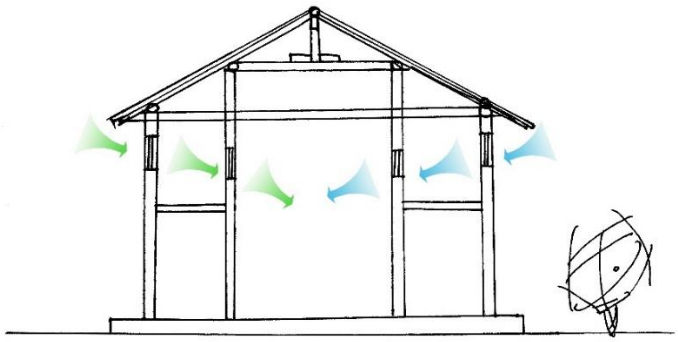

Figure 4-13. Attic profile.

(2) Courtyard

Traditional houses in southern Shaanxi are mostly low-rise buildings. In order to alleviate direct sunlight, flowers and trees are planted in the courtyard to shade the sun [12]. In summer, plants absorb solar radiation and produce photosynthesis, which reduces air temperature through evaporation of branches and leaves and improves the thermal environment of buildings. The combination of architecture and courtyard forms the closed and semi-closed space form of residential houses in southern Shaanxi.

A. Spatial characteristics conducive to cold insulation

Due to the influence of monsoon climate, the winter in southern Shaanxi is wet and cold, and residents in the process of construction, in order to resist the cold. Its construction means include: the north wall does not open windows or small windows, the courtyard building is high in the north and low in the south, the size of the window is small and other means, so that the residential building space has a closed feeling.

a. North wall

In southern Shaanxi, the wind is northwest in winter. In the construction process of residential houses, in order to resist cold and reduce the influence of wind on indoor temperature. The building is built with no windows or small windows to the north, which is designed to resist cold wind.

b. Building height

Traditional residential houses in southern Shaanxi are courtyard style, and the overall building height is different. The height of the north hall is higher than the height of the south room. In order to resist the influence of the northwest wind on the interior space of the building, and with the rise and fall of the terrain building, the interior space uses the height difference to vary.

(3) Spatial characteristics of light environment adaptation

There is sufficient sunshine in southern Shaanxi, and indoor lighting is abundant. Therefore, the influence of light environment on the space of houses in southern Shaanxi includes shading in summer, increasing the irradiation range of houses in winter and other construction techniques.

Affected by the monsoon climate, the southern Shaanxi region has high temperature and long sunshine duration in summer. During the construction process of residential houses, courtyard, eaves, architectural forms and other technical means are used to meet the demand of summer sun shading, creating the spatial diversity of residential houses in southern Shaanxi.

A. Natural lighting

By analyzing the solar radiation of villages in southern Shaanxi, it can be seen that the radiation received by buildings is related to the building density (Figure 4-14 a). The higher the density of the building, the less solar radiation it receives (Figure 4-14 b).

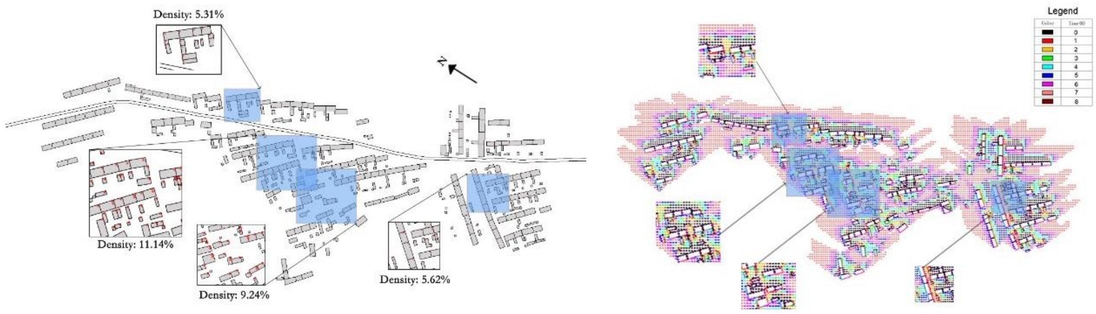

(a) (b)

Figure 4-14. (a) Buildings are divided according to different building densities; (b) Solar radiation analysis divided according to different building densities.

a. Patio

The southern Shaanxi region is hot in summer and cold in winter. The design of the patio meets the function of lighting and ventilation. Sunlight scatters to each room through the patio to meet the lighting demand of the room (Figure 4-15 a).

b. Overhangs

Overhanging eaves is a common component of traditional Chinese architecture. People take advantage of the high Angle of the sun in summer. During the construction of folk houses, the eaves are picked out a certain distance, which reduces the range and duration of sun irradiation and improves the architectural light environment. In this way, the architectural shape of folk houses in southern Shaanxi looks grand and thick as a whole (Figure 4-15 b).

(a) (b)

Figure 4-15. (a) Patio; (b) Overhangs.

c. Doors and windows

Doors and windows are the main means of lighting in residential buildings, but due to technical reasons, the scope of lighting from doors and windows is small (Figure 4-16).

Figure 4-16. Doors and windows.

B. Architectural form

Under the irradiation of the sun, the shadow produced by the building itself includes its own shadow, daily shadow and permanent shadow. The shadow of the building itself refers to that one part of the building blocks the other parts. All day shadow refers to the building is blocked by the outside, no sunshine all day; Permanent shadow means that the building itself is shielded from sunlight all year round.

The architectural forms of traditional folk houses in southern Shaanxi include rectangle, square, L-shaped and U-shaped. Rectangle and square have no shadow of their own, and l-shaped and U-shaped are easy to form their own shadow.

(4) Spatial characteristics of wind environment adaptation

Influenced by the monsoon climate, the houses in southern Shaanxi are southerly in summer and northerly in winter. In the construction process of traditional houses in southern Shaanxi, in order to ensure ventilation in summer and windproof in winter, consideration has been given to the site selection, building space and details. The spatial characteristics of wind environment adaptation are as follows:

A. Ventilation in summer

In southern Shaanxi, there is heavy rain and high temperature in summer, so ventilation can reduce indoor temperature and humidity and improve the comfort of wind environment. Natural ventilation is the preferred way for residents in life, and natural ventilation includes wind pressure and thermal pressure. Wind pressure is when the wind blows to the building, the building is blocked by the surface to form positive pressure, air flow from the side of the building, when the air flow from the front of the building through the back of the building, called "draught". Hot pressure means that the indoor temperature is higher than the outdoor temperature, and the outdoor airflow enters the room through the bottom of the building. The hot air from the upper part of the room is excluded from the upper part, and the indoor air forms the airflow.

Ventilation effect has a great relationship with the size, location and building orientation of the opening of windows in folk houses. Through the influence of different opening positions of doors and windows on ventilation, we can know the influence of doors and windows on ventilation. The opening size of windows in folk houses in southern Shaanxi is small. When the opening and the dominant wind direction into a vertical Angle, the larger the opening area, the better the indoor ventilation effect. Doors and windows are the main air inlet, affecting the ventilation of the whole residential building. The location of doors and windows has a positive influence on the architectural space. The larger the size of doors and windows, the more open the architectural space will be (Figure 4-17).

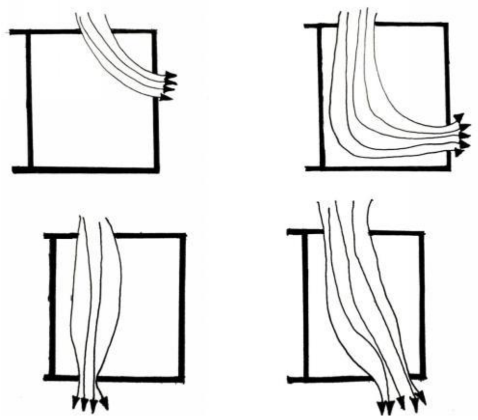

Figure 4-17. The influence of different openings of doors and windows on ventilation.

B. Windbreak in winter

In the thermal division, southern Shaanxi is located in cold winter and hot summer areas, so residents should consider wind protection in winter during construction. The winter wind is northwest in southern Shaanxi, and the building site is generally located in the north wind area, which is the dominant wind direction in winter, so as to prevent cold wind from entering by taking advantage of the terrain characteristics. In traditional folk houses in southern Shaanxi, courtyard style, according to the dominant wind direction, the room on the north side of the building is higher than the room on the south side. The architectural space takes advantage of this feature, and the interior space fluctuates, such as steps, attic and other construction techniques.

4.5 Influencing Factors of Traditional Dwellings

4.5.1 Natural Factors

(1) Topography and landform

Located in the southern part of Shaanxi, southern Shaanxi includes hanzhong, Ankang, and Shangluo. Qinling Mountains in the north and Daba Mountains in the south, the Han River flows from west to east. The Qinling-Bashan mountains in southern Shaanxi account for 36% of the total land area of the province. Mountainous terrain area and hilly terrain area occupy the vast majority of southern Shaanxi, pingba occupies a very small part of the entire southern Shaanxi area, southern Shaanxi has a typical valley landform [13].

The landforms in southern Shaanxi are mainly divided into four types: mountain stream valley type, terrace valley type, plateau valley type and river channel valley type, which are characterized as follows (Figure 4-18):

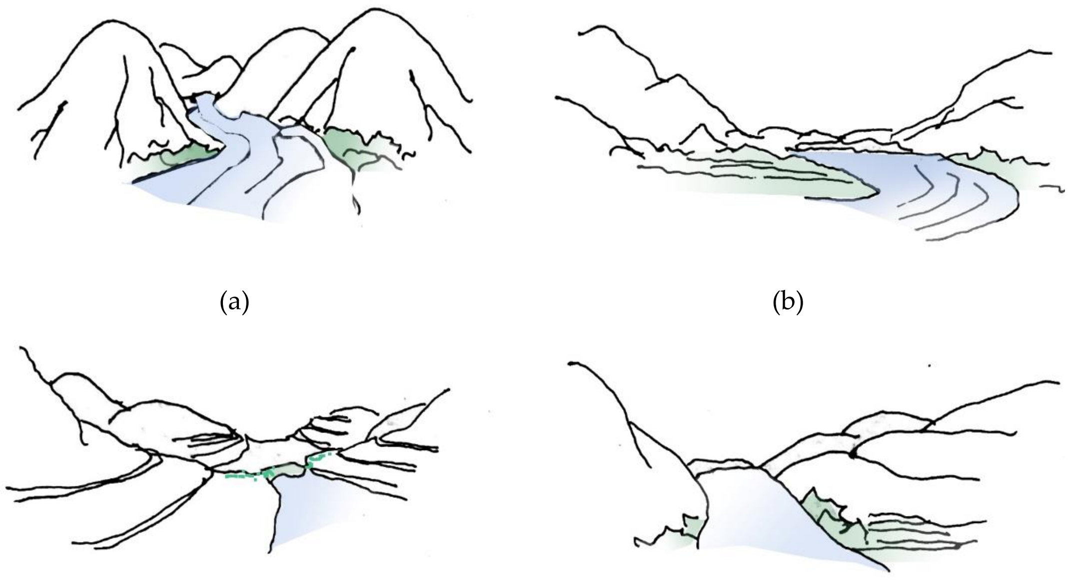

(a) (b) (c) (d)

Figure 4-18. (a) Mountain stream valley type; (b) Terrace valley type; (c) Tableland valley type; (d) River valley type.

A. Mountain stream valley type

The mountains on both sides are steep, and the river flows through. The riverbed area is relatively narrow. Buildings are generally distributed on the riverbed, and most of them are stilted buildings, which are supported by columns to prevent floods.

B. Terrace valley type

The mountains on both sides are impacted by the river, forming a stepped mountain. The river is distributed between the mountains, and the buildings are affected by the mountains and distributed in the stepped mountain.

C. Tableland valley type

The terrace of the river valley is distributed in strips along the river, and the terrace is inclined toward the river valley. The buildings are less distributed on the terrace, and the architectural form is mostly "one font".

D. River valley type

The mountain slope on both sides is relatively gentle, and the river flows through slowly. The riverbed area is relatively spacious. This type of landform has various architectural forms, including courtyard type, "U" type, "L" type and "one-character" type.

Southern Shaanxi is rich in terrain, including mountains, hills and flat dams, of which flat dams account for a small area of Southern Shaanxi. There are typical river valley landforms in southern Shaanxi. The folk houses in southern Shaanxi are distributed on these landforms, resulting in various forms of folk houses.

In the process of spatial form evolution, the folk houses in southern Shaanxi are obviously affected by topographic and geomorphic factors. In the early days, people built folk houses mainly in flat and spacious places along the river, and most of the architectural forms of their folk houses are courtyard style, which can meet the needs of people's production and life. With the increase of population, the former Pingba area could not meet the needs of people, and the houses began to be distributed in the smooth and long places along the river. The forms of the houses before were not suitable for such terrain, and the space of the houses began to change.

The houses adopted the "U" and "L" shapes to make up for the relatively limited land use. As most of southern Shaanxi is mountainous, resident's layout along the contour line during construction, and use the slope of the mountain to divide the interior functions. Their architectural forms pursue simple and generous, so most of their architectural forms are Stripe type.

The layout and spatial form of residential houses in southern Shaanxi are greatly influenced by mountain areas, among which "L" shape, Stripe shape and open courtyard dam are all formed under the restriction of mountain areas. The residential houses near rivers in southern Shaanxi adopt the form of stilted houses, which are also formed under the influence of geographical factors.

(2) Climatic conditions

Southern Shaanxi is affected by the monsoon climate, with sufficient sunshine in summer, high temperature, wet and rainy, dry and little rain in winter, and the rainfall is extremely unstable and varies greatly year by year [14]. In addition, due to the special topography and landform in southern Shaanxi, it is easy to form valley wind and have an impact on the layout of residential houses. Through analyzing the climate in southern Shaanxi, the following characteristics are summarized (Figure 4-19).

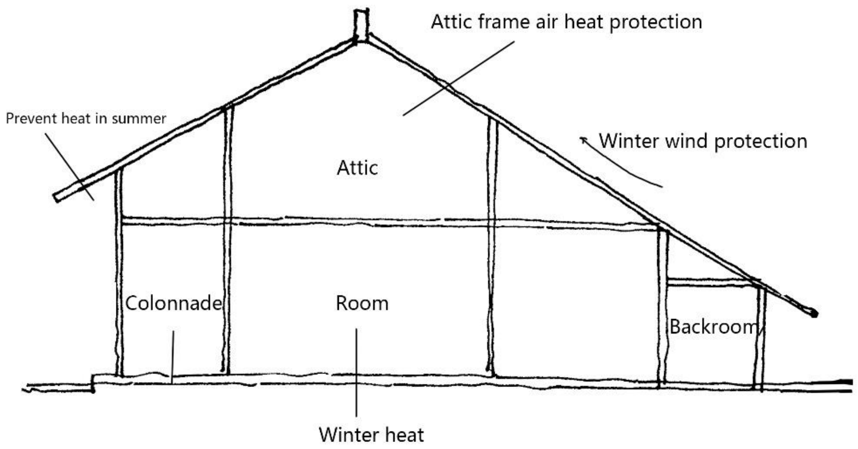

Figure 4-19. Representation diagram of residential space climate suitability.

The climatic conditions of southern Shaanxi affect the spatial form evolution of residential houses mainly by solar radiation, humidity and wind direction.

A. Solar radiation

In southern Shaanxi, there is sufficient sunshine and strong solar radiation in summer, resulting in high indoor temperature. In traditional courtyard style, the east and west wing rooms are exposed to the sun for a long time and the irradiation range is wide. The indoor temperature is easy to rise, and the north-south rooms are well ventilated. In the process of spatial form evolution of residential houses in southern Shaanxi, the residential land is irregular due to the diversity of landform, and the spatial form evolution of residential houses gradually changes from courtyard type to Stripe type.

B. Temperature and humidity

Affected by the monsoon climate, southern Shaanxi is characterized by hot summer and cold and wet winter. In order to adapt to this climate, traditional houses in southern Shaanxi adopt the construction technique of heat prevention in summer and heat preservation in winter.

a. Prevent heat in summer

Because of the high temperature in summer, the site selection of traditional houses is generally located in a better natural environment. The earthen ground and surrounding greening prevent solar radiation. The traditional residential buildings generally adopt the form of colonnade and the ratio of height to width is suitable for the local sun height Angle in winter and summer. The height of traditional residential buildings is generally 4~7m, and the partial indoor overhead adopts the form of attic for heat prevention.

b. Winter insulation

When it is cold in winter, residents use the slope of pitched roof to prevent the invasion of cold wind to the indoor environment. Colonnade and eaves are used to resist cold wind, but also meet the winter sun on the indoor environment. The back facade of the building is generally open or not open Windows, which is conducive to the insulation of the building; The architectural space with high south and low north is the expression of climate suitability.

In conclusion, affected by monsoon climate, southern Shaanxi is hot in summer and cold in winter. Dwellings adopt various construction techniques to meet the characteristics of heat prevention in summer and heat preservation in winter.

(3) Hydrological environment

There are many rivers in Shangluo city, Ankang City and Hanzhong City, which are rich in water resources. Han River water runs through the east and west, making gullies crisscrossed and rivers densely covered in southern Shaanxi. According to the location distribution of rivers and villages, it can be divided into three types: village rivers, parallel rivers and nearby rivers (Figure 4-20).

The river in the village: the river flows through the village and is about 6-9m away from the buildings. The general buildings are mostly in the form of water on the back of the mountain, and the "stilted buildings" are mostly used for the buildings using the terrain.

Parallel river: the water is arranged in parallel with the houses, and the water is 10-50m away from the buildings. Most of the buildings are "L" and Stripe shaped. Such building space reduces land use and forms a concentrated area, which is convenient for people to live and get water.

Tied river: The distance between the river and residential houses is about 400-900m. Residents use the distance to irrigate farmland.

Earlier resident in site selection, generally choose the location of the river in our village, its purpose is to facilitate water, building generally takes the form of mountain surface water, but as a result of geological hazards, such as high temperature summer rain prone to floods in southern shaanxi, residents in siting chose tied for the position of the river, the building body relax, choose courtyard type is in the majority. With the increase of population, the original architectural space could no longer meet the demand of population increase, so residents chose nearby rivers for site selection. However, influenced by the mountainous area in southern Shaanxi, the architecture changed during this period. The form of residential houses was Stripe and "L", which was in line with the shortage of land in southern Shaanxi.

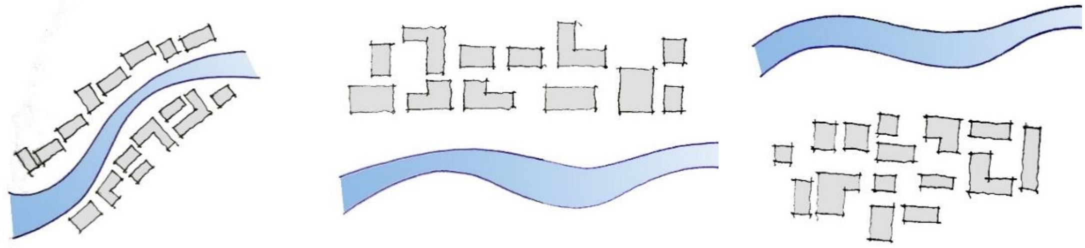

(a) (b) (c)

Figure 4-20. (a) The river in the village; (b) Tied river; (c) Nearby river.

4.5.2 Social Factors

(1) Economic development

Architectural structure, construction technology and other aspects have an important impact on the spatial form of residential buildings. The spatial form evolution of residential buildings cannot be separated from the support of technology. The selection of appropriate construction technology under different circumstances is of great significance to the development of residential buildings [15].

In primitive society, people pursued shelter from wind and rain during construction. In slave society, people made important development in construction technology. For example, the appearance of rammed earth technology led to the development of wooden frame. Ceramic tiles have replaced traditional construction materials. During the feudal society, the construction technology had remarkable improvement, and there appeared "Qin brick and Han tile", residential buildings and courtyards and other residential buildings. In modern and modern times, the construction techniques and materials of residential buildings have changed. In the long history of people building residential buildings, the development of technology has been promoting the spatial evolution of residential buildings, economic development has driven the development of technology, and the two are in a positive proportion, so economic development is one of the factors affecting the spatial form evolution of residential buildings.

Due to the unique geographical environment, the economic development in southern Shaanxi is relatively slow. The development of residential buildings in southern Shaanxi is different from that of urban residential buildings. The residential buildings in southern Shaanxi have certain dependence on the natural environment, and the development of construction technology is also relatively slow.

(2) Cultural environment

In the process of spatial form evolution of residential houses in southern Shaanxi, residents' customs, cultural inheritance, physiological and psychological needs are all important factors affecting the spatial form evolution. Under the specific regional environment, the construction of folk houses is not only based on the natural environment, economic development and other factors, but also includes the influence of the past customs, culture and other factors, so as to form the specific traditional folk houses in southern Shaanxi. The special geographical environment in southern Shaanxi has brought up the situation of diversified cultures in southern Shaanxi. In the process of spatial development, the houses also have diverse regional cultures, including traditional culture, immigrant culture, religious culture and surrounding culture [16].

A. Traditional culture

Under the influence of "rites" in traditional culture, the houses in southern Shaanxi have three aspects: strong hierarchy, clan concept and ethical culture.

a. Hierarchy

Residential buildings are arranged symmetrically along the axis, and the concept of high hierarchy is reflected in the residential buildings. For example, the darkroom on both sides of the main room is for the elders to live, while the wing room is for the younger generation to live, which reflects the hierarchical relationship between the superior and inferior of the family. Restricted by the ritual system, the carving of architectural details is limited to simple patterns such as plants and animals [17].

b. Concept of clan

The height and shape of the houses should be consistent with the external environment and should not be too conspicuous. Therefore, the height, form and orientation of the houses are consistent, which reflects that the houses in southern Shaanxi are influenced by the concepts of the clans [18].

c. Confucianism culture

In terms of spatial layout, the main house of the main house is the core, symmetrical layout along the central axis, the main rooms are arranged in the longitudinal axis direction, such as the main house; Secondary use of rooms arranged in the horizontal direction of the axis, such as the wing; Lower level rooms are free and flexible, such as toilets [19].

In the furniture arrangement, in the middle of the hall placed the ancestors of the row, under the layout of the table, table on both sides of the layout of the chair, is generally the position of the elderly.

B. Immigrant culture

Due to its unique geographical environment, Southern Shaanxi is adjacent to Gansu in the west, Guanzhong in the north, Sichuan and Chongqing in the south, and Hubei and Henan in the east. According to the local Chronicles, it can be seen that immigrants from southern Shaanxi flocked to sichuan, Chongqing, Gansu, Hubei, Henan and other provinces, resulting in diverse cultures that make the houses in southern Shaanxi have regional characteristics (Figure 4-21).

(a) (b) (c)

Figure 4-21. (a) Hanzhong houses; (b)Ankang houses; (c) Shangluo houses.

Under the influence of immigrant culture, the houses in Hanzhong, Ankang and Shangluo have slight differences. Due to the influence of Bashu culture, hanzhong residential houses mostly adopt white walls and blue tiles, hanging mountain roof and eaves are far-reaching. Under the influence of Chu culture, the houses in Ankang are mostly made of green tile earth walls, and the roofs are mostly of hard mountains, among which the walls are marked bycooking heating walls. Influenced by the qin and Chu cultures, hanzhong folk houses are mostly made of earthen walls and blue tiles, with hard mountain roofs and shorter eaves than hanzhong and Ankang folk houses [20].

C. Religious culture

Under the influence of Taoism, Buddhism, Christianity and other religious cultures, people in southern Shaanxi adopt symmetrical arrangement and clear priorities in the construction of residential buildings, which are influenced by Buddhism. Taoism believes that nature is nature and should keep nature, so that the residential buildings tend to nature in the construction process and integrate with nature [21].

D. Surrounding culture

It borders Gansu in the west, Guanzhong in the north, Sichuan and Chongqing in the south, and Hubei and Henan in the east. Gansu province is a region of multi-ethnic and multi-cultural symbiosis, among which the Yellow River culture is the developing relationship between man and the Yellow River, reflecting the relationship between man and the river, nature and society.

It affects the location selection of residential houses in southern Shaanxi, generally with mountains behind water and negative Yin embracing Yang. In the construction, the use of blue and black tiles and yellow earth walls to make the houses better integration with nature. Guanzhong region is located in the middle of Shaanxi Province, where temple fair culture is the concentration of primitive religion, worship, divination and other customs. Therefore, when the houses in southern Shaanxi were built, the north side of the Ming Hall was generally arranged as a place for ancestor worship. Bashu culture in Sichuan pays attention to Taoism and Confucianism, and southern Shaanxi is also influenced by Bashu culture. During the construction of folk houses, the main house is located in the north for the elders to live, and the wing house is located on the east and west sides for the juniors to live, reflecting the hierarchical relationship between superiors and subordinates. Hubei province is dominated by Chu culture, which is characterized by openness, compatibility and romanticism. Influenced by the culture of northwest Hubei province, the roofs of houses in southern Shaanxi are generally decorated with alligators, and the doors and Windows are generally carved with wood and brick [22].

(3) Historical evolution

Southern Shaanxi experienced many immigration activities, the earliest from the end of the Western Zhou Dynasty, to the Spring and Autumn Period and the Warring States period, southern Shaanxi formed a bas-Shu culture pattern, after the unification of the Qin Dynasty, southern Shaanxi flooded into the Qin culture, in the Ming and Qing dynasties immigration movement [23].

Adjacent to Sichuan, Gansu and Guanzhong regions, Hanzhong region has experienced the influence of immigration culture in different periods, making Hanzhong region under the influence of Bashu culture, Central Plains culture, Jingchu culture, and formed a gathering place with diverse cultures. A large number of foreign cultures have influenced the architectural form, spatial layout, building materials and construction techniques of traditional residential houses in Hanzhong. In the construction of residential houses, they advocate nature and pursue "Buddhism and Taoism". The architectural space of traditional residential houses in Hanzhong area is influenced by both natural environment and human environment. According to the terrain and geomorphology, it can be divided into plain basin, low mountain and hill, and middle and high mountain [24].

Due to the unique geographical environment and several immigration movements, Ankang region has bashu culture, Sanqin culture, Jingchu culture, Lingnan culture, Wu Yue culture and other cultures, which shows the diversity and inclusiveness of ankang region culture. Because ankang area and Hanzhong area are adjacent, they are influenced by similar culture, so there is little difference between the traditional houses [25].

4.5.3 Technical Factors

(1) Construction materials

There are abundant forestry resources in southern Shaanxi. The building materials of folk houses are mostly soil, wood, stone, brick, concrete and steel, etc. The building materials can be divided into three types: structural materials, decorative materials and functional materials. Structural materials include soil, wood, stone, brick, concrete, steel; Decorative materials: walls, doors and Windows, etc. Functional materials: heat preservation, waterproof, fire prevention, etc.

A. Structural materials

According to the material, the building structure can be divided into rammed earth structure, civil structure, brick and wood structure, brick and concrete structure, reinforced concrete frame structure [26].

Rammed earth structure is easy to obtain materials, simple construction techniques, low cost, but the performance of the wall itself is poor, the residential space is relatively simple. The seismic performance of civil structure and brick and wood structure is better than that of rammed earth structure, and the residential space has changed from a single space to a form of multiple space coexistence. The appearance of brick and concrete structure makes the residential space has a clear division. With the development of technology, the appearance of reinforced concrete frame structure makes the residential houses have the space form of large span [27].

B. Decorative materials

The wall of rammed earth structure comes from loess, and the texture of the wall comes from layer upon layer of loess masonry, but due to its low strength, it is gradually eliminated [28]. The wall of brick and wood structure is usually built by staggered layer of brick, which shows the symmetry of brick texture (Figure 4-22).

(a) (b) (c)

Figure 4-22. (a) Wall material for rammed earth structure; (b) Wall material of brick and wood structure; (c) Walls of reinforced concrete frame structures.

C. Functional materials

Residential buildings in thermal insulation, waterproof performance has been improving, making residential space has changed. In terms of thermal insulation, earthen walls and attics were used to meet this demand in the early stage, which made the height of residential buildings higher, and the rooms were arranged around the courtyard and relatively concentrated [29]. With the increase of heating means, the single building with the main room as the core was adopted in the residential space. In terms of waterproofing, the walls of early houses were built by loess masonry [30]. In order to prevent rain from attacking, courtyard style and roof were used for organized drainage in the space of houses. In the later period, the depth of eaves was deepened, so that houses no longer used courtyard style and were mainly single buildings [31].

(2) Building structure

Different building materials create a variety of building structures [32]. The materials of traditional residential houses in southern Shaanxi are earth, wood, stone, etc. According to the materials, the building structure can be divided into civil structure, brick and wood structure, brick and concrete structure, and reinforced concrete frame structure [33].

From civil structure to brick structure, architectural space by a single space to a variety of space form, the emergence of brick structure, makes the local-style dwelling houses in southern shaanxi has the division of architectural space, the reinforced concrete frame structure made of local-style dwelling houses in the space has the construction technique of large span, the framework system of wall enclosure and segmentation effect, in addition to the burden of self-respect, not under other loads.

(3) Environmental control technology

Environment control technology including electric lighting, ventilation and other equipment to use, in terms of ventilation, early residential use colonnade, ventilation Windows, patio, architectural layout is given priority to with courtyard type, relatively concentrated, with the increase of ventilation way, people usecooking heating wall, attic, such as the open courtyard for ventilation, the layout of architectural space is given priority to with individual buildings.

4.6 Chapter Summary

This chapter analyzes the spatial development process of residential houses in southern Shaanxi, and then summarizes the inheritance elements in three aspects, such as the appropriate use function, construction technology and style of residential houses, combined with the influence of the special natural environment and social conditions in southern Shaanxi. It provides a strong support for the analysis of spatial characteristics of residential houses in southern Shaanxi.

Reference

[1] Wang, P. Tan Gang. Natural ventilation in Ecological Building. World Architecture. 2000, 4, 62-65.

[2] Yoshinobu, A. External Space Design. Urban Housing. 2017, 09, 95.

[3] Yann, G. Communication and Space. China Architecture and Architecture Press. 2002.

[4] Lu, Y. Architectural Journal. 2007, 11, 66-69.

[5] Sun, D. Research on Chinese Dwellings. China Architecture and Architecture Press. 2004.

[6] Zhang, B.; Liu, Z. Shaanxi Folk Houses. China Architecture and Architecture Press. 1993.

[7] Wang, J. Northwest Folk Houses. Beijing: China Architecture and Architecture Press. 2009. 8

[8] Xu, J. Study on rural Settlement Planning and Construction Strategy in Qinling-Daba Mountain Area. Xi 'an University of Architecture and Technology. 2011.

[9] Wu, X. Research on Regional Style characteristics of Traditional Residential Houses in Small Towns in Southern Shaanxi. Xi 'an University of Architecture and Technology. 2016.

[10] Yang, H. Study on the Evolution and Development of Town building Types in Valley of Qinling Mountains. Chang 'an University. 2013.

[11] Zhang, G.; Xu, Y.; Han, Y. Journal of northwest university (natural science edition). 2014, 44, 661-666.

[12] Zhang, Y.; Gong, X.; Yang, W.; Guo, Wei. Journal of xi 'an university of architecture and technology (social science edition). 2015, 34, 31-35.

[13] Hu, Y.; Shi, F.; He, W.; Li, W. Journal of xi 'an university of architecture and technology (natural science edition). 2009, 41, 841-845.

[14] Zhang, Z.; Han, L. Mining and Inheritance of local knowledge of traditional settlement landscape -- A Case study of Fenghuang Ancient Town in Zhashui County, Southern Shaanxi. Chinese Landscape Architecture. 2018, 8, 50-55.

[15] Lu, Y. Chinese Residential Architecture. South China University of Technology Press. 2003.

[16] Xing, G.; Xu, Y.; Zheng, Y. Economic Geography. 2007, 27. (in Chinese with English abstract)

[17] Abraham, M. The theory of Human Motivation. Finance: Management Science. 2008.

[18] Rossi. Urban Architecture. China Architecture and Architecture Press. 2006.

[19] Wen, X. Environmental Psychology. Environmental Science and Technology. 1989, 2, 16-16.

[20] Wu, L. Introduction to Human Settlements And Environment Science. China Architecture and Building Press. 2001.

[21] Ma, X. Study on commercial and Residential Blocks and Architectural Design of Valley towns in Qinling Mountains. Chang 'an University. 2016.

[22] Meng, F. Research on land use and Layout strategy of Villages and towns in Qinling Valley tourism. Chang 'an University. 2017.

[23] Zhang, J. Research on ecological construction strategy of river channel landscape in Valley towns of Qinling Mountains. Chang 'an University. 2017.

[24] Cao, Y. Study on green Courtyard Design of Valley towns in Qinling Mountains. Chang 'an University. 2017.

[25] Ding, R. Study on spatial expansion and land layout strategy of Valley towns in Qinling Mountains. Chang 'an University. 2017.

[26] Bin, L. Research on Spatial Form of Old Streets and Ancient Courtyards in Shiquan Ancient City in Southern Shaanxi. Xi 'an University of Architecture and Technology. 2015.

[27] Chi, F.; Wang, R. Li, G. Xu, L. Wang, Y. Peng, C. Integration of sun-tracking shading panels into window system towards maximum energy saving and non-glare daylighting. Applied Energy. 2020, 260, 114304.

[28] Hussain, H.; Alzoubi, A.H. Assessment of building façade performance in terms of daylighting and the associated energy consumption in architectural spaces: Vertical and horizontal shading devices for southern exposure facades. Energy Conversion and Management. 2010, 51, 1592-1599.

[29] Saifelnasr, S.S. A Design Chart to Determine the Dimensions of a Horizontal Shading Device over an Equator-facing Window as a Function of the Latitude and the Shading Height. Procedia - Social and Behavioral Sciences. 2016, 216, 724-735.

[30] Yu, G. Yang, H. Luo, D. Cheng, X.; Mark, K.A. A review on developments and researches of building integrated photovoltaic (BIPV) windows and shading blinds. Renewable and Sustainable Energy Reviews. 2021, 149, 111355.

[31] Huang, M.; Wang, J.; Jin, H.; Li, A. Analysis on Wind Environment in Winter of Different Rural Courtyard Layout in the Northeast. Procedia Engineering. 2016, 146, 343-349.

[32] Wang, Y. Agkathidis, A. Andrew Crompton, Parametrising historical Chinese courtyard-houses: An algorithmic design framework for the digital representation of Siheyuan iterations based on traditional design principles. Frontiers of Architectural Research. 2020, 9, 751-773.

[33] Kolokotsa, D. Santamouris, M.; Gen, Y.Y. Passive Solar Architecture, Reference Module in Earth Systems and Environmental Sciences. Elsevier. 2021.

Chapter 5. Research on Passive Cooking Heating Wall System of Traditional Residence in Southern Shaanxi

5.1 Introduction and Simulation of Cooking Heating Wall System in Traditional Residential Buildings

5.1.1 Research Motivation

Nowadays, with the vigorous development of construction, industry, transportation, agriculture, and other industries, total global energy consumption has constantly increased [1]. The ratio of energy consumption in the building industry was 29.36% [2], making the industry one of the main areas of energy consumption in 2018 [3]. Based on the current energy consumption of the building industry, it is estimated that the carbon emissions of the building industry will increase to 50% in 2050 [4]. For developing countries, the energy consumption of the construction industry is even more severe [5]. The building industry accounts for 46.5% of the total energy consumption and 51.3% of the national carbon emissions in China [6]. However, China's building industry for energy demand and carbon emissions will continue to increase [7]. It is expected that in 2050, these numbers will triple [8]. The residential sector is the main component of the building industry [9]. The residential energy consumption increased from 291,435 to 346,713 Ktoe from 1990 to 2018 [2]. Thus, the residential energy consumption has shown a rapid increase trend. In response to this trend phenomenon, many experts and scholars have proposed green, zero-energy, low-carbon, and other types of residential buildings to reduce the demand for energy [10,11].

To reduce the energy demand of residential buildings, national government departments have also put forward urban residential energy conservation design codes and related laws and regulations in China [12]. Many experts and scholars have put forward many research strategies for urban residential energy conservation through field research, data collection, model analysis, mathematical calculations, and other research methods [13]. However, due to the diversity of residential buildings in rural areas of China and the fact that most of them are self-built, residents pay little attention to energy conservation during construction [14]. As of 2018, the total rural residential construction area is about 23.8 billion m2 [6]. Hence, it is necessary to design energy-saving houses in rural areas. However, there are essential differences between urban residences and rural residences, such as building form, height, material, space function, etc., so it is not feasible to simply apply the energy-saving designs used for urban residences to rural residences [15]. Compared with urban residential buildings, rural residential buildings have advantages of being able to be more flexible in terms of space and having larger sites. There-fore, it is convenient to implement the construction of rural residential buildings [16]. In this regard, when designing passive energy-saving technologies for residential buildings the local living habits and natural conditions should be fully considered, and energy-saving design concepts should be applied to rural residential buildings [17]. This is of great significance to the design of modern rural residences [18]. This research's main proposal is to establish a new passive cooking and heating system in winter, effectively using production and lifestyle to increase indoor temperature and reduce energy consumption.

5.1.2 Status Quo of the Model

The study is located in Zhongshan Village, Zhaowan Town, Xunyang County, Ankang City, Shaanxi Province, which is an area with a hot summer and a cold winter (Figure 5-1a).

Covering an area of about 0.02534 km², it hugs the border crossing road in a belt-like shape, following the natural topography [19,20]. The village was included in the second batch of villages in the list of traditional Chinese villages [21,22]. Most of the residential buildings in the village date back to the Qing Dynasty, so the residential buildings are generally one-story or two-story, with the one-story buildings accounting for 85.3% of the total. The floor height of the one-story residential buildings is 4.0–4.8 m, the floor height of the two-story residential buildings is 5.4–6.0 m, and building density is 24.06%. The local climate is humid and mild, with four distinct seasons: a long frost-free period, cold winters with little rain, and summers with drought and rain [23,24,25]. Affected by mountainous areas, villages are arranged in clusters, the houses are arranged relatively close together, and the streets are generally narrow [26,27,28]. Therefore, residential houses are less affected by solar radiation in winter, which makes the air temperature of residential houses lower in winter [29,30,31,32]. The lowest temperature in the village in winter is −3 ℃, the highest temperature in summer is 34 ℃, and the average wind speed of the whole year is 7 m/s (Figure 5-1 b–d).

The research object was traditional residences in southern Shaanxi located in Zhongshan Village (Figure 5-2). Most of the buildings were one-story, some were two-story, the height of the first story was 3 m, and the height of the second story was 1.8 m (Figure 5-4 a). The walls of the residential buildings were enclosed by blue bricks and the roofs were sloped roofs, which help to block the sun and organize drainage. There was little consideration for village planning in southern Shaanxi. Due to the influence of the mountainous terrain, the arrangement of the houses was relatively close, and the roofs had deep overhanging eaves. As a result, residential houses were less affected by solar radiation, so the houses generally felt damp and cold indoors in winter. To improve the temperature of the indoor space, local residents have adopted different heating methods, such as fire ponds, charcoal fire basins, and fire ponds. No matter which method is adopted, its purpose is local heating to increase the surface temperature of human body and the local air temperature, and it is generally used in halls [33,34]. Traditional heating methods are not used in bedrooms, to prevent carbon monoxide poisoning from occurring during deep sleep at night. By using the heat storage capacity of walls, this method stores the heat of the flue gas generated when cooking and releases the heat energy into the room so as to improve the indoor thermal comfort. Walls with this characteristic are called the walls.

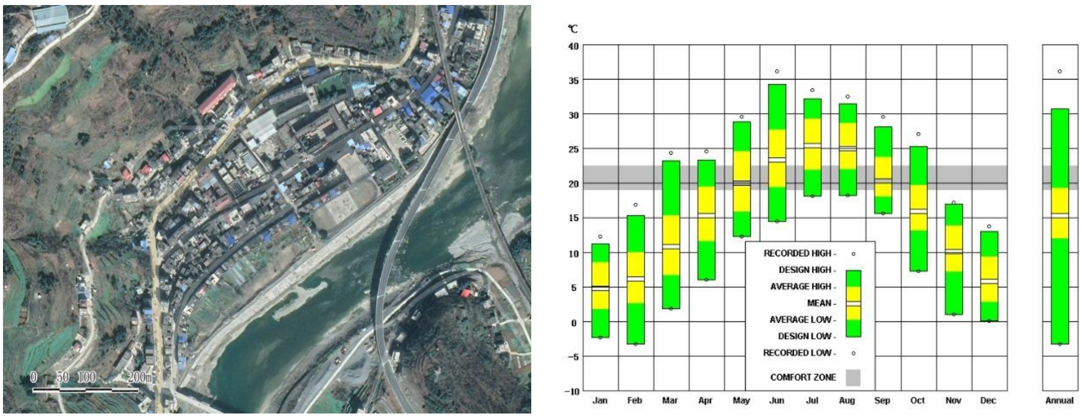

(a) (b)

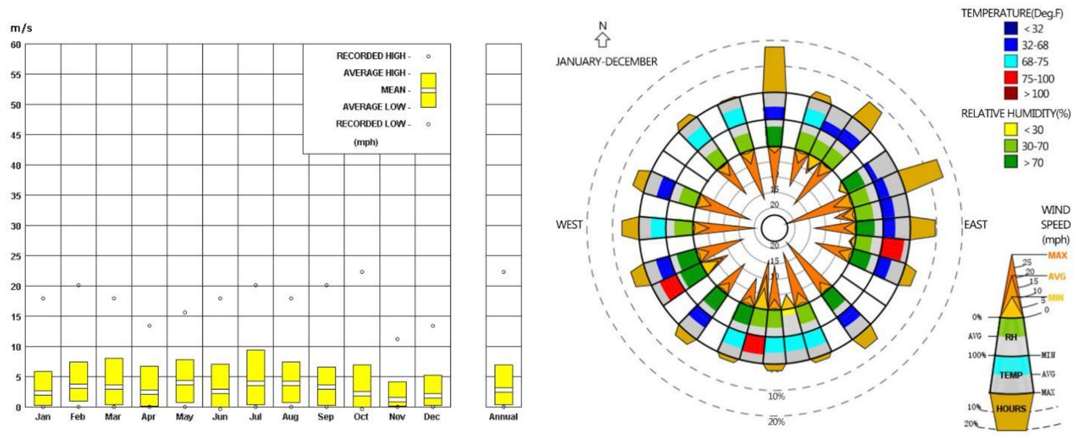

(c) (d)

Figure 5-1. (a) Village satellite map; (b) Average annual temperature; (c) Average annual wind speed; (b) Temperature, humidity and air velocity distribution throughout the year.

Figure 5-2. Photo of the present situation of folk houses in southern Shaanxi.

5.1.3 Design of Heated Cooking Wall

We used three research methods in this case and the cooking heating wall heating research; we mainly wanted to investigate how to use cooking heating walls to passively improve indoor temperature. The dimensions of the dwellings are shown in the figure 5-3. Our main idea was to use high-temperature flue gas to heat the pipes of the cooking heating wall during cooking and thus influence indoor temperature through the heat radiation of the cooking heating wall (Figure 5-4 b). In addition, to prevent the high-temperature cooking heating wall from affecting indoor temperature in summer, a valve should be installed at the stove. Therefore, in the summer opening the valve will cause smoke to be quickly discharged indoors; in the winter, the valve is closed to heat the flue gas around the wall (Figure 5-4 c–d). When using cooking heating wall heating technology, to improve the heating effect, the pipes must be aluminum and the wall must generally be S shaped. Using the heat storage and release of the cooking heating wall to improve indoor temperature, the effect of the outdoor temperature on indoor temperature can be decreased.

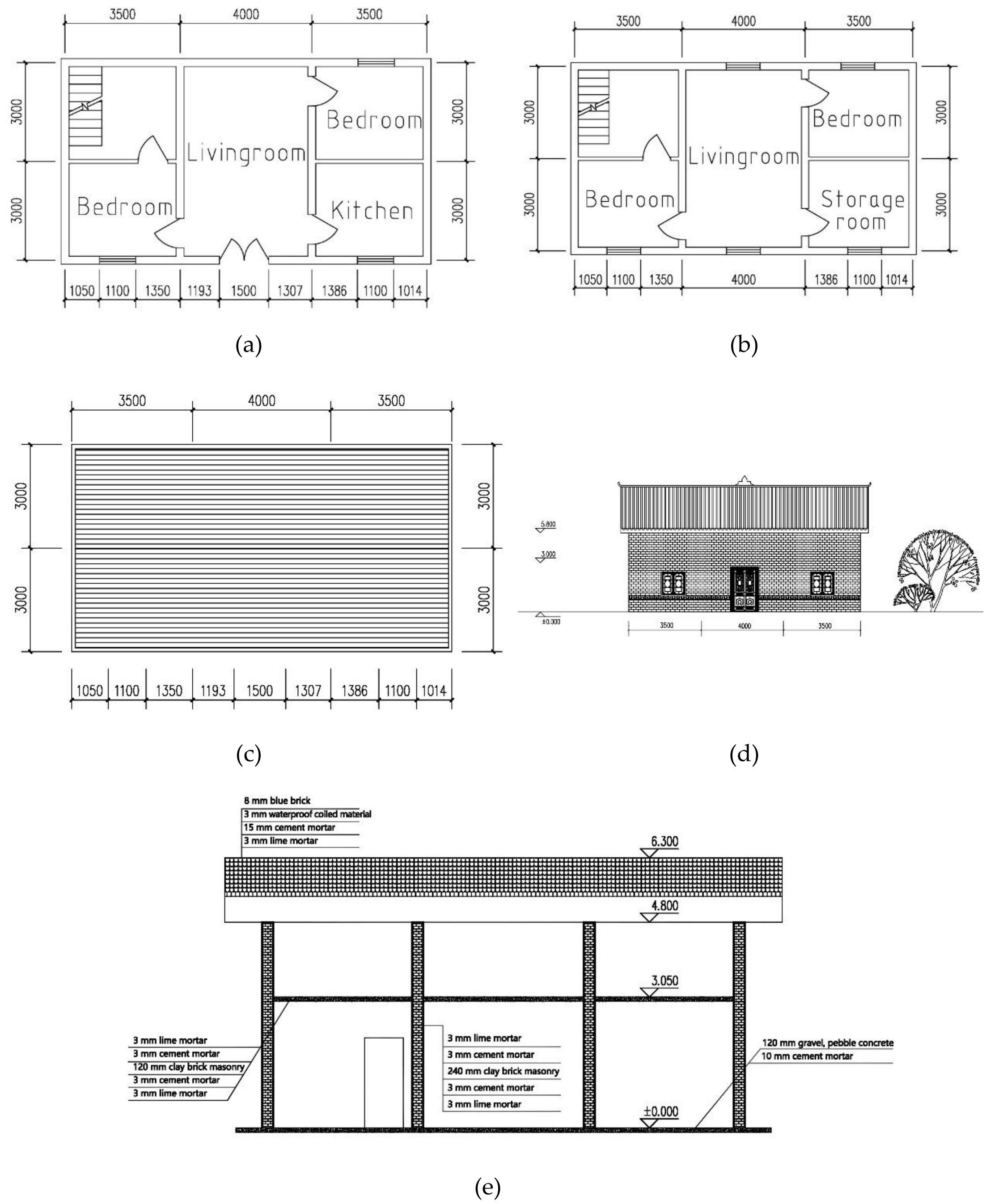

Figure 5-3. (a) First floor plan; (b) Second floor plan; (c) Roof plan; (d) Front elevation; (e) Composition of wall and floor.

The building is oriented north–south, and the plane function is composed of three parts: bedroom, living room, and kitchen. The building has three rooms with two depths, and the wall thickness is 240 mm. The east side is composed of a kitchen and a bedroom, the middle is used as the living room, and the west side has two bedrooms. The trans-formed cooking heating system scheme is as follows: Between the bedroom and kitchen on the east side, a heating wall is installed to raise indoor temperature. The red area in the picture indicates the location of the cooking heating wall (Figure 5-4 a). The specific structure is that a smoke exhaust port with a diameter of 100 mm is set inside the stove and a 2 mm thick aluminum pipe is placed in the smoke exhaust port. To increase the heating area, the aluminum tube is placed in an “S” shape with a total length of 11.68 m. Its major function is to use the high temperature of the cooking heating wall to increase the indoor temperature. First of all, the high-temperature flue gas heats the aluminum tube through thermal convection, and the heated aluminum tube heats the cooking heating wall through heat conduction and thermal radiation. Between the walls, convection heat exchange and thermal radiation are used to increase the temperature of the wall, thus increasing indoor temperature. Secondly, we compare the wall with or without solar radiation for the cooking heating system. This new cooking heating system can raise the overall temperature compared to the previous heating methods, rather than just offering local heating.

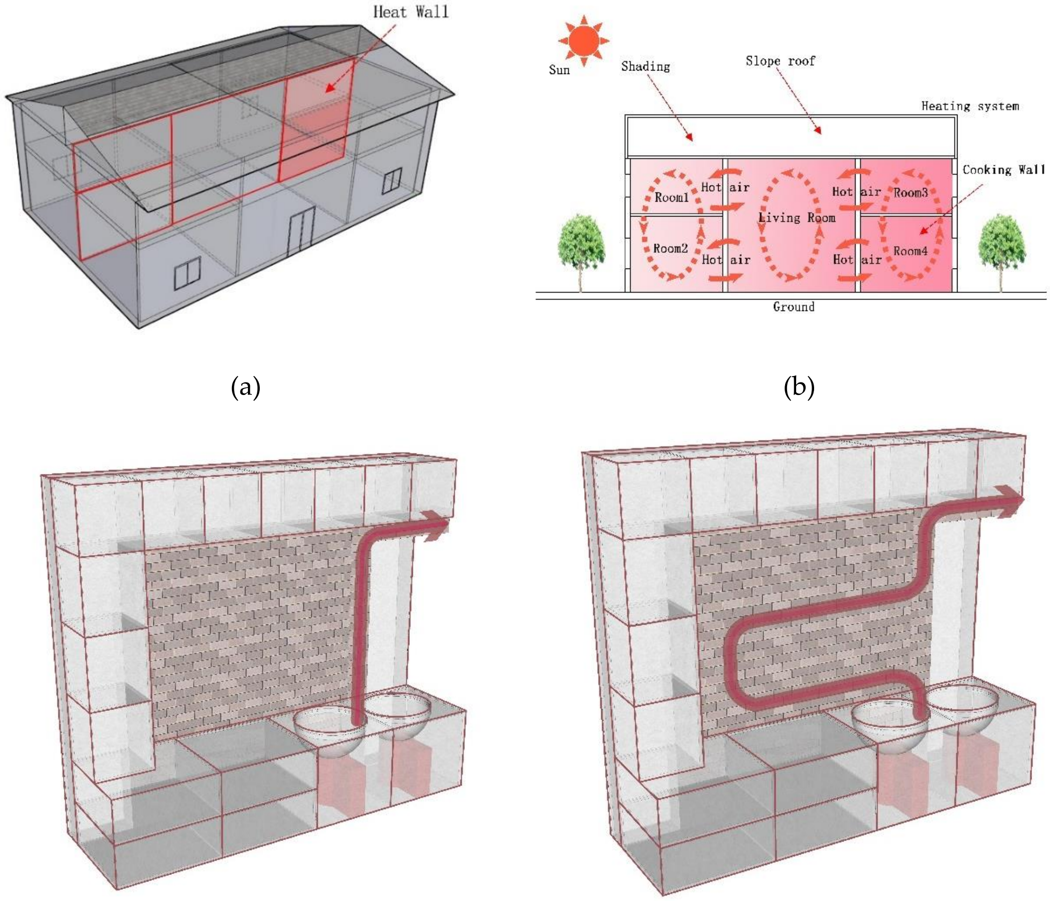

(a) (b)

(c) (d)

Figure 5-4. (a) The location of the cooking heating wall; (b) Thermal effect diagram; (c) Summer cooking equipment design; (d) Winter cooking equipment design.

5.1.4 The Working Principle of the Heated Cooking Wall

The working principle of the cooking heating wall is using the heat storage capacity of the wall to store the heat generated by flue gas during cooking and releasing the accumulated heat indoors, thereby improving the indoor thermal comfort to a certain extent. The cooking heating wall can be regarded as a cooking equipment heat recovery device. The whole heat transfer process is affected by many factors, such as the energy density of the combustion, the material properties of the wall, the material and size of the pipe, the size of the room, the indoor temperature and humidity, sunshine, and other factors. To facilitate understanding, this heat transfer process is divided into three parts: First of all, the burning material of the stove produces high-temperature flue gas, and flue gas flows through the aluminum tube, thereby forming turbulence. In the software simulation, the turbulence intensity needs to be calculated. The formula is as follows:

$$I=0.16re^{(-1/8)} \quad (1)$$

where: I is the turbulence intensity and re is the Reynolds number.

This flow process heats the aluminum tube by a heat transfer process dominated by heat convection, and the heat transfer process is divided into three parts. The turbulence generated by the flue gas in the aluminum tube causes transient heat transfer. After a period of time, the steady-state heat transfer is the mainstay. At the end of the cooking, the transient heat transfer is the mainstay. This heat transfer is a fluid–solid coupling transfer of heat. In the process of convective heat transfer, we follow the basic calculation formula—Newton's law of cooling.

$$\Phi=qA=Ah\Delta t=\Delta t/(1/hA) \quad (2)$$

where: Φ is the heat transfer power, q is the heat flux density, convection heat transfer coefficient h is material, A is the heat transfer area, 1/hA is the convective heat resistance, and Δt is the surface temperature and environmental temperature difference value.

A stable heat pipe heats the wall through heat conduction and heat radiation. Its heat transfer belongs to solid–solid coupling heat transfer, which follows Fourier's Law in the process of heat conduction. The calculation formula is as follows:

$$Q/A=q=-K(\partial T/\partial X+\partial T/\partial Y+\partial T/\partial Z) \quad (3)$$

where Q is the heat transfer rate, q is the heat flux density, K is the thermal conductivity, and A is the heat transfer area.

Secondly, the heated wall heats space between the walls through convection heat transfer and heat radiation, thus improving indoor temperature. This heat transfer process is coupled with fluid and solid heat transfer. In the process of thermal radiation, Stefan–Boltzmann's law is followed, and the calculation formula is as follows:

$$M(T)=\sigma T^4 \quad (4)$$

where M(T) is the radiation energy, T is the absolute temperature of the object, and σ is the constant 5.67×10^{-8}.

When cooking is stopped, the temperature of the aluminum tube begins to drop, thus stopping the heating of the cooking heating wall.

5.1.5 Simulation Process

The software used in this simulation was Ansys, Openstudio, Ladybug, Energyplus. The boundary condition is whether the wall has solar heat radiation or not. The software Ansys mainly calculates the heating time of the room and final temperature of the room after heating. The software products OpenStudio, Ladybug, and EnergyPlus are mainly used to calculate the thermal load reduction. The software Ansys was mainly used for turbulence simulation, steady-state thermal power, transient thermal power, and thermal radiation simulation calculation. Turbulence simulation mainly calculates the time taken for flue gas to pass through the aluminum tube, the wind vector of the flue gas, and the temperature of the tube wall. The steady-state thermal power and transient thermal power are mainly used to calculate the temperature of the heat pipe heating the wall and the time required for this. Thermal radiation simulation is mainly used to calculate the thermal radiation of the cooking heating wall and the heat exchange between walls. Heating load after adopting the new heating system is calculated and simulated using OpenStudio, Ladybug, and EnergyPlus. The steps are as follows: the model was established in OpenStudio, the model was imported into the ladybug to set relevant parameters, and the heat load was calculated using EnergyPlus.

The simulation was divided into three parts. The first part was the simulation of natural heating. The model was established by measuring data, and the local winter climate conditions data were used, including temperature and humidity, wind speed, sunshine, and so on. The simulation content includes the temperature of the room equilibrium and the time required. The second part is to simulate the heating of the cooking heating wall. Firstly, we establish the cooking heating wall system, which mainly includes the hearth, flue, and cooking heating wall. The simulation content is the velocity and temperature of flue gas, the heating time of the cooking heating wall, and the indoor temperature and the required time after equilibrium. The third part is the simulation calculation of the appropriate time of the cooking heating wall system and the reduction in heat load. The basic data statistics are as follows: Table 5-1 shows the basic information of residential buildings and the construction methods and materials used for walls, windows, floors, roofs, and other structures. Table 5-2 shows the heat storage coefficient, specific heat capacity, and other thermal indexes of different structural materials.

Table 5-1. Basic information of residential buildings.

Traditional Houses in Southern Shaanxi	Data Information
Basic information	The number of rooms is 5. The building area is 12.6 m2 for the bedroom, 12.6 m2 for the kitchen, and 17.64 m2 for the living room.
Roof	8 mm blue brick + 3 mm waterproof coiled material + 15 mm cement mortar + 3 mm lime mortar
Wall	3 mm lime mortar + 3 mm cement mortar + 240 mm clay brick masonry + 3 mm cement mortar + 3 mm lime mortar
Window	Wooden windows are made of 6 mm single-layer colorless transparent glass, the heat transfer coefficient is 4.7 W/(m2·K), the shading coefficient is 0.8, the visible light transmittance is 0.77, the air permeability is 1.0 m3/ (m· h).
Door	50 mm wood
Floor	120 mm gravel, pebble concrete + 10 mm cement mortar

Table 5-2. Properties of residential materials.

Material	Density (Kg/m^3)	Thermal Conductivity (W/m·K)	Specific Heat Capacity (J/Kg·K)	Thermal Storage Coefficient W/(m^2·K)	Vapor Permeability Coefficient g/(m·h·kPa)
Cement mortar	1800	0.93	1050	11.37	0.021
Clay brick masonry	1700	0.76	1050	9.933	0
Lime mortar	1600	0.81	1050	10.07	0.0443
Crushed stone, pebble concrete	2300	1.51	920	15.36	0.0173
Blue brick	2000	1.16	920	12.56	0
Waterproof materials	600	0.17	1470	3.302	0
Wood	500	0.14	2510	3.575	0
Aluminum	2700	203	920	191.495	0

Note: The data come from the thermophysical properties and data manual of building materials.

5.2 Cooking Heating Wall System and Natural Heating System with Solar Radiation on Wall

5.2.1 Natural Heating with Solar Radiation on the Wall

A. System Introduction

In the winter, a natural heating system relies mainly on solar radiation to raise the temperature of the interior through the walls. The heat transfer process mainly includes three parts: the first is that the wall surface absorbs heat, and the outer surface of the wall absorbs heat energy through convection heat exchange and thermal radiation. The second is the heat transfer of the wall itself, which transfers from the high-temperature outer surface to the low-temperature inner surface. Finally, the inner surface radiates heat, and the inner surface of the wall radiates heat to an indoor environment. The heat transfer method of each part is a comprehensive process of heat transfer, convection, and heat radiation. In the case of natural heating, the difference between the indoor temperature and the outdoor temperature is 2.5 ℃ (Figure 5-7 e).

B. System Simulation

To better verify effectiveness of the cooking heating system, comparisons were made with the natural heating effect as a benchmark. The construction materials of the folk houses in southern Shaanxi include cement mortar, clay brick masonry, lime mortar, gravel, gravel, pebble concrete, blue brick, waterproof membrane, wood, and aluminum. The specific simulation method is as follows: use the Ansys software to simulate, import the model into Ansys, set the grid, activate the energy equation, select the turbulence model, and set the radiation model. Add the thermal properties of the above materials, set the boundary conditions, and solve the method. Finally, the flow field is initialized to solve the simulation process. Through comparison with multiple sets of measurement data, the day when the outdoor temperature is least affected by solar radiation in winter is selected, and the temperature distribution is shown in Figure 5-6. First of all, from 18:00 to 9:00 is the time period that is least affected by solar radiation 24 h a day, and the difference between the indoor temperature and outdoor temperature is small. Without solar radiation indoors, the heat source mainly depends on the indoor heat disturbance source. The indoor heat disturbance source mainly refers to the heat generated by electrical appliances and human body. In addition to the influence of indoor thermal disturbance, the influence of indoor temperature changes is also related to the building scale, window size, and ventilation frequency. However, in past passive heating design research, the lack of solar radiation was not considered. To a certain extent, this makes software simulations more accurate and usable compared with reality. In the case of natural heating without considering solar thermal radiation, the indoor temperature changes with the outdoor temperature and the change range is small, with an indoor temperature to outdoor temperature difference of 0.2 ℃.

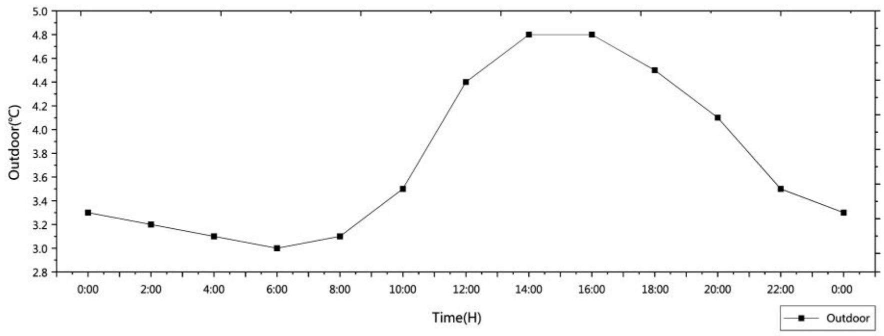

Figure 5-5. Outdoor temperature distribution

Natural heating mainly relies on solar radiation through the wall, glass, roof, and other structures to improve the indoor temperature. However, with the increase in solar radiation from 9:00 to 18:00, the wall began to be affected by solar radiation, and the indoor temperature began to change. Therefore, the simulation time was selected from 8:00 to 18:00. It can be seen from the simulation calculation that, from 8:00 to 11:30, as the sun's altitude angle changes, the temperature of the room on the first floor on the east side and the meeting room in the middle begins to increase from the initial average temperature of 6 to 7 ℃ (Figure 5-7 a, b). The temperature of the rooms on the second floor on the east side rises slowly, and the four rooms on the west side are less affected by solar radiation, so the temperature is slightly reduced. From 11:30 to 14:30, the range of indoor temperature change is small, the indoor temperature tends to be stable, and the average indoor temperature is 7 ℃ (Figure 5-7 c). From 14:30 to 18:00, the solar radiation is mainly distributed in the west side of the room (Figure 5-7 d). At 16:30, the room on the first floor in the west side reaches a maximum temperature of 7.5 ℃ and this then begins to decline (Figure 5-7 e). At 18:00, the temperature of the room on the east side decreases due to the influence of solar radiation, and the temperature of the room begins to drop, from 7 to 6.5 ℃ (Figure 5-7 f). In the case of natural heating with solar radiation, the indoor mean temperature is 7 ℃, which is a 2.5 ℃ difference from the outdoor average temperature.

Natural heating (with solar radiation)

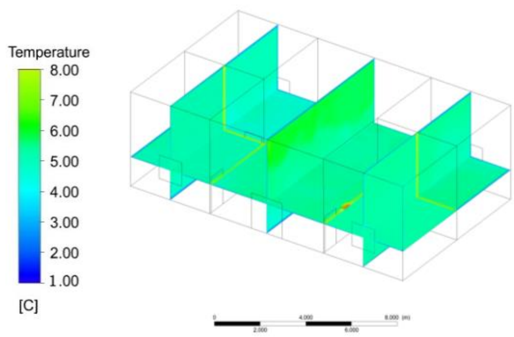

(a) 8:00 a.m.

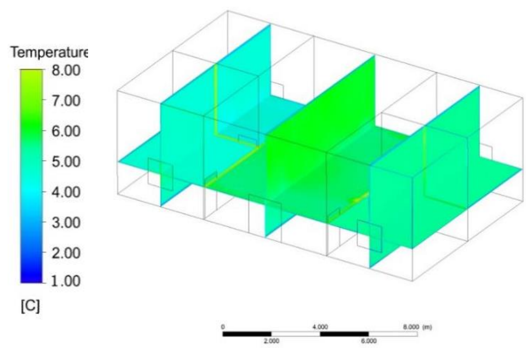

(b) 10:30 a.m.

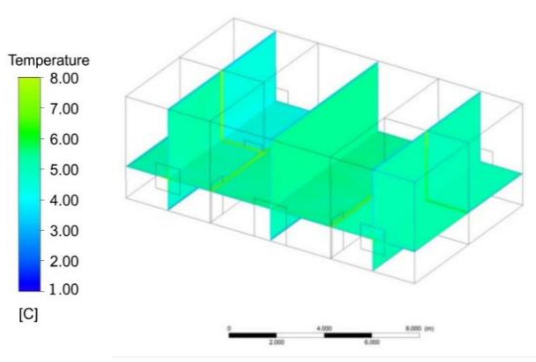

(c) 11:30 a.m.

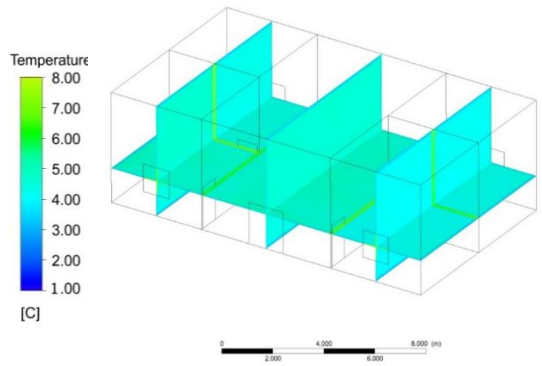

(d) 14:30 p.m.

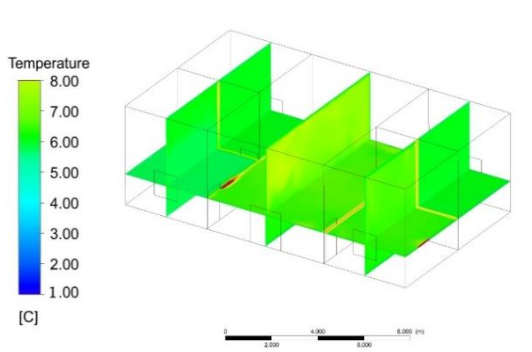

(e) 16:30 p.m.

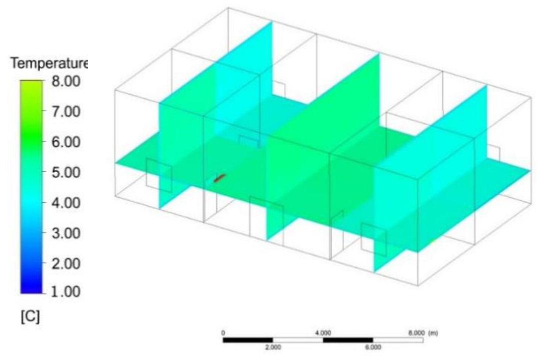

(f) 18:00 p.m.

Figure 5-6. Natural heating at defined times.

5.2.2 Cooking Heating Wall System with Solar Radiation on the Wall

A. System Introduction

To increase indoor temperature, the heat generated during cooking is used to heat the wall, and the heat absorption and heat storage capacity of wall is used to increase indoor temperature and reduce the effect of the outside temperature. The cooking heating wall is a double-sided heating wall that can simultaneously use heat radiation to heat the rooms on both sides of the cooking heating wall. The effect of flue gas entering the pipe wall and heating the pipe wall is shown in Figure 5-7 c–f. When the heat pipe heats the cooking heating wall, the temperature of the cooking heating wall increases significantly (Figure 5-9 a–f). A period of time after the cooking heating wall becomes hot, the temperature of the bedroom rises significantly compared to in natural heating. Using a cooking heating system, in the case of solar heat radiation, heating is stopped when the heating time is 48 min, and the heating effect of residential buildings is better (Figure 5-10 f). The temperature after equilibrium and the time spent were improved, and the heat load of the building was also reduced.

B. System Simulation

In comparing the simulation results with the results of natural heating, we can see that the outdoor temperature distribution is the same as the natural heating outdoor distribution and the initial indoor temperature is also 6 ℃ (Figure 5-6). The process of cooking and burning is divided into four stages: material ignition, open flame ignition (continuous fuel supply), smokeless combustion (closed flue), and material ignition. After the measurement, the flue gas enters the aluminum tube at an average speed of 2.5 m/s after the material is ignited. Through Ansys simulation, it can be seen that the speed at the turn is 1.6 m/s and the wind pressure is

1.1 pa (Figure 5-8 a). The speed of the flue gas to the smooth part of the aluminum tube is increased to 3.2 m/s, and the wind pressure is 1.4 pa (Figure 5-8 b). Finally, it is discharged from the aluminum tube at a speed of 2.6 m/s. The change in the flue gas velocity is mainly caused by the hot pressure generated by the flue gas in the aluminum tube and the shape of the aluminum tube. The temperature of the flue gas depends on the amount of heat generated when the material is burned. After many measurements, the temperature of the flue gas is generally 60~70 ℃. The flue gas enters the aluminum tube at a temperature of 60 ℃. At 38 s, the inlet of the aluminum tube is 12.65 ℃, and the temperature of the remaining aluminum tubes is maintained at 2 ℃ (Figure 5-8 c). At 84 s, the average temperature of the aluminum tube is 36.94 ℃ (Figure 5-8 d). At 102 s, the average temperature of the aluminum tube is 42.55 ℃ (Figure 5-8 e). At 134 s, the aluminum tube reaches a constant temperature of 60 ℃ (Figure 5-8 f). Since the thermal conductivity of the aluminum tube is higher than 203 W/m· k, the temperature of the aluminum tube increases faster.

Fumes from aluminum pipes

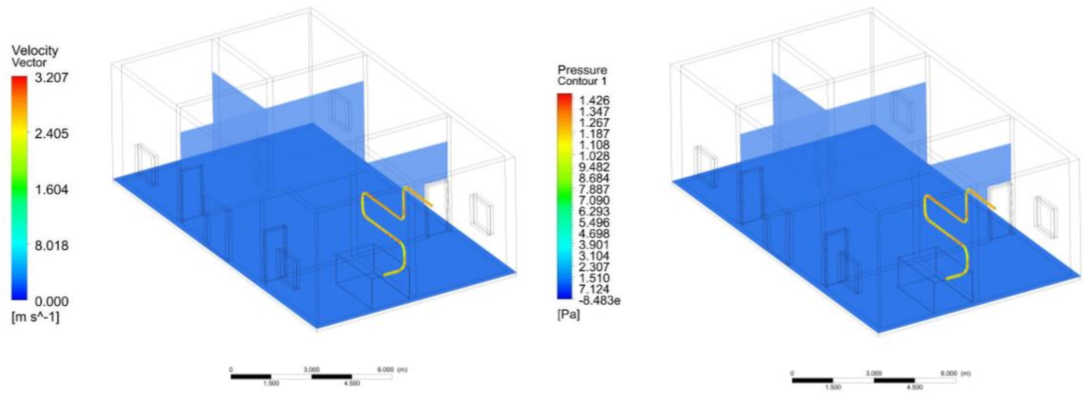

(a) Speed (b) Pressure

Aluminum tube temperature

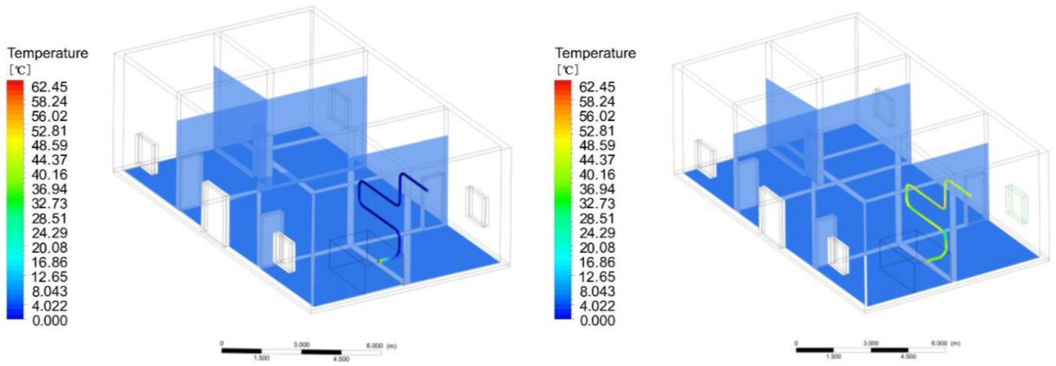

(c) 38S (d) 84S

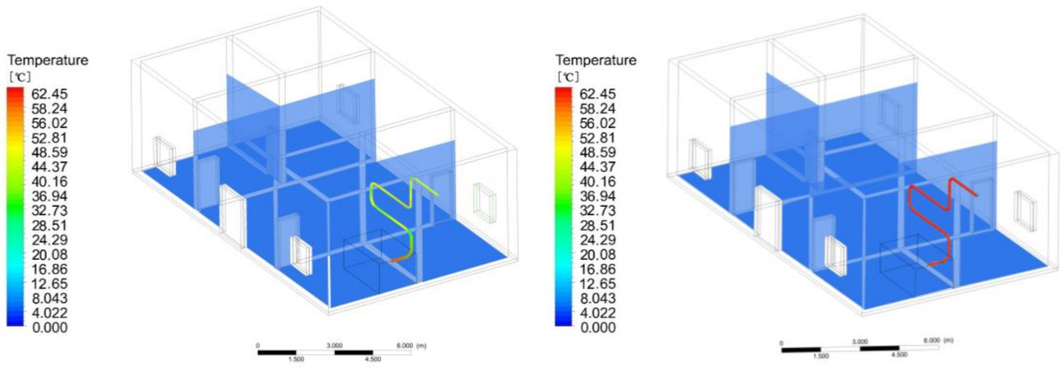

(e) 102S (f) 134S

Figure 5-7. Wall heating for specific times. (a) Flue gas velocity in aluminum tube; (b) Flue gas pressure in aluminum pipe; (c) The temperature of 38s aluminum tube; (d) The temperature of 84s aluminum tube; (e) The temperature of 102s aluminum tube; (f) The temperature of 134s aluminum tube.

After the aluminum tube is heated, the heat wall is heated by heat conduction and thermal radiation. At 5 min and 15 s, the average temperature of the cooking heating wall is 9.07 ℃, which is mainly distributed around the aluminum tube, and the lowest temperature on the ground is 5.94 ℃ (Figure 5-9 a). At the time of 8 min and 30 s, the average temperature of the cooking heating wall is 12.15 ℃, and the lowest temperature at the ground is 5.88 ℃ (Figure 5-9 b). With the increase in heating time, the average temperature of the cooking heating wall reaches 15.22 ℃ at 12 min and 45 s, representing an average increase of 2 ℃ (Figure 5-9 c). At 16 min and 27 s, the temperature of the cooking heating wall gradually increases. The average temperature of the cooking heating wall is 21.44 ℃, and the lowest temperature at the ground is 5.67 ℃ (Figure 5-9 d). At20 min and 24 s, the average temperature of the cooking heating wall is 24.51 ℃ (Figure 5-9 e). At 25 min and 35 s, the temperature of the cooking heating wall no longer changes, reaching a constant value of 30.78 ℃, and the lowest temperature at the ground is 5.24 ℃ (Figure 5-9 f).

Heating wall system

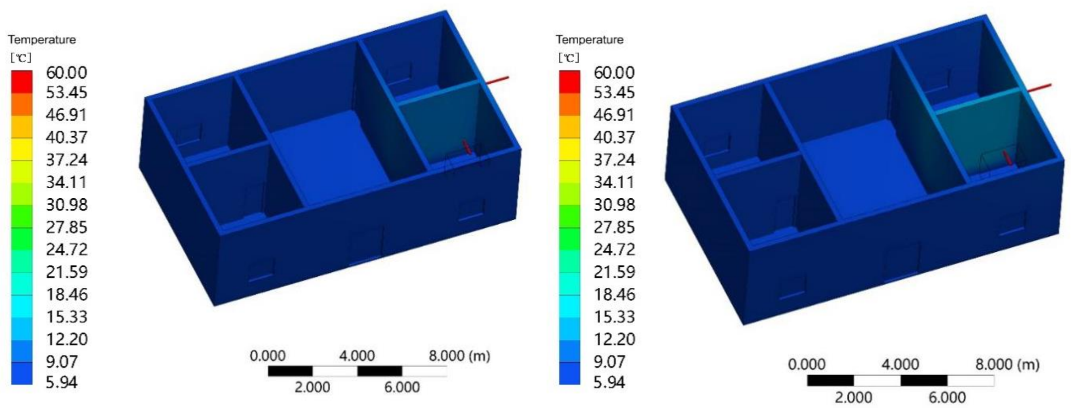

(a) 5min 15s (b) 8min 30s

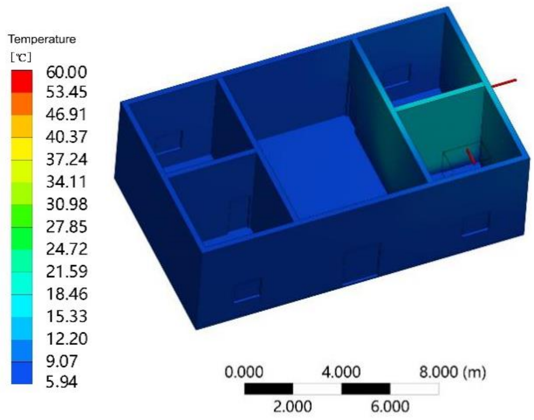

(c) 12min 45s

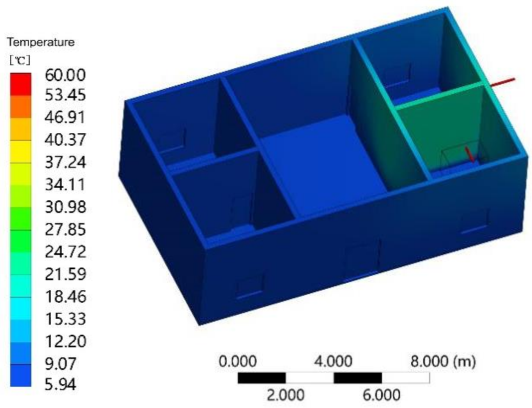

(d) 16min 27s

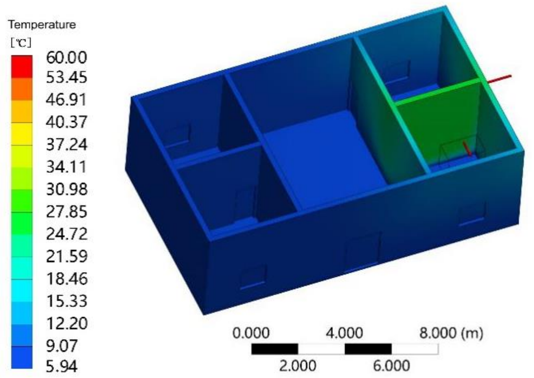

(e) 20min 24s

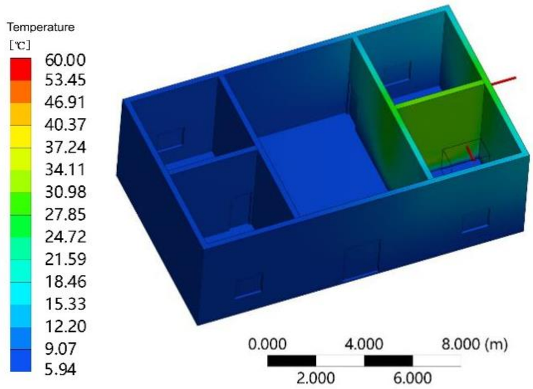

(f) 25min 35s

Figure 5-8. Wall heating for specific times.

From the above survey on the length of a single cooking time, it can be known that 60–90 min is the main one. To make the simulation more realistic, we chose a single cooking time of 75 min. When the cooking heating wall temperature reaches a constant value, it takes 27 min and 49 s to cook. There should be 48 min and 11 s remaining for the cooking heating wall to heat up. To simulate the influence of the cooking heating wall on the indoor temperature through convective heat transfer and thermal radiation, the simulation time started at 6 o'clock, and the initial indoor temperature was 6 ℃. With solar radiation, at 6:05, the temperature of the first and second floor rooms on both sides of the cooking heating wall began to rise from 6 to 7 ℃ (Figure 5-10 a). The temperature of the living room and the other rooms remained basically unchanged. At 6:10, the temperature in the rooms on both sides of the wall rose to 7.8 ℃, while the temperature in other rooms rose to 6.5 ℃ (Figure 5-10 b). At 6:20, the room temperature on both sides of the cooking heating wall was 9.5 ℃, and the temperature in the other rooms was 7.2 ℃ (Figure 5-10 c). At 6:30, the temperature of the room on both sides of the cooking heating wall was 11.5 ℃, and temperature of the other rooms was 7.9 ℃ (Figure 5-10 e). At 6:40, the temperature of the room on both sides of the cooking heating wall was 13.6 ℃, and the temperature of the other rooms was 8.7 ℃ (Figure 5-10 f). At 6:48, the temperature of the rooms on both sides of the cooking heating wall was 14.6 ℃, the temperature of other rooms was 9.8 ℃, and the cooking heating wall heating was stopped (Figure 5-10 f).

Cooking heating wall (with solar radiation)

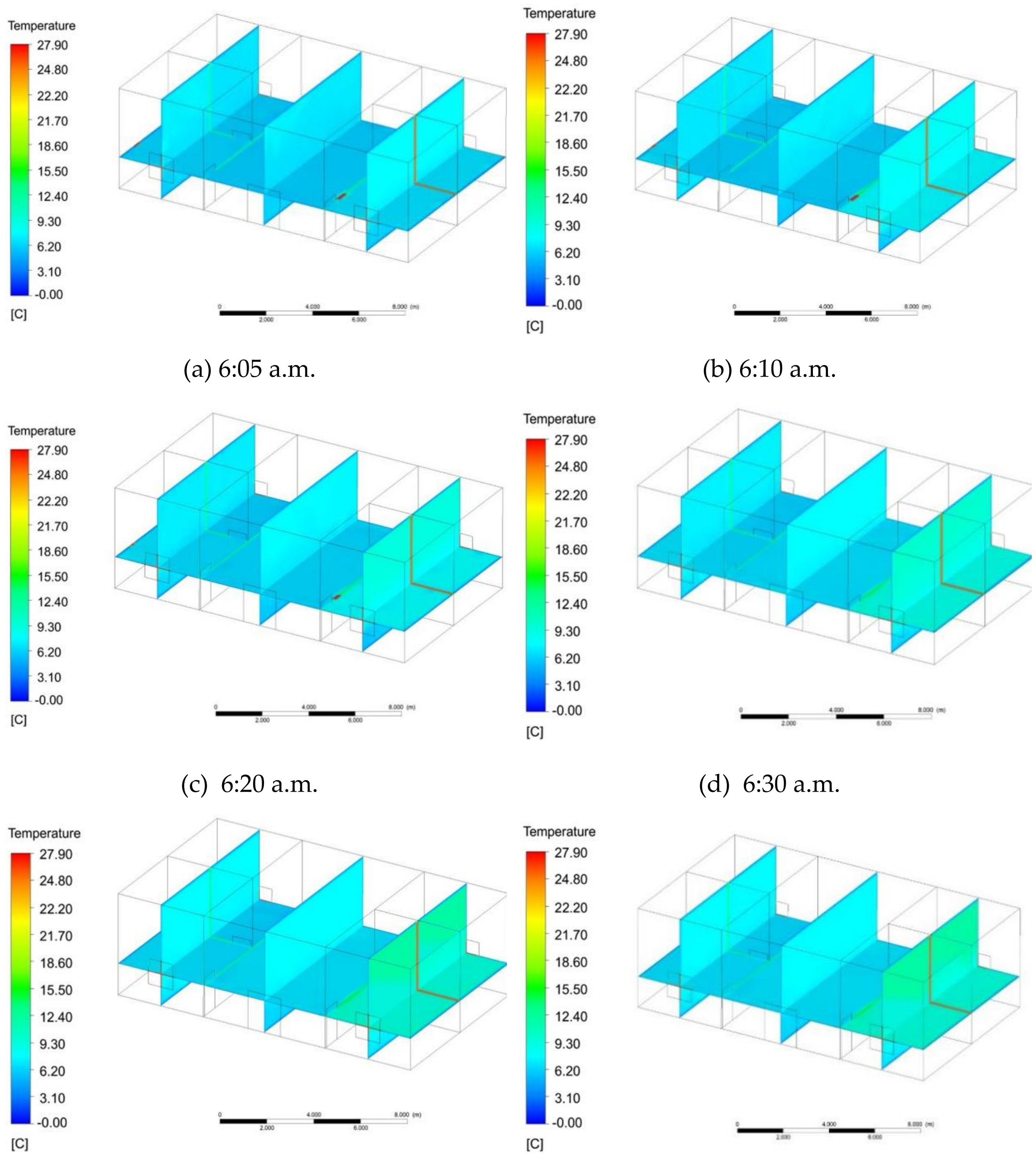

(a) 6:05 a.m. (b) 6:10 a.m.

(c) 6:20 a.m. (d) 6:30 a.m.

(e) 6:40 a.m. (f) 6:48 a.m.

Figure 5-9. Cooking and heating at defined times.

With the closure of the cooking heating wall cooking system, the indoor temperature began to slowly drop. Within 30 min of stopping cooking, the indoor temperature was in a stable state. The temperature of the first and second floors on both sides of the cooking heating wall was still maintained at 14.6 ℃, and the temperature in the other rooms was maintained at 9.8 ℃. The mean indoor temperature was 12.2 ℃. The temperature increased by 6.2 ℃. Thirty minutes after stopping cooking, the temperature of the rooms on the second floor on both sides of the cooking heating wall dropped to 11.2 ℃, the temperature of the room on the first floor was 10.5 ℃, and the temperature of the other rooms dropped to 8 ℃ (Figure 5-11 a). Forty-five minutes after cooking was stopped, the temperature of the second-floor room on both sides of the cooking heating wall dropped to 10.2 ℃, the temperature of the first-floor room was basically in equilibrium with the temperature of other rooms, and the temperature was 8 ℃ (Figure 5-11 b). One hour after stopping cooking, the indoor temperature was steady at 8 ℃, but due to the influence of solar radiation the temperature in the east room was 8.5 ℃ (Figure 5-11 e).

Cooking and heating system stopped (with solar radiation)

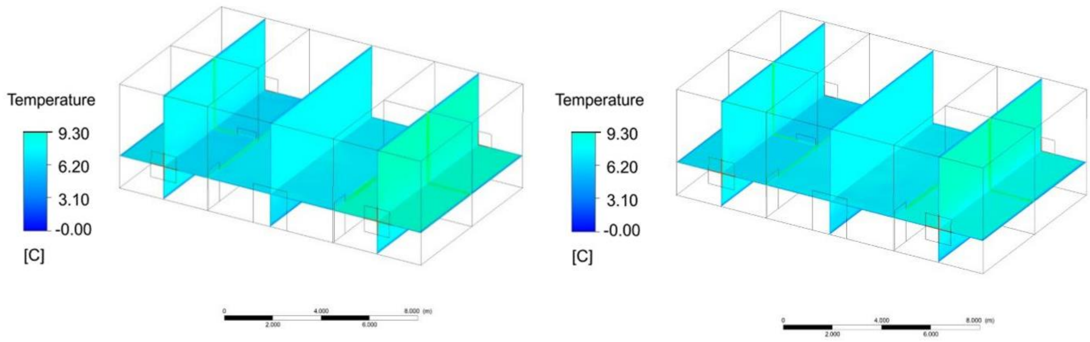

(a) After 30 min (b) After 45 min

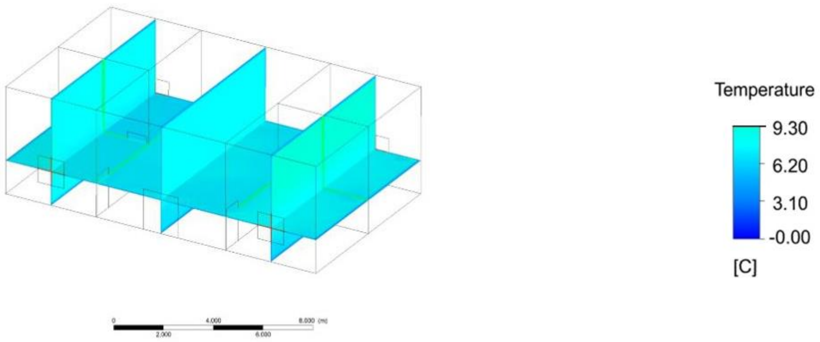

(c) After 1h

Figure 5-10. Temperature after the heating system was powered off.

5.2.3 Comparison and Analysis

In natural heating with or without solar radiation, the difference between the indoor temperature and the outdoor temperature is small. In the case of solar radiation, the heating time is 4.30 h; the equilibrium temperature is 7 ℃, which is a 2.5 ℃ difference from the outdoor value; and the heating efficiency is 0.22 ℃/h. The heating effect of solely relying on so-lar radiation is poor and the heating time is longer. In the process of natural heating, the heat generated by solar radiation first heats the wall, and the heat passes through the wall to heat the room. This heating method is greatly affected by the weather, the heating efficiency is extremely low, and the effect of improving indoor temperature is not good.

Due to the cooking and heating system, the cooking time is limited. The early stage of the cooking heating wall system requires 27 min and 49 s, so the heating time is 48 min and 11 s. In the case of solar radiation, the indoor temperature remains basically unchanged for 30 min after the cooking activity stops. The temperature of the rooms on both sides of the cooking heating wall is 14.6 ℃ and the other rooms are kept at 9.8 ℃. The mean indoor temperature is 12.2 ℃and temperature increases by 6.2 ℃.

5.3 Cooking Heating Wall System and Natural Heating System without Solar Radiation on the Wall

5.3.1 Natural Heating System without Solar Radiation on Wall

A. System Introduction

Without solar radiation indoors, the heat source mainly depends on the indoor heat disturbance source. The indoor heat disturbance source mainly refers to the heat generated by electrical appliances and human body. In addition to the influence of indoor thermal disturbance, the influence of indoor temperature changes is also related to the building scale, window size, and ventilation frequency. However, in past passive heating design research, the lack of solar radiation was not considered. To a certain extent, this makes software simulations more accurate and usable compared with reality. In the case of natural heating without considering solar thermal radiation, the indoor temperature changes with the outdoor temperature and the change range is small, with an indoor temperature to outdoor temperature difference of 0.2 ℃.

B. System Simulation

Through software simulation calculation, the indoor temperature is basically the same as the outdoor temperature in the case of natural heating without solar radiation. The simulated time is the same as the natural heating with solar radiation, and the time is also from 8:00 to 18:00. From 8:00 to 12:00, the average temperature of the first and second floors indoors is 4.5 ℃, mainly because the outdoor temperature is relatively low (Figure 5-12 a, b, c). From 12:00 to 14:00, the indoor temperature is basically the same. From 14:00 to 17:00, the outdoor temperature begins to rise slowly, and the indoor temperature of the first floor also begins to rise slowly (Figure 5-12 d, e). After equilibrium, the temperature is 4.8 ℃, and the second floor remains unchanged. The temperature begins to drop from 17:00 to 18:00, and the temperature on the first and second floors is 4.5 ℃ (Figure 5-12 f). The research results show that in the case of natural heating without solar radiation, the mean indoor temperature is 4.7 ℃ and the temperature change range is small, with only a 0.2 ℃difference from the average outdoor temperature.

Natural heating (without solar radiation)

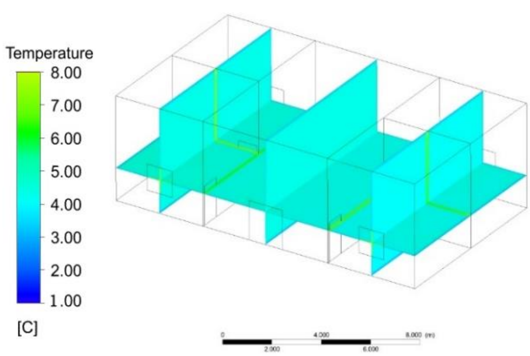

(a) 8:00 a.m.

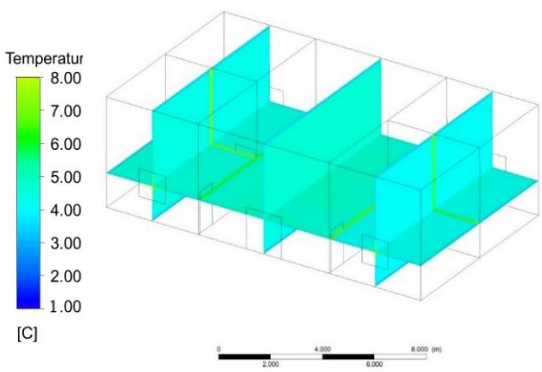

(b) 10:30 a.m.

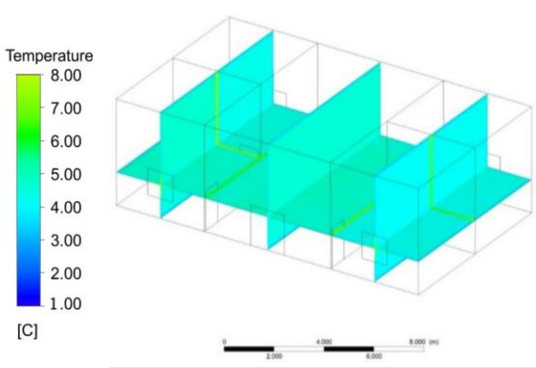

(c) 11:30 a.m.

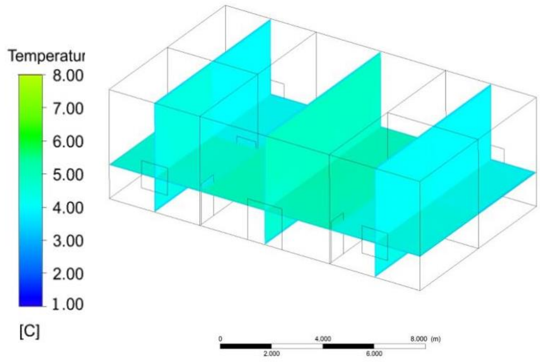

(d) 14:30 p.m.

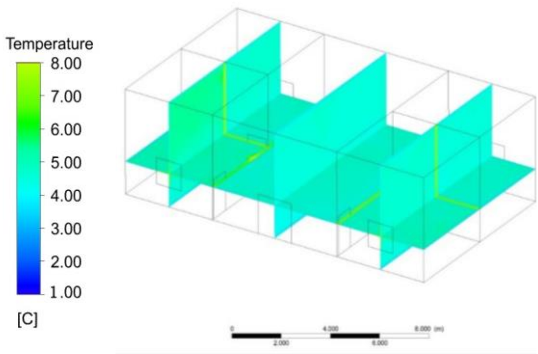

(e) 16:30 p.m.

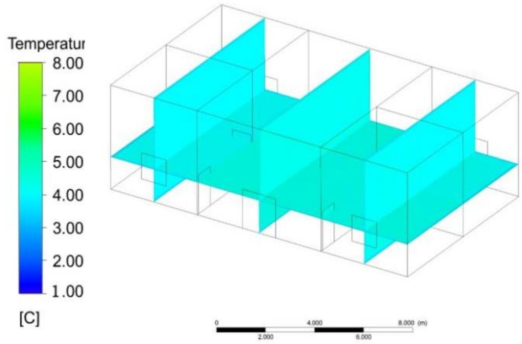

(f) 18:00 p.m.

Figure 5-11. Natural heating at defined times (heating without solar radiation).

5.3.2 Cooking Heating Wall System without Solar Radiation

A. System Introduction

Without solar heat radiation, the cooking system stops heating when the heating time is 48 min, and the indoor temperature increases (Figure 5-14 a). Using a cooking heating system, in the case of solar heat radiation heating is stopped when the heating time is 48 min, and the heating effect of residential buildings is better (Figure 5-11 a). The temperature after equilibrium and the time spent were improved, and the heat load of the building was also reduced.

B. System Simulation

To prove the effectiveness of the cooking heating wall heating system, simulations were carried out without solar radiation. The simulation time also started at 9 o'clock. At 6:05, the temperature of the rooms on both sides of the cooking heating wall began to rise, the temperature was 6.5 ℃, and the temperature of other rooms was 6 ℃ (Figure 5-13 a). At 6:10, the temperature of the rooms on both sides of the cooking heating wall was 7 ℃ and the temperature of the other rooms remained unchanged (Figure 5-13 b). At 6:20, the temperature in the first and second floor rooms on both sides of the cooking heating wall was 7.5 ℃, while the temperature in the other rooms began to drop to 5.5 ℃ (Figure 5-13 c). This happened because there was no solar radiation and the outdoor temperature dropped, so the temperature of the rooms without a cooking heating wall system began to drop. At 6:30, the temperature of the rooms on both sides of the cooking heating wall was 9.3 ℃ and the temperature of the other rooms was 6.5 ℃ (Figure 5-13 d). This situation occurred because when the temperature of other rooms is in balance with the outdoor temperature, the increase in the temperature of the rooms on both sides of the cooking heating wall affects other rooms, causing the indoor temperature to rise. At 6:40, the temperature of the rooms on both sides of the cooking heating wall was 10.5 ℃ and the temperature of the other rooms was 7.1 ℃ (Figure 5-13 e). At 6:48, the temperature in the rooms on both sides of the cooking heating wall was 11.8 ℃ and the temperature in the other rooms was 7.6 ℃ (Figure 5-13 f). When the heating system of the cooking heating wall was stopped for 20 min, the indoor temperature on both sides of the cooking heating wall began to drop to 8 ℃ and the average temperature of the other rooms was 6.0 ℃ (Figure 5-14 a). Fifty minutes after the heating was stopped, the average indoor temperature was 5.5 ℃ (Figure 5-14 b). 1hour after the heating was stopped, the average indoor temperature was maintained at 5.5 ℃ (Figure 5-14 e).

Cooking heating wall heating (without solar radiation)

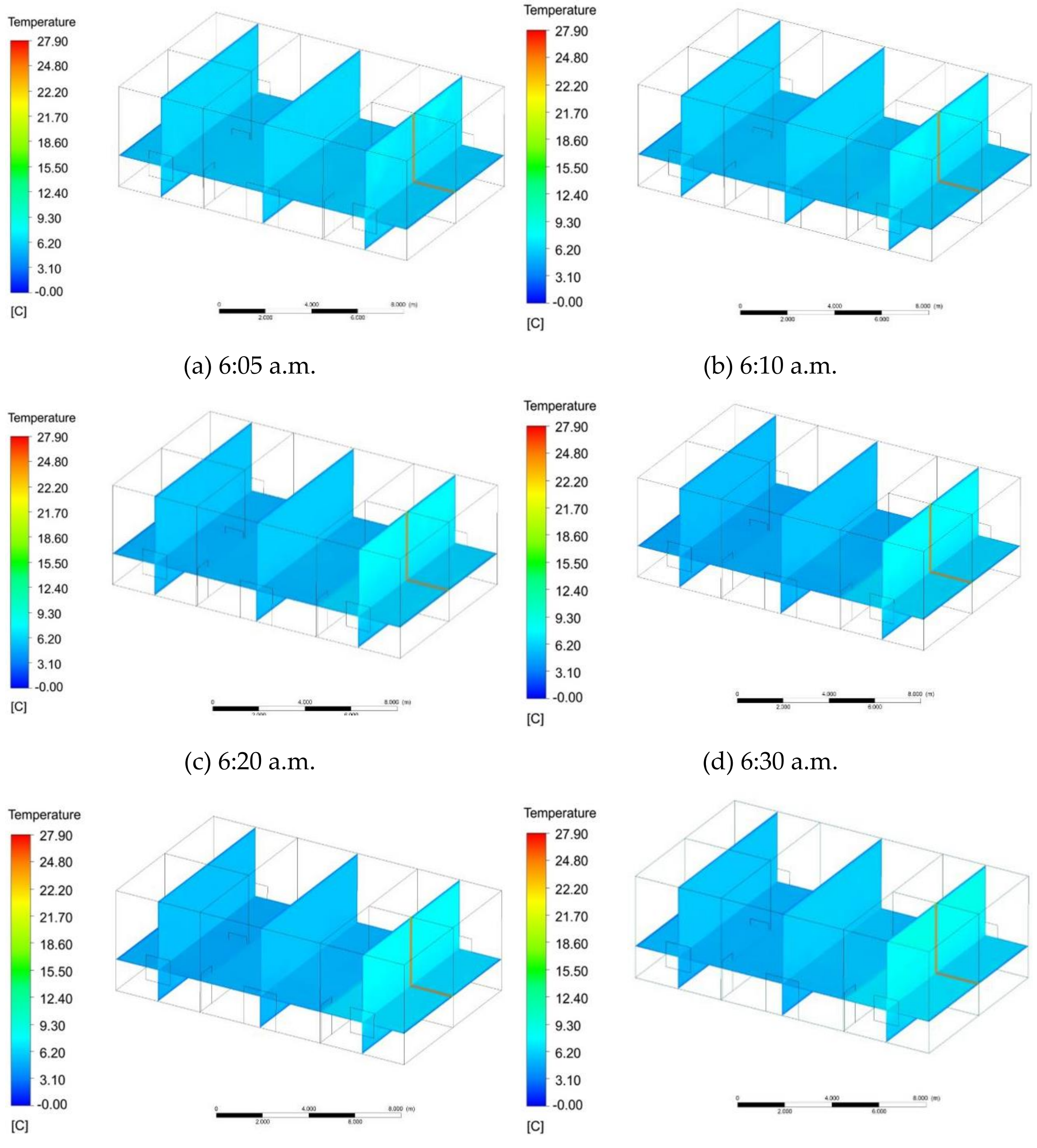

(a) 6:05 a.m. (b) 6:10 a.m.

(c) 6:20 a.m. (d) 6:30 a.m.

(e) 6:40 a.m. (f) 6:48 a.m.

Figure 5-12. Cooking and heating at defined times (heating without solar radiation).

Cooking and heating system stopped (with solar radiation)

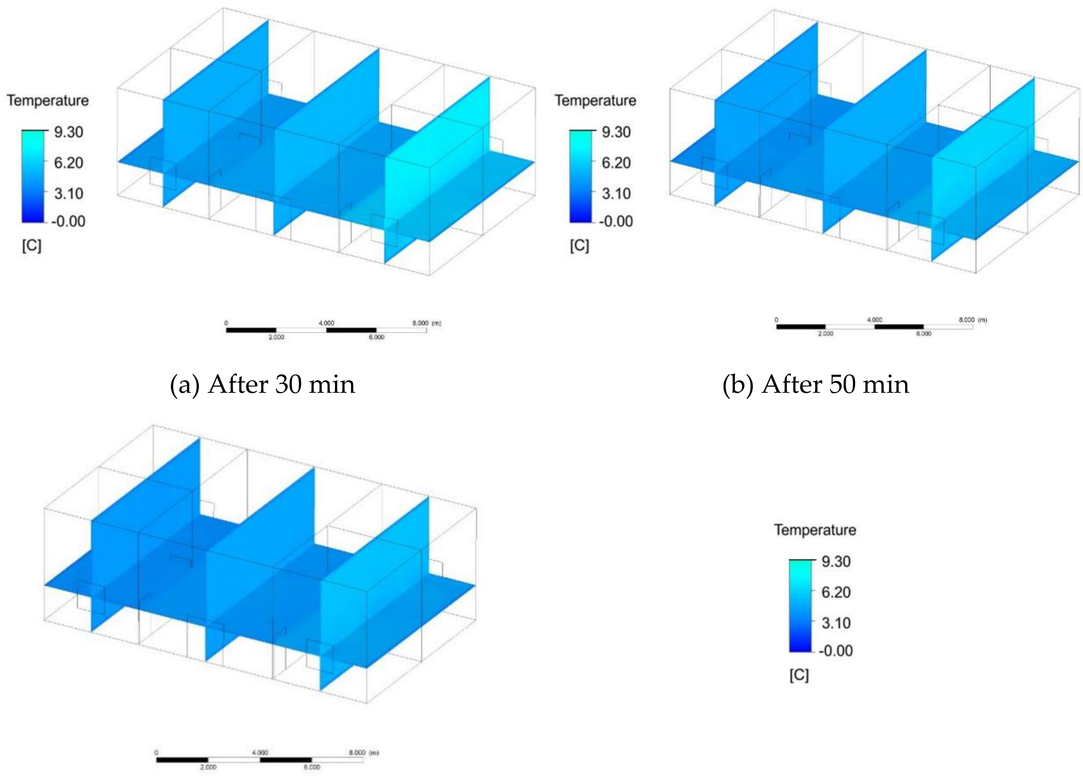

(a) After 30 min (b) After 50 min

(c) After 1h

Figure 5-13. Temperature after the heating system was powered off (heating without solar radiation).

5.3.3 Comparison and Analysis

Without solar radiation, the indoor temperature remained basically unchanged for 20 min after cooking stopped. The temperature of the first and second floors on both sides of the cooking heating wall was 11.8 ℃, and that of the other rooms was 7.6 ℃. The average indoor temperature was 9.7 ℃, which increased by 3.7 ℃. Without of solar radiation, the heating time for natural heating is 6 hours. The temperature after equilibrium is 4.8 ℃, which is a 0.2 ℃ difference from the outdoor temperature.

Natural heating systems mainly rely on solar radiation to generate heat in the walls to affect the interior temperature. However, when a cooking heating system is heated, it mainly relies on a cooking heating wall for heating, which greatly increases the heating efficiency. Without considering solar radiation, the average heating efficiency for cooking and heating is 2.34 ℃/h. Considering solar radiation, the average heating efficiency for cooking and heating is 3.54 ℃/h.

5.4 Suitable Time for Applying New System

The heating system, whether with or without solar radiation, has an effect on the heating time, heating efficiency, post-heating equilibrium temperature, and reduced heat load. The time taken to use the cooker for heating, changes in indoor temperature, and reduced heat load were estimated with and without solar radiation throughout the year. The most suitable time to use the heating system is mainly in January, February, March, November, and December. Due to the limitations of cooking heating time, in the case of solar radiation, the annual use of cooking heating system is 667 h, accounting for 7.71% of the total time of the year (Figure 5-15 a). In the case of there being no solar radiation, the annual use of cooking heating system is 424 h, accounting for 4.91% of the total time of the year (Figure 5-15 b).

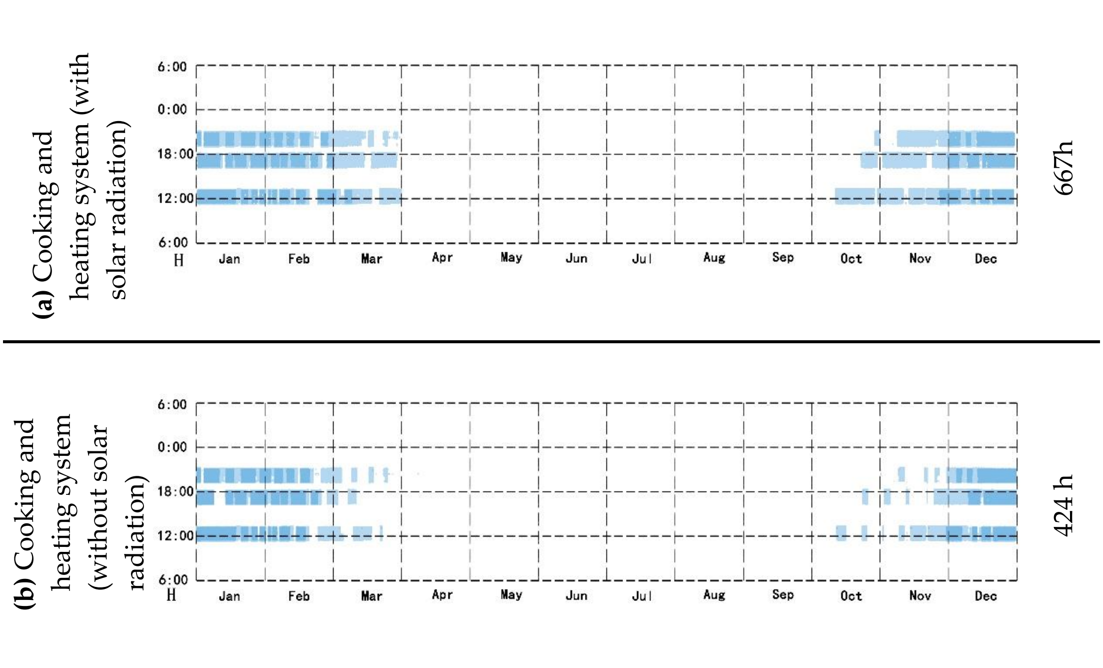

Figure 5-14. (a) Suitable time of the annual average for cooking and heating system with solar radiation; (b) Suitable time of the annual average for cooking and heating system without solar radiation.

5.4.1 Total Thermal Load Reduced by the New System

Using Energyplus to simulate the annual heat load of the cooking and heating system, when the wall experiences solar radiation, the annual heat load of the building is reduced by 1104.723 kW· h, with a reduction rate of 19.84% (Figure 5-16 a). When there is no solar heat radiation on the wall, the annual heat load of the building will be reduced by 440.8318 kW· h, which is a reduction rate of 7.91% (Figure 5-16 b). The thermal load difference between the two is 663.8912 kW· h.

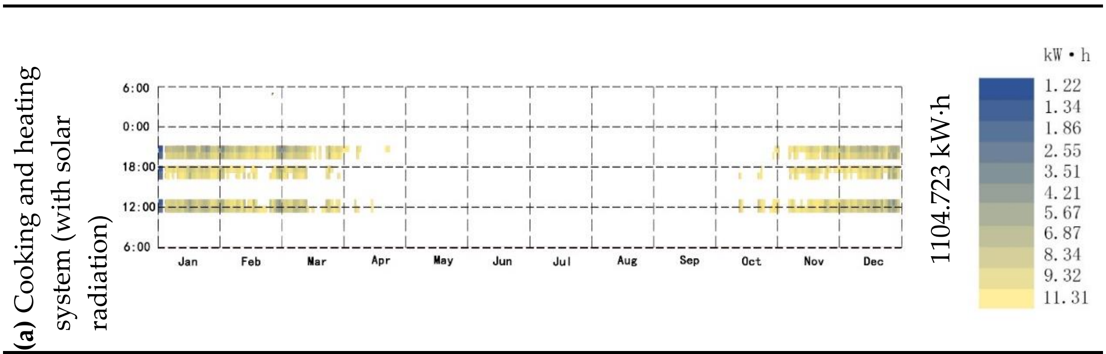

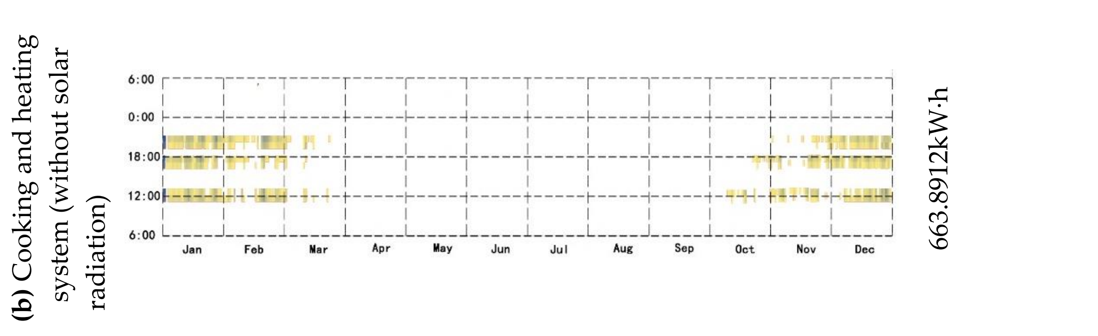

Figure 5-15. (a) The annual average load reduction in the cooking and heating system with solar radiation; (b) The annual average load reduction in the cooking and heating system without solar radiation.

5.4.2 Room Temperature below 18°

The figure 5-15 shows the variation in indoor temperature with or without solar radiation when the building adopts a natural heating system. We take 18 ℃ as the limit of the passive heating of the building and calculate the time below 18 ℃. In the case of natural heating, the total annual time when the temperature in the building is below 18 ℃ is 4430 h, accounting for 51.27% of the total annual time (Figure 5-17 a). When the cooking system is used and the wall experiences solar radiation, the annual time when the temperature in the building is lower than 18 ℃ is 3763 h, accounting for 43.55% of the total time of the year (Figure 5-17 b). Without solar radiation on the wall, the total annual time when the building is below 18 ℃ is 4006 h, accounting for 46.36% of the total annual time (Figure 5-17 c).

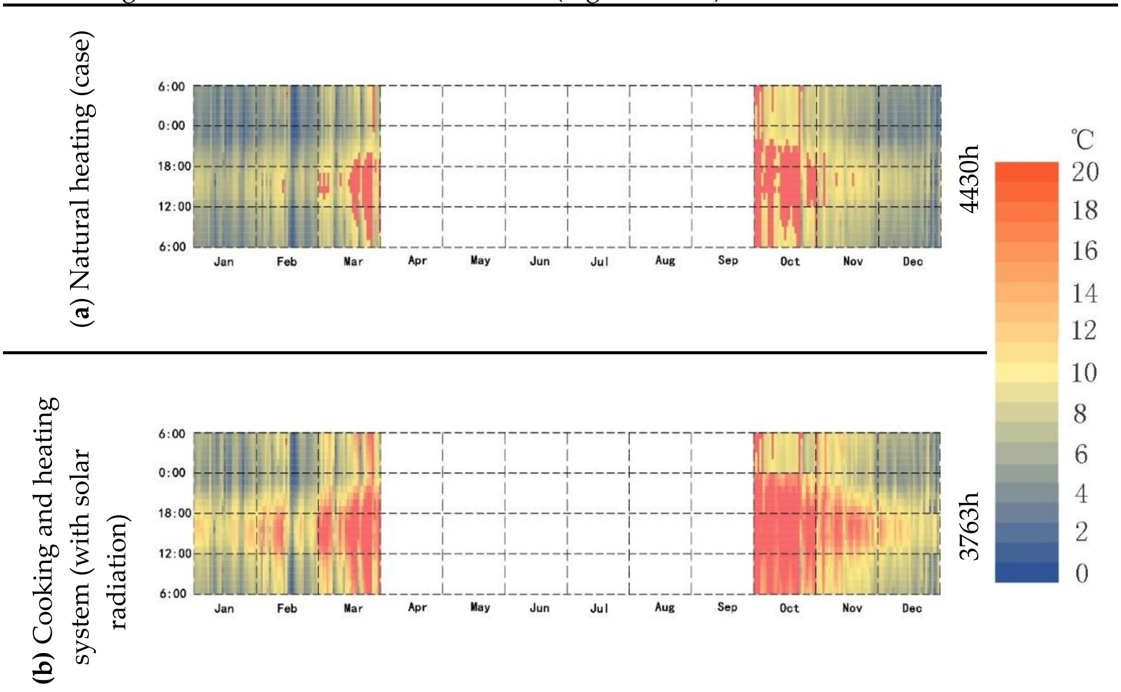

(c) Cooking and heating system (without solar radiation)

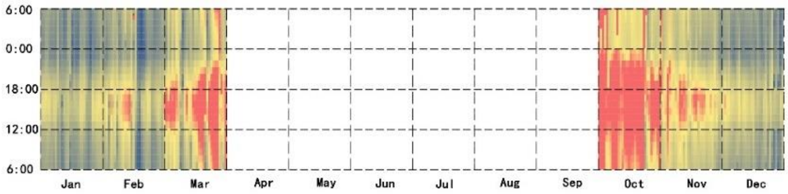

4006h

Figure 5-16. (a) The time when the average annual temperature of natural heating is lower than 18 ℃; (b) The annual time when using cooking heating with solar radiation when the average temperature is below 18 ℃; (c) The annual time when using cooking heating without solar radiation when the average temperature is below 18 ℃.

5.5. Chapter Summary

This chapter mainly describes the application of cooking heating wall system in traditional residential houses in southern Shaanxi. The first part is a detailed introduction to the cooking heating wall system of traditional houses in southern Shaanxi. This paper introduces the definition and modeling of cooking heating wall, its design, working principle and software simulation process. Secondly, through software simulation comparative analysis of natural heating and cooking heating wall system heating situation, summed up the cooking heating wall system can effectively improve the indoor temperature. In addition, the annual adaptation time and reduced heat load of the cooking heating wall system are summarized, which provides new ideas for passive heating design of rural residential houses in the future.

Reference

[1] Liu, M.; Huang, X.; Chen, Z.; Zhang, L.; Qin, Y.; Liu, L.; Zhang, S.; Zhang, M.; Lv, X.; Zhang, Y. The transmission mechanism of household lifestyle to energy consumption from the input-output subsystem perspective: China as an example. Ecol. Indic. 2021, 122, 107234.

[2] IEA. IEA Online Data Services. Available online: https://www.iea.org/subscribe-to-data-services/world-energy-balances-and-statistics (accessed on 20 Feb 2021).

[3] EIA, U.S. Annual energy outlook 2018; DOE: Washington, DC, USA, 2018.

[4] Rhodes, C.J. The 2015 Paris Climate Change Conference: Cop21. Sci. Prog. 2016, 99, 97–104.

[5] Building Energy Efficiency Research Center of Tsinghua University. Tsinghua University annual report on China building energy efficiency; China Architecture & Building Press: Beijing, China, 2017.

[6] China Association of Building Energy Efficiency. 2018 China building energy research report. Available online: https://www.cabee.org/site/term/107.html (accessed on 20 Feb 2021).

[7] International Energy Agency. Transition to sustainable buildings: strategies and opportunities to 2050; Organization for Economic: Paris, 2013.

[8] Mi, Z.; Zheng, J.; Meng, J.; Shan, Y.; Zheng, H.; Ou, J.; Guan, D.; Wei, Y.-M. China’s Energy Consumption in the New Normal. Earths Future. 2018, 6, 1007–1016.

[9] Jiang, Z.; Lyu, P.; Ye, L.; Zhou, Y.W. Green innovation transformation, economic sustainability and energy consumption during China’s new normal stage. J. Clean Prod. 2020, 273, 123044.

[10] Liu, C.; Xu, W.; Li, A.; Sun, D.; Huo, H. Energy balance evaluation and optimization of photovoltaic systems for zero energy residential buildings in different climate zones of China. J. Clean Prod. 2019, 235, 1202–1215.

[11] Liu, Z.; Liu, Y.; He, B.-J.; Xu, W.; Jin, G.; Zhang, X. Application and suitability analysis of the key technologies in nearly zero energy buildings in China. Renewable and Sustainable Energy Reviews 2019, 101, 329–345.

[12] Siwei, L.; Yu Joe, H. Energy conservation standard for space heating in Chinese urban residential buildings. Energy 1993. 18, 871-892.

[13] Hu, S.; Yan, D.; Guo, S.; Cui, Y.; Dong, B. A survey on energy consumption and energy usage behavior of households and residential building in urban China. Energy Build. 2017, 148, 366-378.

[14] Xu, C.; Li, S.; Zhang, X. Energy flexibility for heating and cooling in traditional Chinese houses based on adaptive thermal comfort: A case study in Nanjing. Build. Environ. 2020, 179, 106952.

[15] He, B.-j.; Yang, L.; Ye, M.; Mou, B.; Zhou, Y. Overview of rural building energy efficiency in China. Energy Policy 2014, 69, 385–396.

[16] Ding, J.; Ma, S. Comparative analysis of habitation behavioral patterns in spatial configuration of traditional houses in Anhui, Jiangsu, and Zhejiang provinces of China. Frontiers of Architectural Research 2020, 9, 54–66.

[17] Merzoug, W.; Chergui, S.; Cheikh, Z.M. The impact of reinforced concrete on the modern-day architectural heritage of Algeria. Journal of Building Engineering 2020, 30, 101210.

[18] Andreescu, I.; Gaivoronsch, V.; Mosoarca, M. Old and New—The Complex Problem of Integrating New Functions into Old Building. Procedia Eng. 2016, 161, 1103–1108.

[19] Ren, J.; Zhao, Z.; Zhang, J.; Wang, J.; Guo, S.; Sun, J. Study on the hygrothermal properties of a Chinese solar greenhouse with a straw block north wall. Energy and Buildings. 2019, 193, 127-138.

[20] Zheng, W.; Li, B.; Cai, J.; Li, Y.; Qian, L. Microclimate characteristics in the famous houses: A case study of the Hakka Tulou in Hezhou, China. Urban Climate. 2021,37, 100824.

[21] Mangesh, V.; Madurwar, R.V.; Ralegaonkar, S.A.; Application of agro-waste for sustainable construction materials: A review, Construction and Building Materials. 2013, 38, 872-878.

[22] Deepa, G.; Nair, K.S.; Jagadish, A.F. Reactive pozzolanas from rice husk ash: An alternative to cement for rural housing. Cement and Concrete Research. 2006, 36, 1062-1071.

[23] Taha, A.; Heiko, G.; Wei, W. Performance of straw bale wall: A case of study. Energy and Buildings. 2011, 43, 1960-1967.

[24] Song, G.; Song, J.; Zhang, S. Modelling the policies of optimal straw use for maximum mitigation of climate change in China from a system perspective. Renewable and Sustainable Energy Reviews. 2016, 55, 789-810.

[25] Binici, H.; Eken, M.; Kara, M. and Dolaz, M. An environment-friendly thermal insulation material from sunflower stalk, textile waste and stubble fibers. 2013 International Conference on Renewable Energy Research and Applications (ICRERA). 2013, 833-846.

[26] Li, J.; Li, Y.; Bo, Y.; Xie, S. High-resolution historical emission inventories of crop residue burning in fields in China for the period 1990–2013, Atmospheric Environment. 2016, 138, 152-161.

[27] Zhang, L. Production of bricks from waste materials – A review, Construction and Building Materials. 2013, 47, 643-655.

[28] Rahman, M.A. Properties of clay-sand-rice husk ash mixed bricks. International Journal of Cement Composites and Lightweight Concrete. 1987, 9, 105-108.

[29] Zulcão, R.; Calmon, J.L.; Thais, A.R.; Darli, R.V. Life cycle assessment of the ornamental stone processing waste use in cement-based building materials. Construction and Building Materials. 2020, 257, 119523.

[30] Dina, M.; Sadek, M.M.; El-Attar, H.A. Reusing of marble and granite powders in self-compacting concrete for sustainable development, Journal of Cleaner Production. 2016, 121, 19-32.

[31] Bacarji, E.; Filho, R.D.; Koenders, E.A.B.; Figueiredo, E.P.; Lopes, J.L.M.P. Sustainability perspective of marble and granite residues as concrete fillers, Construction and Building Materials. 2013, 45, 1-10.

[32] Madhura, Y.; Mahek, A. Biobased building materials for sustainable future: An overview, Materials Today: Proceedings. 2021, 43, 2895-2902.

[33] Chao, W.; Xu, G. Gu, X. Gao, Y. Zhao, P. High value-added applications of coal fly ash in the form of porous materials: A review, Ceramics International. 2021, 47, 22302-22315.

[34] Roya, A.; Bubak, S.; Masood, E. Evaluation of wheat straw to insulate fired clay hollow bricks as a construction material. Journal of Cleaner Production. 2020, 254, 120043.

Chapter 6. Research on Passive Cooking Heating Wall with an Additional Sunlight Room System in Traditional Houses in southern Shaanxi

6.1 Introduction and Simulation of the System between Cooking Heating Wall and Additional Sunlight

6.1.1 Current Situation Model

The research site was Hong Village, Houliu Town, Shiquan County, Ankang City, Shaanxi Province, covering an area of approximately 0.01625 km² (Figure 6-1 a). The development of the village along the Han River is ribbon-shaped, and the terrain is mostly mountainous [1,2]. This area is hot and humid in summer with more rainstorms, and cold and humid in winter with less rain. According to the field survey, the lowest temperature is –2 ℃, and the highest wind velocity is 5 m/s (Figure 6-1 b,c). Due to the constraints posed by the river valleys and mountains, the distribution of villages is mainly in clusters, and the layout of residential buildings is relatively close. The residential buildings in the Ming and Qing dynasties were mostly of the one- or two-floor, sloped roof type [3,4,6,7,8,9]. Among them, the one-story residential houses accounted for 88.2% of the total, with a floor height of 4–4.5 m; meanwhile, the two-story residential houses had a floor height of 5.5–6.0 m, and the building density was 23.15% (Figure 6-1 d). Due to the influence of the building form and structure, the indoor solar radiation received by the residential houses are relatively small, and the influence of the climate causes the residential houses to feel damp and cold in winter.

The research objects were the traditional houses in southern Shaanxi. The buildings of the folk houses are primarily one-story, although some parts of the houses are two story [10,11,12,13,14,15]. The overall height of the buildings is 4.8 m; the height of the first floor is 3.3 m and the height of the local second floor is 1.5 m. The walls of the building are made of blue bricks; the roof has double slopes of blue tiles and the eaves are longer, which is conducive to blocking the sun and organizing rainwater drainage. Local houses are mostly self-built, and the construction method is based on years of construction experience. Restricted by economic conditions and building materials, less consideration is given to the passive heating of residential buildings in winter, resulting in lower indoor temperatures in winter (Figure 6-2).

(a)

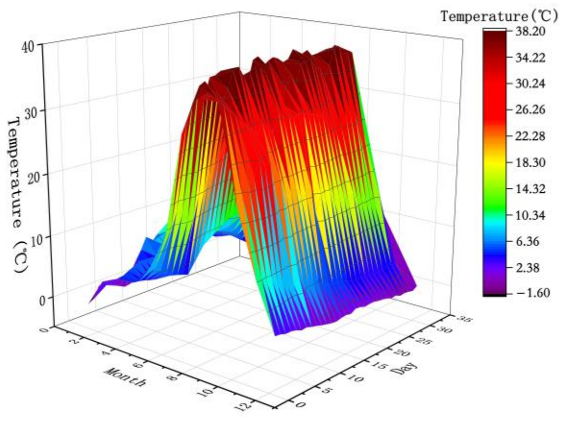

(b)

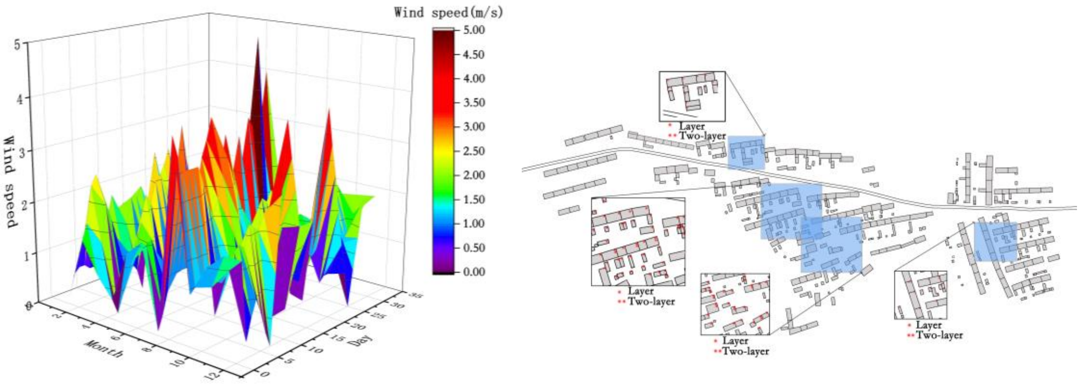

(c) (d)

Figure 6-1. (a) Topographic satellite map of Hong village; (b) Annual temperature distribution map; (c) Distribution map of wind velocity throughout the year; (d) Village plan.

Figure 6-2. Photos of folk houses in southern Shaanxi.

6.1.2 Model Design of Cooking Heating Wall and Additional Sunlight System

For effectively increasing the indoor temperature in winter, residents use different heating equipment, such as braziers and fire tables. These heating devices can only increase the temperature of a part of the room and are mostly used in the daytime, and have disadvantages such as a poor heating effect and inflexible use [16,17,18,19,20,21]. This paper presents a cooking heating wall system with an additional sunlight room, which consists of two parts. The first part is the cooking heating wall; its working principle is to use the heat storage capacity of the wall to heat said wall, with the residual temperature generated by cooking raising the indoor temperature (Figure 6-3 a). The second part is the additional sunlight room. Since the heating time of the cooking heating wall mainly depends on the duration and frequency of cooking, in order to solve this problem, an additional sunlight room was designed on the basis of the cooking heating wall (Figure 6-3 b). The additional sunlight room refers to a closed space made of transparent materials such as glass. When solar radiation is irradiated in this transparent and enclosed space, the ability of the wall and the ground to absorb and release heat is used to heat the indoor temperature in the form of thermal radiation and thermal convection, thereby prolonging the indoor heating time (Figure 6-3 c). This research mainly used the advantages of the cooking heating wall system and the sun room system to make up for the shortcomings of a single system, so as to improve heating efficiency and energy saving.

The key technology to be solved in this study was how to use cooking heating walls and additional sunlight for passive heating to raise the indoor temperature. By analyzing the local winter sunshine, it is known that when designing a cooking heating wall system with an additional sun room, the sun room should be combined with the kitchen, so that the sun room can collect the waste heat generated by cooking (Figure 6-3 d–f). Second, the sun room should be designed on the side facing the sun, so that the sun room can fully collect and receive solar radiation. At the junction of the pipe and the furnace body, two valves are provided. In winter, valve 1 is opened and valve 2 is closed, letting the flue gas pass through flue 1 to be exhausted outdoors and to heat flue 1 (Figure 6-3 g). In summer, valve 2 is opened and valve 1 is closed, allowing the flue gas to pass through flue 2 to the outside (Figure 6-3 h). The additional sunlight room system needs to be equipped with sliding glass to prevent the indoor temperature from becoming too high in summer.

Based on comprehensive research and comparison, residential buildings with four bays and one depth were selected as the object of this study. According to the established model, the spatial distribution from west to east is the bedroom, the living room, the bedroom, and the kitchen. The reformed cooking heating wall plan is as follows: The cooking heating wall is set between the bedroom and the kitchen on the east side (Figure 6-3 a). The specific structure is as follows: A circular hole with a diameter of 100 mm is set inside the hearth, and an aluminum tube with a thickness of 3 mm is inserted into the hole and placed inside the wall in an S shape, with an overall length of 11.37 m. After renovation, the plan of the additional sunlight room is as follows: A 1.5 m × 3.0 m × 19.34 m confined space is built on the sunny side of the dwelling with the kitchen, which is the additional sunlight room. As shown in the purple area, the outer protective structure is composed of glass curtain walls (Figure 6-3 b). The glass adopts a single-layer glass of 6 mm, and the visible light transmittance is 0.77. The combined design of cooking heat and sunlight can not only make up for the lack of cooking-based heating time but can also meet the overall needs of heating the indoor temperature.

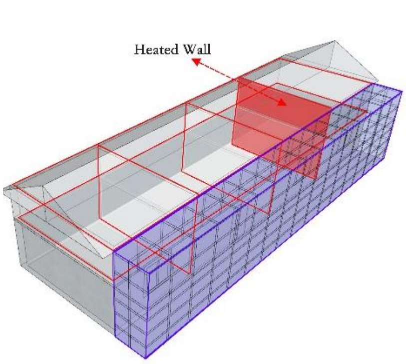

(a)

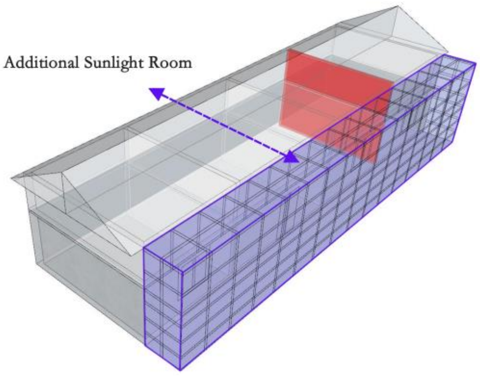

(b)

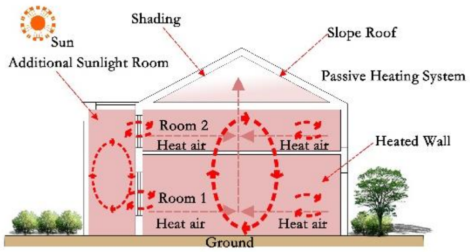

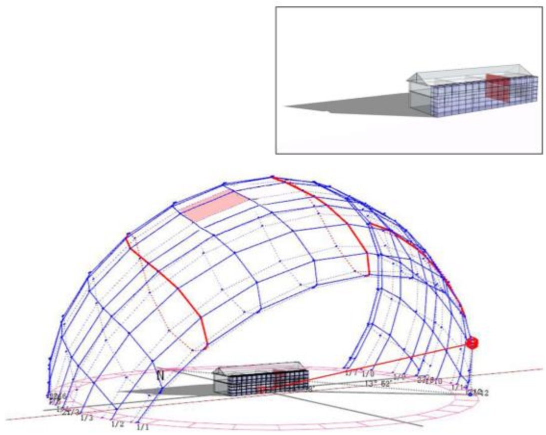

(c) (d)

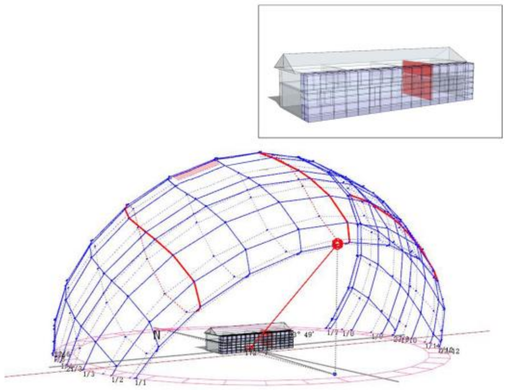

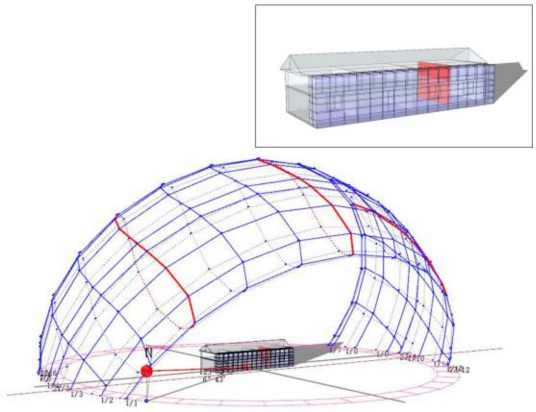

(e) (f)

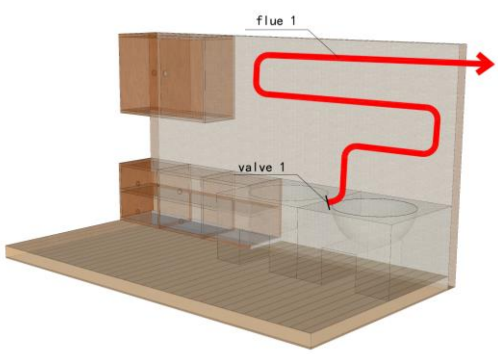

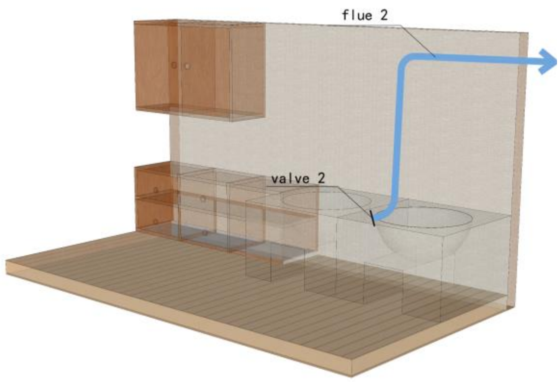

(g) (h)

Figure 6-3. (a) The location of the cooking heating wall; (b) The location of additional sunlight; (c) Heat transfer effect picture; (d) Sunshine conditions in winter at 8:00 a.m.; (e) Sunshine conditions in winter at 12 a.m.; (f) Sunshine conditions in winter at 5:00 p.m.; (g) Cooking heating wall system design in winter; (h) Cooking heating wall system design in summer.

6.1.3 Working Principle of Additional Sunlight Room

The working principle of the cooking heating wall is that the hot gas generated by cooking enters the aluminum tube heating wall, and the tube wall heats the wall after reaching a constant temperature. Using the heat storage capacity of the wall, the indoor temperature is heated to enhance the thermal comfort of the human body. The design of the cooking heating wall is similar to the cooking waste heat recovery equipment. For better analyzing the heat transfer process of the cooking heating wall, the heat transfer process includes three steps: First, the material burned during cooking produces high-temperature gas, and the hot gas enters the aluminum tube to heat the tube wall. The entire heat transfer process is dominated by heat convection, which belongs to the coupled heat transfer between fluid and solid states. In the process of software simulation, hot air enters the aluminum tube and forms a turbulent flow. When the speed of the hot gas reaches a relatively constant value, the hot gas heats the tube, and the heat transfer mainly takes the form of heat convection. When the tube is heated to a constant temperature, the wall is heated in the form of heat conduction and thermal radiation.

This process is a solid–solid coupling heat transfer. In addition, the heated wall heats the interior of the wall in the form of heat radiation and convection to raise the temperature. Finally, when the cooking is over, no more smoke is produced, the temperature of the cooking heating wall begins to drop, and the heat transfer process also ends. The working principle of the additional sun room is that the sun heats the air in the sun room through the glass and irradiates the wall and the ground to absorb and store part of the heat energy. The other part of the sunlight can be directly irradiated into the room through the windows, thereby increasing the indoor temperature. From the perspective of the indoor heating principle, the mechanism is the same as the principle of the heat collection and storage wall type, which is a combination of the direct revenue type and the heat collection and storage type. In order to understand the whole heat transfer process, it is split into three steps: First, sunlight heats the temperature in the room through the glass. This heat transfer process is mainly in the form of heat transfer by heat radiation and convection. The time sequence in the heat transfer process is transient heat transfer–steady heat transfer–transient heat transfer. When the fluid is heated, it follows Newton's law of cooling, and its calculation formula is

$$q = h(T_w - T_f) \tag{1}$$

where formula h is the surface heat transfer coefficient, Tw and Tf are the wall temperature and fluid temperature, respectively, and q is heat flux.

When the temperature reaches a certain level, the wall begins to absorb and store heat. The heat transfer in this process is mainly heat conduction and heat convection. In heat conduction, Bouriet's law is followed and its calculation formula is

$$q = \frac{Q}{A} = -\lambda\left(\frac{dt}{dx}\right) \tag{2}$$

where formula Q is the heat conduction rate, Q is the heat flux, and λ is the proportionality coefficient. When the temperature t increases along the x direction, $dt/dx > 0$ and $q < 0$, indicating that the heat is transferred in the direction where X decreases. On the contrary, $dt/dx < 0$ and $q > 0$ explain that heat is transferred along the increasing direction of the x-axis at this time.

When the indoor temperature is lower than the temperature of the room with additional sunlight, the high temperature exterior of the wall conducts heat to the low temperature indoor wall. The temperature between the walls is heated in the form of thermal convection and thermal radiation, thereby increasing the overall temperature. In heat radiation, it follows the fourth power law and its calculation formula is

$$\Phi = \varepsilon A \sigma T^4 = \varepsilon C_0\left(\frac{T}{100}\right) \tag{3}$$

where formula Φ is the radiation energy, T is the thermodynamic temperature, A is the radiation surface area, ε is the emissibility of the object, σ is the constant 5.67×10^{-8}, and C_0 is the constant 5.67 [22,23,24,25,26,27].

6.1.4 Simulation Process

This simulation mainly includes three parts. Part one was to build a model based on the data measured on the spot, and to set up a cooking heating wall model, which mainly included the stove, aluminum tube, and wall. The content of the simulation calculation was mainly the temperature and time required for the aluminum tube, the cooking heating wall, and the indoor temperature and time after equilibrium. In the second part, based on the original cooking heating wall model, the additional sunlight interval model was established, including the size and area of the sunlight interval. The content of the simulation was mainly the temperature between the sunlight, the heat transfer of the wall, and the indoor temperature and time after the balance. The third part mainly involved simulating and calculating the annual heat load of the new system and the appropriate time.

6.2 Natural heating, Cooking Heating Wall and Additional Sunlight Room System with Solar Radiation on the Wall

6.2.1 Natural Heating with Solar Radiation on the Wall

A. System Introduction

The ordinary heating of residential buildings mainly relies on the heat radiation of the sun through the heat transfer of the walls to raise the indoor temperature. The heat transfer process is as follows: The wall absorbs heat and solar radiation through thermal convection and thermal radiation as the main heat transfer methods. Second, the wall self-generates heat conduction, and the high-temperature outer surface transfers heat to the low-temperature inner surface. The inner surface of the wall radiates heat between the walls, thus heating the indoor temperature. In short, ordinary heating is a synthesis of heat convection, conduction, and radiation.

B. System Simulation

To confirm the effectiveness of the cooking heating wall system with an additional sunlight room, a comparison was made to ordinary heating as the benchmark. For verifying the practicability of the results of the software simulation, the indoor temperature was measured for three consecutive days. The test took place from 25 to 28 December 2020. The test interval was measurement every 1 h. The testing equipment included four thermometers and hygrometers (type: PM6508). and four rangefinders (type: D508). The indoor measuring points were mainly selected in the middle of the room, and the outdoor measuring points were mainly selected at 2 m away from the building (Figure 6-4 a). During the test, the sensor of the instrument was perpendicular to 1.5 m on the ground, and the data were read after standing for 1 min. The test results were as follows: From 2:00 to 4:00 p.m. in the afternoon, the highest outdoor temperature was 5.0 ℃ and the average temperature was 3.5 ℃ (Figure 6-4 b). From 9:00 to 11:00 a.m. in the morning, the average indoor temperature rose from 5.0 to 5.4 ℃. At 2:00 p.m., the average indoor temperature rose to 6.4 ℃, and by 5:00 p.m., the indoor temperature began to drop. At 7:00 p.m., the indoor temperature was 4.4 ℃ (Figure 6-4 c). In order to make the simulation more realistic, through the comparison of multiple sets of data, the day that was least affected by solar radiation in the winter was selected and the initial indoor temperature was 5 ℃ (Figure 6-4 d). The plane details of the dwellings are shown in the figure 6-4 e-g. In order to compare the situation to solar radiation, a simulation time during the day was selected, and the simulation time was mainly from 9:00 a.m. to 7:00 p.m. The main reason is that the wall is affected by the solar thermal radiation, which causes the indoor temperature to rise. From 9:00 to 11:00 a.m., under the influence of solar radiation, the indoor temperature began to rise slowly, from an average temperature of 5 to 5.5 ℃ (Figure 6-5 a,b). At 3:00 p.m., the solar radiation altitude angle changed, and the average indoor temperature rose to 6.5 ℃, which is 1.9 ℃ different from the outdoor temperature (Figure 6-5 c,d). From 5:00 p.m., the indoor temperature began to slowly drop, and the average temperature was 6 ℃ (Figure 6-5 e). At 7:00 p.m., the average indoor temperature dropped to 4.5 ℃ (Figure 6-5 f). Therefore, ordinary heating mainly relies on solar radiation to improve the indoor temperature through the irradiation of walls, glass, and other structures. By comparing the software simulation results with the actual measurement results, it can be seen that the temperature difference between the two is 0.1 ℃ (Figure 6-6). Within the allowable range of error, it was proven that the results of the software simulation were close to the actual situation.

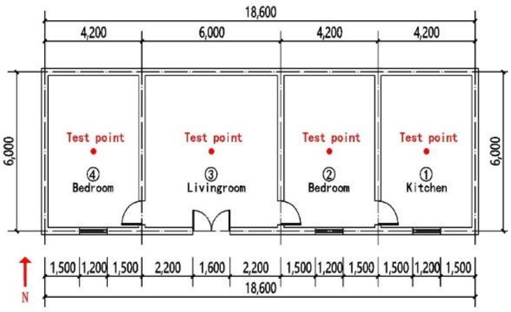
18,600
4,200
6,000
4,200
4,200
6,000
6,000
Test point
Test point
Test point
Test point
④ Bedroom
③ Livingroom
② Bedroom
① Kitchen
1,500 1,200 1,500 2,200 1,600 2,200 1,500 1,200 1,500 1,500 1,200 1,500
18,600
N

(a)

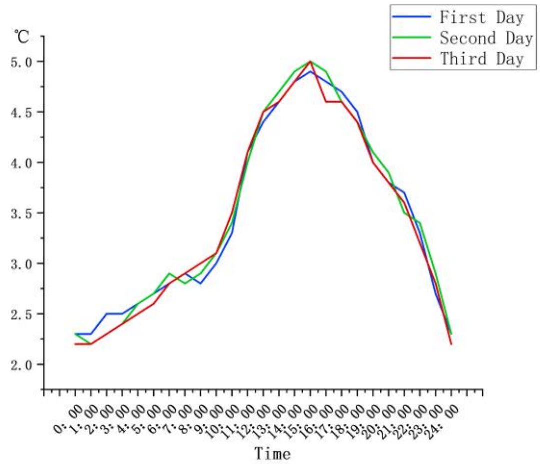
℃
First Day
Second Day
Third Day
5.0
4.5
4.0
3.5
3.0
2.5
2.0
Time

(b)

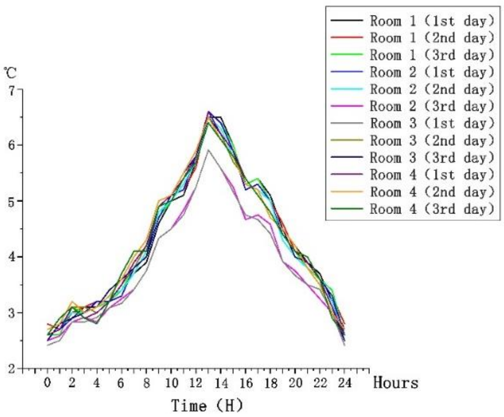
℃
Room 1 (1st day)
Room 1 (2nd day)
Room 1 (3rd day)
Room 2 (1st day)
Room 2 (2nd day)
Room 2 (3rd day)
Room 3 (1st day)
Room 3 (2nd day)
Room 3 (3rd day)
Room 4 (1st day)
Room 4 (2nd day)
Room 4 (3rd day)
0 2 4 6 8 10 12 14 16 18 20 22 24
Hours
Time (H)

(c)

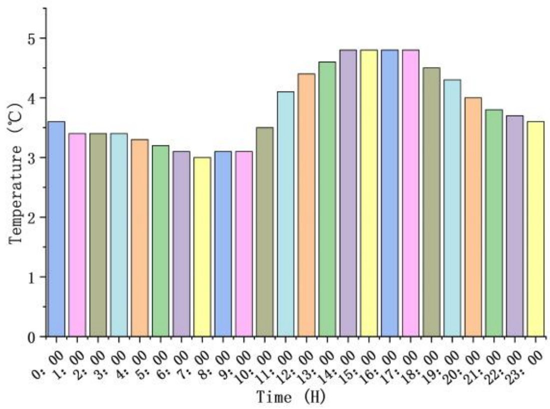
Temperature (℃)
Time (H)

(d)

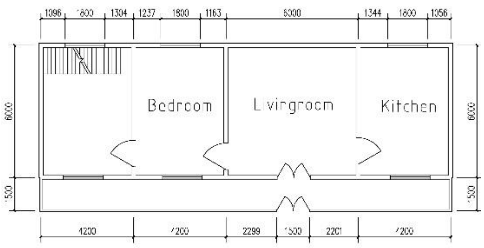
Bedroom
Livingroom
Kitchen

(e)

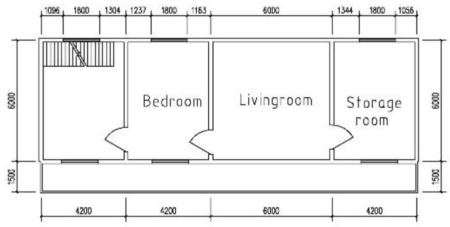
Bedroom
Livingroom
Storage room
4200
4200
6000
4200

(f)

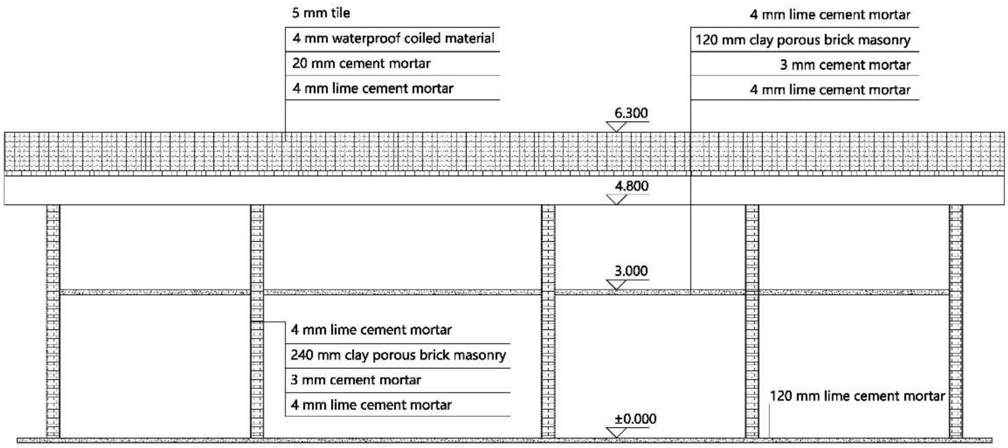

(g)

Figure 6-4. (a) Building layout; (b) Outdoor temperature distribution map; (c) Indoor temperature distribution map; (d) Outdoor temperature distribution during a day; (e) First floor plan; (f) Second floor plan; (g) Composition of wall and floor.

The temperature change of the ordinary system with WSR

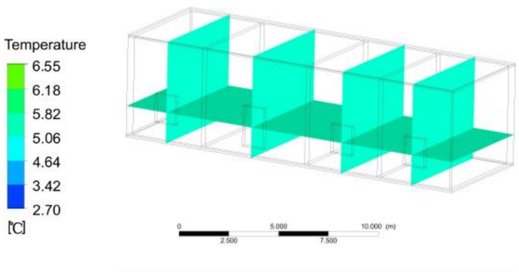

(a) 9:00 a.m.

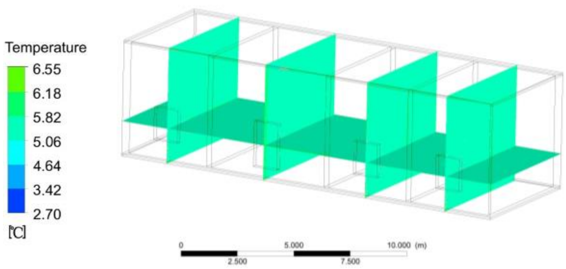

(b) 11:00 a.m.

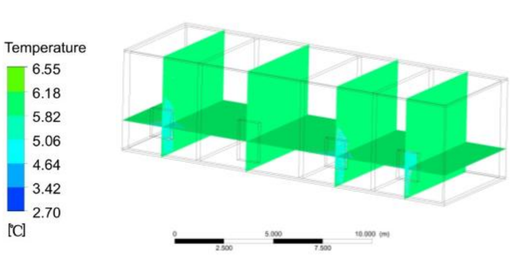

(c) 1:00 p.m.

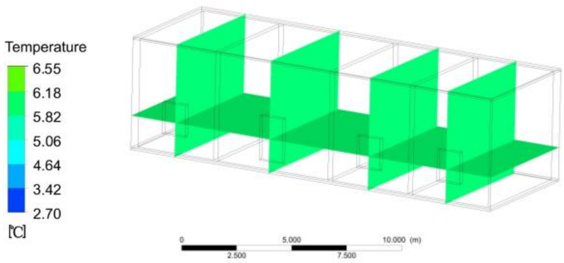

(d) 3:00 p.m.

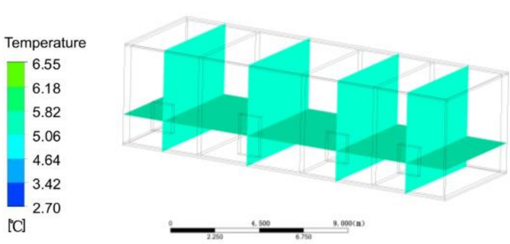

(e) 5:00 p.m.

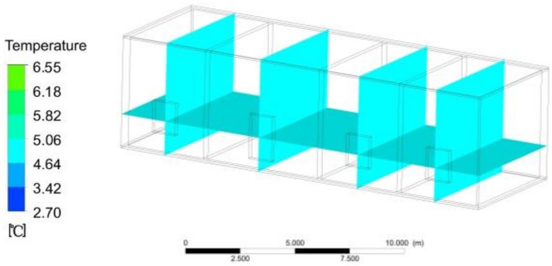

(f) 7:00 p.m.

Figure 6-5. (a) At 9:00 a.m. the temperature of the ordinary heating (with WSR); (b) At 11:00 a.m. the temperature of the ordinary heating (with WSR); (c) At 1:00 p.m. the temperature of the ordinary heating (with WSR); (d) At 3:00 p.m. the temperature of the ordinary heating (with WSR); (e) At 5:00 p.m. the temperature of the ordinary heating (with WSR); (f) At 7:00 p.m. the temperature of the ordinary heating (with WSR).

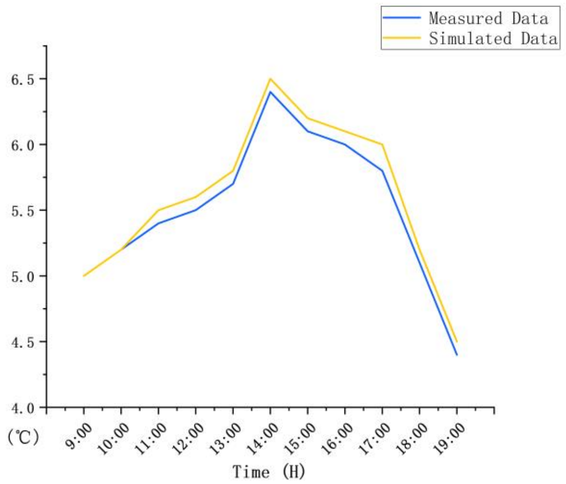

Figure 6-6. Comparison between the measured and simulated data.

6.2.2 Cooking Heating Wall and Additional Sunlight Room System with Solar Radiation

A. System Introduction

In order to effectively improve the limitation of cooking and heating time, a passive cooking heating wall and additional sunlight heating are proposed. Not only can the heating time be extended, but it can also make up for the insufficient heating effect of the additional sunlight on cloudy days. When the sun shines on the additional sunlight room, the temperature starts to rise slowly, and cooking has stopped by this point. When the temperature in the additional sunlight room reaches a relatively constant value, the indoor temperature is heated through the heat absorption and heat release effect of the wall. The wall, through the form of heat radiation and convection, raises the temperature of the room. Compared to single-cooking heating wall, the passive cooking heating wall and additional sunlight heating effect is better; after the balance of the temperature has been significantly increased, the heating time is extended.

B. System Simulation

In order for a comparison with ordinary heating, the indoor and outdoor temperature distributions were basically the same when the cooking heating wall was simulated and the sun room was added. The heating of the cooking heating wall is inseparable from the energy released when cooking. After the cooking has started, the cooking heating wall starts to work. The combustion of cooking is mainly divided into four parts: firewood burning, firewood burning, stop adding firewood, and firewood burning out. According to the actual measurement, when the firewood is ignited, the flue gas enters the aluminum pipe at a speed of 2.3 m/s. The software simulation shows that the average velocity of gas in the aluminum pipe is 2.26 m/s and the average pressure is 1.56 Pa (Figure 6-7 a,b). The temperature of the gas depends on the energy of cooking and burning biomass. Through multiple measurements, the average temperature of the gas was shown to be 60 ℃. Taking 60 ℃ as the initial temperature of the gas, software simulations can be conducted. At 25 s, the temperature at the inlet of the pipe was 60 ℃ and the outlet was 0 ℃ (Figure 6-8 a). As the time increased, at 65 s, the mean temperature of the pipe was 28.32 ℃ (Figure 6-8 b). At 95 s, the mean temperature of the pipe was 42.62 ℃ (Figure 6-8 c). At 125 s, the temperature of the pipe reached equilibrium, and the final temperature was 60.22 ℃ (Figure 6-8 d).

Speed and pressure of flue gas

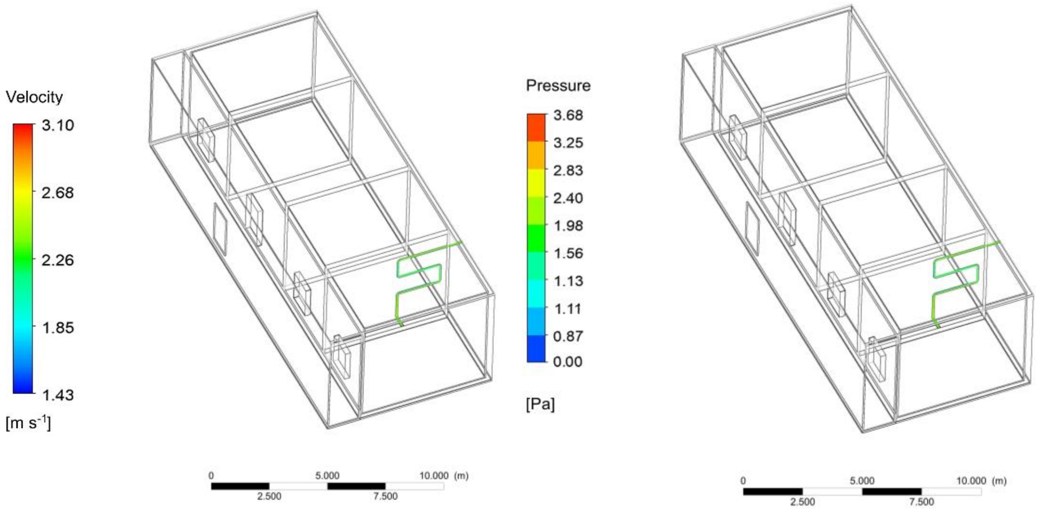

(a) Speed (b) Pressure

Figure 6-7. (a) Speed of the flue gas; (b) Pressure of the flue gas.

Temperature of the pipe

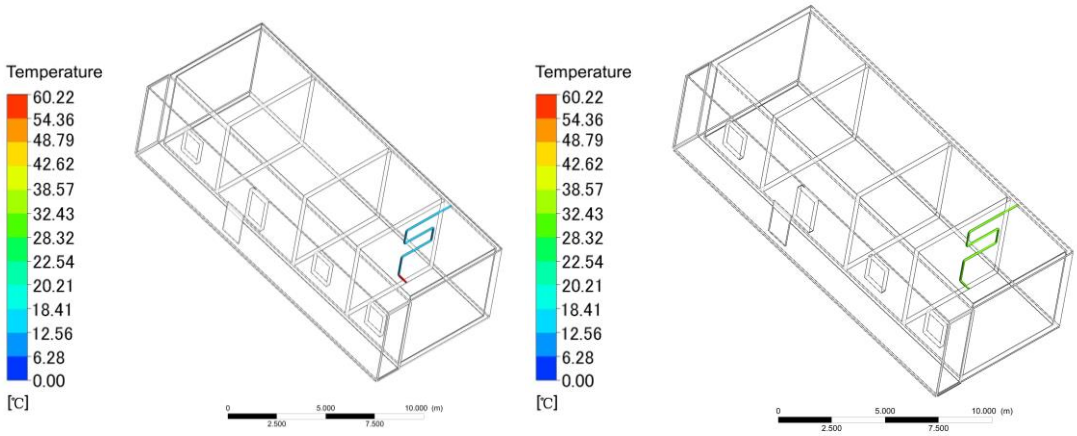

(a) 25s (b) 65s

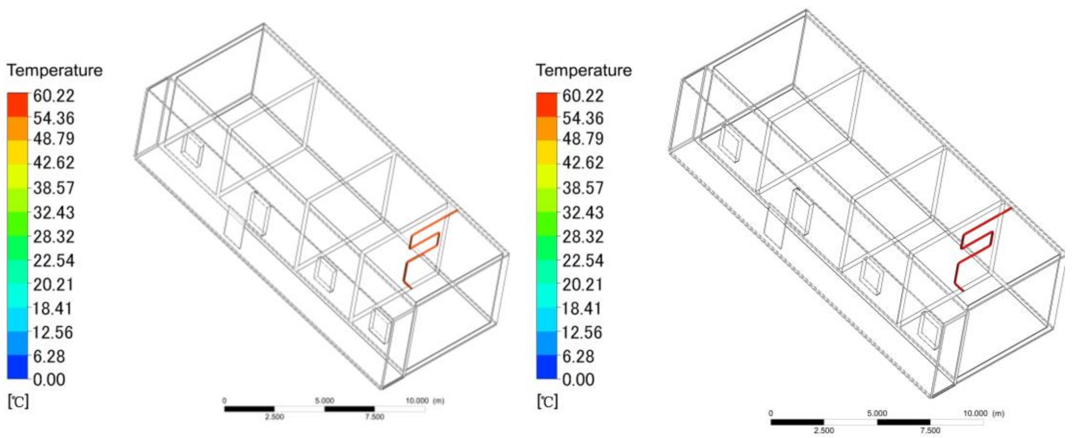

(c) 95s (d) 125s

Figure 6-8. (a) Pipe heating in 25 s; (d)Pipe heating in 65 s; (c) Pipe heating in 95 s; (d) Pipe heating in 125 s.

When the aluminum tube reached a constant temperature, the cooking heating wall is heated by heat conduction. At 4 min and 43 s, the average temperature of the cooking heating wall was 4.38 °C (Figure 6-9 a). At 7 min and 45 s, the average temperature of the cooking heating wall was 9.43 °C (Figure 6-9 b). With the increase in heating time, the average temperature of the cooking heating wall was 14.49 °C at 11 min and 30 s (Figure 6-9 c). At 16 min and 10 s, the average temperature of the cooking heating wall gradually increased to 19.55 °C (Figure 6-9 d). At 20 min and 10 s, the average temperature of the cooking heating wall was 24.60 °C (Figure 6-9 e). At 24 min and 20 s, the temperature of the cooking heating wall reached a stable value of 29.66 °C, and the temperature of the additional sunlight room remained unchanged (Figure 6-9 f).

Wall heating

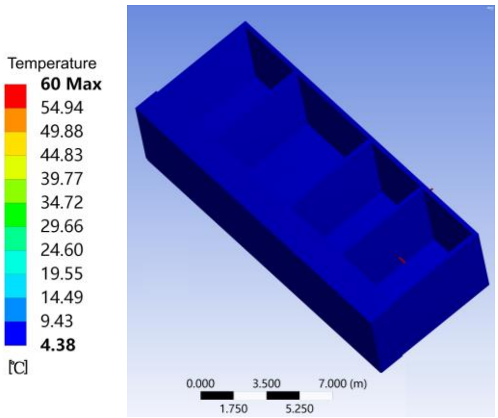

(a) 4 min and 43 s

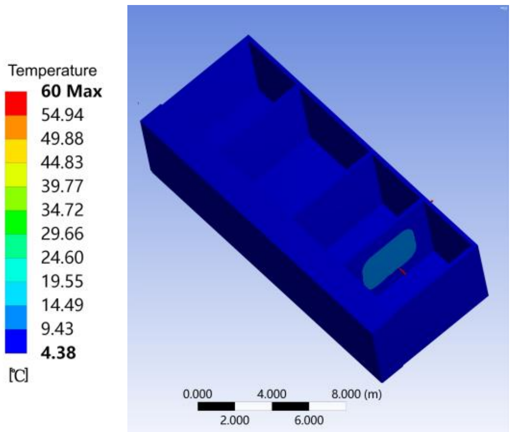

(b) 7 min and 45 s

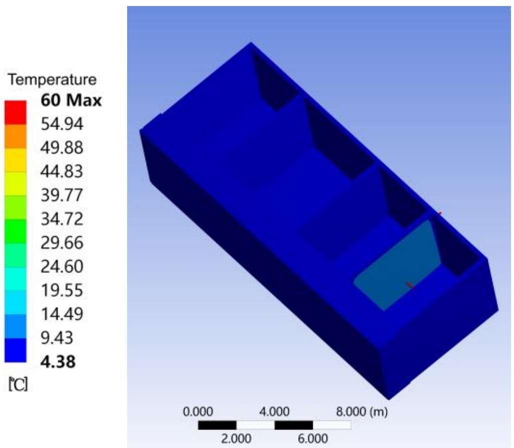

(c) 11 min and 30 s

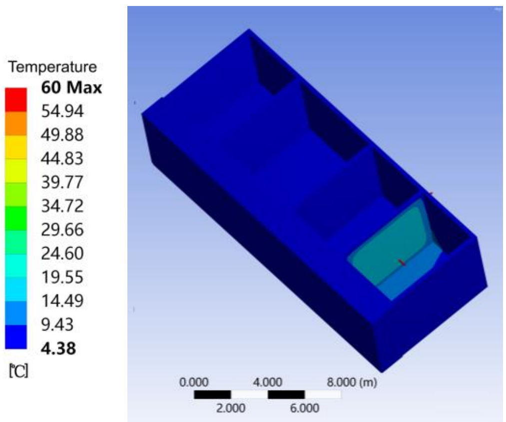

(d) 16 min and 10 s

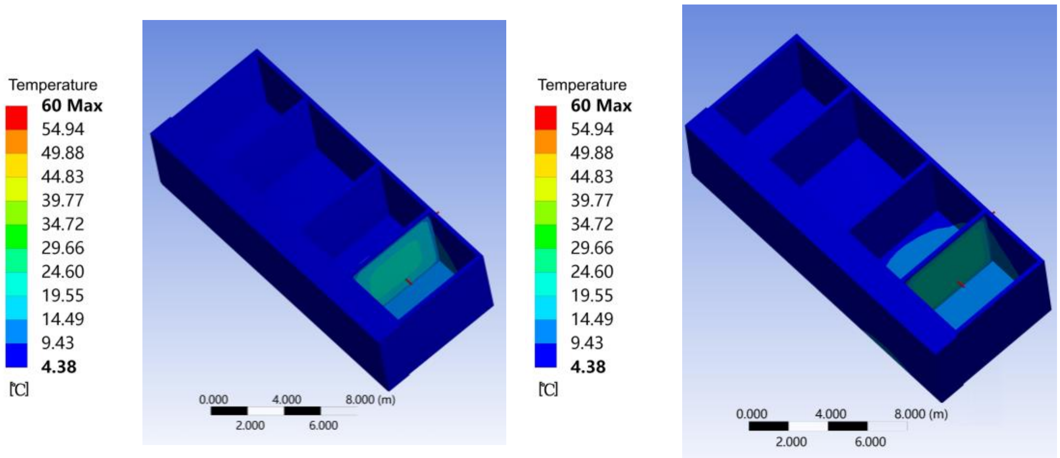

(e) 20 min and 10 s (f) 24 min and 20 s

Figure 6-9. (a) Wall heating in 4 min and 43 s; (b) Wall heating in 7 min and 45 s; (c) Wall heating in 11 min and 30 s; (d) Wall heating in 16 min and 10 s; (e) Wall heating in 20 min and 10 s; (f) Wall heating in 24 min and 20 s.

Through the investigation of the duration of cooking in winter, a single cooking event took 60 min, where the initial cooking heating wall time was 26 min and 25 s, and the remaining time was 34 min and 35 s. In order for a comparison to ordinary heating, the simulation started at 9:00 a.m., and the initial temperature was also 5 °C. Under the condition of solar radiation, the adjacent cooking heating wall room began to rise slowly at 9:10 a.m., from the initial temperature of 5 °C to 7.24 °C, and the temperature in the room with additional sunlight remained basically unchanged (Figure 6-10 a). At 9:20 a.m., the temperature of the adjacent cooking heating wall room rose to 9.16 °C, and the temperature in other rooms began to rise slowly (Figure 6-10 b). At 9:30 a.m., the temperature of the adjoining cooking heating wall room rose to 11.07 °C, and the temperature in the other rooms was 8.2 °C (Figure 6-10 c). At 9:34 a.m., the temperature of the adjacent cooking heating wall room rose to 13.56 °C, while the temperature in other rooms was 9.12 °C, and the temperature in the additional sunlight room began to slowly rise to 6.23 °C (Figure 6-10 d). When the cooking system stopped, the room temperature remained unchanged within 30 min; meanwhile, the temperature of the additional sunlight room started to rise slowly. At 10:10 a.m., the temperature in the additional sunlight room was 7.55 °C, and the temperature in the other rooms dropped to 6.14 °C (Figure 6-10 e). At 10:30 a.m., the temperature in the additional sunlight room was 8.16 °C, and the temperature in the other rooms began to slowly rise to 6.32 °C (Figure 6-10 f). At 10:50 a.m., the temperature in the additional sunlight room was 10.39 °C, and the temperature in the other rooms began to slowly rise to 6.42 °C (Figure 6-10 g). At 11:20 a.m., the temperature in the room with additional sunlight reached a stable value of 13.99 °C, and the temperature in the other rooms began to rise slowly to 6.53 °C (Figure 6-10 h). At this time, the heat transfer of additional sunlight through the wall heated the indoor temperature. At 11:36 a.m., the average indoor temperature was 7.55 °C (Figure 6-10 i). At 2:16 p.m., the indoor temperature rose to the highest value of 9.16 °C (Figure 6-10 j). With the increasing time, the temperature between the additional rays began to drop. At 6:00 p.m., the temperature in the additional sunlight room was 10.55 °C, and the temperature indoor was 8.73 °C (Figure 6-10 k). At 6:24 p.m., the temperature in the additional sunlight room was 9.43 °C, and the indoor temperature changed little (Figure 6-10 l). At 6:45 p.m., the temperature in the additional sunlight room was 7.88 °C, and the indoor temperature dropped to 6.73 °C (Figure 6-10 m). At 7:00 p.m., the temperature in the additional sunlight room was 6.93 °C, and the indoor temperature dropped to 6.53 °C (Figure 6-10 n). At this time, there was a difference of 2.53 °C from the outdoor temperature.

New system (with WSR)

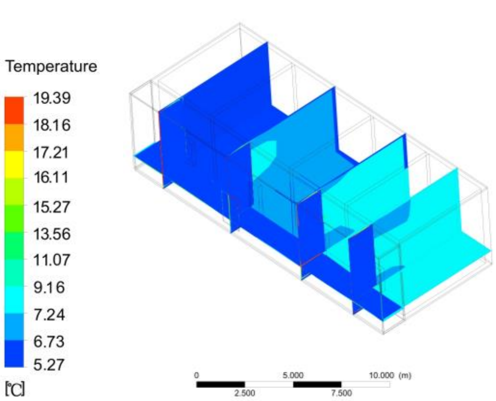

(a) 9:10 a.m.

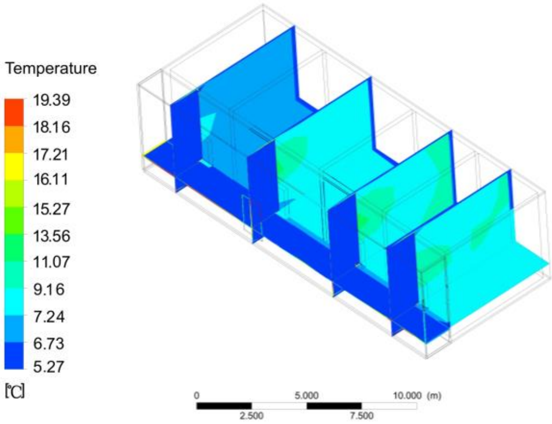

(b) 9:20 a.m.

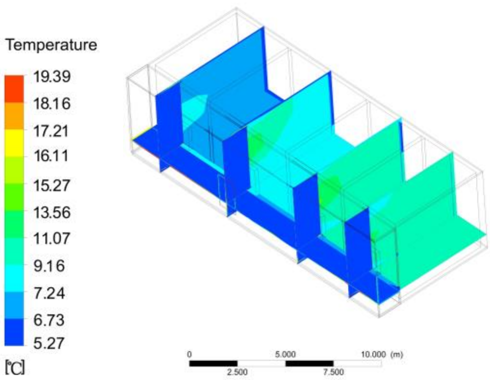

(c) 9:30 a.m.

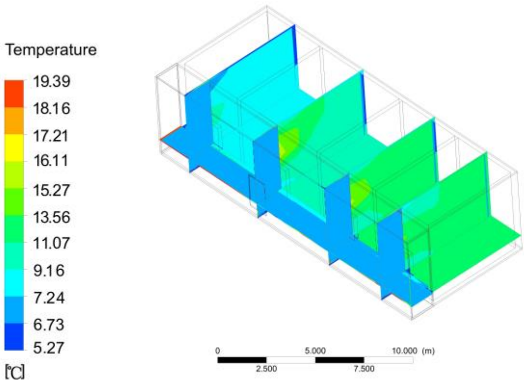

(d) 9:34 a.m.

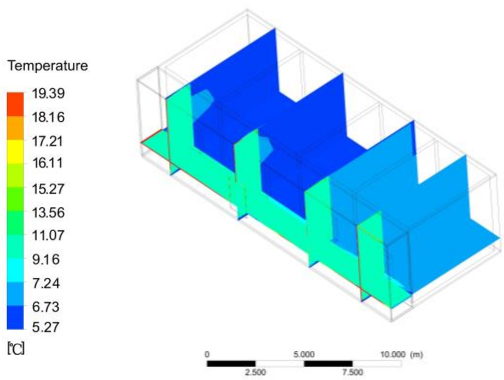

(e) 10:10 a.m.

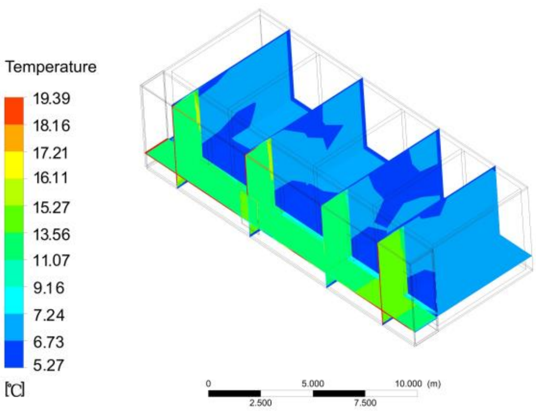

(f) 10:30 a.m.

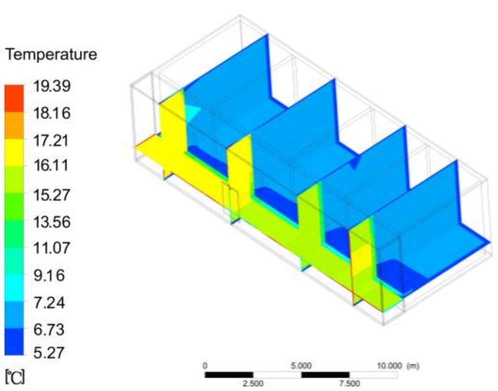

(g) 10:50 a.m.

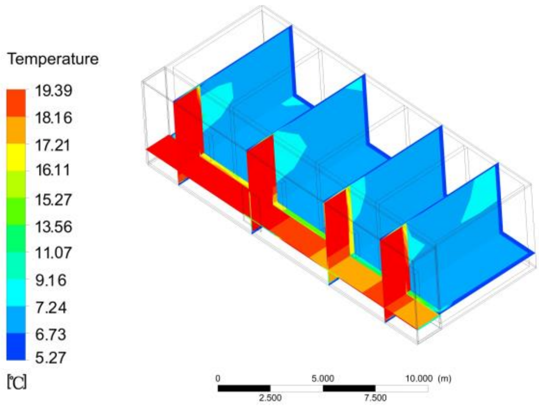

(h) 11:20 a.m.

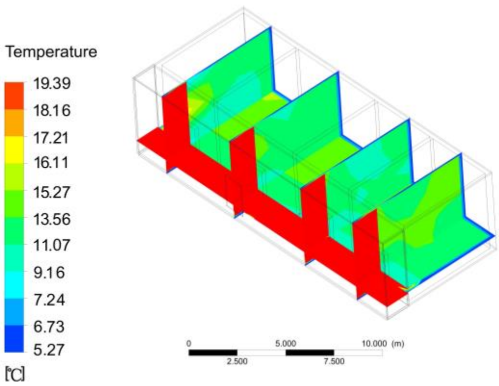

(i) 11:36 a.m.

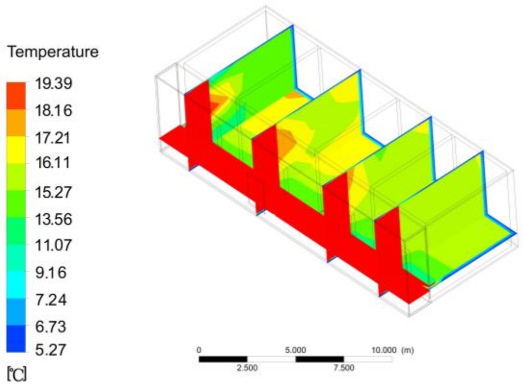

(j) 2:16 p.m.

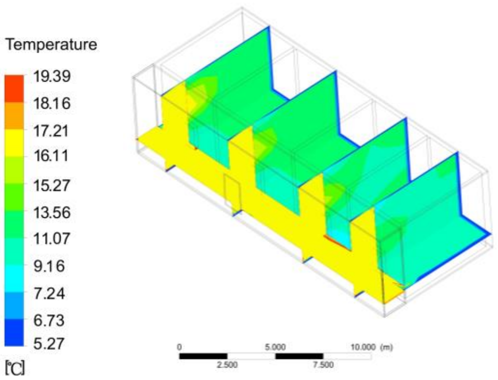

(k) 6:00 p.m.

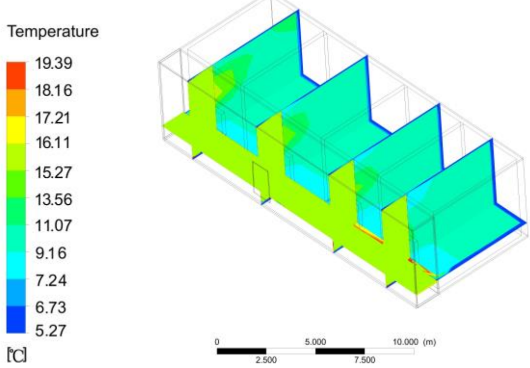

(l) 6:24 p.m.

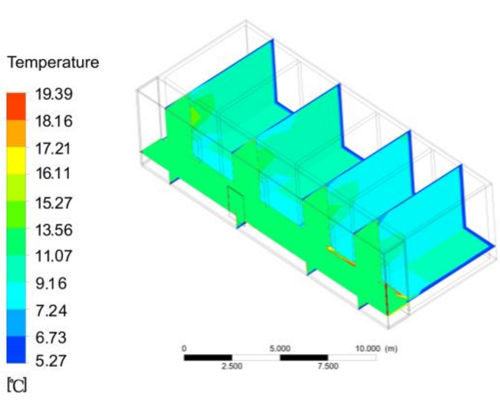

(m) 6:45 p.m.

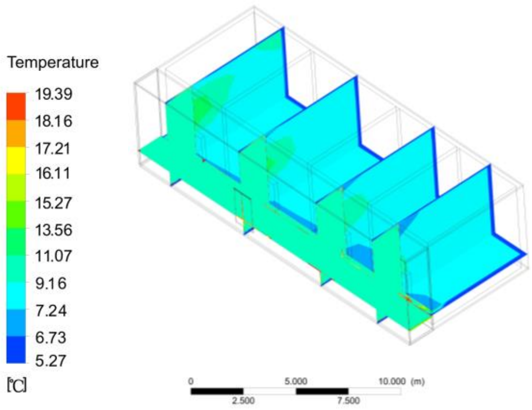

(n) 7:00 p.m.

Figure 6-10. (a) At 9:10 a.m. the temperature of the new system (with WSR); (b) At 9:20 a.m. the temperature of the new system (with WSR); (c) At 9:30 a.m. the temperature of the new system (with WSR); (d) At 9:34 a.m. the temperature of the new system (with WSR); (e) At 10:10 a.m. the temperature of the new system (with WSR); (f) At 10:30 a.m. the temperature of the new system (with WSR); (g) At 10:50 a.m. the temperature of the new system (with WSR); (h) At 11:20 a.m. the temperature of the new system (with WSR); (i) At 11:36 a.m. the temperature of the new system (with WSR); (j)At 2:16 p.m. the temperature of the new system (with WSR); (k) At 6:00 p.m. the temperature of the new system (with WSR); (l) At 6:24 p.m. the temperature of the new system (with WSR); (m) At 6:45 p.m. the temperature of the new system (with WSR); (n) At 7:00 p.m. the temperature of the new system (with WSR).

6.2.3 Comparison and Analysis

Due to the heating system between cooking and additional sunlight, the heating time is intermittent. First, the cooking heating wall system was 26 min and 25 s in the early stage, and the remaining time was 34 min and 35 s. At this time, the temperature of the additional sunlight room remained basically unchanged. The indoor temperature basically stayed the same within 30 min after the cessation of cooking activities. The temperature of the adjacent cooking heating wall room was 13.56 °C, and the other rooms were kept at 9.12 °C. The average indoor temperature was 11.34 °C, and the temperature increased by 6.34 °C. With the increase in temperature in the additional sunlight room, after 4 h and 16 s, the indoor temperature was 9.16 °C, with a 4.76 °C difference to the outdoor temperature, and the temperature increased by 4.16 °C. In winter, relying on ordinary heating alone is not enough to meet the thermal comfort requirements of the human body, mainly because the heating time is long and the temperature change is not obvious.

For ordinary heating, the heating time is 6.5 h, the temperature after equilibrium is 6.5 °C, which is 1.9 °C different to the outdoor temperature, and the heating efficiency is 0.23 °C/h. Ordinary heating is mainly affected by solar radiation, so there are requirements for weather conditions. This heating method has no obvious effect on increasing the indoor temperature.

6.3 Natural Heating, Cooking Heating Wall and Additional Sunlight Room System without Solar Radiation on the Wall

In order to verify the effectiveness of the cooking heating wall and the additional sunlight room system, ordinary heating was used as a benchmark for comparison to the new system. Ordinary heating refers to keeping the body of the residential house unchanged, and only relying on solar energy to heat the interior. The new system is the cooking heating wall system with an additional sunlight room mentioned in a previous article [62], which refers to the renovation of residential buildings, adding cooking heating walls and additional sunlight rooms. Heating the interior using the heat generated by the cooking heating wall from cooking while relying on absorption of additional sunlight and storing and converting solar energy, so as to heat the interior more effectively.

In order to make the test and experiment results accurate, the room and windows were kept closed during the test and experiment, forming a relatively closed space indoors. At the same time, during the simulation process, the room was set up as an independent closed fluid space, thereby reducing the influence of outside temperature on the room.

6.3.1 Natural Heating without Solar Radiation on the Wall

A. System Introduction

In the process of basic heating, the indoor temperature changes significantly, and the indoor temperature differs from the outdoor temperature. Moreover, the change in indoor temperature should also be considered when there is no wall solar radiation (WSR). The indoor thermal disturbance is the main source of indoor temperature change. The heat disturbance mainly includes personnel activities, household appliances, room size, window size, and other such factors. For making the simulation results more compatible with the actual situation and therefore usable, does not have the ordinary heating of WSR, and the indoor temperature changes in a small range, which is different from the outdoor temperature.

B. System Simulation

In addition to the presence of WSR, the absence of WSR should also be considered. The simulation time, method, and initial indoor temperature are consistent with the previous situation with solar radiation. According to the software simulation, the indoor temperature changed slowly. From 9:00 a.m. to 12:00 p.m. (noon), the indoor and the outdoor temperatures basically remained unchanged, and the average indoor temperature dropped from the initial 5 ℃ to 4.5 ℃ (Figure 6-11 a,b). At 3:30 p.m., the indoor temperature began to rise slowly, and the average indoor temperature was 5.5 ℃ (Figure 6-11 c). With the time increasing from 4:00 to 7:00 p.m. in the evening, the indoor temperature began to drop. The average indoor temperature reached a minimum of 4.6 ℃ at 7:00 p.m., a difference of 0.1 ℃ compared to outdoors (Figure 6-11 d). The results showed that if ordinary heating has no radiation, the indoor and outdoor temperatures are similar.

The temperature change of the ordinary system without WSR

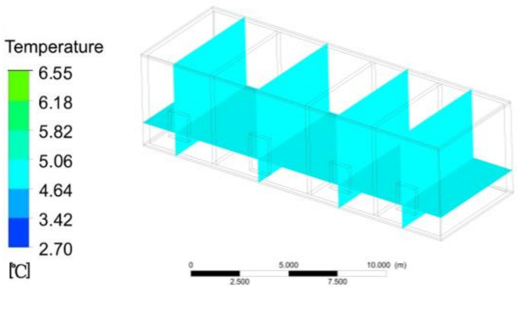

(a) 9:00 a.m.

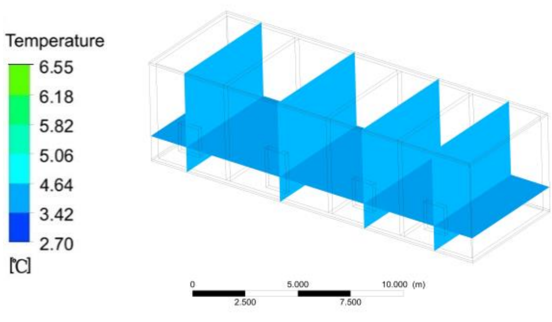

(b) 12:00-noon.

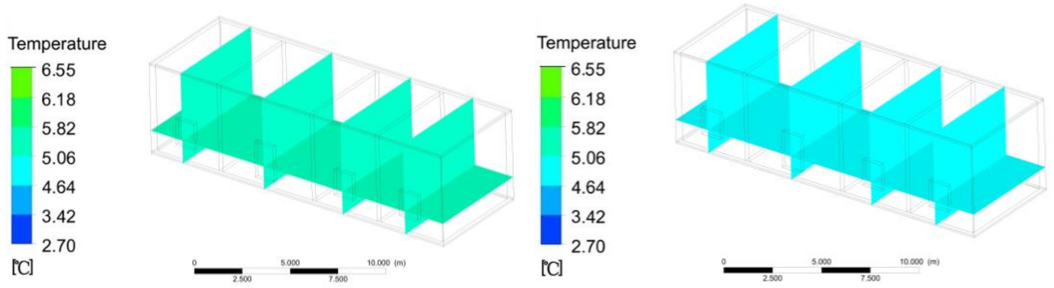

(c) 3:30 p.m. (d) 7:00 p.m.

Figure 6-11. (a) At 9:00 a.m. the temperature of the ordinary heating (without WSR); (b) At 12:00-noon the temperature of the ordinary heating (without WSR); (c) At 3:30 p.m. the temperature of the ordinary heating (without WSR); (d) At 7:00 p.m. the temperature of the ordinary heating (without WSR).

6.3.2 Cooking Heating Wall and Additional Sunlight Room System without Solar Radiation

A. System Introduction

In addition to considering the presence of WSR, the absence of WSR is also considered. In the absence of WSR, the temperature between the wall and the additional sunlight room rises slowly. When the temperature in the sunlight room reaches a relatively constant value, the indoor temperature starts to rise slowly. In the absence of solar radiation, compared to a separate cooking heating wall system, the cooking heating wall and additional sunlight room combination is more effective in raising the indoor temperature. In the absence of solar radiation, a cooking heating wall combined with additional sunlight is more effective at raising the indoor temperature than a cooking heating wall system alone.

B. System Simulation

The simulation of the new system also started at 9:00 a.m., and the initial indoor temperature was also 5 ℃. At 9:10 a.m., the temperature of the adjacent cooking heating wall room began to rise slowly, from the initial temperature of 5 ℃ to 5.52 ℃ (Figure 6-12 a). Meanwhile, the temperature of the additional sunlight room remained basically unchanged. At 9:20 a.m., the temperature of the adjoining cooking heating wall room rose to 6.03 ℃, and the temperature in other rooms began to rise slowly (Figure 6-12 b). At 9:30 a.m., the temperature of the adjacent cooking heating wall room rose to 6.53 ℃, and the temperature in the other rooms was 5.84 ℃ (Figure 6-12 c). At 9:34 a.m., the temperature of the adjacent cooking heating wall room rose to 8.79 ℃, the temperature in other rooms was 7.41 ℃, and the temperature in the room with additional sunlight remained basically unchanged (Figure 6-12 d). When the cooking system stopped, the room temperature within remains unchanged15 min, and the temperature of the additional sunlight room started to rise slowly at this time. At 9:45 a.m., the temperature in the additional sunlight room was 5.44 ℃, and the temperature in the other rooms dropped to 6.64 ℃ (Figure 6-12 e). At 9:55 a.m., the temperature of the additional sunlight room was 5.45 ℃, and that of other rooms is 6.32 ℃ (Figure 6-12 f). At 10:10 a.m., the temperature in the additional sunlight room remained basically unchanged, and the temperature in the other rooms was 5.57 ℃ (Figure 6-12 g). At 10:20 a.m., the temperature in the additional sunlight room reached a stable value of 5.45 ℃, and the temperature in the other rooms was 5.43 ℃ (Figure 6-12 h). This is mainly because the temperature in the additional sunlight room mainly depends on solar radiation. When there is no solar radiation, the indoor temperature range is small. At 6:00 p.m., the temperature in the additional sunlight room began to drop to 5.11 ℃, and the indoor temperature was 5.23 ℃ (Figure 6-12 i). At 6:24 p.m., the temperature in the additional sunlight room was 4.98 ℃, and the indoor temperature was 5.11 ℃

(Figure 6-12 j). At 6:45 p.m., the temperature in the additional sunlight room was 4.73 ℃, and the indoor temperature dropped to 4.86 ℃ (Figure 6-12 k). At 7:00 p.m., the temperature of the additional sunlight room and indoor remained basically unchanged (Figure 6-12 l). At this moment, there was a difference of 0.86 ℃ to the outdoor temperature.

New system (without WSR)

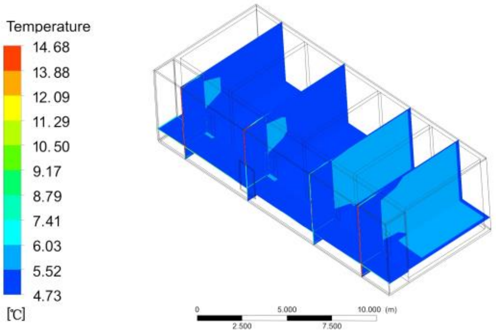

(a) 9:10 a.m.

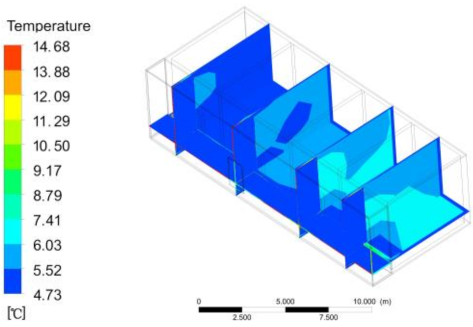

(b) 9:20 a.m.

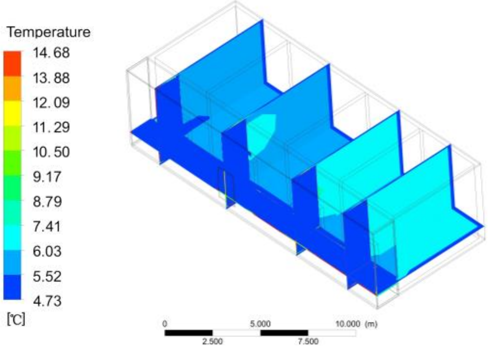

(c) 9:30 a.m.

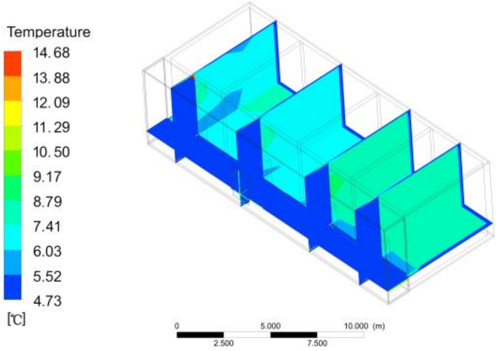

(d) 9:34 a.m.

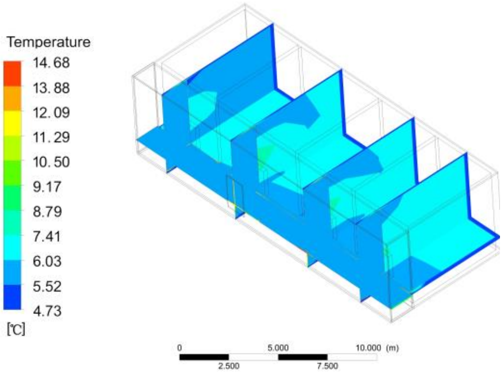

(e) 9:45 a.m.

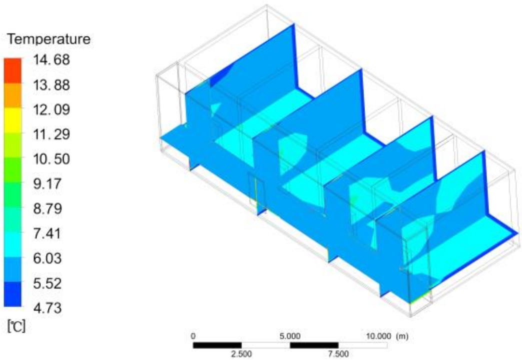

(f) 9:55 a.m.

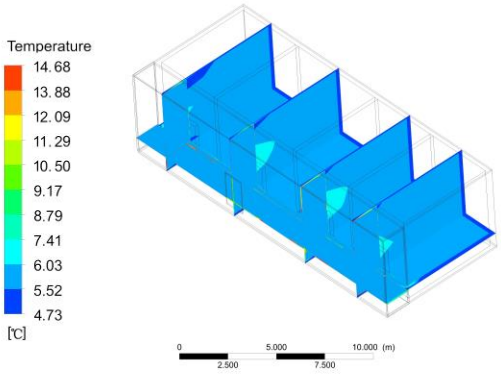

(g) 10:10 a.m.

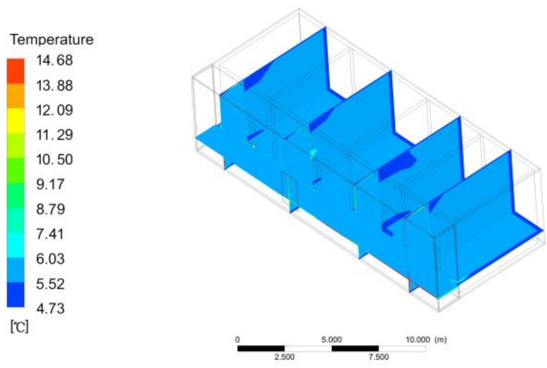

(h) 10:20 a.m.

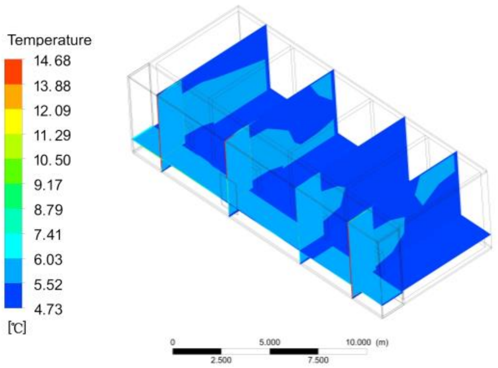

(i) 6:00 p.m.

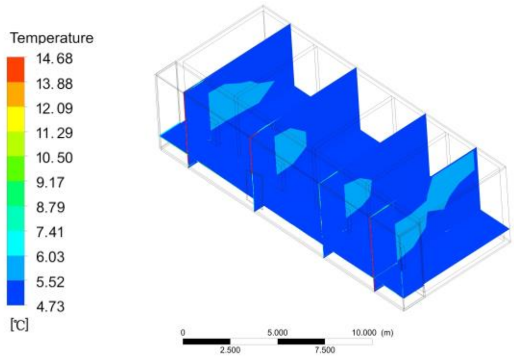

(j) 6:24 p.m.

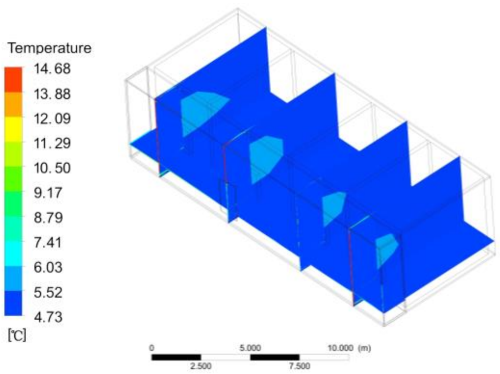

(k) 6:45 p.m.

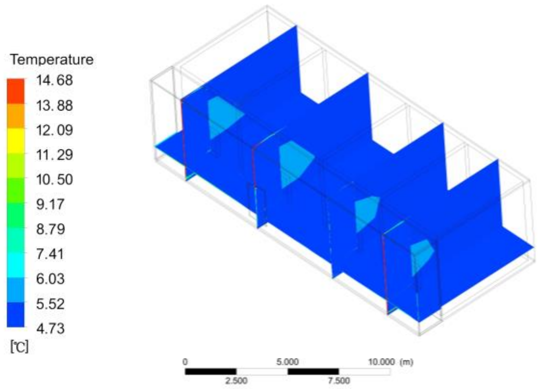

(l) 7:00 p.m.

Figure 6-12. (a) At 9:10 a.m. the temperature of the new system (without WSR); (b) At 9:20 a.m. the temperature of the new system (without WSR); (c) At 9:30 a.m. the temperature of the new system (without WSR); (d) At 9:34 a.m. the temperature of the new system (without WSR); (e) At 9:45 a.m. the temperature of the new system (without WSR); (f) At 9:55 a.m. the temperature of the new system (without WSR); (g) At 10:10 a.m. the temperature of the new system (without WSR); (h) At 10:20 a.m. the temperature of the new system (without WSR); (i) At 6:00 p.m. the temperature of the new system (without WSR); (j)At 6:24 p.m. the temperature of the new system (without WSR); (k) At 6:45 p.m. the temperature of the new system (without WSR); (l) At 7:00 p.m. the temperature of the new system (without WSR).

6.3.3 Comparison and Analysis

In the absence of WSR, the indoor temperature remained basically unchanged within 15 min after the cessation of cooking activities. The temperature on both sides of the cooking heating wall was 8.79 °C, the temperature in other rooms was 7.41 °C, and the mean indoor temperature was 7.95 °C, increasing by 2.55 °C. With the increase in temperature in the additional sunlight room, the indoor temperature was 5.43 °C after 1 h and 20 min, which was 1.43 °C different to that outdoors—an increase of 0.43 °C. Ordinary heating systems mainly rely on WSR. Yet, when cooking and additional sunroom systems are used, the heating time is greatly increased. Without considering the WSR, the mean heating efficiency between cooking and additional sunlight was 2.87 °C/h. Considering WSR, the mean heating efficiency between the cooking heat and additional sunlight was 4.09 °C/h.

In the case of ordinary heating without WSR, the heating time is 7.3 h, the temperature after equilibrium is 5.5 °C, which is 0.5 °C different to the outdoor temperature, and the heating efficiency is 0.06 °C/h. If ordinary heating has no radiation, the indoor and outdoor temperatures are similar.

6.4 Thermal Comfort Time and Thermal Load Reduction of the System

6.4.1 Thermal Comfort Time

The presence or absence of WSR between the cooking heating wall and the additional sunlight room affects the temperature of the room after heating, the extension of heating time, the efficiency of heating, and the reduced heat load. For this system, the time required for heating using the cooking heating wall system with an additional sunlight room, the change in indoor temperature, and the decreased heat load value were estimated for the system in the presence or absence of solar radiation throughout the year.

The suitable times of the year for using the system are mainly distributed in January, February, March, November, and December. In the presence of WSR, the annual cooking heating wall and additional sunlight room system were used for 1155 h, accounting for 13.11% of the total time of the year (Figure 6-13 a). In the absence of WSR, the cooking heating wall system with an additional sunlight room was used throughout the year for 882 h, accounting for 10.01% of the total time of the year (Figure 6-13 b).

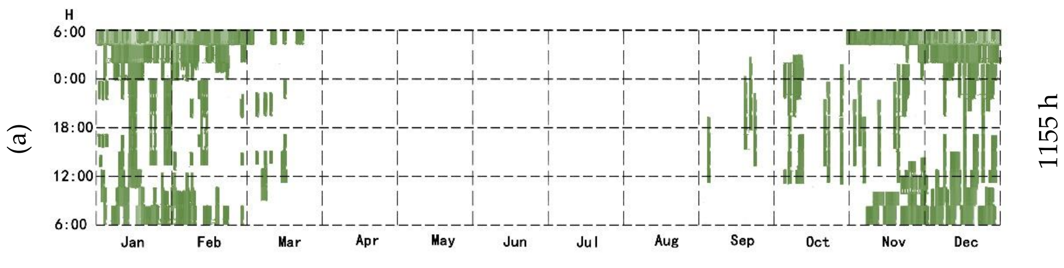

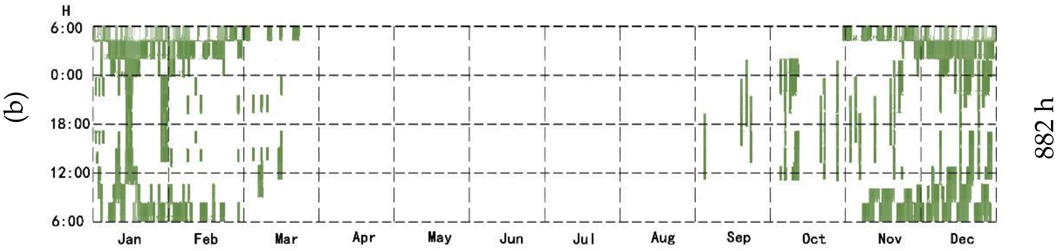

Figure 6-13. (a) Heated cooking wall–Sunlight system (with WSR); (b) Heated cooking wall–Sunlight system (without WSR).

6.4.2 Adopting the Standard Time of Thermal Comfort of the Heated Cooking Wall–Sunlight System

Software simulation was used to calculate the thermal comfort range of residential houses. The indoor thermal comfort was significantly improved under the action of the new system. In this study, the three cases of ordinary heating and the new system with or without WSR were compared and analyzed, and the time for each room to be below 18 °C was calculated. Taking 18 °C as the standard value of the building's winter thermal comfort, the proportion of time when the temperature was lower than 18 °C throughout the year was calculated. In the case of ordinary heating, the annual temperature below 18 °C was 4532 h, accounting for 51.45% of the total annual time (Figure 6-14 a). In the presence of WSR, when the cooking heating wall system with an additional sunlight room was used, the time when the temperature was lower than 18 °C was 3733 h, which is a decrease of 799 h, meaning a reduction rate of 17.63%, accounting for 38.34% of the total time of the year (Figure 6-14 b). In the absence of WSR, the annual time below 18 °C was 4006 h, which is a decrease of 526 h, meaning a reduction rate of 11.60%, accounting for 41.43% of the total annual time (Figure 6-15 c). In addition, the time each room was below 18 °C was also calculated. Due to the different location of the room, the indoor time below 18 °C was also different. The indoor time below 18 °C in rooms 1 and 2 was significantly reduced by adopting the new system compared to the ordinary heating system. The time below 18 °C in rooms 3 and 4 was also reduced by adopting the new system compared to the ordinary heating system, and the reduction was lower than that in rooms 1 and 2 (Figure 6-15 d).

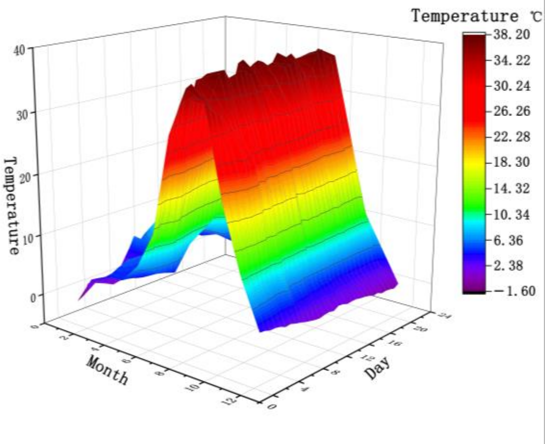

(a)

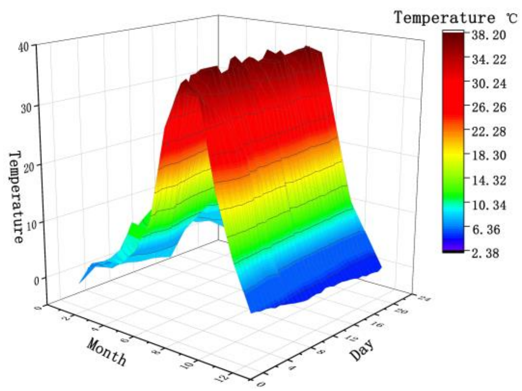

(b)

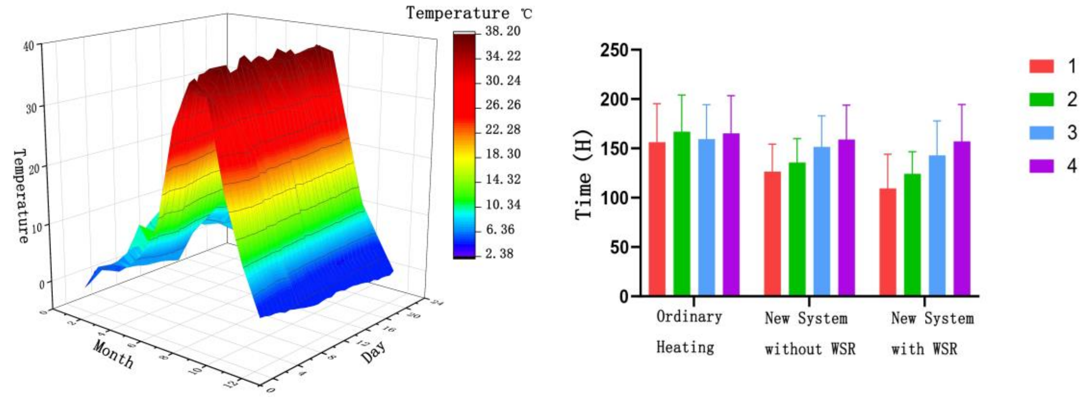

(c) (d)

Figure 6-14. (a) Thermal comfort time under ordinary heating; (b) Thermal comfort time under the new system (with WSR); (c) Thermal comfort time under the new system (without WSR); (d) Thermal comfort time of the rooms.

6.4.3 Heat Load Reduction of the Heated Cooking Wall–Sunlight System

The annual heat load of the cooking heating wall system with the additional sunlight room was simulated and calculated by Energyplus software. When there was WSR, the annual heat load reduction of the building was 1436.731 kW· h (Figure 6-15 a), a decrease rate of 20.21%. When there was no WSR, the annual heat load reduction of the building was 735.919 kW· h, a decrease rate of 8.56%. The thermal load difference between the two was 840.812 kW· h (Figure 6-15 b).

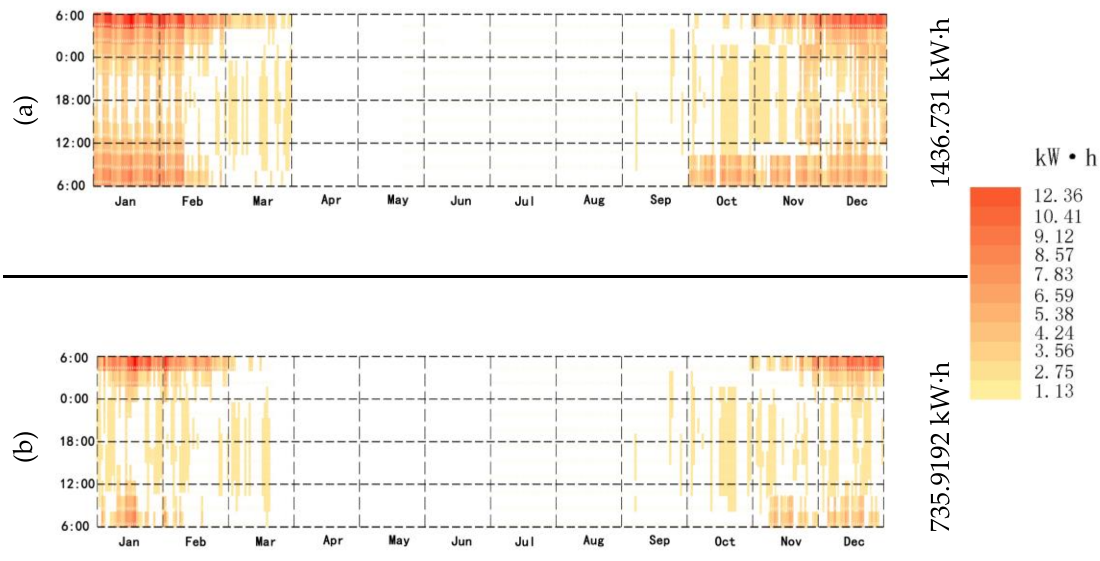

Figure 6-15. (a) Heated Cooking Wall–Sunlight system (with WSR); (b) Heated Cooking Wall–Sunlight system (without WSR).

6.5 Chapter Summary

This chapter mainly elaborates the additional solar system based on the cooking heating wall. The first part is a detailed introduction to the cooking heating wall-additional sunshine room system of the traditional houses in southern Shaanxi. The content of the introduction includes the definition and model establishment of the cooking heating wall-additional sunlight room, the design of the cooking heating wall-additional sunlight room, the working principle and the simulation process of the software. Secondly, the heating situation of natural heating and the cooking heating wall-additional sunlight room system is compared and analyzed through software simulation, and it is concluded that the cooking heating wall-additional sunlight room system can effectively improve the indoor temperature. In addition, it also summarizes the adaptation time of the cooking heating wall-additional sunlight room system throughout the year and the reduced heat load, which provides new ideas for the passive heating design of rural houses in the future.

Reference

[1] Sha, C.; He, W.; Yan, H. Yang, L. Cong, S. Influences of vernacular building spaces on human thermal comfort in China's arid climate areas. Energy and Buildings. 2021, 244, 110978.

[2] Yu, H.; Niu, J. Chung, T. Comprehensive analysis on thermal and daylighting performance of glazing and shading designs on office building envelope in cooling-dominant climates. Applied Energy. 2014, 134, 215-228.

[3] Ashrafian, T. Moazzen, N. The impact of glazing ratio and window configuration on occupants' comfort and energy demand: The case study of a school building in Eskisehir, Turkey. Sustainable Cities and Society. 2019, 47, 101483.

[4] Liu, J.; Wang, L.; Yasuko, Y.; Liu, Y. The thermal mechanism of warm in winter and cool in summer in China traditional vernacular houses. Building and Environment. 2011, 46, 1709-1715.

[5] Ma, L. Shao, N. Zhang, J. Zhao, T. The Influence of Doors and Windows on the Indoor Temperature in Rural House. Procedia Engineering. 2015, 121, 621-627.

[6] Yi, L.; Zhou, P.; Ni, P.; Peng, X.; Ye, J. Degradation of rammed earth under soluble salts attack and drying-wetting cycles: The case of Fujian Tulou, China. Applied Clay Science. 2021, 212, 106202.

[7] Zhou, Z.; Wang, C.; Sun, X.; Gao, F.; Wei, F.; George, Z. Heating energy saving potential from building envelope design and operation optimization in residential buildings: A case study in northern China. Journal of Cleaner Production. 2018, 174, 413-423.

[8] Hou, X.; Cheng, B. Yang, J. A quantitative study on the exterior wall texture of stone-built houses in traditional villages in China: A case study of the xisuo village in the Jiarong Tibetan area. Journal of Building Engineering. 2021, 42, 102357.

[9] Yi, L.; Zhou, P. Ni, P.; Peng, X. Ye, J. Degradation of rammed earth under soluble salts attack and drying-wetting cycles: The case of Fujian Tulou, China. Applied Clay Science. 2021, 212, 106202.

[10] Lugt, A.A.J.F.; Dobbelsteen, J.J.A. An environmental, economic and practical assessment of bamboo as a building material for supporting structures. Construction and Building Materials. 2006, 20, 648-656.

[11] Dong, J. Lin, M. Zuo, J. Lin, T. Liu, J. Sun, C. Luo, J. Quantitative study on the cooling effect of green roofs in a high-density urban Area—A case study of Xiamen, China. Journal of Cleaner Production. 2020, 255, 120152.

[12] Ge, J.; Lu, J.; Wu, J.; Luo, X.; Shen, F. Suitable and energy-saving retrofit technology research in traditional wooden houses in Jiangnan, South China. Journal of Building Engineering. 2021, 103550.

[13] Lai, D. Jia, S. Qi, Y. Liu, J. Window-opening behavior in Chinese residential buildings across different climate zones. Building and Environment. 2018, 142, 234-243.

[14] Marwan, M. The effect of wall material on energy cost reduction in building. Case Studies in Thermal Engineering. 2020, 17, 100573.

[15] Steven, G.; Richard, G. Sustainable earth walls to meet the building regulations. Energy and Buildings. 2005, 37, 451-459.

[16] Jiang, B.; Wu, T. Xia, W.; Liang, J. Hygrothermal performance of rammed earth wall in Tibetan Autonomous Prefecture in Sichuan Province of China. Building and Environment. 2020, 181, 107128.

[17] Xiang, D.; Veronica, S.; Michael, Griffith, Achieving thermal comfort in naturally ventilated rammed earth houses, Building and Environment, 82, 2014, Pages 588-598.

[18] Layth, S.; Al-Rukaibawi, Z.S.; György, K. Numerical simulation of the effect of bamboo composite building envelope on summer overheating problem. Case Studies in Thermal Engineering. 2021, 28, 101516.

[19] Eduardo, W.; Michael, R. The impact of policy instruments on the first generation of Tall Wood Buildings. Building Research & Information 0:0. 2021, 1-21.

[20] Bai, Y.; Gao, J.; Pitts, A.; Gao, Y.; Bai, W.; Tao, Z. Improving the Sustainability of Traditional Dwellings in Yunnan, China: Seismic Resistance Testing of Wood-frame and Earth-Built Wall Dwellings. Sustainability. 2019, 11, 977.

[21] Asif, M. 2 - Sustainability of timber, wood and bamboo in construction, Editor(s): Jamal M. Khatib, In Woodhead Publishing Series in Civil and Structural Engineering, Sustainability of Construction Materials, Woodhead Publishing. 2009, 31-54.

[22] Michael, H.; Ramage, H.B.; Marta, B.W.; George, F.; Thomas, R.; Darshil, U.; Shah, G.; Wu, L.; Yu, P.F.; Danielle. D.T.; Julian, A.; Paul, D.; Linden, P.F.; Scherman, O. The wood from the trees: The use of timber in construction. Renewable and Sustainable Energy Reviews. 2017, 68, 333-359.

[23] Li, Q. You, R. Chen, C.; Yang, X. A field investigation and comparative study of indoor environmental quality in heritage Chinese rural buildings with thick rammed earth wall. Energy and Buildings. 2013, 62, 286-293.

[24] Amada, S. Untao, S. Fracture properties of bamboo. Composites Part B: Engineering. 2001, 32, 451-459.

[25] Yu, D. Tan, H. Ruan, Y. A future bamboo-structure residential building prototype in China: Life cycle assessment of energy use and carbon emission. Energy and Buildings. 2011, 43, 2638-2646.

[26] Bhavna, S.; Ana, G.; Maximilian, B.; Michael, R. Engineered bamboo for structural applications. Construction and Building Materials. 2015, 81, 66-73.

[27] Li, Y.; Yao, J.; Li, R. Zhang, Z.; Zhang, J. Thermal and energy performance of a steel-bamboo composite wall structure. Energy and Buildings. 2017, 156, 225-237.

Chapter 7. Optimization of Passive Heating System of Cooking Heating Wall and Additional Sunlight Room

This chapter mainly introduces the optimization of the system between the cooking heating wall and additional sunlight. The first five chapters are based on the basic theory of the study and the establishment of the initial model and parameter setting, using the simulation software EnergyPlus to simulate the traditional residential houses in southern Shaanxi.

Has nothing to do in order to rule out a variety of factors, this section of the simulation will be a single change between cooking heating wall and additional examples of simulation data, other parameters remain the same, using the "typical day" method to simulate the sun room and master bedroom at room temperature and the basis of the annual heating load index, through the analysis of the simulated data both the indoor temperature change, the impact on the building annual energy consumption, etc.

7.1. Influencing Factors of the System between the Cooking Heating Wall and Additional Sunlight

7.1.1 Different Glass Window Materials

The improvement of outer envelope structure of residential buildings includes the improvement of exterior window performance. Different glass window materials have an important impact on building energy conservation. In 1982, Rubin studied the calculation model of glass heat transfer and the calculation model of glass solar optical performance, developed the calculation program and developed a variety of related calculation software. A database of optical properties of glass, NFRC_300, has been established, including DOE-2 and EnergyPlus for energy simulation of the entire building, window for thermal performance simulation of exterior windows and optics for optical performance simulation of window glass [1]. The development of these software and the establishment of database have important significance for users to choose energy-saving windows and glass, manufacturers to develop new energy-saving windows and glass products, architectural design engineers and scientific research workers [2]. In 2001, Baird studied the calculation of heat transfer and solar optical properties of ordinary glass, which has been widely recognized. However, scholars around the world have not reached a consensus on the theoretical calculation of coated single-layer glass, and further exploration is still under way. With the support of ASHRAE research project, Klems et al., [3] Lawrence Berkeley National Laboratory, USA, theoretically derived the detailed calculation formula of solar radiation heat gain coefficient (SHGC) of inner and outer shading, and tested the bidirectional optical performance of complex shading system. Wright et al. derived a theoretical calculation formula for solar radiation heat gain coefficient of sunshade facilities between glasses in 1997 [4]. In 2007, Dutch scholar R.Bokel studied the influence of exterior windows on building energy conservation, and established the functional relationship between the location, size and shape of exterior windows and the building's annual cooling and heating energy consumption [5].

In 2002, China promulgated the standards for the classification and detection methods of thermal insulation performance, daylighting performance, air tightness and water tightness of building exterior windows, and revised them in 2008. The Institute of standards and quotas of the Ministry of construction has systematically studied the energy-saving classification and certification identification system of doors and windows, and achieved many research results [6]. Dong of Chongqing University made a detailed study of the heat gain of Windows in hot areas, the thermal performance of windows and the shading of windows, and came up with a simplified calculation method for the heat gain of windows [7,8]. In 2003, Zhang Wen of Zhejiang University used DOE-2 software to simulate the energy consumption of exterior Windows of residential buildings in Hangzhou, obtained the key points of energy saving design of exterior Windows, and summarized the influencing factors [9]. Bu from Shenzhen

Building Research Institute and Yang from Tsinghua University have simulated and analyzed the influence of heat transfer coefficient and shading coefficient of low-E glass on air conditioning load and energy consumption under different climate conditions [10,11]. Xie et al. [12] from Tianjin University analyzed the energy-saving effect of shading in residential buildings in different regions. Jian et al. [13] from Beijing University of Technology used DeST software to analyze the influence rules of window-wall ratio parameters on annual heating energy consumption, annual air conditioning energy consumption and annual total energy consumption of buildings under different orientations. Fang of Hunan University used equest, an energy-simulation software, to study the performance of exterior windows, window orientation, window-wall ratio and building orientation of residential buildings in Beijing, Changsha and Shenzhen [14]. Wang of Tianjin University has studied the energy-saving design of window frames, glass, ventilation and air tightness in residential buildings in cold northern regions, and has made in-depth research on the relationship between external Windows and solar radiation [15].

7.1.2 Different Depths

In 1989, Faist et al. from Switzerland put forward a complete design system according to different architectural themes, including data input related to energy saving, such as building structure design, electrical equipment and cost estimation [16]. Hanna in Poland in 2001, such as people in order to promote the energy conservation level of private houses and apartments, through optimizing the structure of the envelope, building plane shape and achieve the goal of building energy efficiency building heating system, which uses the mathematical analysis method to study the rectangle and trapezoid flat energy-saving design contrast, architectural plane size with the influence of the energy conservation equation [17]. In 2002, G.A. Florides et al. used TRNSYS software to conduct comprehensive simulation analysis on ventilation, shading, various forms of exterior windows, orientation, shading and walls of a typical building, emphasizing the importance of building thermal insulation research. In the study of building orientation, it is pointed out that from the perspective of energy saving, the long side of cuboid building faces north and south is the most reasonable [18]. In 2006, Wang et al. [19] from Canada used the genetic algorithm to study the influence of building plane shape on building performance in green building design. By establishing a model, they discussed the great variability of building plane. The resulting impact on building performance is also varied. In 2010, Eddine et al. [20] in Italy adopted the method of variance analysis to study the contribution of various design variables to building energy conservation in the conceptual design stage of office buildings, so as to guide architects to better carry out building energy conservation design. Taking buildings in five typical Italian cities as examples, the author extracted six factors affecting energy saving, namely, shape coefficient, surface area fineness, solar radiation coefficient, external shading coefficient, building orientation and effective internal heat capacity. It is concluded that the influences of these factors on building heating and air conditioning energy consumption are significantly different, and the shape coefficient has the greatest influence on heating energy consumption, accounting for 0.54 to 0.69. The surface area coefficient has the greatest influence on building air conditioning energy consumption, accounting for more than 0.8, while the shading coefficient has the least influence, accounting for only 0.07.

In the 1980s, a famous architectural physicist in China, studied the relationship between the building plane, shape and orientation of residential and public buildings and energy saving, and found that the cylindrical building has the best energy saving effect from the perspective of reducing the exposed area of buildings. In addition, by analyzing the comparative relationship among building shape, height and shape coefficient, it is concluded that the most economical and practical slab house has 4-6 floors, 9m-13m depth and 25m-50m length. Finally, the relationship between building orientation and energy saving is analyzed, and it is concluded that the most favorable residential plane is north and south orientation [21]. In 1983, Feng and Xiang studied the relationship between building shape coefficient and building energy consumption and proposed that "building energy saving is not only related to the exposed area of the building, but also related to the thermal performance of the building envelope and various loads inside the building". By using the method of energy consumption calculation, the author obtained the cube with the ideal energy-saving building shape of 32V side length and 3V4 height (V is the building volume), and concluded that the ideal energy-saving building shape should not only have a small exposed area, but also reduce the area of the building envelope with poor thermal performance to a minimum. In addition, by changing the building shape parameters, the relationship between building energy consumption index and building volume is inversely proportional to the cube root, multi-storey building is beneficial to energy saving and so on [22].

In 1990, Cai et al. [23] from school of Architecture, Tsinghua University calculated and analyzed the heat transfer and heat consumption indexes of strip residential buildings commonly used in Beijing, Xi 'an and Harbin under different volumes, and obtained the curve of the relationship between the increase of residential building volume and the decrease of heat consumption per unit floor area. And draw the following conclusions:

The larger the volume of a single building is, the smaller the heat transfer and heat consumption per unit building area. With the increasing volume, the decreasing trend of heat consumption becomes smaller and smaller, and tends to be gentle after a certain stage.

If the number of floors of a single building is the same but the building depth is different, the greater the building depth is, the more significant the energy saving effect will be caused by the increase of the building volume.

For a single building with the same depth but different floors, the higher the number of floors, the more significant the energy saving effect will be caused by the increase of the volume.

Buildings of different volumes have the lowest energy consumption.

In 2000, Song and Zhang from Tongji University first studied the relationship between building shape coefficient and energy consumption from the perspective of building shape coefficient, and obtained four laws, including the law of simultaneous decline, the law of inverse height ratio, the square limit law and the L/A substitution law. Then, the relationship between different plane combinations and building energy saving is studied, and the relationship curves of building orientation, plane shape and building energy consumption are obtained. The relationship between building shape coefficient and building plane size, building height and building arrangement was studied, and the energy-saving design principles related to controlling building shape coefficient were put forward [24]. Through model experiments, the energy-saving effects of buildings with different plane shapes under wind, heat and other environmental conditions were analyzed, and conclusions were drawn:

Circular plane is best for energy saving, triangular plane is worst for energy saving.

The influence of solar radiation should be fully considered when analyzing the plane shape of buildings.

The influence of Angle coefficient should be fully considered and the Angle coefficient should be minimized in energy saving design.

Strictly controlling the exterior area of buildings is the key to energy saving control.

Improving environmental microclimate index is of great significance to control energy saving.

7.1.3 Window Wall Ratio

Window wall area ratio (hereinafter referred to as window wall ratio) refers to the ratio of window opening area to room facade unit area (i.e. the area surrounded by building floor height and bay positioning axis). The appendix of the code for thermal design of civil buildings (GB 50176) makes corresponding provisions on the window wall ratio applicable to residential buildings in most areas of China. For the north direction, the window wall ratio shall not exceed 0.25, the east-west direction shall not exceed 0.3, and the south direction shall not exceed 0.35. Of course, this is considered from the perspective of energy conservation. The large opening area makes the outdoor heat quickly enter the room through the window in summer, and the indoor heat will be lost to the outside in winter. If the opening area is too small, the lobby of traditional folk houses in southern Shaanxi will have large "cornices", which will affect the indoor daylighting, and the overall building proportion will be unbalanced, Thus affecting the overall beauty of the building. In fact, for the folk houses in southern Shaanxi, at this stage, most of them are "brick concrete structure". Limited by the structural form, the window area will also be affected. If the window area is too large, or the window on the most side of the facade is too close to the edge of the outer wall, the overall strength of the building will be affected. Based on the above analysis, combined with the higher requirements for indoor ventilation in summer in southern Shaanxi, the south window wall ratio of local houses will generally reach the upper limit of the specification requirements, i.e. 0.35 [25].

Taking the existing residential buildings in Qingdao as an example, Zhang uses grasshopper to establish the building model and ladybug + honeybee for visual processing. Based on the relationship between the value of heat transfer coefficient and solar heat gain coefficient and building energy consumption, he puts forward the strategy of selecting energy-saving external windows for existing residential buildings with different window wall ratio and different thermal performance envelope structures [26]. Cheng et al. [27] Took the translucent photovoltaic window as the research object and took the daylighting area ratio as a new measurement standard to quantify the daylighting quality. On this basis, they analyzed it in different directions and window wall ratio. The results show that this type of window is beneficial to improve the lighting quality and reduce the annual energy consumption of the office. In order to effectively reduce the air conditioning load caused by the energy loss of the external window, Zhang invented a new type of external window structure that can be ventilated and insulated. The structure is composed of three layers of glass and built-in louvers with automatic adjustment function, which has good sun shading effect. At the same time, the middle glass cavity layer can also participate in indoor air ventilation, ventilation and heat recovery. In this way, the temperature of the inner glass of the outer window is equal to the indoor temperature, so as to effectively reduce the energy consumption of the air conditioner and have a good energy-saving effect [28]. Lai et al. [29] Analyzed the optimal constant SHGC in several typical climatic regions of the United States and China, and compared the SHGC values according to their latitudes. Based on the grid shadow configuration of window, the energy-saving grid spacing is optimized. The results show that the optimal SHGC decreases gradually with the decrease of latitude, and the effect of shading device is more obvious. The window with the best SHGC can reduce the total construction load by up to 37.8% and 24.8% in some cities in the United States and some cities in China. For the same city and grid spacing, the difference from summer to winter is more than 6 times. The minimum geometric shadow coefficient (GSC) of mesh shadow increases with the decrease of latitude. Chen Sha studied the climate adaptability of Guangfu traditional residential buildings, analyzed the light and heat environment of different types of residential doors and windows in subtropical humid and hot climate, studied the climate adaptation modes and similarities and differences of different types of residential buildings, and put forward the climate adaptation strategies of residential doors and windows from four aspects: ventilation and daylighting, sun shading and heat insulation, moisture and rain protection and psychological comfort, Finally, it analyzes the layout, orientation, scale, form, material and structure of doors and windows of traditional folk houses in Guangfu area, and summarizes its climate adaptability [30].

7.1.4 Wall Materials

Because the energy consumption of heating and air conditioning accounts for a large proportion in the daily operation energy consumption of buildings and even the whole building energy consumption, the research on the thermal performance of peripheral protective structures has naturally become the focus of building energy conservation in many countries. Denmark revised the heat loss value of each part of the building stipulated in the code twice in 1977 and 1982, and made specific provisions on the materials and components of each part of the building in the code in 1982 [31]. In 1992, barozzi established a two-dimensional model to simulate the passive cooling effect of roof solar chimney, which was verified by experiments with a small model of 1:12 [32]. In the same year, kossecka and others began to study the influence of room structural characteristics on thermal performance, focusing on the energy consumption of medium and heavy wall structures, and analyzed the influencing factors of building energy consumption under different composite walls [33]. In 2000, bouchlaghem proposed to optimize the thermal performance of buildings through the design of building envelope, so as to achieve the best effect of energy conservation and comfort. The author puts forward what is the thermal design index to minimize the deviation of thermal comfort under given conditions [34]. In 2006, collet et al. [35] Concluded that the traditional wall has high thermal performance and should be used in modern buildings. In the same year, lollini and others studied the heat transfer value of the optimal insulation layer of each component of the envelope structure of newly-built residential buildings in Italy under the condition of winter heat load, focusing on the economic benefits of using materials with different thickness [36]. In 2008, Utama and gheewala studied the energy consumption composition of residential building envelope in Indonesia, and analyzed the relationship between different envelope component materials and energy consumption of air conditioning system [37].

China's research on building envelope energy conservation began in the 1980s, and has always been the focus of domestic production enterprises and scientific research institutions in building energy conservation research. In the 1990s, Chen of Chongqing University studied the heat and moisture transfer of building walls and compiled the basis of building thermophysics [38]. In 2000, Yu and Yang introduced the design technology of slope roof insulation layer in Shanghai, including construction method, selection of insulation materials and calculation and determination of insulation layer thickness, and put forward the minimum thickness of various insulation materials available [39]. In 2003, according to the climate characteristics of hot summer and cold winter areas, Sun focused on the auxiliary sun shading and heat insulation design of Xishan wall in residential architectural design, so as to reduce the impact of "western sun" [40]. In 2004, Xue and Jiang from Tsinghua University analyzed the energy consumption status and energy-saving potential of large public buildings in Beijing, and analyzed the building energy consumption status and energy-saving ways of residential and ordinary public buildings in Beijing [41,42]. In 2007, Xu of Tianjin University used CFD technology to analyze the composite wall solar wall and double-layer ventilation glass curtain wall commonly used in residential buildings in Tianjin, and designed the intelligent control system of artificial cold and heat source in the building on the basis of MATLAB simulation analysis [43]. The thermal insulation structure of double-layer residential buildings in Wang University was studied by using the computer simulation method in 2008 [44]. In 2009, according to the characteristics of residential buildings in Lhasa, Tibet, Sang of Xi'an University of architecture and technology established a mathematical and physical model to study the structural system of low-energy residential buildings from the aspects of heat collection, heat storage, thermal insulation and heat distribution [45]. In 2009, Yu of Hunan University and others proposed EETP evaluation index for the overall thermal performance of residential building envelope in hot summer and cold winter areas, analyzed the envelope of many residential buildings in Shanghai, Changsha, Shaoguan and Chengdu, and put forward the economic analysis and energy efficiency identification system of envelope in the whole life cycle [46]. In 2010, Wang and Wan of Wuhan University of technology used computer simulation technology to simulate the energy consumption of three buildings in Wuhan, and analyzed the energy-saving potential of building envelope [47]. In 2010, Masoud Taheri of South China University of technology took residential buildings in Iran as an example, studied the new wall with thermal insulation materials by using the methods of laboratory measurement and software simulation, and obtained the energy-saving characteristics of the new external wall through the results of on-site actual building test [48].

7.2. Simulation and Optimization of Different Glass Window Materials

7.2.1 Simulation of Glass Window Materials

The selection of the model object is based on the protruding sunlight room of the initial model (Figure 7-1). The rural house area of the model and the initial model is the same, the floor height is the same, and the peripheral protection structure parameters are the same. Low-E glass (low transmittance type), ordinary insulating glass (6mm + 9mm + 6mm) and ordinary three-layer insulating glass (6mm + 9mm + 6mm + 9mm + 6mm) were selected as the window materials for the simulation, and compared with the ordinary 6mm single-layer glass of the initial model (Table 7-1).

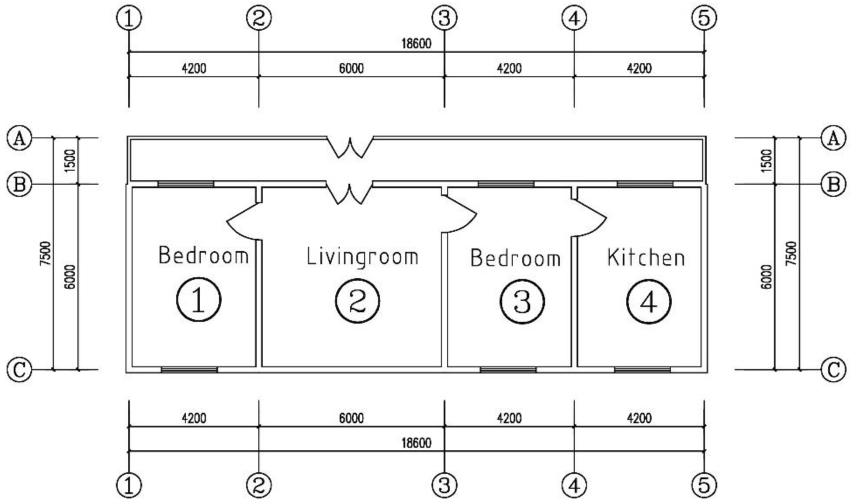

Figure 7-1. Model floor plan.

Table 7-1. Glass window material.

Number	**Name**	**Material thickness (mm)**	**Heat transfer coefficient W/(m2·K)**
Case 1	Ordinary 6mm, colorless, single layer glasser insulating glass	6	5.7
Case 2	Low-e glass (Low permeability)	6+9+6	2.1
Case 3	Ordinary insulating glass	6+9+6	3.1
Case 4	Ordinary three lay	6+9+6+9+6	2.3

Four window materials are simulated by DeST-h simulation software, and the data of outdoor temperature, basic room temperature in sunshine room and basic room temperature in master bedroom on typical days are sorted into curve distribution diagram (Figure 7-2 7-3).

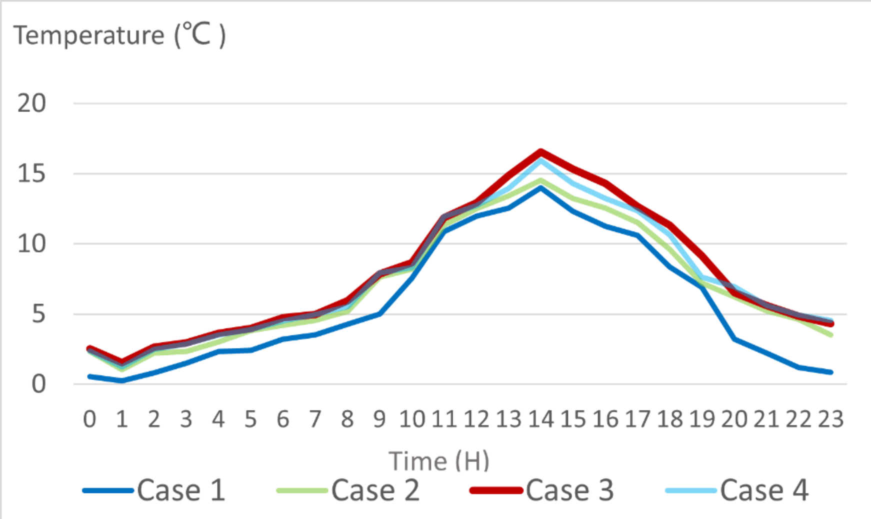

Figure 7-2. Temperature distribution of the sunlight room.

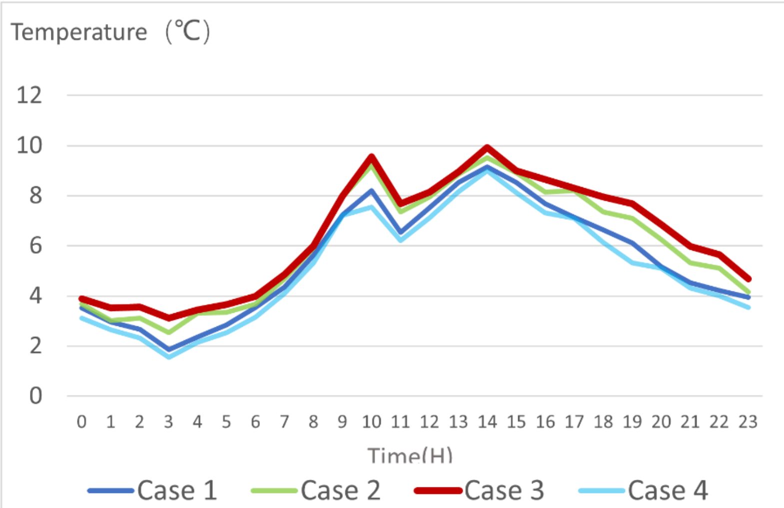

Figure 7-3. Room temperature distribution.

Four window materials are simulated by DeST-h simulation software, and the annual energy consumption and heat load corresponding to the four materials are analyzed (Table 7-2).

Table 7-2. Energy consumption simulation results.

Number	Case 1	Case 2	Case 3	Case 4
Annual cumulative heat load (KW·h)	6853.25	5862.87	5523.24	5663.24

7.2.2 Analysis of Simulation Results

(1) Basic Room Temperature Simulation Analysis

In a day, the temperature fluctuation value in the sunshine room is large at day and night. The reason is that the sunlight is direct during the day, the radiation is good, there is no direct sunlight at night, and the sunshine room needs to transfer heat to the room through the south wall of the building. The temperature fluctuation between ordinary insulating glass and sunlight is the largest, about 20 ℃. The second is ordinary glass sunlight, with temperature fluctuation of about 15 ℃. The most stable temperature is between Low-E glass and sunlight, and the temperature fluctuation is about 11 ℃. The lowest temperature of the sunshine room of the four materials appears around 1 a.m. in the morning. The main reason is that the sunshine room absorbs a lot of solar radiant heat during the day. When there is no direct sunlight at night, it gradually transmits its own heat to the bedroom and living room through convection and radiation. The maximum temperature appears at about 3:00 pm, and the minimum and maximum temperatures of case 1, case 2, case 3 and case 4 are 0.25 ℃, 13.99 ℃, 1.05 ℃ and 14.52 ℃ respectively; 1.55℃、16.55℃、1.25℃、15.96℃.

Compared with the sunshine room, the day and night temperature fluctuation of the master bedroom is small in a day. The temperature fluctuation of the bedrooms in the ordinary glass sunshine room, the Low-E glass sunshine room and the ordinary three-story insulating glass sunshine room is about 2 ℃, while the temperature fluctuation of the bedrooms in the ordinary insulating glass sunshine room is the largest, only about 3 ℃. The maximum temperature of the bedrooms of the three materials appears around 2 p.m., which is 9.16 respectively ℃, 9.92 ℃, 9.52 ℃ and 9 ℃, while the lowest temperatures of ordinary glass, Low-E, ordinary insulating glass and ordinary three-story insulating glass all appeared at 3 a.m., which were 1.85 ℃, 2.54℃and 3.12 ℃ 1.54℃. According to the above data analysis:

A. The number of window layers has an effect on the basic room temperature.

Rooms with different window layers are affected by direct sunlight and radiation. Double layer window glass has a greater impact on the temperature fluctuation in the sunshine room than single-layer window glass. The average room temperature of the sunshine room of ordinary double-layer glass is about 8 ℃ higher than that of single-layer ordinary glass. The average temperature of ordinary three-layer glass is less than 1 ℃ higher than that of ordinary double-layer insulating glass. In addition to ordinary single-layer glass, the other three materials have little effect on the temperature fluctuation of the bedroom, which is about 2 ℃. In terms of raising the indoor temperature, the room temperature of the other three kinds of bedrooms is about 3 ℃ higher than that of the single-layer ordinary glass bedroom.

B.The heat transfer coefficient has an effect on the basic room temperature.

The glass material with small heat transfer coefficient and low transmittance has less influence on the room temperature fluctuation between sunlight than the glass material with large heat transfer coefficient and high transmittance. It has little effect on the temperature fluctuation of the room in indirect contact with Yangguan. In terms of increasing the indoor temperature, the temperature difference between the ordinary double glass bedroom and the Low-E glass bedroom is small and can be ignored.

(2) Simulation Analysis of Building Heat Load

When the room temperature is maintained at 16℃ in winter, the heat load in winter heating season of four different window materials can be seen that the heat load in winter heating season is the largest when the ordinary single-layer window is used in the sunlight room. The heat load of winter heating season using ordinary insulating glass form material is the smallest, which is 43% lower than that of ordinary glass. Low-e glass falls somewhere in between, but also has a 32 percent lower winter heating load than single-layer regular glass. The heat load of ordinary insulating glass form material in winter heating season is only 10% lower than that of ordinary double-layer insulating glass. (Figure 7-4).

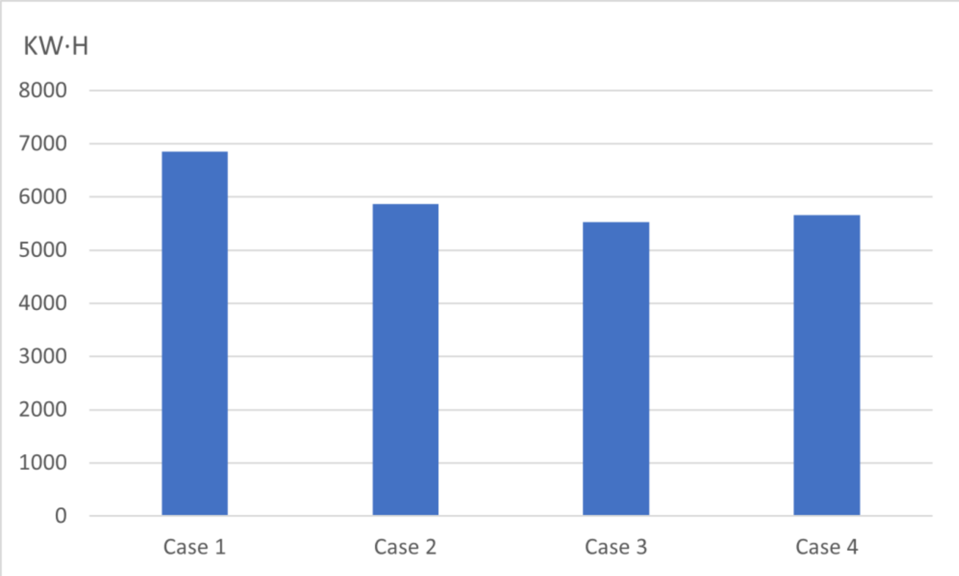

Figure 7-4. Simulation results of annual energy consumption.

7.2.3 Optimization Design Strategy

Through this study, it is found that under the condition that other factors remain unchanged, only changing the window material and number of floors, the indoor temperature and heating load in heating season still change greatly. By changing the window material and the number of layers in the additional sunlight room, it is of great help to reduce the heat load in the heating season. In the passive heating design of residential cooking heating wall and additional sunshine room in southern Shaanxi, under the condition that other factors remain unchanged and only the window material of sunshine room is changed, the following suggestions are given:

(1) Increase the number of window layers appropriately.

According to the simulation experimental data of different window layers, increasing the number of window layers can not only improve the indoor temperature, but also reduce the building energy consumption. However, it can be seen from the above data that the heating seasonal heat load of ordinary double-layer insulating glass is 32% lower than that of single-layer glass, and only 7% more than that of three-layer ordinary insulating glass. Therefore, in terms of the selection of window layers, considering its economy and construction difficulty, the author suggests that the window with two layers should be selected.

(2) Select the appropriate glass heat transfer coefficient.

According to the simulated experimental data of heat transfer coefficient of different window materials, it is concluded that the basic room temperature of the room in direct contact with sunlight is higher when the window material with high heat transfer coefficient and high transmittance is used than that of the room with low heat transfer coefficient and low transmittance. When the number of window layers is the same, the heat transfer coefficient of window material in sunlight room has little effect on the bedroom temperature. However, the glass material with low heat transfer coefficient is better than the window material with high heat transfer coefficient in building energy saving.

(3) Choose an economical and reasonable form material.

According to the market price of the three window materials, Low-E glass is expensive. Although the energy-saving efficiency is higher, it is 140 yuan /m^2more expensive than ordinary insulating glass. According to the calculation of the glass area of the sunshine room in the initial model, compared with the installation of ordinary insulating glass, the installation of Low-E glass costs about 4100 yuan more, and the installation of ordinary three-layer insulating glass costs about 3000 yuan more. Its economy is poor. While the price of ordinary insulating glass is relatively low, its energy-saving efficiency is not poor, so it is more economical and reasonable as the window material of sunshine room (Table 7-3).

Table 7-3. Form material price list.

Number	Name	Price (yuan / m2)
Case 1	Ordinary 6mm, colorless, single layer glass	40
Case 2	Low-e glass (Low permeability)	240
Case 3	Ordinary insulating glass	100
Case 4	Ordinary three lay	200

7.3. Different Depth Simulation and Optimization

7.3.1 Depth Simulation

The depth of the sunlight room is the distance from the south wall of the sunlight room to the south wall of the building. This distance has a significant impact on the heat load of the building and the indoor temperature. When the depth of the sunlight room increases, the sunlight directly entering the room decreases, but the East-West wall of the sunlight room increases and the volume of the sunlight room increases, which can make the room absorb more long wave radiation from the sun.

This section simulates the sunshine room temperature, indoor temperature and building heat load at different depths, and compares and analyzes the simulation data. The depth of sunlight simulated below is 600mm, 900mm and 1200mm respectively. The simulation results are compared with 1500mm of the initial model to analyze its economy (Table 7-4).

Table 7-4. The depth of the sunroom.

Number	The depth of the sunroom（mm)
Case 1	600
Case 2	900
Case 3	1200
Case 4	1500

Four groups of data are simulated by DeST-h simulation software, and the data of outdoor temperature, basic room temperature in sunshine room and basic room temperature in master bedroom on typical days are sorted into curve distribution diagram (Figure 7-5 7-6).

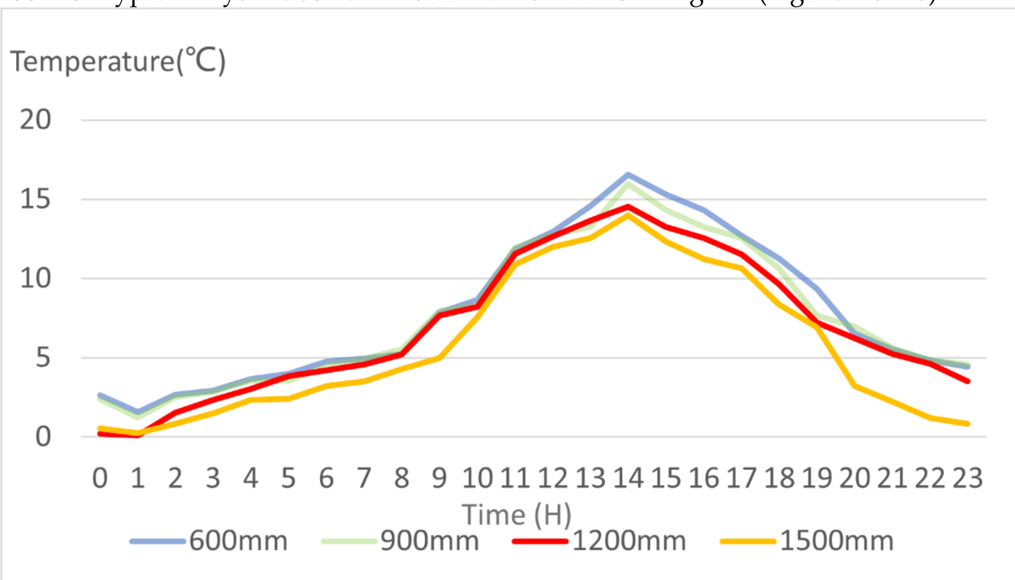

Figure 7-5. Temperature distribution of the sunlight room.

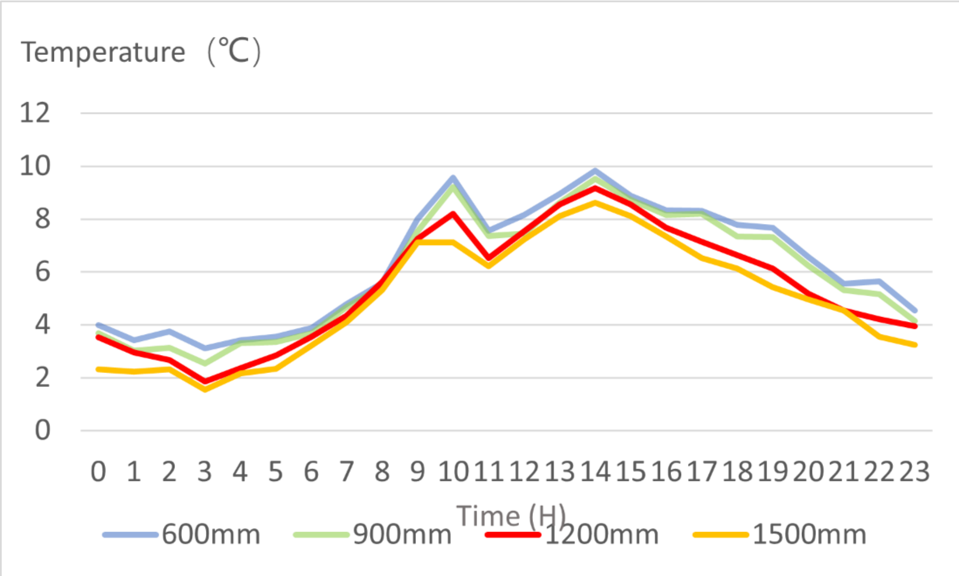

Figure 7-6. Room temperature distribution.

The four groups of data are simulated by DeST-h simulation software. The corresponding annual energy consumption and heat load, and the annual energy consumption and heat load of the four groups of data are sorted out (Table 7-5).

Table 7-5. Energy consumption simulation results.

	600 mm	900 mm	1200mm	1500mm
Annual cumulative heat load (KW·h)	6532.48	6685.32	7325.68	7753.25

7.3.2 Analysis of Simulation Results

(1) Basic Room Temperature Simulation Analysis

The temperature between the sunlight changes regularly with the increase of the depth between the sunlight. With the increase of sunshine depth, the temperature curve increases from 7:00 a.m. to 18:00 p.m. and decreases from 24:00 p.m. to 4:00 a.m. because the rate of heat gain in the daytime is greater than that of heat loss. During the day, the main way to increase the temperature in the sunlight is the direct radiant energy of the sun. In this time period, the smaller the depth of sunlight, the smaller the volume of sunlight. Therefore, in the daytime, the same amount of direct sunlight is obtained, and the higher the temperature is when the depth of sunlight is small. At night, when there is no solar radiation, there are two main ways to lose heat in the sunshine room. First, the sunshine room will lose some heat through the windows in the sunshine room. Second, in order to maintain the stability of indoor temperature, the sunlight room transfers the heat accumulated during the day to the building room through convection, radiation and other forms. Because the window area and wall area are the same, the heat released to the room is also the same, and the more heat stored in the deep and large sunlight room, the higher the temperature of the deep and large sunlight room in this time period.

During the day, the temperature in the bedroom tends to be stable, and the difference between the lowest temperature and the highest temperature is only about 2 ℃. At the same time, the temperature of the bedroom decreases with the increase of the depth of the sunlight room, but the range is small. The main reason is that with the increase of the depth of the sunlight room, the heat loss speed of the sunlight room is accelerated, so the heat transferred indoors is reduced, so the heat available indoors is also reduced.

From the above data analysis, it can be seen that in the severe cold area of Northeast China, with the increase of the depth of sunlight, the indoor temperature decreases gradually. The main reason is that the increase of heat caused by the increase of the volume of sunlight can not make up for the faster increase of heat loss.

(2) Simulation Analysis of Building Heat Load

It can be seen that the heating load of the building increases by 3% in winter, and the heating load of the building increases by 1% in winter. The reasons are as follows: the south wall and its glass window are the main components to absorb solar energy in the sunlight room. When the depth of the sunlight room increases, the sunlight directly shining on the south wall decreases, so the heat supply in the sunlight room decreases. At the same time, the increase of heat caused by the increase of the volume of the sunlight room can not make up for the faster heat loss (Figure 7-7).

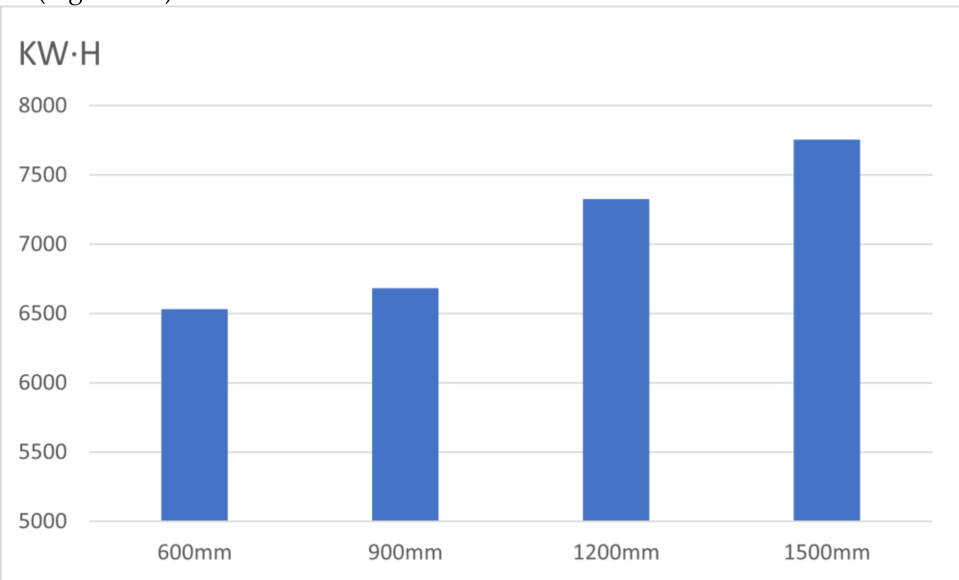

Figure 7-7. Simulation results of annual energy consumption.

7.3.3 Optimization Design Strategy

Through the above simulation and analysis of different window materials in the sunshine room, we can get the relationship between the depth of the sunshine room and the thermal comfort of the passive solar room and the energy consumption in the heating season. When other variables remain unchanged, the changes of the temperature in the sunshine room, the temperature in the bedroom and the thermal load in the heating season change regularly with the increase of the depth of the sunshine room.

The optimal design obtained from the simulation experimental data can provide more objective theoretical support for the future rural residential design in southern Shaanxi. On the premise that other design factors remain unchanged, the optimal design of sunshine depth is as follows:

1. With the increase of sunshine depth, the temperature between sunshine changes greatly. It has little effect on the indoor temperature. The temperature decreases by less than 1 ℃ for every 300 mm increase in the depth of the sunlight room.

2. With the increase of the depth of sunlight, the heat load of the building shows an upward trend. In architectural design, if the sunlight room is only used as a heat collection and storage component, the depth of the sunlight room should be 600mm. With the continuous

improvement of people's living standards, the villagers' requirements for the living space in the farm house are also increasing. When designing the sunshine room, we should also consider the functional requirements and body size of the sunshine room. The functional requirements of the sunshine room include the physiological needs, the spiritual needs and the functional needs derived from the basic composition of the farm house, Functional zoning between sunshine rooms.

In terms of human scale factors, it is mainly considered that people will carry out appropriate leisure activities and necessary auxiliary transportation functions in the sunshine room in winter. When the weather is cold in winter, people can exercise in the sunshine, communicate with neighbors, and children can also play in it. In addition to improving the indoor thermal environment, the sunshine room often becomes a display platform for family personality and characteristics, such as raising birds, fish and pets. All these activities need appropriate space to carry out, and these basic life activities need appropriate space scale to carry out smoothly.

When people climb, dry or walk, the scale can be carried out smoothly between 650mm and 1200mm, so the depth of additional sunlight should be greater than or equal to 1200mm as far as possible; When normal people exercise in a large range, for example, the size of exercise is about 1600mm, but when people exercise and other activities, they can choose the direction of the human body parallel to the width of the farm house.

Through the above analysis, it can be seen that in the construction of the passive solar house with additional sunshine room in southern Shaanxi, the depth of the sunshine room should be as wide as possible without affecting the indoor thermal comfort, so as to leave some space for human activities, but it is not the wider the better. Too wide will increase the energy consumption in the heating season. Therefore, the author believes that the depth range is 1200mm ~ 1500mm.

7.4. Simulation and Optimization of Window Wall Ratio

7.4.1 Window Wall Ratio Simulation

This section simulates the indoor temperature of sunshine room, indoor temperature of bedroom and building heat load with different window wall ratio of sunshine room, and compares and analyzes the simulation data. The window wall ratio of the sunlight room simulated below is 0.8, 0.7, 0.6 and 0.5 respectively. The simulation results are compared with 0.9 of the initial model to analyze its economy.

Five groups of data are simulated by DeST-h simulation software, and the basic room temperature data of sunshine room and master bedroom on typical days are sorted into curve distribution diagram (Figure 7-8 7-9).

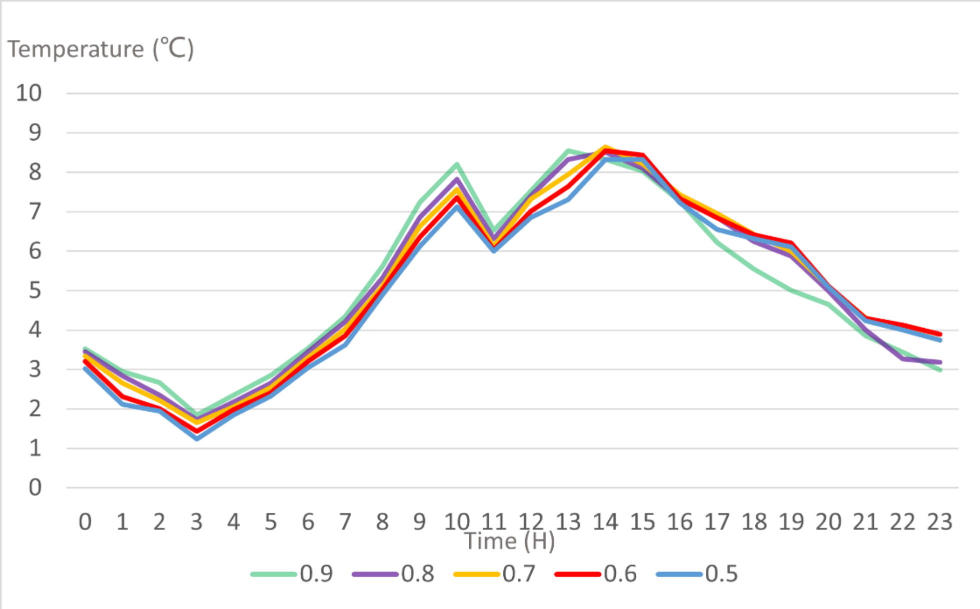

Figure 7-8. Temperature distribution of the sunlight room.

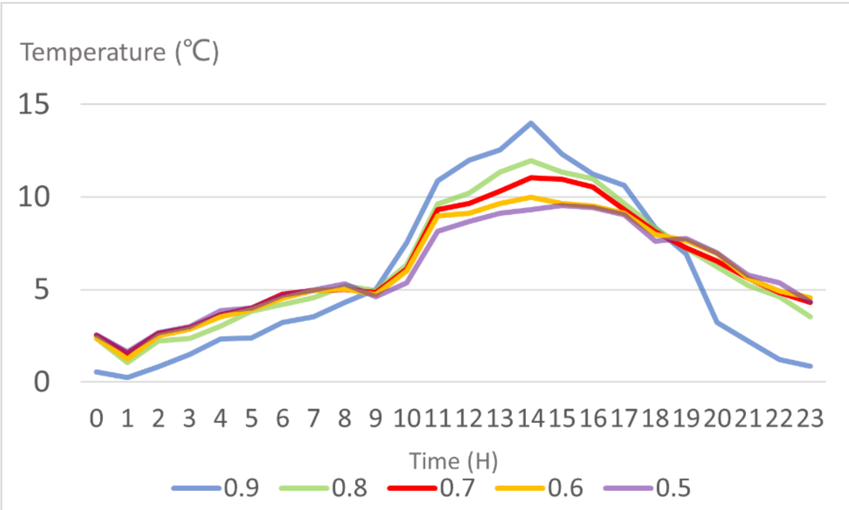

Figure 7-9. Room temperature distribution.

Through DeST-h simulation software, simulate the five groups of data, the corresponding annual energy consumption and heat load, and sort out the annual energy consumption and heat load of the five groups of data (Table 7-5).

Table 7-6. Energy consumption simulation results.

	0.9	**0.8**	**0.7**	**0.6**	**0.5**
Annual cumulative heat load (KW·h)	6853.25	5968.26	5468.95	5132.69	4869.23

7.4.2 Analysis of Simulation Results

(1) Basic Room Temperature Simulation Analysis

The temperature between sunlight changes regularly with the decrease of window wall ratio. With the decrease of the window wall ratio in the sunlight room, the temperature curve increases from 7:00 a.m. to 16:00 p.m. and decreases from 24:00 p.m. to 4:00 a.m. because the rate of heat gain in the sunlight during the day is greater than the rate of heat loss. During the day, the main way to increase the temperature in the sunlight is the direct radiant energy of the sun. The heat gain of this way is inseparable from the window, and the window plays a decisive role. Therefore, the larger the window wall ratio of the sunlight room wall during this time period, the higher the indoor temperature. At night, when there is no solar radiation, there are two main ways to lose heat in the sunlight room. First, the sunlight room will lose some heat through the windows in the sunlight room. Second, in order to maintain the stability of indoor temperature, the sunlight room will transfer the heat accumulated during the day to the building through convection, radiation and other forms, As a result, the rate of heat gain between the sunlight is much less than the rate of heat loss. Therefore, in this time period, the smaller the window wall ratio between the sunlight, the higher the temperature between the sunlight.

With the decrease of window wall ratio in sunlight room, the indoor temperature curve changes regularly. With the decrease of window to wall ratio, the temperature curve increases from 7:00 a.m. to 14:00 a.m The temperature curve between 14:00 and 23:00 shows a decreasing trend. The main reason is that during the day, with the increase of the window wall ratio in the sunlight room, the indoor heat gain speed is greater than the heat loss speed. When there is no solar radiation at night, the indoor heat gain speed is less than the heat loss speed. Therefore, the smaller the window wall ratio in the sunlight room is, the heat loss will be relatively reduced, The temperature will drop relatively slowly.

The data show that the change of window wall ratio in the additional sunshine room has a significant impact on the temperature change of one day in the additional sunshine room and bedroom. Changing the window wall ratio of the additional sunlight room has a direct impact on the temperature of the sunlight room and the bedroom, and the temperature curves during the day and night show the opposite trend.

(2) Simulation Analysis of Building Heat Load

When the room temperature of the farm house is maintained at 16 ℃ in winter, the heat load of the winter heating season of the five groups of data is shown in Figure 4-15. It can be seen that when the window wall ratio of the additional sunlight room increases, the heat load of the building shows a decreasing trend, and the heat load of the heating season under condition 4 is 21% lower than that under condition 0. The heat load in the heating season of condition 1 is 5% less than that of condition 0, the heat load in the heating season of condition 2 is 5% less than that of condition 1, the heat load in the heating season of condition 3 is 5% less than that of condition 2, and the heat load in the heating season of condition 4 is 6% less than that of condition 3. It can be seen from the data that when the window wall ratio of the additional sunlight room decreases by 0.1, the heat load in the heating season will be reduced by 5% ~ 6%. The reasons are as follows: when the window wall ratio of the additional sunlight room increases, the solar radiation heat obtained during the day will increase, but when there is no sunlight, the heat loss will increase greatly. In a day, the time without direct sunlight is much longer than the time with direct sunlight. Therefore, when the window wall ratio of the additional sunlight room decreases, the heat load in the heating season will decrease, compared with the window wall, it is more energy-saving than the large additional sunlight room (Figure 7-10).

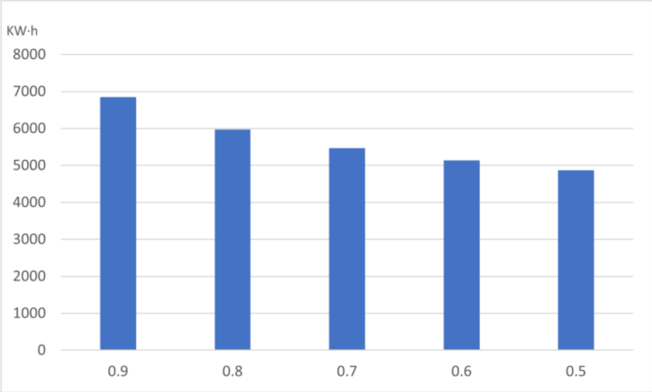

Figure 7-10. Simulation results of annual energy consumption.

7.4.3 Optimization Design Strategy

Through the research on the window wall ratio of the additional sunlight room for the indoor thermal comfort of rural houses and the heat load in the heating season in this section, it is found that when other factors remain unchanged, only the window wall ratio of the additional sunlight room is changed, and the change of the indoor temperature is different in the case of direct sunlight and no direct sunlight. Therefore, we can not simply make a judgment, but through the combination with practice and comprehensive analysis, the results can be more objective and persuasive. For the design of additional sunshine room passive solar house in villages and towns in the severe cold area of Northeast China, under the condition that other factors remain unchanged and only the window wall ratio of sunshine room is changed, the following suggestions are given:

(1) With the increase of the window wall ratio of the additional sunshine room, the indoor temperature curve of the sunshine room decreases at night and increases during the day. The appropriate window wall ratio should be selected according to the difference between day and night. The temperature curve change in the master bedroom is consistent with that in the sunshine room. In southern Shaanxi, after setting up an additional sunshine room, the temperature during the day is ideal, and there is still time to cook during the day, so the bedroom can be heated artificially. The night should be the key factor to be considered, because there is no direct sunlight at night and there is no time period for artificial heating. Therefore, when considering the window wall ratio of the additional sunlight room, the temperature at night should be mainly analyzed. According to the above data, the smaller the window wall ratio of the additional sunlight room at night, the higher the indoor temperature. Therefore, the scheme of small window wall ratio should be selected. However, the window wall ratio is the main component of heat absorption during the day, so it cannot be designed too small. Too small design will also affect the indoor daylighting and cause too dark light in the room.

(2) From the perspective of building heat load, the smaller the window wall ratio of the additional sunshine room, the smaller the heat load in the heating period. It can be seen from the data that the heat load in the heating period with the window wall ratio of 0.5 in the additional sunshine room is 21% less than that with the window wall ratio of 0.9 in the additional sunshine room, and the difference in energy consumption is still relatively large. Therefore, in the design, the window wall of the additional sunshine room is relatively smaller than that in the design. The wall of the sunshine room should also be made into the same thermal insulation treatment as the main wall of the farm house, so as to have a better thermal insulation effect and better structural practice. Through the comprehensive consideration of indoor temperature, heat load and daylighting, the window wall ratio of additional sunlight room should be 0.6 ~ 0.7.

7.5 Simulation and Optimization of Wall Materials

7.5.1 Simulation of Wall Materials

The thermal inertia of the south wall of the additional sunlight room is the main link of heat collection in the sunlight room, and it is also one of the important indexes of the performance of the sunlight room. During the day, while the south wall transfers heat to the room, it also accumulates some heat. At night, when there is no sun, its own heat will be transferred to the room to keep the room as constant as possible. The thermal inertia of enclosure structure is generally expressed by D, and its calculation formula is:

$$D=R\times S \quad (1)$$

Where R - thermal resistance of structural layer, unit: $M^2 \cdot K/W$

S -- heat storage coefficient, unit: $w/(m^2 \cdot K)$

Table 7-7. Thermal parameters of wall materials.

Number	Name	Density kg/m³	Heat storage coefficient W/（m2·K）	Thermal inertia index	Heat transfer coefficient W/（m2·K）
Case 1	Solid clay brick	1800	6.3	3.5	0.814
Case 2	Concrete porous brick	1450	2.8	2.6	0.62
Case 3	Reinforced concrete	2500	14.6	1.7	1.628

It can be seen that the greater the thermal resistance of the material, the better its thermal inertia and the smaller the heat transfer coefficient. In this section, concrete perforated brick, reinforced concrete and solid clay brick of the initial model are used as wall materials respectively, and the indoor temperature and heat load are simulated under the condition that other structures remain unchanged (Table 7-7).

7.5.2 Analysis of Simulation Results

(1) Thermal Inertia Simulation

Three groups of data are simulated by DeST-h simulation software, and the basic room temperature data of the master bedroom on typical days are sorted into a curve distribution diagram. Simulate the three groups of data through DeST-h simulation software, the corresponding annual energy consumption and heat load, and sort out the annual energy consumption and heat load of the three groups of data (Figure 7-11).

A. Basic room temperature simulation analysis

The average indoor temperature values of the three groups with different thermal inertia are 5.45 ℃, 5.73 ℃ and 5.02 ℃respectively. It can be seen that the average indoor temperature value of the bedroom with concrete perforated brick is the highest and that of the reinforced concrete wall is the lowest. The reason is that the thermal inertia value of solid clay brick is higher than that of concrete. When a certain amount of heat is stored indoors, due to its large thermal resistance, the indoor heat is not lost through the wall quickly.

The indoor average temperature values of the three groups of wall materials are 5.45 ℃, 5.73 ℃ and 5.02 ℃ respectively. It can be seen from the indoor average temperature that the indoor average temperature of reinforced concrete is the smallest and that of concrete perforated brick is the largest. The reason is that although the thermal resistance of solid clay brick is the largest, due to the gap of concrete porous brick, when building the wall, the wall will form an air isolation layer, so the concrete porous brick performs better in maintaining indoor temperature.

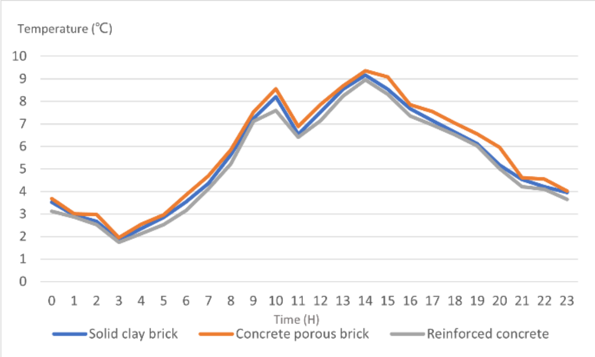

Figure 7-11. Master bedroom basic room temperature contrast.

From the analysis of the above data, it can be seen that in the severe cold area of Northeast China, the indoor temperature has a direct relationship with the thermal inertia of the main structure wall. Selecting materials with high thermal inertia as the wall enclosure can make the indoor temperature gentle, or increase the indoor temperature without too fast loss. The internal structure of the material is also the main evaluation basis of the indoor temperature. When the porous brick quality material is used as the wall, the indoor temperature performance in winter is more excellent.

B. Simulation analysis of building heat load

When the room temperature of rural houses is maintained at 16 ℃ in winter, according to the heat load in winter heating season of the three groups of data, it can be seen that the heat load in reinforced concrete heating season is the highest, followed by concrete perforated brick, and solid clay brick is the best. The main reason is that the thermal inertia and thermal resistance of solid clay brick are the highest, and the less heat loss is estimated. Therefore, in the selection of the above three materials as the outer enclosure structure, concrete perforated brick is the first choice. Although the performance of solid clay brick is also excellent, considering its waste of land resources, the country has banned the use of this product in 2010 (Figure 7-12).

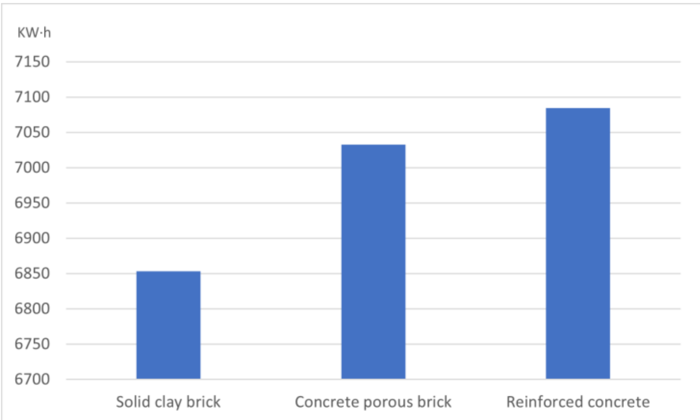

Figure 7-12. Simulation results of annual energy consumption.

(2) Simulation of Wall Insulation Materials

The simulated insulation material was selected by straw board, XPS insulation board, polyurethane foam board and initial EPS insulation board model test. The thickness of insulation layer was 100mm, and the data were compared (Table 7-8).

Table 7-8. Thermal parameters of wall insulation materials.

Number	Name	Material thickness (mm)	Thermal conductivity	Heat transfer coefficient W/

			W/ (m2·K)	(m2·K)
Case 1	EPS insulation board	100	0.047	0.383
Case 2	Grass plate	100	0.108	0.696
Case 3	XPS insulation board	100	0.03	0.284
Case 4	Polyurethane foam board	100	0.037	0.314

Four groups of data are simulated by DeST-h simulation software, and the basic room temperature data of the master bedroom on typical days are sorted into a curve distribution diagram (Figure 7-13).

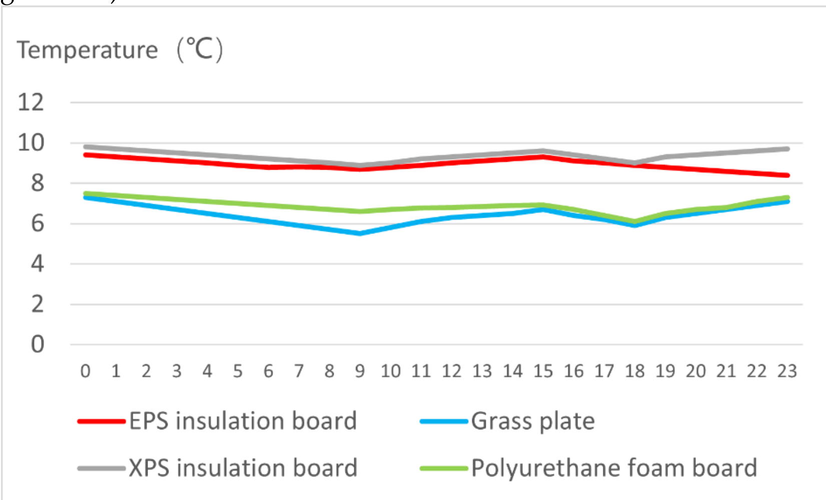

Figure 7-13. Master bedroom basic room temperature contrast.

Through DeST-h simulation software, simulate the four groups of data, the corresponding annual energy consumption and heat load, and sort out the annual energy consumption and heat load of the four groups of data (Table 7-9).

Table 7-9. Energy consumption simulation results.

Number	Case 1	Case 2	Case 3	Case 4
Annual cumulative heat load (KW·h)	7028.81	7198.46	5842.50	5924.22

A. Basic room temperature simulation analysis

Among the four thermal insulation materials, except straw board, the other three materials meet the specification requirements and can be used in the construction of agricultural houses. In a day, the indoor temperature of the XPS insulation board is the highest, followed by the polyurethane foam board. The indoor temperature of the EPS insulation board is worse than that of the previous two, but the indoor temperature is much better than that of the grass board.

From the above data analysis, it can be seen that in the severe cold area of Northeast China, the application of new wall insulation materials for external insulation treatment can greatly improve the indoor temperature in winter. The EPS insulation board, XPS insulation board and polyurethane foam board can be applied in the farmhouses of the northeast cold region.

B. Simulation analysis of building heat load

When the farmhouse temperature is maintained at 16 ℃ in winter, the heat load of the four sets of data in winter heating season shows that the insulation performance of XPS insulation board is the best, and the grass plate is the worst. The heating load of XPS insulation board is 15% less than that of EPS insulation board in winter, and the thermal load of polyurethane foam board is 14% less than that of EPS insulation board in winter. It can be seen from the above data that the thermal load of XPS insulation board and polyurethane foam board is very good and can be applied to construction (Figure 7-14).

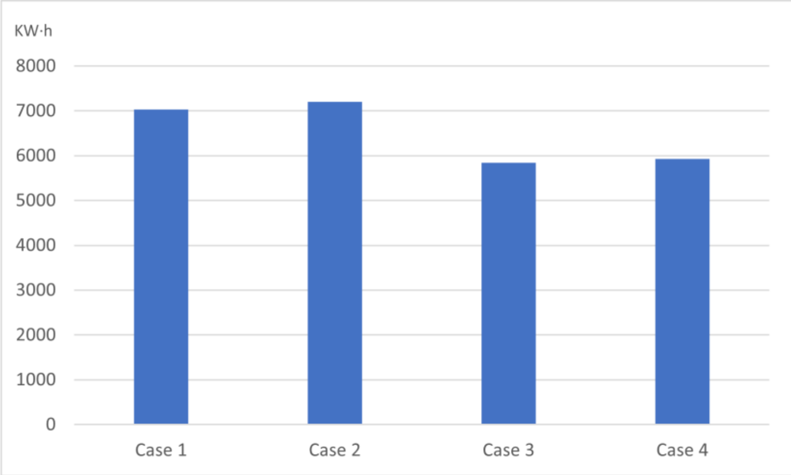

Figure 7-14. Simulation results of annual energy consumption.

7.5.3 Optimization Design Strategy

Through the research and analysis of the relationship between indoor temperature, heating load in heating season and the enclosure structure of the south wall of rural residence, it is found that changing the parameters of the south wall will affect the indoor temperature and heating load in heating season. Through the above simulation and analysis of different thermal inertness of enclosure structure, the following design optimization strategies are obtained.

(1) Considering the maintenance of indoor temperature, the indoor temperature of the envelope with high thermal inertia index is higher than that of the material with low thermal inertia in winter. When materials such as porous bricks are used as the outer envelope, we can not only consider the single index of thermal inertia, but also comprehensively consider the porosity of the envelope. The problem of keeping warm in winter needs to be considered in the envelope structure, so the material with large porosity should be selected in the selection of material, which can play a better heat preservation effect (Figure 7-15).

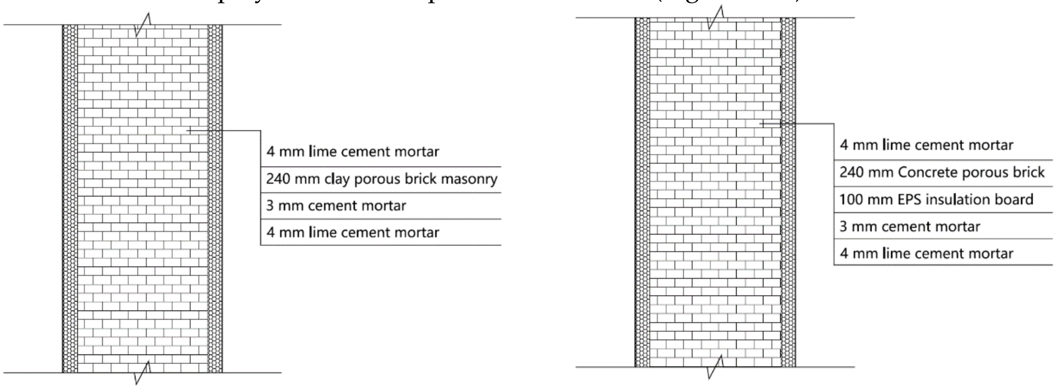

(a) The wall before the renovation (b) The wall after renovation

Figure 7-15. Wall material changes.

(2) The higher the thermal inertia index of the enclosure, the greater the thermal resistance, the higher the temperature in the room, and the temperature fluctuation of the room is small and the stability is good.

Through the above simulation and analysis of thermal insulation materials, the following design optimization strategies are obtained. When the thickness of insulation layer is the same, the insulation material with low heat transfer coefficient is better than the insulation material with high heat transfer coefficient in maintaining indoor temperature and heat load in winter heating season. It can be seen from the data that EPS insulation board, XPS thermal insulation board and polyurethane foam board can be used for the construction of external insulation of farm house wall. However, when the insulation layer is in phase, the performance of XPS insulation board and polyurethane foam board is better than that of EPS insulation board. According to the market price of the three insulation materials, XPS insulation board is expensive. Although the energy-saving efficiency is higher, it is 80 yuan / m3 more expensive than EPS insulation board， The price of polyurethane insulation board is 70 yuan / M3 higher than that of EPS insulation board. Therefore, considering that the energy-saving efficiency of EPS insulation board is not low compared with XPS insulation board, but its price is much lower than XPS insulation board, EPS insulation board is the most suitable external insulation material for rural houses (Table 7-10).

Table 7-10. Price list of insulation materials.

Number	Name	Price (yuan / m2)
Case 1	EPS insulation board	399
Case 2	XPS insulation board	480
Case 3	Polyurethane foam board	470

7.6 Chapter Summary

This chapter mainly introduces the optimization of cooking heating wall and additional sunlight room system, and analyzes the influencing factors of cooking heating wall and additional sunlight room system. Through analysis and comparison, it is concluded that the main influencing factors of the system are glass window material, depth, window wall ratio and wall material. Using software simulation, determine the best value of influencing factors (window material, depth, window wall ratio and wall material of glass). In addition, Energyplus software is used to calculate the annual heat load of the building when the optimal value is adopted.

Reference

[1] Arasteh, D.K.; Reilly, M.S.; Rubin, M.D. A versatile procedure for calculating heat transfer through windows. ASHRAE Transaction. 1989, 95, 755-765

[2] Versluis, R.; Powles, R.; Rubin, M.D. Optics. 2002，LBNL report 52148.

[3] Baird, J. American society of heating refrigerating and air-conditioning engineers ASHRAE fundamentals handbook. 2001, 30.

[4] Wright. Calculating the central-glass performance indices of the windows. ASHRAE Transactions. 101, 802-818.

[5] Bokel, R.M.J. The Effect of window position and window size on the energy demand for heating, cooling and electric lighting. The 10th International Building Performance Simulation Association Conference and Exhibition. 2007, 117-121.

[6] General Administration of Quality Supervision, Inspection and Quarantine of the People's Republic of China, Standardization Administration of China, Gbt7106-2008. Classification and Testing method for Air tightness, Water tightness and Wind Pressure Resistance of Building Windows, Beijing: Standards Press of China. 2008, 11.

[7] Dong, Z.; Xu, Y.; Wen, Y.; Chen, Q. Study on the thermal process of windows in hot area in summer. Warm Air Conditioning. 2003, 33, 93-96.

[8] Dong, Z.; Xu, Y. A simplified method for calculating the heat transfer coefficient of windows. Advanced Building Materials. 2002, 40-44.

[9] Zhang, W. Research on energy saving design of exterior windows of residential buildings -- a case study of Hangzhou. Zhejiang University. 2003, 10-30.

[10] Bu, Z.; Mao, H.; Yang, H. Effect of low-E glass on air conditioning load and building energy consumption. HVAC Air Conditioning. 2005, 35, 119-121.

[11] Di, H.; Yang, Y. study on energy saving of low radiant glass windows. Journal of Solar Energy. 2001, 22, 296-301.

[12] Xie, Y.; Liu, Y. Analysis on energy-saving Effect of sunshade Rolling curtain for residential Buildings in summer. Construction Science and Technology. 2006,76-77.

[13] Jian, Y.; Jiang, Y. Effect of window-wall ratio on total energy consumption of residential heating and air conditioning. HVAC, 2006, 36, 1-5.

[14] Fang, S. Research on energy saving of exterior windows of residential buildings in different areas. Hunan University. 2008.

[15] Wang, L. study on energy saving design of exterior windows of residential buildings in cold area of north China. Tianjin University, 2007.

[16] Faist, A.; Hagen, F.; Morel, N. An expert system for passive and low energy building design，Clean and Safe Energy Forever. Proceedings of the 1989 Congress of the International Solar Energy Society. 1990, 931-935.

[17] Hanna, J.; Wojciech, M. Optimization of shape and functional structure of buildings as well as heat source utilization. Building and Environment. 2002, 37, 1037-1043.

[18] Florides, G.A.; Tassou, S.A.; Kalogirou, S.A. Measures used to lower building energy consumption and their cost effectiveness. Applied Energy. 2002, 73, 299–328.

[19] Wang, W.; Hugues, R.; Radu, Zmeureanu. Floor shape optimization for green building design, Advanced Engineering Informatics. 2006, 20, 363-378.

[20] Houcem, E.M.; Alfonso, C.; Vincenzo, C. Use of the Anova approach for sensitive building energy design. Applied Energy. 2010, 10, 3073-3083.

[21] Lin, H. Building plane-form-orientation and energy saving. Journal of Architecture, 1981, 06, 37-41.

[22] Feng, Y.; Xiang, S. Also on building shape and energy saving. Architectural Journal, 1983, 08, 33-35.

[23] Cai, J. Residential Energy Saving Design. Beijing: China Architecture and Building Press. 1991.10.

[24] Song, D.; Zhang, Z. Energy saving analysis of building plane shape design. New Building. 2000, 03, 8-11.

[25] Technical Standard for Buildings with near zero Energy Consumption GBT 51350-2019[S]. China Building and Architecture Press. 2019.

[26] Zhang, S. Research on energy saving reconstruction of existing residential buildings in Qingdao. Qingdao University of Technology, 2020.

[27] Cheng, Y.; Gao, M.; Jia, J. An optimal and comparison study on daylight and overall energy performance of double-glazed photovoltaics windows in cold region of China. Energy. 2019, 170, 356-366.

[28] Zhang, C. Research on heat transfer and energy saving characteristics of building exhaust air and insulation windows. Huazhong University of Science and Technology. 2017.

[29] Lai, K.; Wang, W.; Giles, H. Solar shading performance of window with constant and dynamic shading function in different climate zones. Solar Energy. 2017, 147, 113-125.

[30] Chen, S. Study on climate adaptability of doors and windows of Guangfu traditional residential houses. South China University of Technology. 2020.

[31] Building energy saving technology and its application abroad. Wall materials and building decoration. 2004, 01, 7-8.

[32] Barozzi, G.S.; Imbabi, M.S.E.; Noble, E.; Sousa, A.C.M. Physical and numerical modeling of a solar chimney-based ventilation system. Building and Environment, 1992, 27, 433-455.

[33] Kossecka, E. Heat transfer through building wall elements of complex structure. Archives of Civil Engineering. 1992, 38, 117-126.

[34] Bouchlaghem, N. Optimizing the design of building envelopes for thermal performance. Automat Constr. 2000, 10, 101–112.

[35] Collet, F.; Serres, L.; Miriel, J. Study of thermal behavior of clay wall facing south. Building and Environment. 2006, 41, 307–315.

[36] Lollini, B.; Fasano. Optimization of opaque components of the building envelope-energy, economic and environmental issues. Building and Environment. 2006, 41, 1001-1013.

[37] Utama, A.; Gheewala, S.H. Life cycle energy of single landed houses in Indonesia. Energy and Buildings. 2008, 40, 1911–1916.

[38] Chen, Q.; Fundamentals of building thermophysics. Xi 'an: Jiaotong University Press. 1991.

[39] Yu, L.; Yang, X. Insulation layer design of slope roof of multi-storey residence. Journal of Thermal Insulation and Building Energy. 2000, 1, 20-22.

[40] Sun, H. Sunshade and heat insulation design of west gable of residential building unit in hot summer and cold winter area. Industrial Building. 2004, 34, 24-26, 29.

[41] Xue, Z.; Jiang, Y. Analysis of energy consumption status and energy saving potential of large public buildings in Beijing. Hvar Tone. 2004, 34, 8-10, 24.

[42] Jiang, Yi.; Xue, Z. Analysis on current situation of building energy consumption and energy saving approaches in Beijing. Hvar, 2004, 34, 13-16.

[43] Yang, Z.; Xu, X.; Han, J. Analysis of thermal characteristics of solar wall. Acta Solarica Sinica. 2007, 28, 1091-1096.

[44] Wang, P.; Ding, X. Design concept of double-side insulation of building envelope in hot summer and cold winter area. Architectural Festival Energy, 2008, 4, 33-35.

[45] Sang, G. Study on structural system of low energy residential Building in Tibetan Plateau, ph. D. dissertation. Xi 'an Jian Zhu University of Science and Technology. 2009.

[46] Yu, J.; Yang, C.; Tian, L.; Liao, D. Optimal thickness of exterior insulation layer for residential buildings in Changsha area. Journal of Hunan University: Natural Science. 2009, 36, 16-21.

[47] Wan, C. Design and simulation of energy-saving building envelope. Wuhan Institute of Technology University, 2010.

[48] Masoud, T.S.; Zhao, L.; Meng, Q. Multi-storey house in Mashhad, Iran Energy Research, 2010, 5, 1287-1292.

Chapter 8. Conclusion and Prospect

8.1 Conclusion

This work studied the passive heating of traditional houses in southern Shaanxi in winter and proposes a cooking heating wall heating system. First, a model of the cooking heating wall was designed to use the waste heat from cooking to increase the indoor temperature. Secondly, this paper studied the indoor temperature change with or without solar radiation when using the cooking heating wall system and natural heating. Finally, the results of using the cooking heating wall system and natural heating to increase the indoor temperature are compared with or without solar radiation. The indoor temperature changes of the cooking heating wall system were evaluated under the conditions of whether there was solar radiation throughout the year or not. Without solar radiation, the cooking heating wall system can increase the indoor temperature. The specific conclusions are as follows:

● In order to increase the indoor temperature of traditional houses in southern Shaanxi in winter in accordance with local living customs, a cooking heating wall system was designed. Using the waste heat generated by cooking and the characteristics of wall heat storage, the heat was transferred to the room through the system. A software simulation confirmed that the new system caused a significant increase in the indoor temperature, and specifically increased by 3.7 ℃.

● By simulating natural heating, without solar radiation, the indoor temperature will eventually reach 4.8 ℃, and the heating efficiency will be 0.03 ℃/h. With solar radiation, the indoor temperature will eventually be 7 ℃, and the heating efficiency will be 0.22 ℃/h.

● Through the simulation of the cooking heating wall system, without solar radiation, the indoor temperature is increased to 9.7 ℃, and the heating efficiency is 2.34 ℃/h. With solar radiation, the indoor temperature is significantly increased to 12.2 ℃ and the heating efficiency is 3.54 ℃. Compared with natural heating, the heating effect of the cooking heating wall is obvious.

● Using the cooking and heating system, the heat load of the building was reduced by 1104.723 kW· h (reduction rate 19.84%) and 440.8318 kW· h (reduction rate 7.91%) throughout the year with or without solar radiation. In addition, with 18 ℃ as the limit of the passive heating of buildings, the total heat load time of the building throughout the year with or without solar radiation accounted for 43.55% and 46.36% of the total time of the year, respectively.

This research focused on the passive heating of residences in southern Shaanxi in winter, proposing a cooking heating wall–sunlight heating system combining the cooking method and solar heating in southern Shaanxi. The cooking heating wall system uses the hot air generated by cooking to heat the wall and raises the indoor temperature in the form of heat radiation and convection. The sunlight room system establishes an additional sunlight room on the sunny side of the building, using the principle of the greenhouse effect to improve the heating efficiency. The new system combines the advantages of the cooking heating wall system and the sun room system to further improve the indoor temperature. The principle of the additional sunlight room is similar to that of the thermal insulation wall, which effectively blocks the direct contact between the hot indoor air and the cold outdoor air, thereby achieving a thermal insulation effect and reducing the energy demand of the building. Through software simulation, the heating time, heating efficiency, balanced temperature, building heat load reduction, and the time of using the new system throughout the year were calculated in detail. The specific results are as follows:

● Its working principle is not only to use the heat generated by cooking to heat the wall to raise the indoor temperature, but also to increase the heating effect by adding the characteristics of heat transfer between the sun room and the wall through solar radiation heating. The software simulation proved that the new system is effective for increasing the indoor temperature, and the temperature was increased by 4.16 ℃.

● In the presence of solar radiation, the equilibrium temperature in the basic heating room was 6.5 ℃, and the heating efficiency was 0.23 ℃/h. After adopting the new system, the room temperature after equilibrium was 9.16 ℃, and the heating efficiency was 4.09 ℃/h.

● In the absence of WSR, the equilibrium temperature in the basic heating room was 5.5 ℃, and the heating efficiency was 0.06 ℃/h. After adopting the new system, the temperature in the room after equilibrium was 5.43 ℃, and the heating efficiency was 2.87 ℃/h. Therefore, when there was no WSR, the heating effect of the new system was obvious compared to the basic heating system.

● When the cooking heating wall and additional sunlight system were used, the thermal load of the building decreased by 1436.731 kW h during the whole year (with WSR). The thermal load of the building decreased by 735.919 kW· h throughout the year (without WSR). Taking 18 ℃ as the standard value of the building's winter thermal comfort, the annual time below 18 ℃ was 3733 h (the wall has solar radiation) and 4006 h (the wall has no solar radiation).

8.2 Prospect

Future research should mainly focus on the following aspects:

● The results of this study need to be proved in practice. Future research should focus on creating a detailed method of construction for the cooking heating wall system. Additionally, the thermal properties of the cooking heating wall material need to be considered, such as the insulation and air tightness of the material. It is necessary to maximize the heat storage performance of the cooking heating wall, thereby extending the heating time.

● Consideration could be given to building a more comprehensive cooking heating wall system, connecting the various rooms, and discussing indoor temperature changes and the reduction in the overall thermal load of the building.

● Technology for combining the cooking system with a solar chimney can be considered to analyze the temperature changes and extend the heating time.

● According to actual investigations, the wall materials of the residential buildings in southern Shaanxi mainly involve clay porous brick masonry. Therefore, in the simulation analysis, the wall material of the model was set as clay porous brick masonry. As the maintenance structure of the building, walls are important for the insulation of the building. In future studies, the selection of wall materials can be an important research direction. Concrete, bamboo charcoal, or new types of materials can be used to find wall materials suitable for local conditions.

● The research aim of this paper was to put forward a cooking heating wall system with an additional sunlight room, focusing on the analysis of the impact of this system on improving the indoor temperature. It was verified that this system is effective for indoor heating in residential buildings. The ratio of walls to other elements is also an important factor affecting the heating of the system. In future research, this viewpoint can be used as the main research direction. First, the main elements affecting the indoor temperature can be determined based on the local geographical environment and climatic conditions to further determine the proportion of walls and major elements, so as to optimize the system.